ASD TECHNICAL REPORT 61-216

PRESENTATION OF CREEP DATA FOR DESIGN PURPOSES

M. N. Aarnes
M. M. Tuttle

Boeing Airplane Company

JUNE 1961

AERONAUTICAL SYSTEMS DIVISION

NOTICES

When Government drawings, specifications, or other data are used for any purpose other than in connection with a definitely related Government procurement operation, the United States Government thereby incurs no responsibility nor any obligation whatsoever; and the fact that the Government may have formulated, furnished, or in any way supplied the said drawings, specifications, or other data, is not to be regarded by implication or otherwise as in any manner licensing the holder or any other person or corporation, or conveying any rights or permission to manufacture, use, or sell any patented invention that may in any way be related thereto.

Qualified requesters may obtain copies of this report from the Armed Services Technical Information Agency, (ASTIA), Arlington Hall Station, Arlington 12, Virginia.

This report has been released to the Office of Technical Services, U.S. Department of Commerce, Washington 25, D.C., for sale to the general public.

Copies of ASD Technical Reports and Technical Notes should not be returned to the Aeronautical Systems Division unless return is required by security considerations, contractual obligations, or notice on a specific document.

ASD TECHNICAL REPORT 61-216

PRESENTATION OF CREEP DATA FOR DESIGN PURPOSES

M. N. Aarnes
M. M. Tuttle

Boeing Airplane Company

JUNE 1961

Directorate of Materials and Processes
Contract No. AF 33(616)-7201
Project No. 7381

AERONAUTICAL SYSTEMS DIVISION
AIR FORCE SYSTEMS COMMAND
UNITED STATES AIR FORCE
WRIGHT-PATTERSON AIR FORCE BASE, OHIO

FOREWORD

This report was prepared by the Aero-Space Division of the Boeing Airplane Company under USAF Contract No. AF 33(616)-7201, Project No. 7381, "Materials Application," Task No. 73812, "Data Collection and Correlation." The work was administered under the direction of Directorate of Materials and Processes, Applications Laboratory, Deputy for Technology, Aeronautical Systems Division with Mr. C. L. Harmsworth acting as project engineer.

This report covers work done from 1 June 1960 to 31 May 1961.

Testing was done by Materials Laboratory Group, Structures Laboratories Unit, Boeing Airplane Company, under the direction of Mr. John Boysen; New England Materials Laboratory, Inc., under the direction of Dr. Robert Widmer; and Battelle Memorial Institute, under the direction of Mr. John VanEcho. The skill and cooperation of these people are gratefully acknowledged.

The research is identified as D2-7837-1, D2-7837-2, and D2-7837-3 in the records of the Boeing Airplane Company.

ABSTRACT

This program was conducted to obtain additional and comparative creep data, to compare creep data from several sources, and to recommend what values to present and in what form to present creep data for design purposes.

Conventional long time creep tests were performed on A-286 at 1200°F and 1500°F; A110AT at 800°F and 1000°F; and Unimach 2 at 600°F and 900°F for purposes of comparing with existing similar data. Conventional creep tests were performed on Rene' 41 at 1250, 1400, 1550, 1700, 1850, and 2000°F.

Data were analyzed and are presented in the form of activation series equations. Nomographs were derived for each material.

Cyclic creep tests were performed on Rene' 41, in which both stress and temperature were cycled. Cyclic data were found to be comparable to the constant stress constant temperature data.

PUBLICATION REVIEW

This report has been reviewed and is approved.

FOR THE COMMANDER

W. P. Conrardy

W. P. CONRARDY
Chief, Materials Engineering Branch
Applications Laboratory
Directorate of Materials and
Processes

TABLE OF CONTENTS

LIST OF ILLUSTRATIONS

LIST OF ILLUSTRATIONS (Cont'd)

LIST OF ILLUSTRATIONS (Cont'd)

LIST OF ILLUSTRATIONS (Cont'd)

LIST OF ILLUSTRATIONS (Cont'd)

LIST OF SYMBOLS

a	area
c	specific heat
d 1	a physical distance
d 2	a physical distance
d 3	a physical distance
d 4	a physical distance
k	rate constant
k_p	plastic rate constant
k_E	elasto-plastic rate constant
e	natural logarithm
f	a function of
h	hardness
m_x	scale modulus for x axis
m_y	scale modulus for y axis
m_z	scale modulus for z axis
m_q	scale modulus for q axis
m	scale modulus for ϵ axis
n	a constant for activation series method
p	load
t	time
t_a	a constant pertaining to the convergence of stress lines in Manson-Haferd method
v	volume
A	frequency factor

A'	frequency factor assumed to be constant by Manson-Haferd
A_p	plastic frequency factor
A_E	elasto-plastic frequency factor
B	time dependent constant
C_{HJ}	Holloman-Jaffee constant
C_{LM}	Larson-Miller constant
C_p	concentration of moles per unit volume of material for plastic deformation
C_E	concentration of moles per unit volume of material for elasto-plastic deformation
C_1	a constant
C_2	a constant
C_3	a constant
C_4	a constant
D	a constant for activation series method
D'	hardening coefficient
E	modulus of elasticity
F	a constant for activation series method
H	activation energy
ΔH	activation energy
HJ	Holloman-Jaffee tempering parameter
H_p	activation energy for plastic deformation
H_E	activation energy for elasto-plastic deformation
K_p	a reaction velocity constant for plastic deformation
K_E	a reaction velocity constant for elasto-plastic deformation

K_{HJ}	Holloman-Jaffee constant
K	a constant for activation series method
LP	Manson-Haferd parameter
Lx	physical length of x axis
Ly	physical length of y axis
Lz	physical length of z axis
M	a thermal dependent function
N	a thermal dependent function
P	a constant for activation series method
Q	activation energy
ΔQ	activation energy
Q'	activation energy pertaining to Manson-Haferd method
R	the gas constant
S	a constant for activation series method
S'	a constant for activation series method
S"	a constant for activation series method
ΔS	entropy change
T	absolute temperature
T_a	a constant pertaining to the convergence of stress lines in Manson-Haferd method
X	a function
Y	a function
Z	a function
α	a constant for activation series method
β	a constant for activation series method

γ_p	plastic reaction rate
γ_E	elasto-plastic reaction rate
δ	true change in length
$\dot{\epsilon}$	strain rate
ϵ	strain
θ	Sherby-Dorn parameter
κ	an empirical constant
λ	length
μ	a constant for activation series method
μ_o	transverse coefficient
ζ	coefficient of viscosity
ρ	density
σ	stress
ψ	a constant

I. INTRODUCTION[1]

There exists today a large amount of creep data on materials ranging from aluminum alloys to refractory metals. In some cases, the information is adequate and in others very limited. The major problem encountered in utilizing some of these existing data is that the stresses and/or times used to obtain the data are usually not suitable for airframe design usage without extrapolating or interpolating. A state-of-the-art study reveals that several investigations have been conducted in recent years attempting to show by empirical equations the relationship between the creep variables. Such a relationship, if valid, would allow interpolation and perhaps limited extrapolation.

Another problem involved in the use of existing creep data is that of assessing the reliability of the data. It is generally accepted that there is an inherent scatter in test results, including creep data, on materials. Statistical evaluations of creep and rupture properties of several alloys have been reported in the literature. These investigators concluded that metallurgical variation of the material, rather than sampling technique or testing variables is responsible for the scatter in test data. Results of such investigations indicate that there may not be much difference in results between laboratories providing a reasonably common test procedure is used (1, 2, 3).[2]

It is recognized that consideration of conventional creep data is necessary in high temperature design, however, most aircraft structures will be subjected to cyclic temperature and stress conditions rather than steady temperatures and stresses for long periods of time. Various types of cyclic testing have been conducted and results have been reported in the literature (4, 5, 6). Such testing usually has been performed with a specific application in mind, and attempts to correlate such data with steady state data by use of one of the commonly used parametric methods have so far been unsuccessful.

The ultimate use of creep data would be the formulation of an equation relating stress, time, strain, and temperature. This would permit a closed solution to some structural analysis problems.

---

[1]Manuscript released by author(s) June 1961 for publication as an ASD Technical Report.

[2]Numbers in parenthesis refer to references appended hereto.

II. DISCUSSION

PURPOSE

This program was conducted to obtain additional and comparative creep data, to compare creep data from several sources, and to recommend what values to present and in what form to present creep data for design purposes. To accomplish these objectives, the investigation was conducted in three phases as follows:

Phase 1: Experimental work to obtain additional comparative creep data on three alloys, namely: A-286, an iron base super alloy; Unimach 2, an H-11 hot work die steel; and A110AT, a titanium alloy. In addition, cyclic and steady state creep data were obtained on Rene' 41, a nickel base super alloy.

Phase 2: Analysis of the data obtained from Phase 1, and comparison of these data with that previously obtained from other WADD sponsored investigations.

Phase 3: Analysis of the procedures and methods used in presenting creep data, and recommendations for presenting creep data for design use.

COMMONLY USED METHODS OF PRESENTING CREEP DATA

The simplest method of presenting creep data is a plot of creep strain versus time as is obtained directly from the test data. If sufficient strain-time curves are available for different temperatures and stress levels, the data can be cross plotted to yield other types of curves, such as isochronous curves.

A curve is required for each condition of temperature and stress. These curves do not permit interpolation or extrapolation.

There are several methods of correlating creep data which stem from the Arrhenius rate equation:

$$k = Ae^{-Q/RT}$$

where k is the rate constant
A is the frequency factor dimensionally equal to k
Q is the activation energy
R is the gas constant
T is the absolute temperature

Although this equation is semi-empirical in origin, it has found applications to many liquid and gaseous reactions. It was obtained by noting that if the logarithm of the rate is plotted versus the reciprocal of absolute temperature, a straight line develops with intercept at 1/T equal to A, and of slope equal to -Q/R. This is shown in Figure 1, page 4.

The Larson Miller Method

In 1945, Holloman and Jaffee derived a graphical relationship between hardness H, and a parameter depending on time and temperature, applicable to the steel tempering process (9). They assumed that tempering is a function of an activation process:

$$\mathbf{h} = f_1 (te^{-Q/RT}) \tag{1}$$

where **h** is hardness
t is time
Q is the activation energy
R is the gas constant
T is the absolute temperature

It was found that

$$\mathbf{h} = f_2 (Q) \tag{2}$$

and

$$te^{-Q/RT} = t_o = \text{constant} \tag{3}$$

Taking logarithms of Equation 3 and equating Q from Equations 2 and 3

$$Q = RT \left[\ln (t) - \ln (t_o) \right] = f_2 (\mathbf{h}) \tag{4}$$

$$\mathbf{h} = f_3 \left[e^{RT (\ln t/t_o)} \right] \tag{5}$$

or

$$\mathbf{h} = f (T \ln t/t_o) = f \left[T (\ln t - \ln t_o) \right] \tag{6}$$

Let

$$C_{HJ} = -\ln t_o, \text{ or } t_o = e^{-C_{HJ}} \tag{7}$$

$$k = A e^{-Q/RT}$$

Q/R = slope

A = intercept at $1/T = 0$

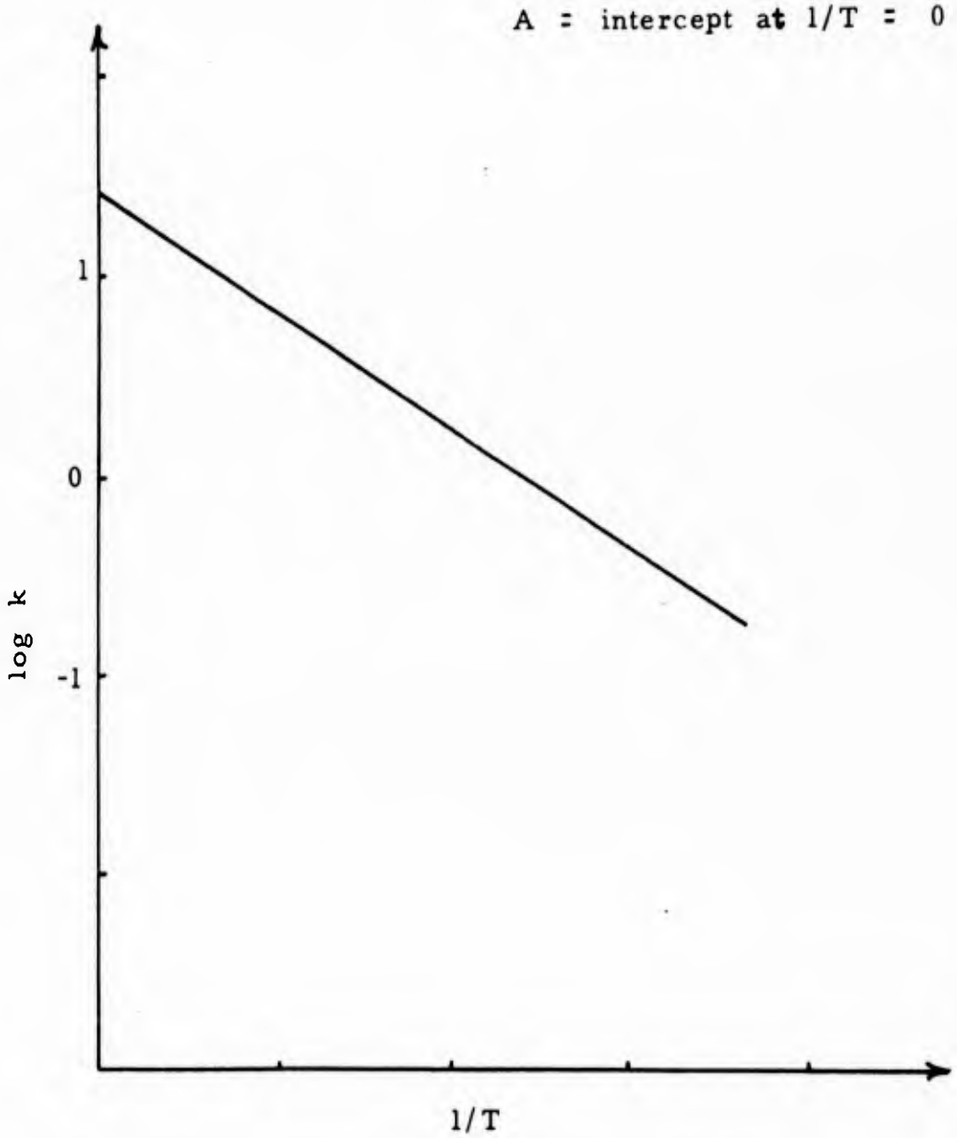

FIGURE 1 - GRAPHICAL REPRESENTATION OF A SINGLE ACTIVATED PROCESS

Then $$h = f\left[T\,(C_{HJ} + \ln t)\right] \tag{8}$$

where the Holloman-Jaffee tempering parameter is

$$Q/R = HJ = f\left[T\,(C_{HJ} + \ln t)\right] \tag{9}$$

or, if $K_{HJ} = e^{-C_{HJ}}$ then

$$t = Ae^{Q/RT} = K_{HJ}e^{HJ/T} \tag{10}$$

By 1952, it had been shown by several investigators that creep, diffusion, and tempering appeared to conform to a rate controlled process (11, 12). Larson and Miller applied the tempering parameter derived by Holloman and Jaffee to the correlation of creep data (7). They assumed that the time to rupture, or the time required to reach a given plastic deformation depends on the summation of the preceding creep rates and that the activation energy, Q, is independent of temperature, but dependent on stress in such a manner that A will be a constant for any material:

$$t = Ae^{Q/RT} \tag{11}$$

and setting $A = e^{-C_{LM}}$

$$Q/R = LM = f\left[T\,(C_{LM} + \ln t)\right] \tag{12}$$

In their original work, Larson and Miller proposed that the constant C_{LM} could be assumed equal to 20 for all materials and testing conditions, and that the error introduced by such an assumption is negligible. However, it is now common practice to select a value of C_{LM} for each material which produces the best correlation of data.

It is important to recognize the limitations of the Larson-Miller method, which are a result of the authors' original assumptions. The assumption that A is constant is erroneous, since A is both strain rate and temperature dependent (10, 14, 19). The assumption that the activation energy Q is independent of temperature can lead to serious errors, especially when predictions are made for long time low temperature behavior using short time high temperature data, or vice versa. However, the Larson-Miller method can be successfully applied if used well within the steady state creep region.

The Sherby Dorn Method

In 1952, Sherby and Dorn also proposed a method for correlation of creep data (8). They proposed that the total creep strain could be expressed by the following relationship:

$$\epsilon = f(\theta\ \sigma) \tag{13}$$

where

$$\theta = \int_0^t e^{-\Delta Q/RT}\, dt \tag{14}$$

where ΔQ is the activation energy for creep.

If temperature is constant, Equation 14 can be written:

$$\theta = te^{-\Delta Q/RT} \tag{15}$$

Rewriting Equation 15 and letting $\theta = A$, the equation takes the same form as Equations 3 and 11:

$$t = Ae^{+\Delta Q/RT} \tag{16}$$

Orr, Sherby, and Dorn extended this method in 1953 to the treatment of deformation and rupture data (13). The rupture parameter is essentially of the same form:

$$\theta_r \cong t_r e^{(-\Delta Qr/RT)} \tag{17}$$

where

$$\epsilon_r \cong \text{constant}$$

$$\theta_r = f(\sigma) = A \tag{18}$$

Sherby and Dorn found that their method is valid as long as the temperatures are greater than the minimum temperature required for rapid recovery of the material, or about 0.4 of the melting point.

The limitations of this method are also a result of the authors' original assumptions. Sherby and Dorn assumed that the activation energy ΔQ is neither stress nor temperature dependent; however, they did assume that A is stress dependent (8, 14).

The method of Sherby and Dorn can be successfully used if applied well within the steady state creep region.

The Manson-Haferd Method

In 1953, Manson and Haferd developed a method for correlation of rupture data and prediction of behavior based on experimental observations (10). Manson and Haferd decided from graphical observations, that at least for some materials and rupture times in excess of 30 hours, the stress rupture data were much better represented by plotting the log of rupture time versus temperature and letting the constant stress lines fan out as straight lines from a common point. In 1958, Manson gave a detailed explanation showing how to select the testing conditions in order to prepare master curves with a minimum expenditure of testing time (14). The Manson-Haferd method is represented by the following equation:

$$t_r = A' e^{-Q'T} \tag{19}$$

where t_r is the time to rupture
A' is a constant
Q' is the activation energy
T is the absolute temperature

The parameter obtained by the Manson-Haferd method is

$$LP = \frac{T - T_a}{\log t_r - \log t_a} \tag{20}$$

where T_a and $\log t_a$ are the constants which are determined graphically from a plot of log time versus temperature. The values T_a and $\log t_a$ represent the point of convergence of the various stress lines on such a plot.

Attempts to mathematically justify Equation 19 have not been successful. It is interesting to note that Q' is stress dependent and that A' is neither stress nor temperature dependent.

The method of Manson and Haferd should be used only in the tertiary creep region, since it was derived using rupture data.

Figure 2, page 8, shows a comparison of the constant stress lines assumed by Larson-Miller, Sherby-Dorn, and Manson-Haferd.

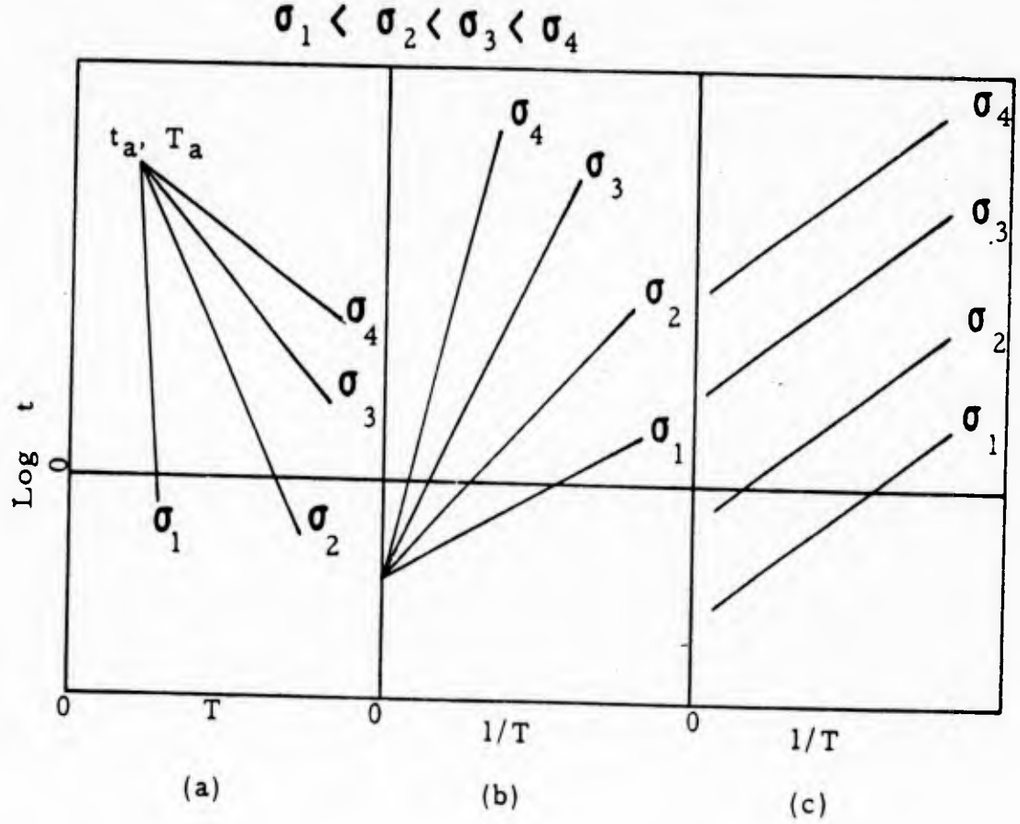

FIGURE 2 - Comparison of Constant Stress Lines
(a) Manson's Method (b) Larson-Miller Method
(c) Dorn's Method

ACTIVATION SERIES METHOD

Figure 3, page 11 shows how the Larson-Miller, Sherby-Dorn, and Manson-Haferd methods represent deformation data. It is readily seen that the Larson-Miller method favors the primary portion, the Sherby-Dorn the central, and the Manson-Haferd the final portion of the deformation curve. When a material deforms, several activated processes occur simultaneously, but reach their maximum intensities at different times. Assuming that these processes obey the Arrhenius rate equation, the overall process can be expressed by the following reaction series:

$$t = A_1 e^{Q_1/RT} + A_2 e^{Q_2/RT} + A_n e^{Q_n/RT} \qquad (21)$$

where

$$A_1 = f(\epsilon_1 \sigma_1);\ A_2 = f(\epsilon_2 \sigma_2);\ A_n = f(\epsilon_n \sigma_n)$$

$$Q_1 = f(\sigma_1 T_1);\ Q_2 = f(\sigma_2 T_2);\ Q_n = f(\sigma_n T_n)$$

In Figure 4, page 12, the isometric graph shows the relationship between frequency factor, A; strain rate, $\dot{\epsilon}$; and stress, σ. Figure 5, page 13, shows the relationship between activation energy, Q; stress σ; and temperature, T.

The activation series equation can be written in terms of strain:

$$\epsilon = P_1 e^{-\mu_1/T} \sigma^{D_1} e^{F_1/T} t^{S_1} e^{n_1/T} + P_2 \ldots\ldots \qquad (22)$$

where P_1, μ_1, D_1, F_1, S_1, n_1, etc. are constants.

Rewriting this expression for constant temperature, it is interesting to note that it contains Hook's Law as well as the Newtonian Law for viscous behavior:

$$\epsilon = K_1 \sigma^{\beta_1} t^{\alpha_1} + K_2 \sigma^{\beta_2} t^{\alpha_2} + \ldots\ldots \qquad (23)$$

where K_1, β_1, α_1, etc. are constants.

The theory and derivation of these equations are detailed in Appendix I, page 52.

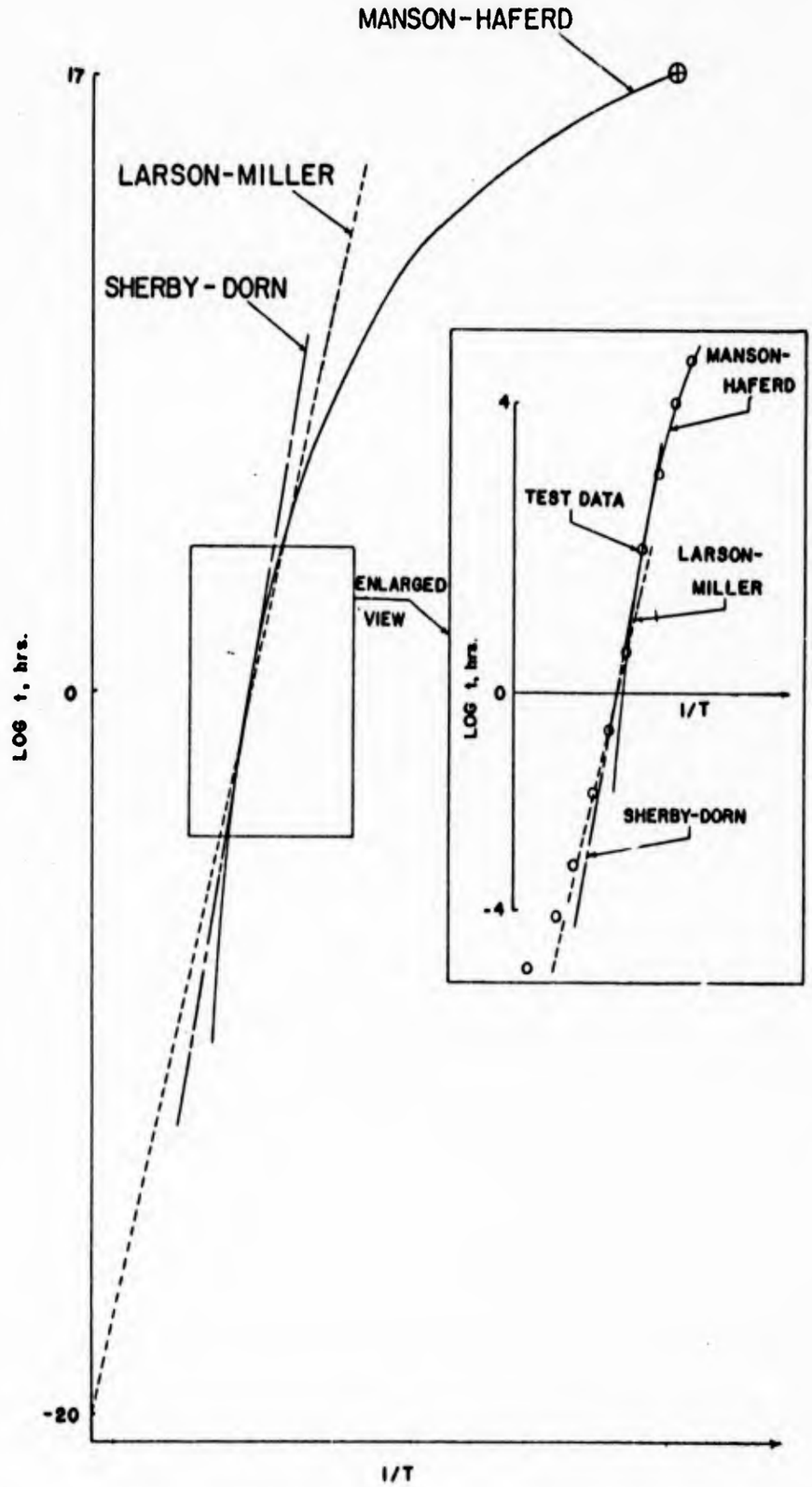

FIGURE 3 - ISOBARIC CREEP DATA REPRESENTED BY MANSON-HAFERD, SHERBY-DORN, AND LARSON-MILLER

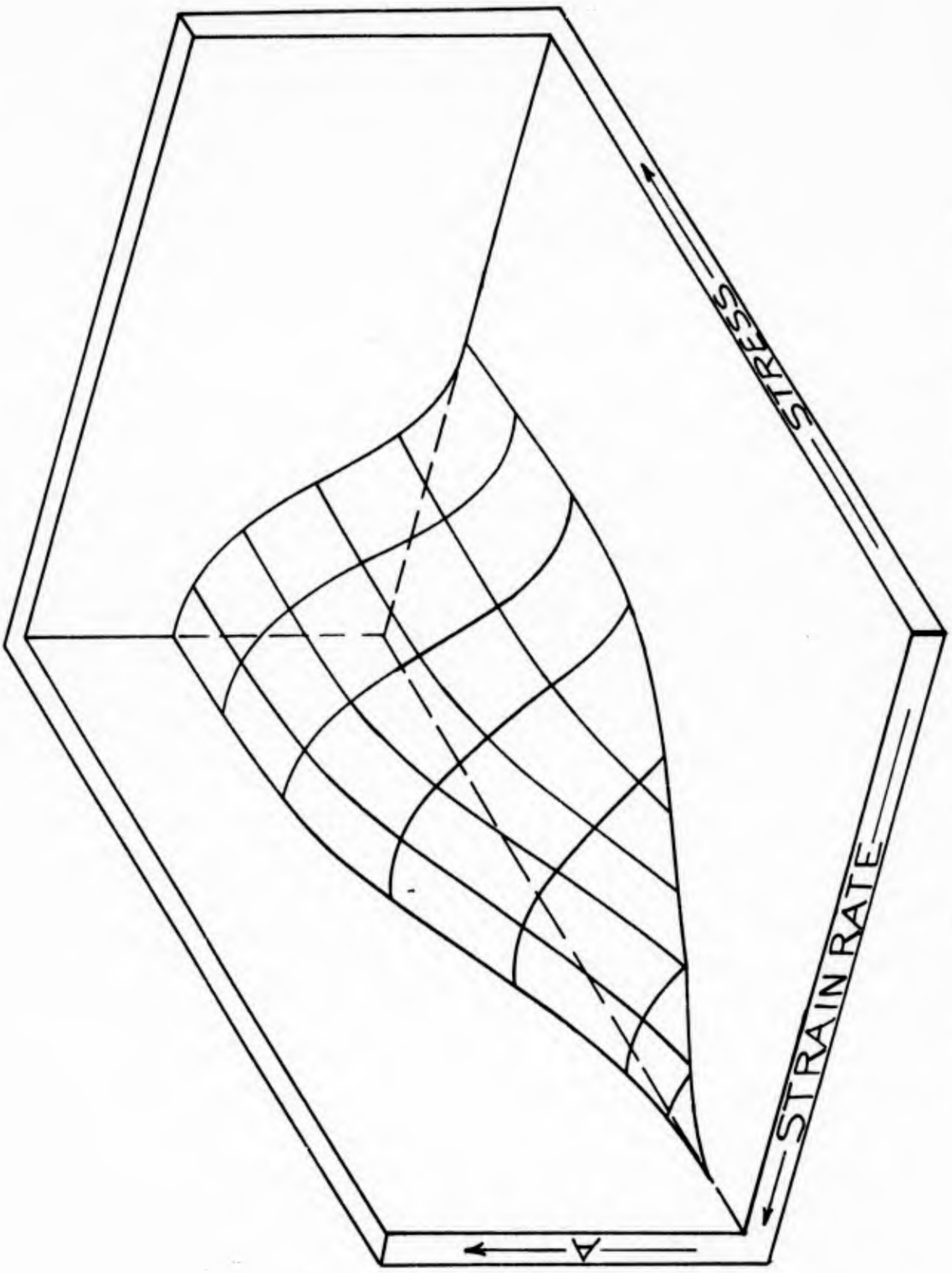

FIGURE 4 - ISOMETRIC STRESS-STRAIN RATE - FREQUENCY FACTOR SURFACE

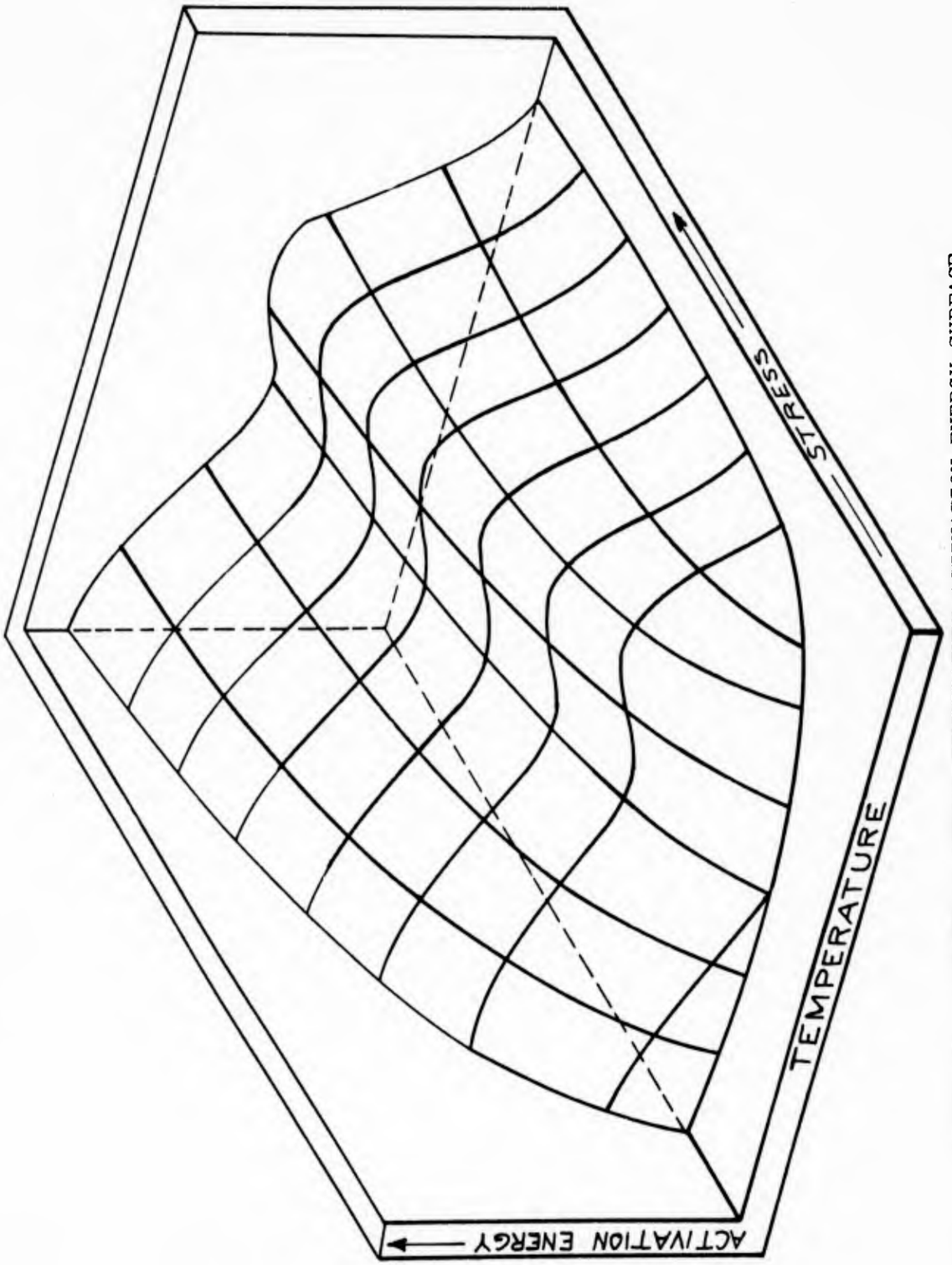

FIGURE 5 - ISOMETRIC STRESS-TEMPERATURE-ACTIVATION ENERGY SURFACE

III. CREEP TESTING

In order to accomplish the objectives of this program, a limited amount of creep testing was done by Boeing. Three alloys which had been tested on other WADD contracts were retested in order to directly compare data from two or more sources for compatibility. These alloys are A110AT, A-286, and Unimach 2. Testing was conducted at two different temperatures, and two stress levels per temperature for each alloy as follows:

Alloy and Heat Treatment	Testing Temp. °F	Testing Stress, KSI	No. of Spec.
A110AT	800	68	2
Mill annealed	800	35	2
	1000	10	2
	1000	6	2
A-286	1200	30	2
Degreased in vapor degreaser	1200	40	2
Solution treated at 1650°F 1 hr in argon	1500	2	2
Cooled in forced argon	1500	3	2
Aged at 1325°F 16 hours in air			
Unimach 2	600	250	2
Solution treated at 1800°F 1/2 hour	600	200	2
Cooled to room temperature	900	60	2
Aged at 800°F 2 hours	900	90	2
Cooled to room temperature			
Aging repeated			
(Neutral atmosphere used for all heat treating operations)			

In addition to these alloys, Rene' 41 was creep tested according to the conditions shown below:

Alloy and Heat Treatment	Testing Temp. °F	Testing Stress, KSI	No. Spec.
Rene' 41	1250	90	4
Solution treated at 1975°F	1250	50	4
Water quenched	1400	50	4
Aged 16 hrs. at 1400°F in air	1400	30	4
Air cooled	1550	20	4
	1550	12	4
	1700	6	4
	1700	4	4
	1850	2	4
	1850	1	4
	2000	.8	4
	2000	.4	4

The stress levels chosen were expected to produce 1% creep in from 500 to 1000 hours. All test results are shown in Appendix II.

It will be noted that some of the Rene' 41 curves show "negative creep" behavior in the early portion of the curve. Rene' 41 is metastable over the range of test temperatures used in this program. In addition to the usual creep deformation, metallurgical changes such as precipitation, agglomeration of very fine precipitates, and resolution of dispersed phases may occur. A volume change can occur in the material as a result of a metallurgical phenomenon such as precipitation, and a portion of the creep curve will display a negative slope. The photomicrographs shown in Figure 6, page 17 indicate that **precipitation** is occurring during exposure at test temperature, thus accounting for the unusual behavior noted in some of the creep curves. In most cases, creep deformation predominates, and a normal time-deformation curve results, where the creep rate is positive.

In order to determine the effect of intermittent creep conditions, cyclic creep tests were conducted on Rene' 41. Eight specimens were tested under cyclic stress and temperature conditions as shown below:

Heat and load in less than 1 minute

Hold for 1 hour

Unload and cool in less than 1 minute

Repeat until 1% creep has been accumulated

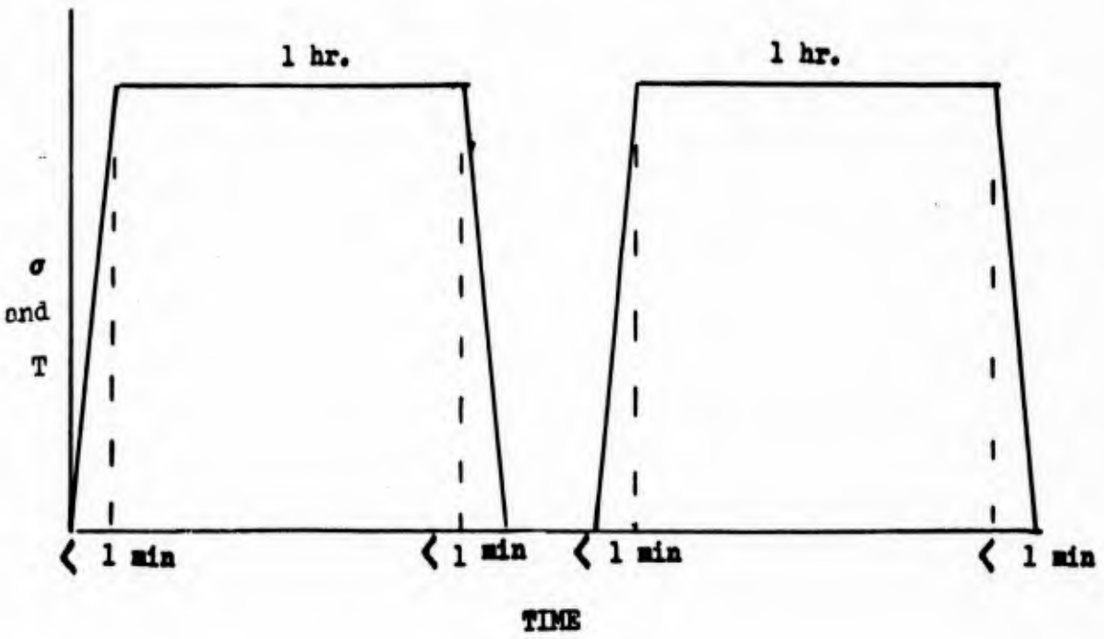

The maximum temperatures and stresses used were as follows:

Maximum Temp. °F	Maximum Stress, KSI	Number of Specimens
1400	50	2
1550	20	3
1700	6	3

The steady state creep testing of Rene' 41 was done at New England Materials Laboratory, Medford, Massachusetts, and the cyclic creep testing was done at Battelle Memorial Institute, Columbus, Ohio.

The test data shown in Appendix II are reported on an arithmetic-semi log plot to provide creep strain reading accuracies of ± .0001 in/in, paralleling that provided by the **ASTM class B-1 extensometer used in testing.** An arithmetic scale is used from 0 to 0.1 hours for better accuracy in the primary portion of the curve. Beyond 0.1 hours, the time is plotted logarithmically.

Tensile control data for all the alloys tested are shown in Appendix II. The manufacturers and heat numbers of alloys tested are also shown in Appendix II, page 98.

Testing procedures and equipment used are reported in Appendix III, page 169.

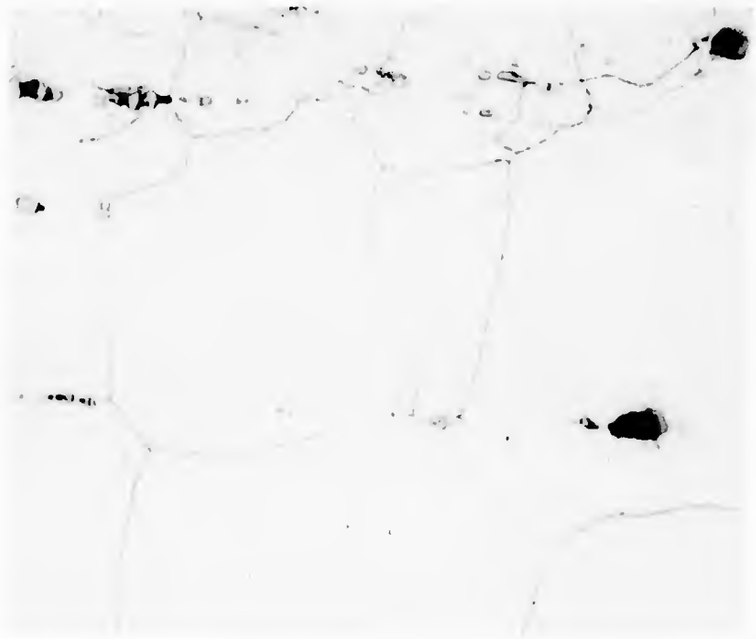

a. Specimen No. 44. Sample taken from "as received" end of test bar. Longitudinal section, etched with mixed acids, 95-3-2; 1000X.

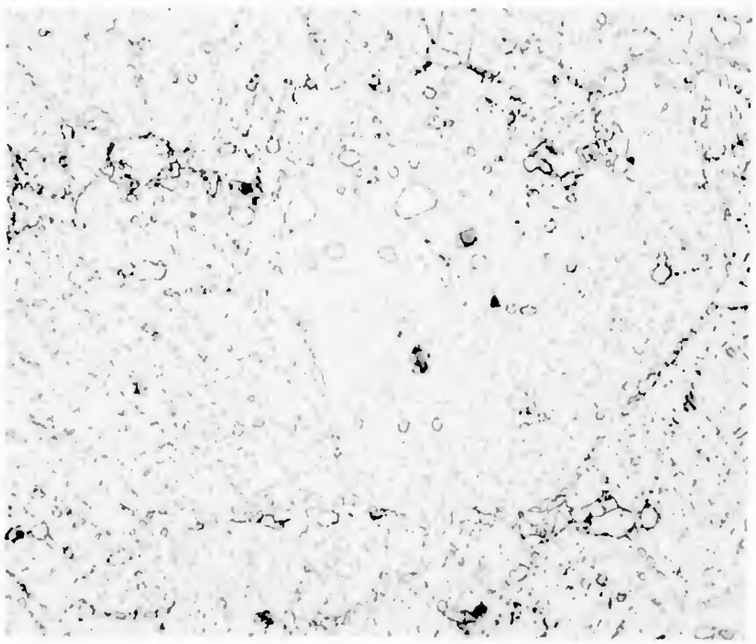

b. Specimen No. 44. Sample taken from section tested at 1850° F and 2000 psi. Longitudinal section etched with mixed acids, 95-3-2; 1000X.

FIGURE 6 - PHOTOMICROGRAPHS RENE' 41

IV. DATA COMPARISON

In order to get a measure of the difference that may occur between creep test results obtained by different investigators, the test data generated in this program were compared with that from other investigations. Comparison curves have been prepared and are shown in Figures 7 through 30, pages 19 through 42. All of the data are shown in these curves.

The Rene' 41 material used in this investigation was heat treated to the condition which results in optimum tensile properties (i.e. solution treated at 1975°F and aged at 1400°F). Most Rene' 41 creep data reported in other investigations have been obtained for material heat treated to the condition which results in optimum rupture properties (i.e. solution treated at 2150°F and aged at 1650°F).

The "cyclic" Rene' 41 data was compared with conventional creep data. These are shown in Figures 21, 23 and 25. The cumulative creep resulting from the cyclic tests is of the same magnitude as the conventional creep, i.e. the cumulative cyclic data falls within the scatter band of the constant temperature, constant stress creep data. It is recognized that the cyclic testing reported in this study covers only a small range of temperature and stress, and that the effect of cycle frequency was not investigated.

The scatter in data appears to be greatest for longer times (500 to 1000 hours) where values for strain approach 1%. In some cases, the data obtained in this investigation fall within the scatter of data from other investigations (e.g. Figure 13, page 25), and in others, the data obtained in this investigation fall outside the data from other investigations (e.g. Figure 11, page 23). The Rene' 41 data which was generated by one laboratory shows scatter generally of a lesser magnitude than that shown by the data for the other alloys.

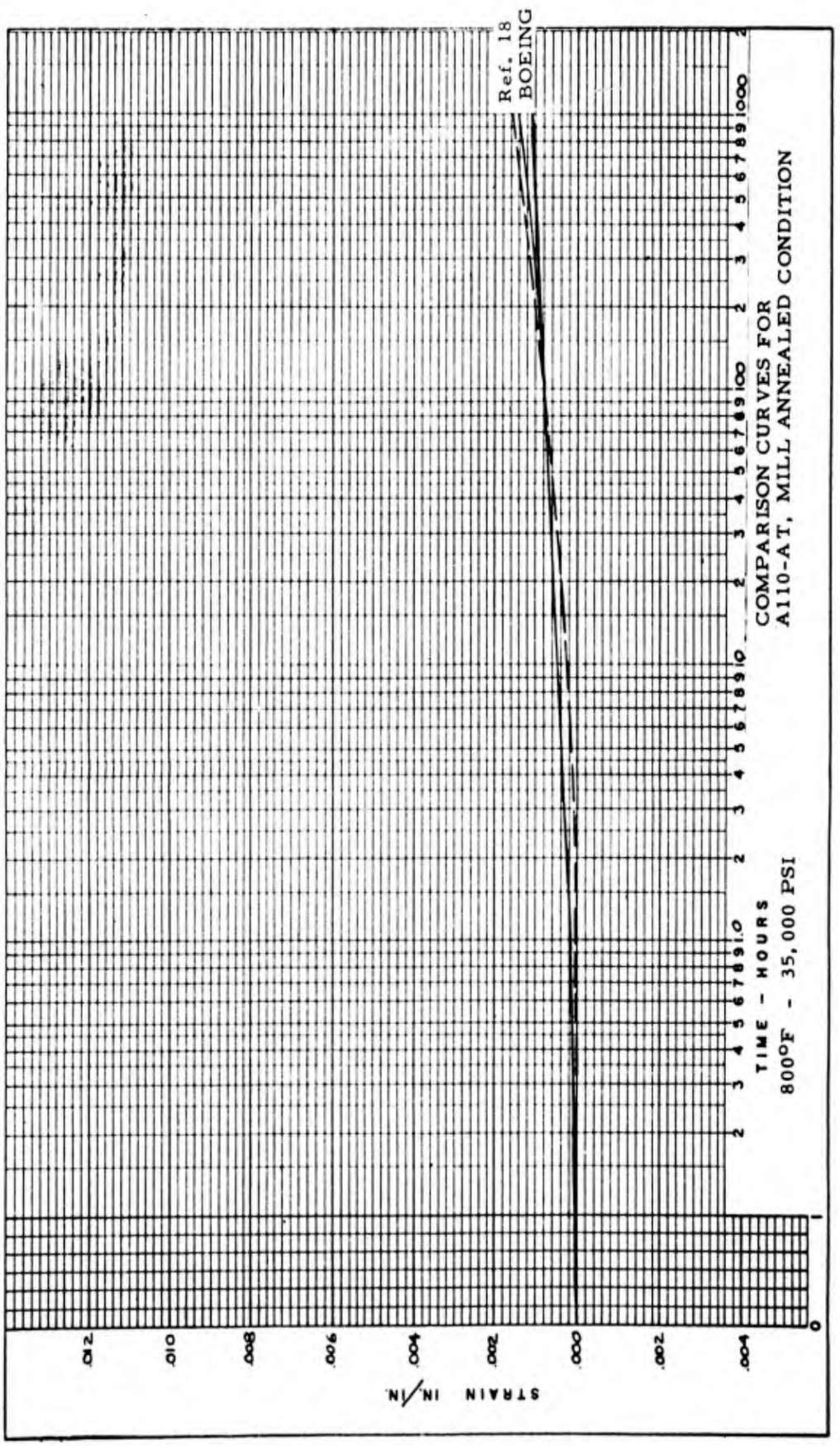

FIGURE 7 - COMPARISON CURVES A110AT 800°F 35,000 psi

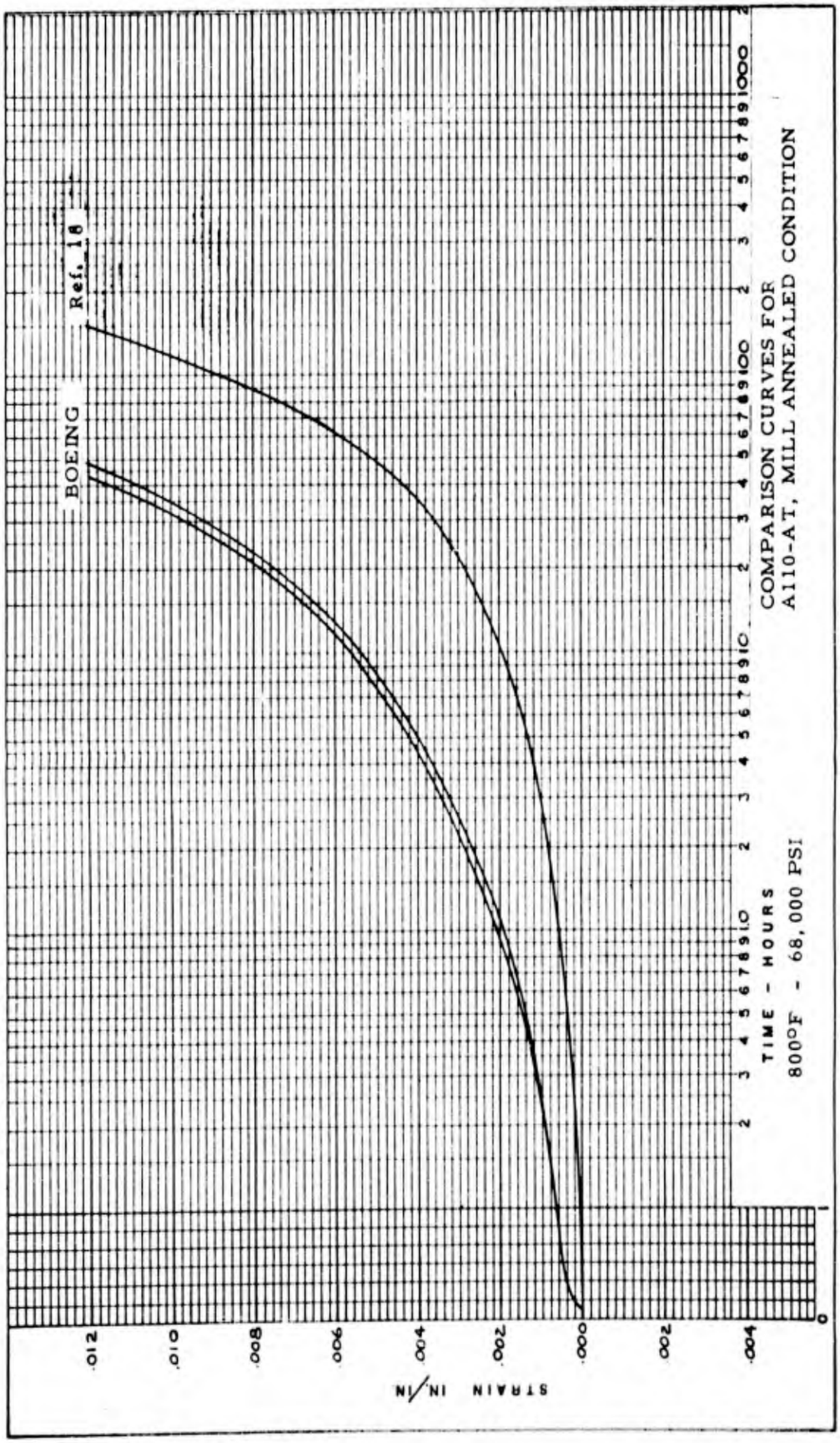

FIGURE 8 - COMPARISON CURVES A110AT 800°F 68,000 psi

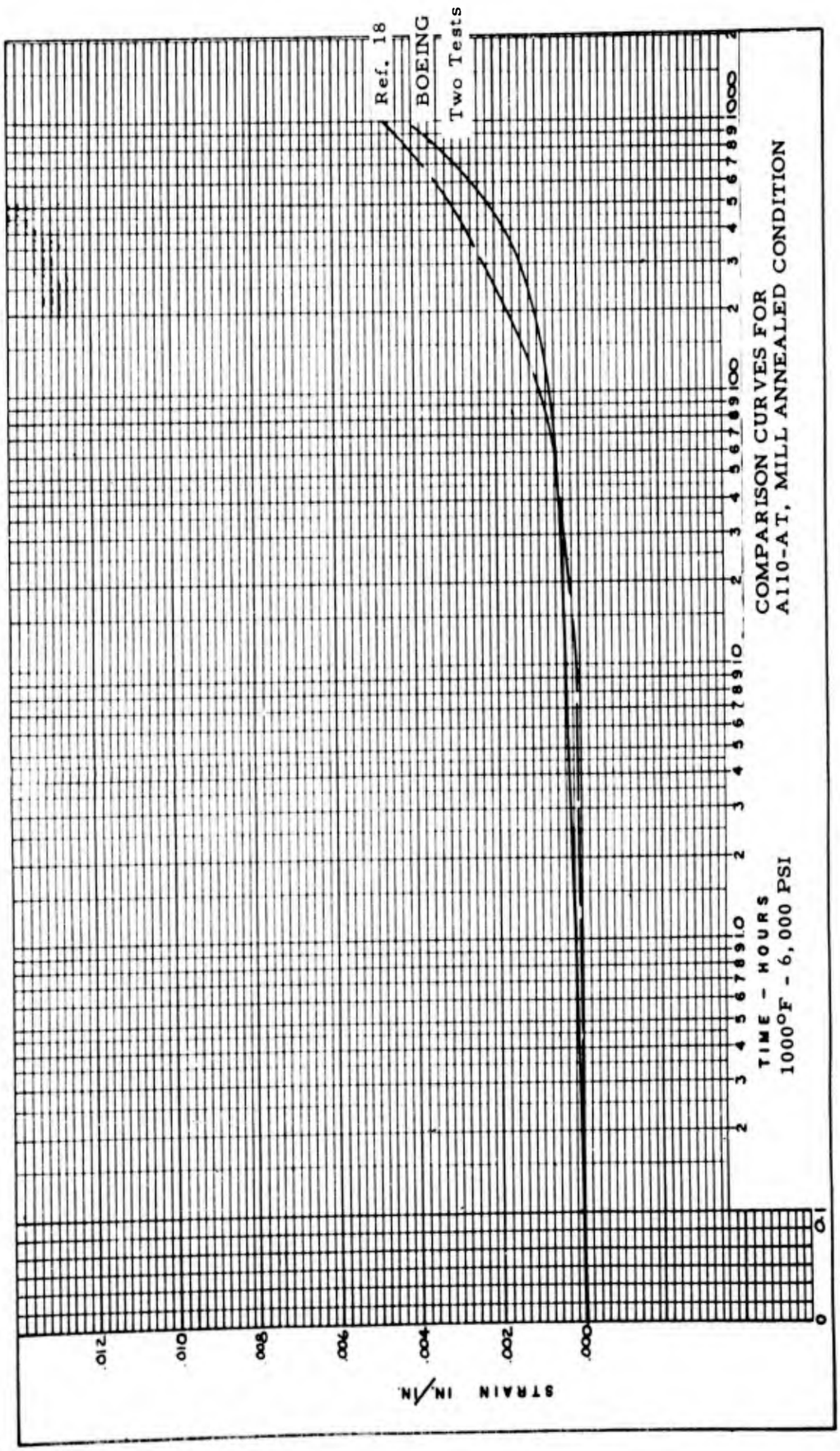

FIGURE 9 - COMPARISON CURVES A110AT 1000°F 6,000 psi

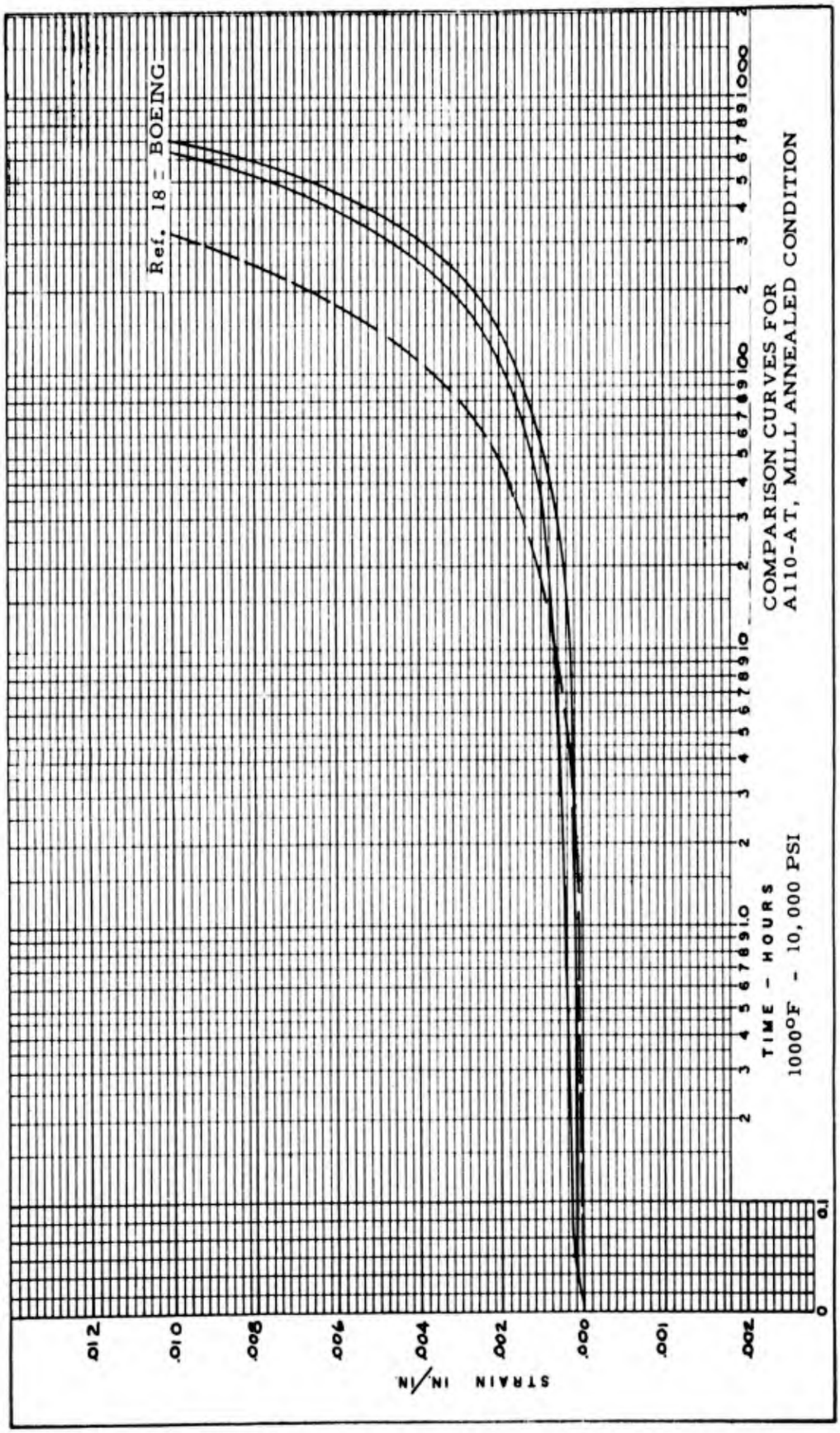

FIGURE 10 - COMPARISON CURVES A110AT 1000°F 10,000 psi

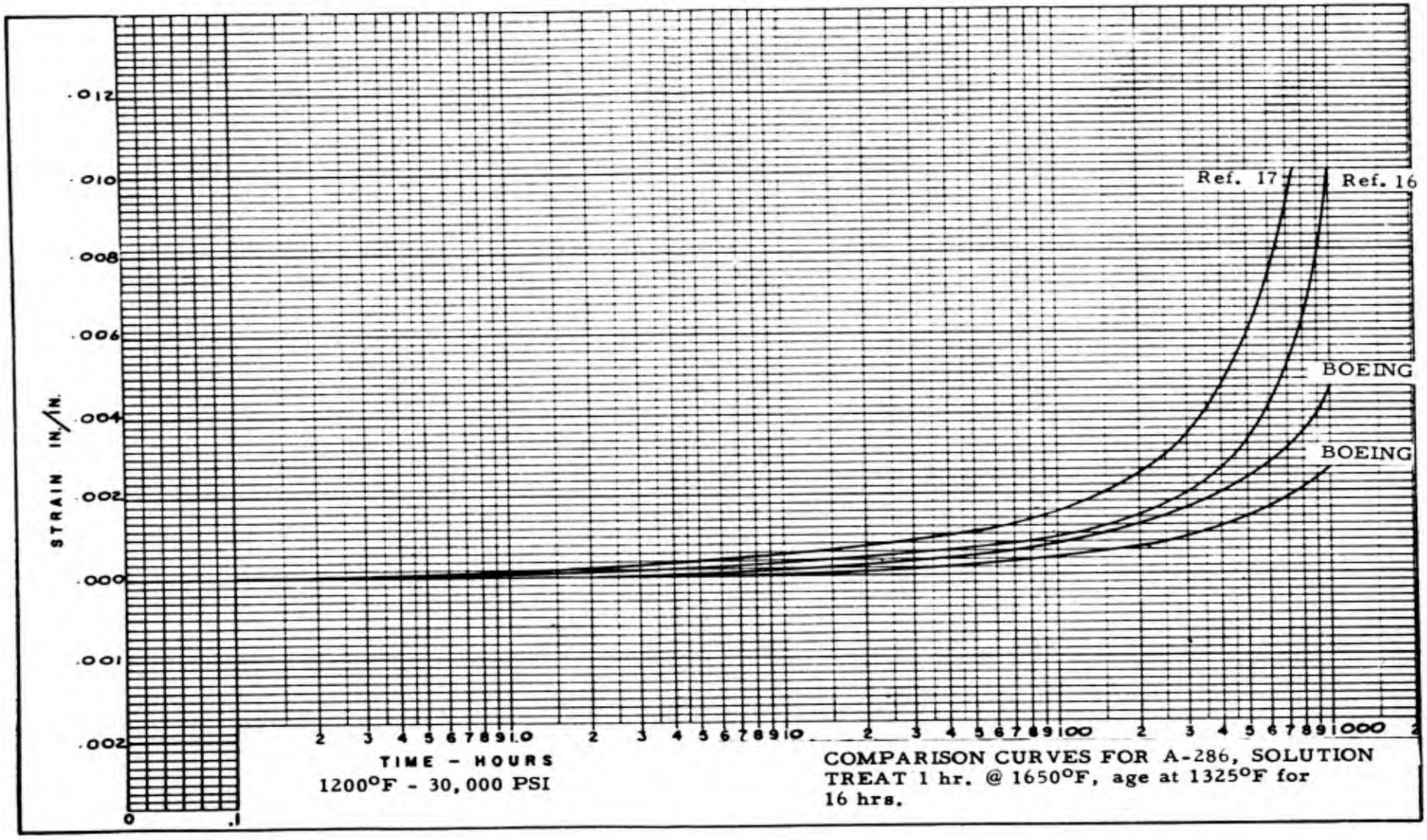

FIGURE 11 - COMPARISON CURVES A286 1200°F 30,000 psi

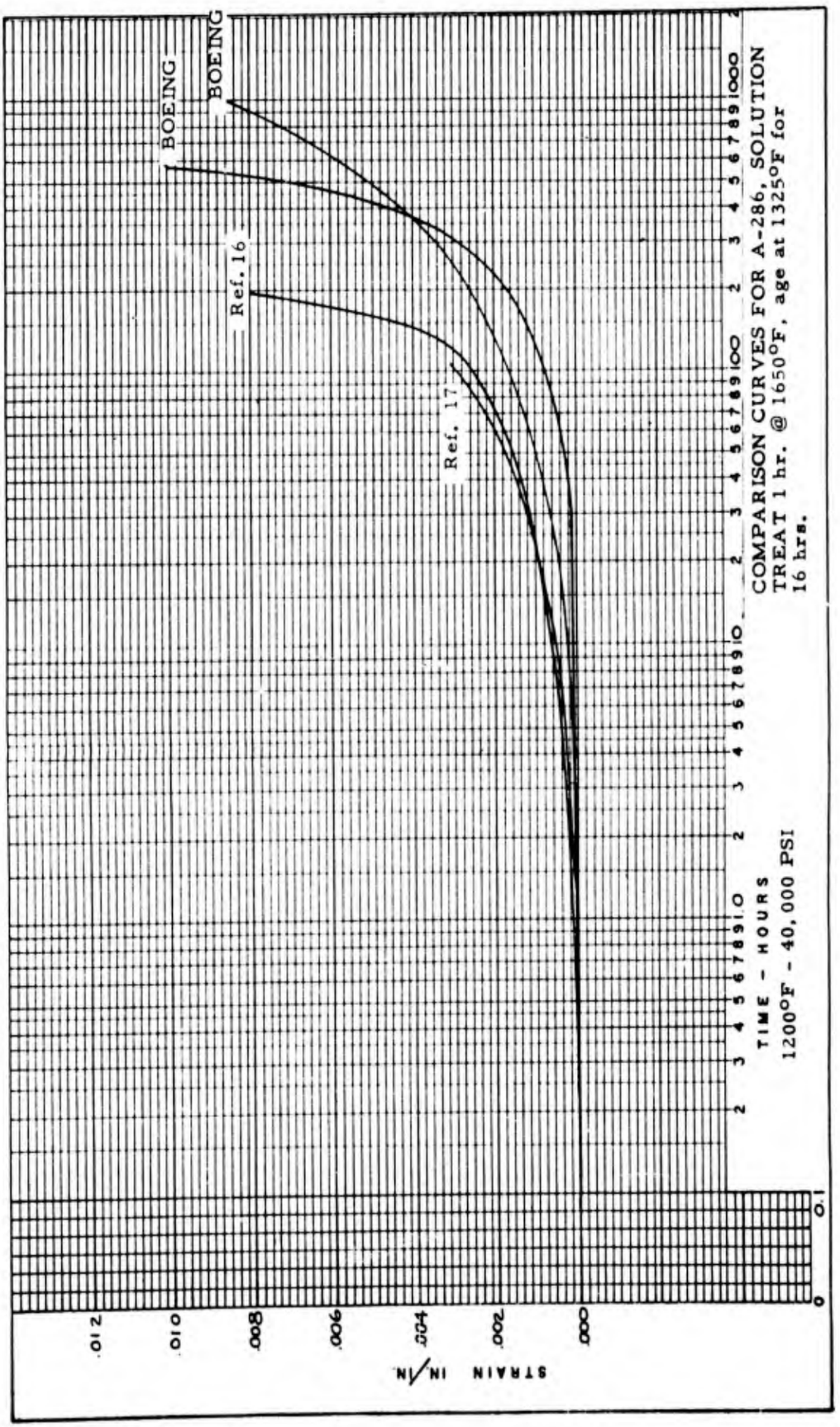

FIGURE 12 - COMPARISON CURVES A286 1200°F 40,000 psi

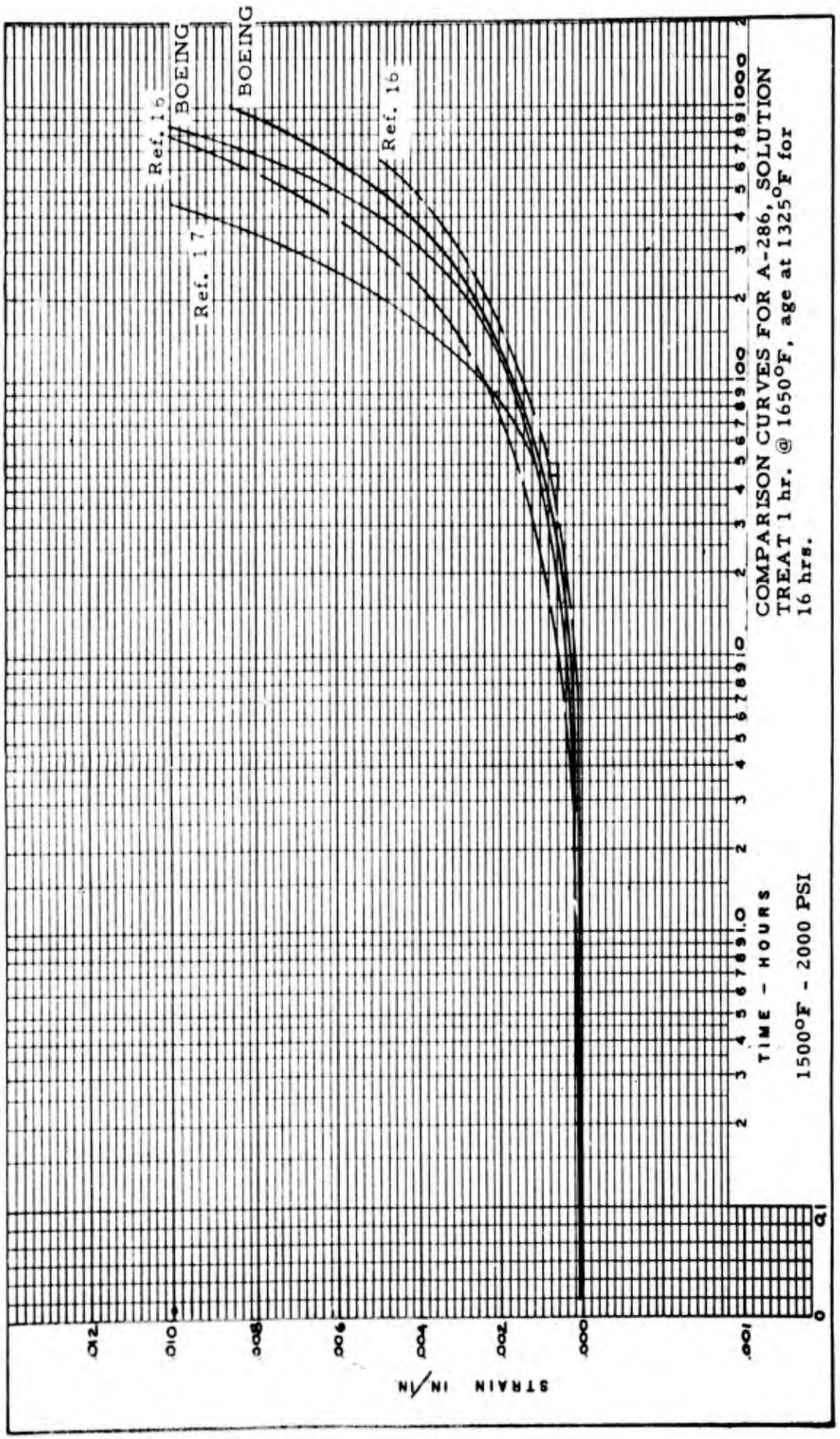

FIGURE 13 - COMPARISON CURVES A286 1500°F 2000 psi

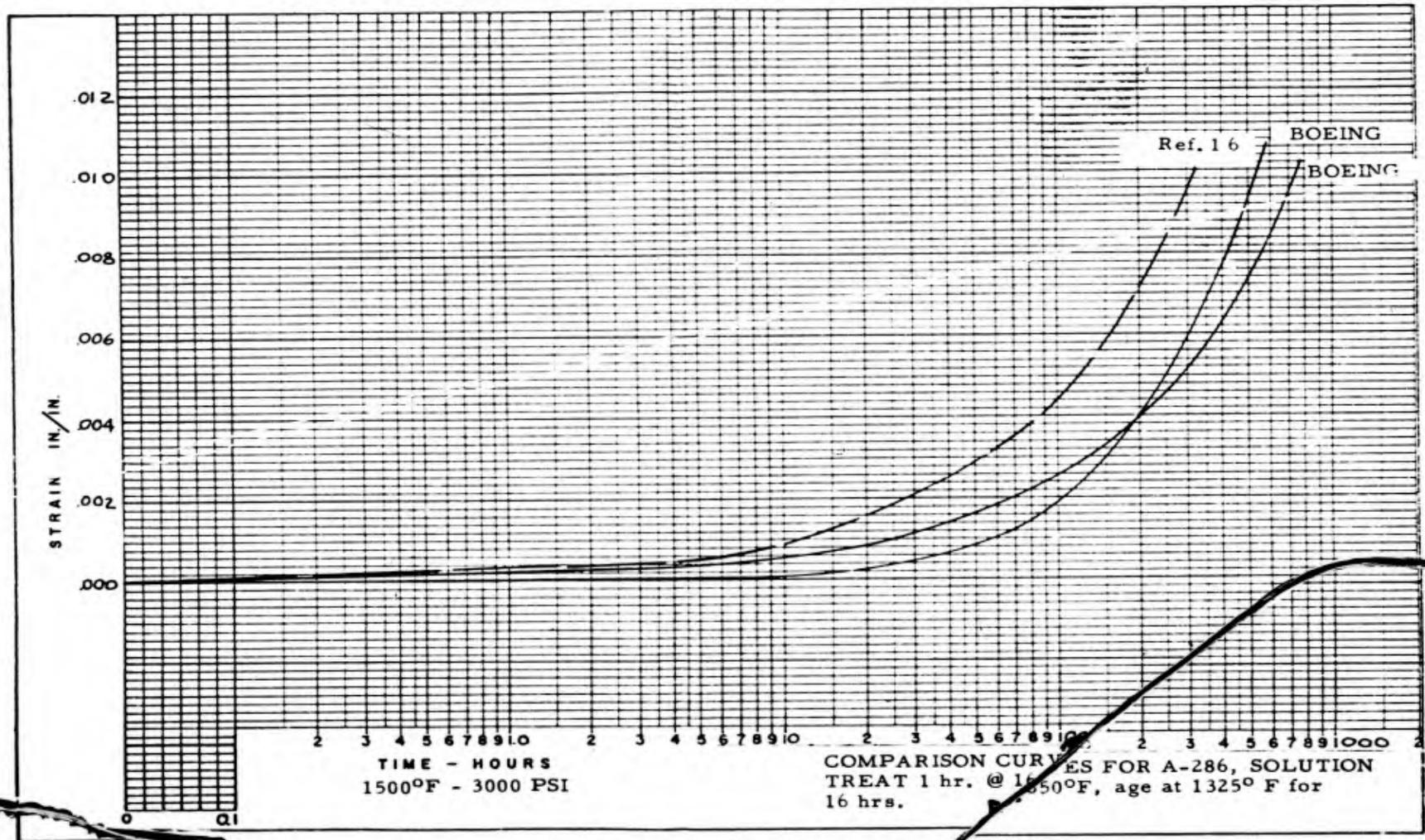

FIGURE 14 - COMPARISON CURVES A286 1500°F 3000 psi

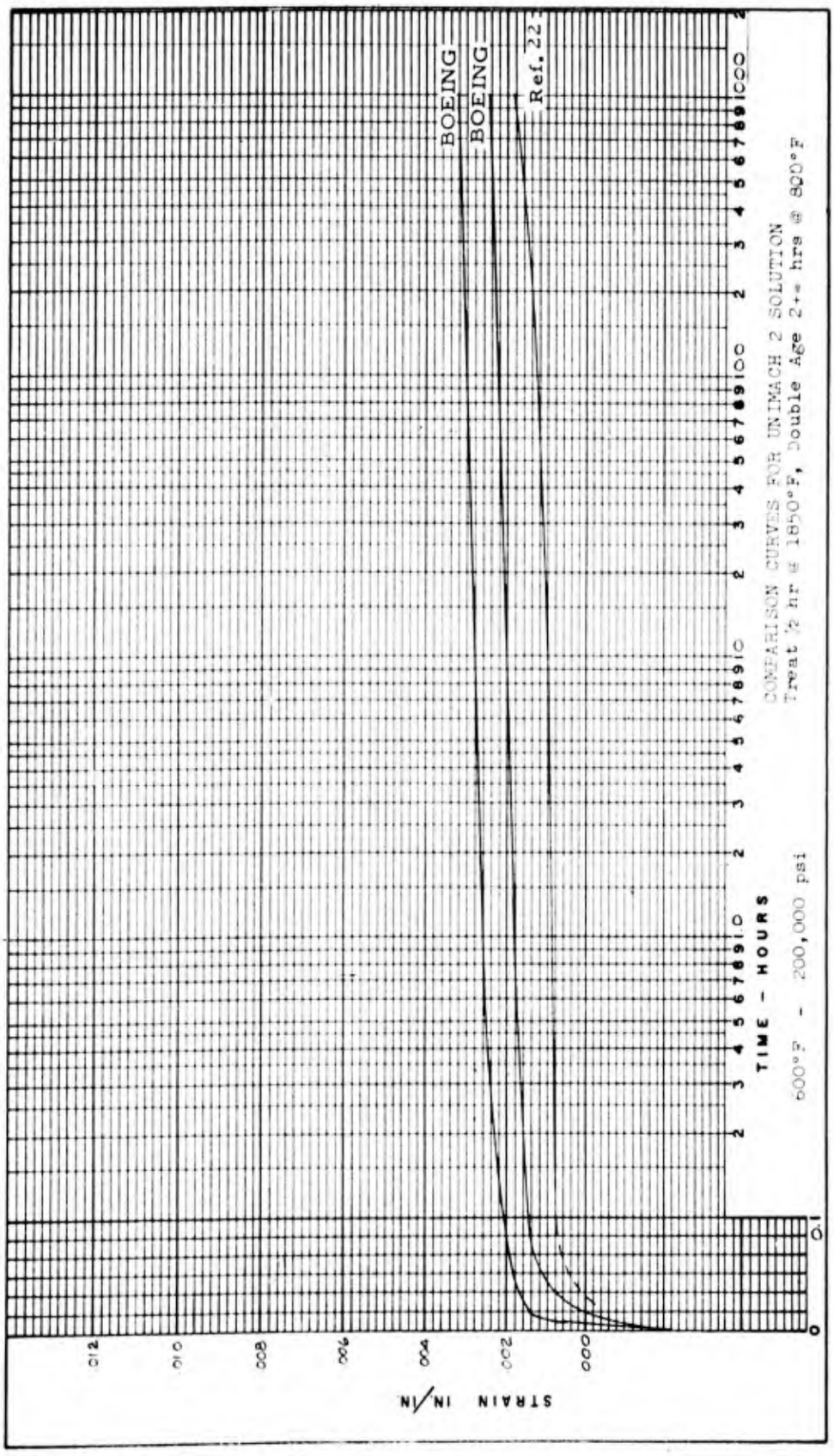

FIGURE 15 - COMPARISON CURVES UNIMACH 2 600°F 200,000 psi

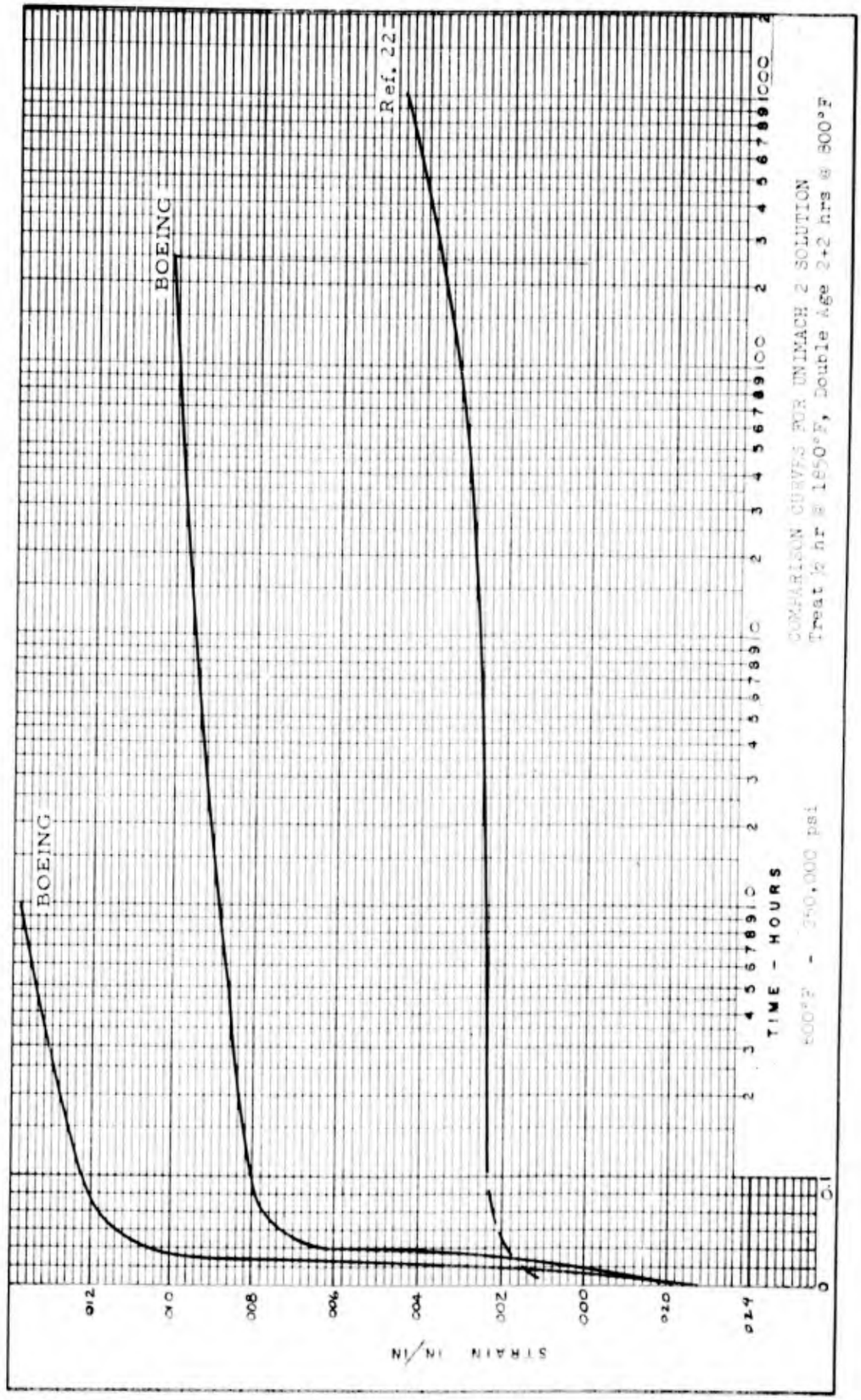

FIGURE 16 - COMPARISON CURVES UNIMACH 2 600°F 250,000 psi

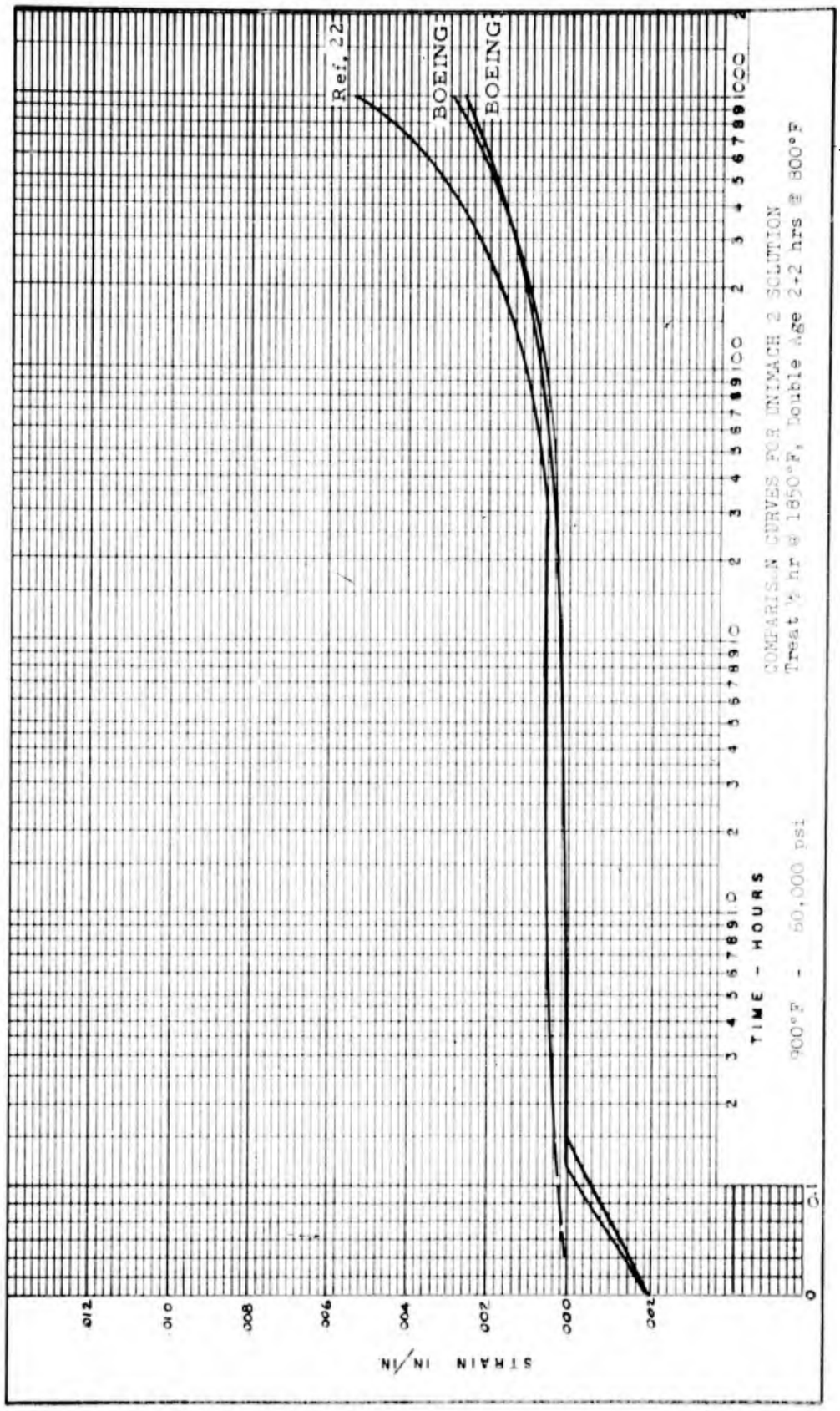

FIGURE 17 - COMPARISON CURVES UNIMACH 2 900°F 60,000 psi

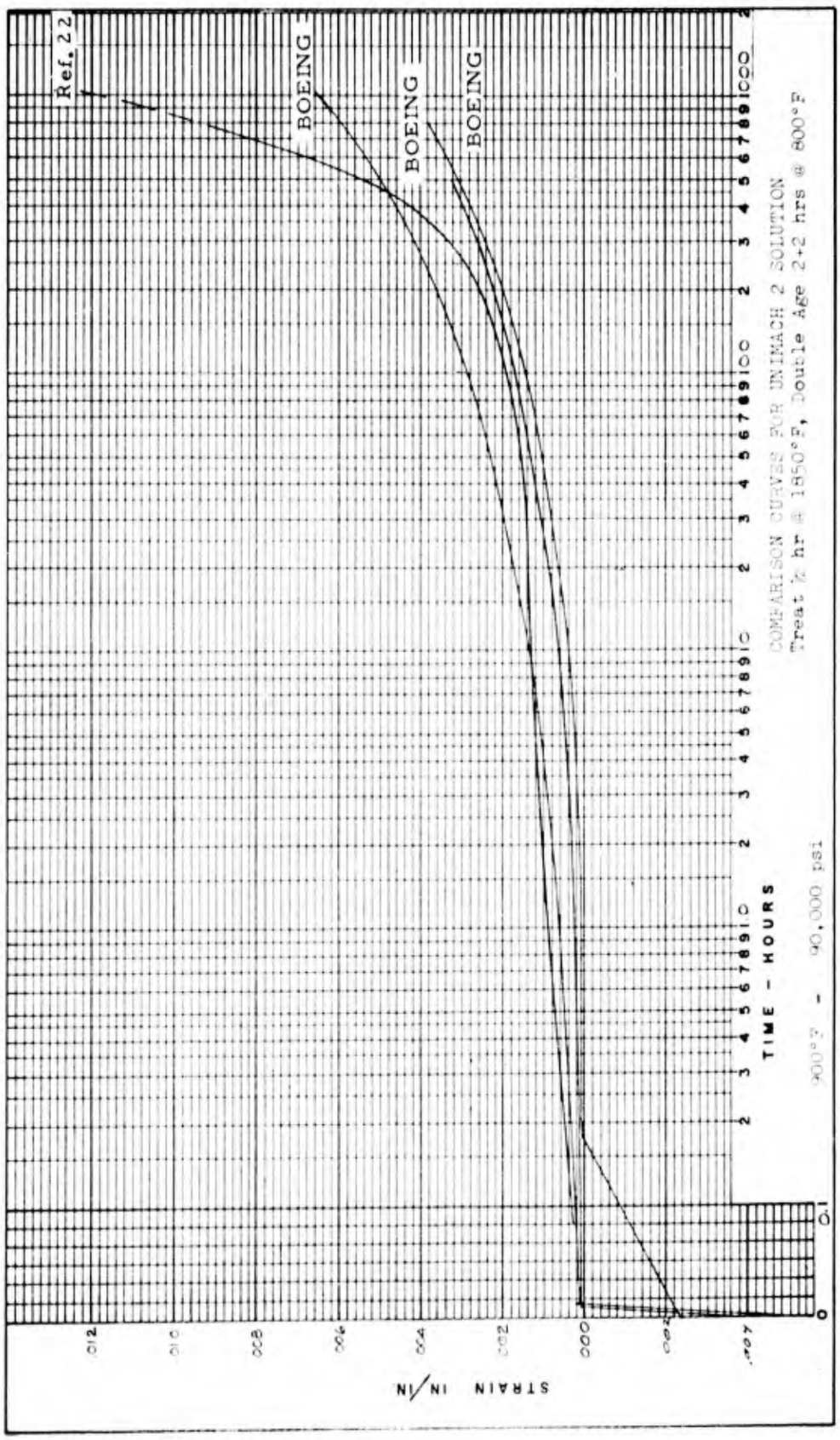

FIGURE 18 - COMPARISON CURVES UNIMACH 2 900°F 90,000 psi

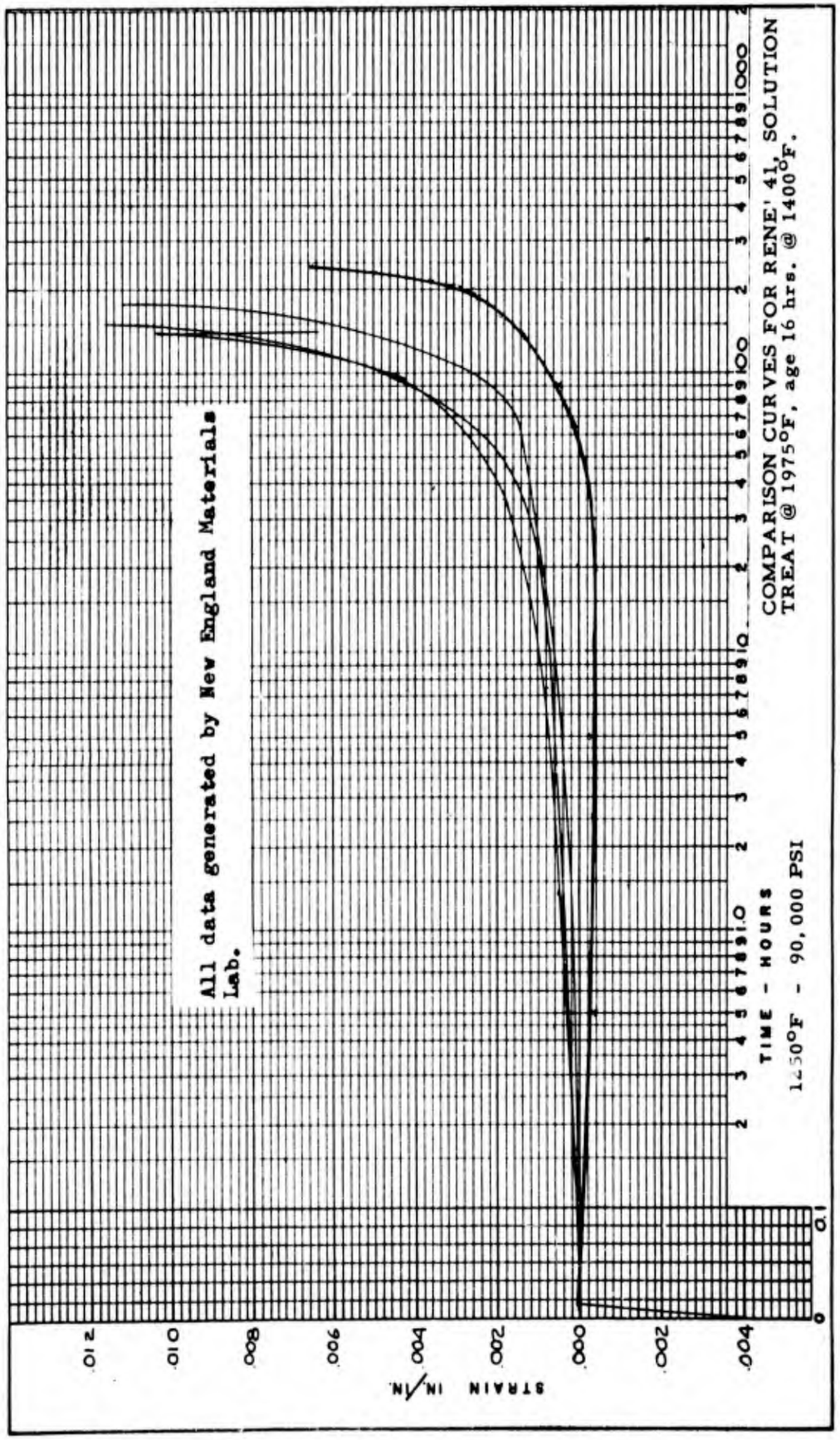

FIGURE 19 - COMPARISON CURVES RENE' 41 1250°F 90,000 psi

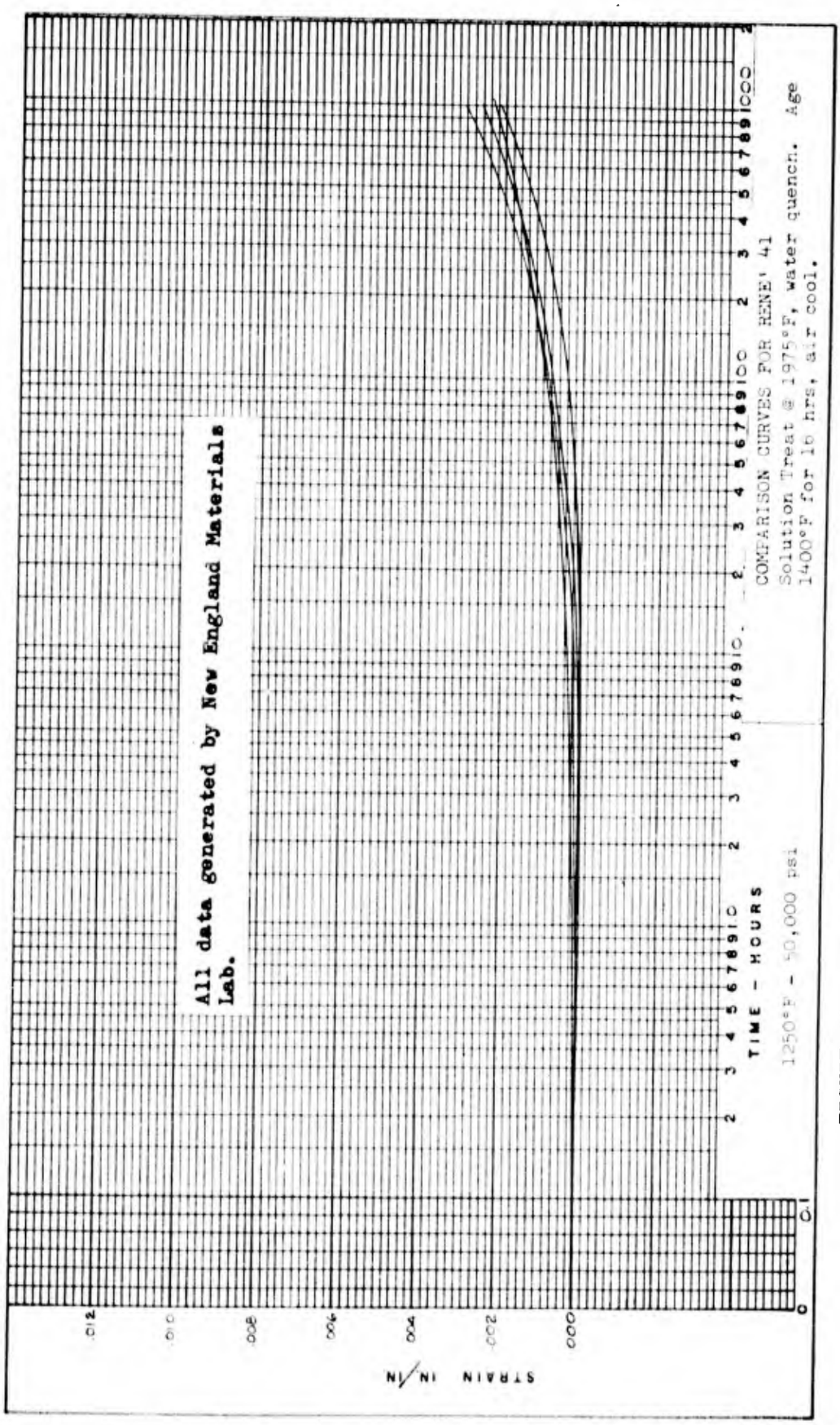

FIGURE 20 - COMPARISON CURVES RENE' 41 1250°F 50,000 psi

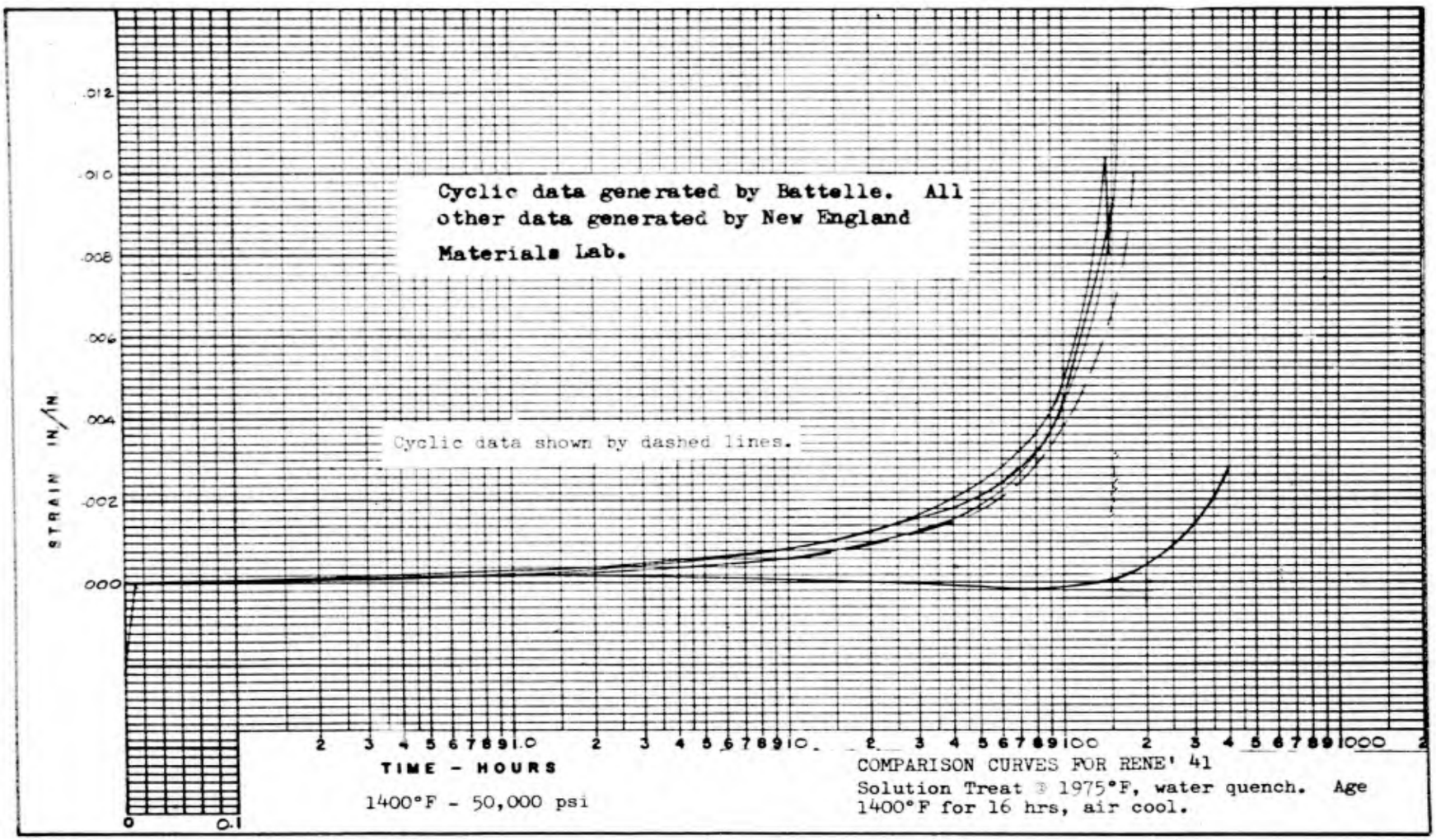

FIGURE 21 - COMPARISON CURVES RENE' 41 1400°F 50,000 psi

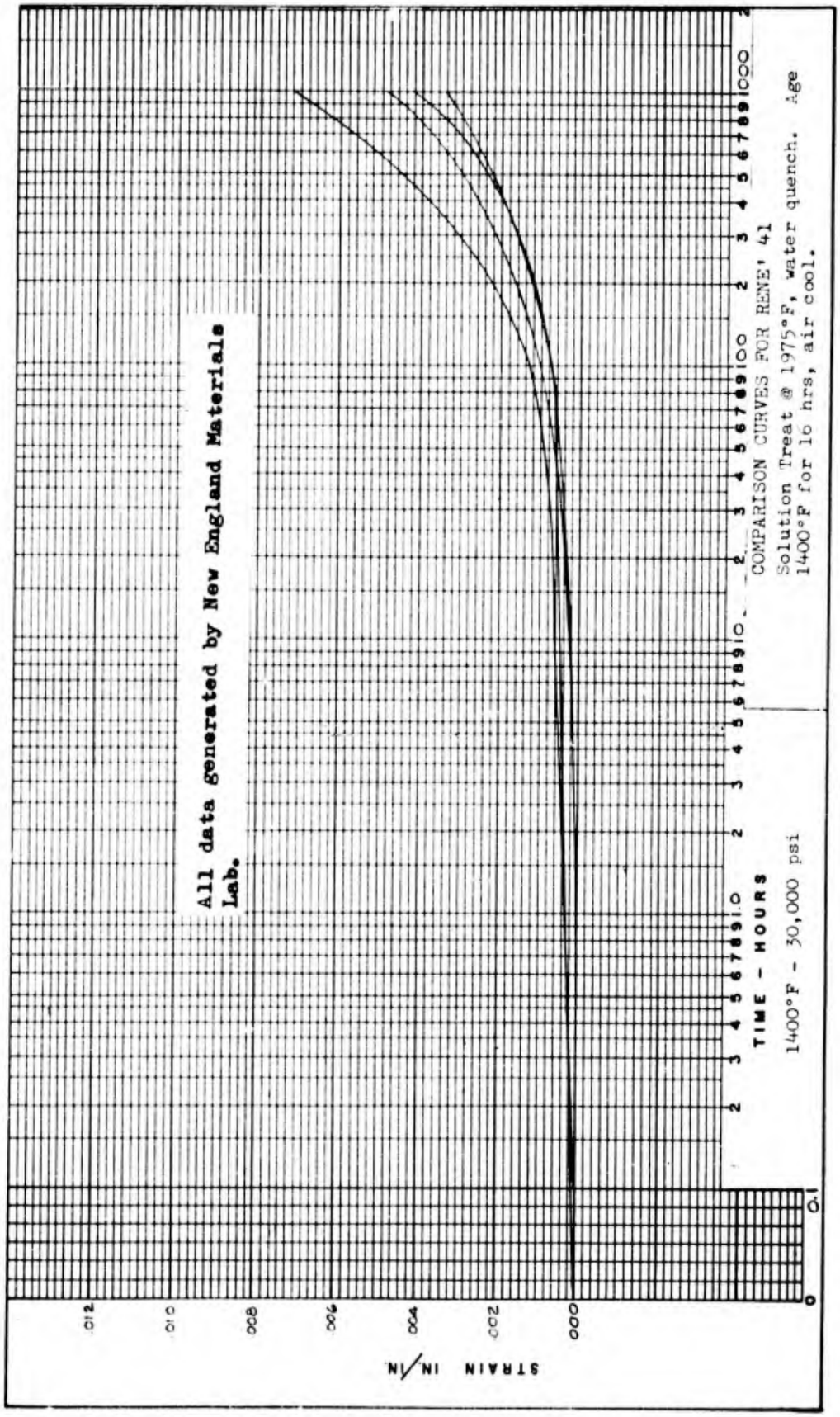

FIGURE 22 - COMPARISON CURVES RENE' 41 1400°F 30,000 psi

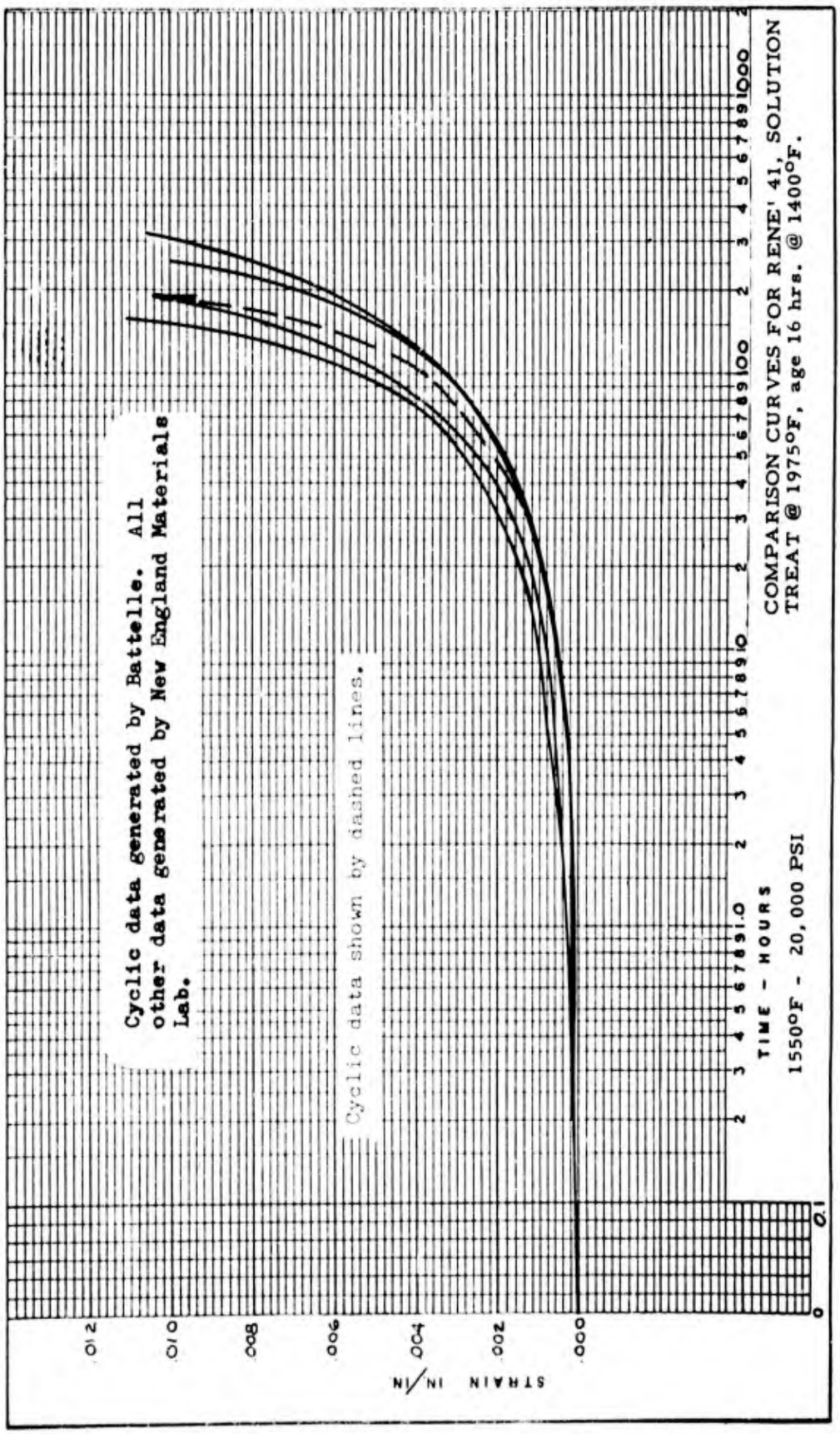

FIGURE 23 - COMPARISON CURVES RENE' 41 1550°F 20,000 psi

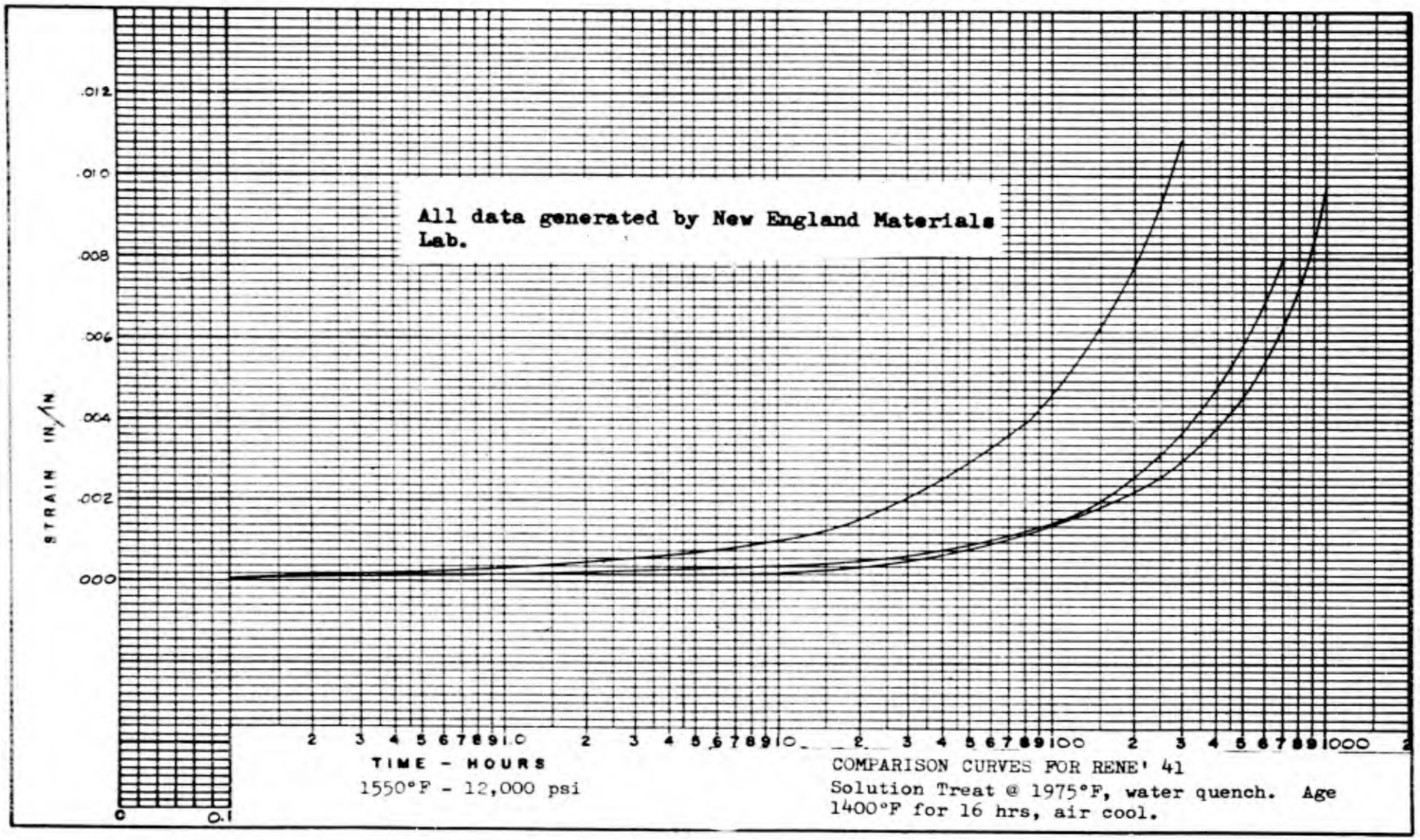

FIGURE 24 - COMPARISON CURVES RENE' 41 1550°F 12,000 psi

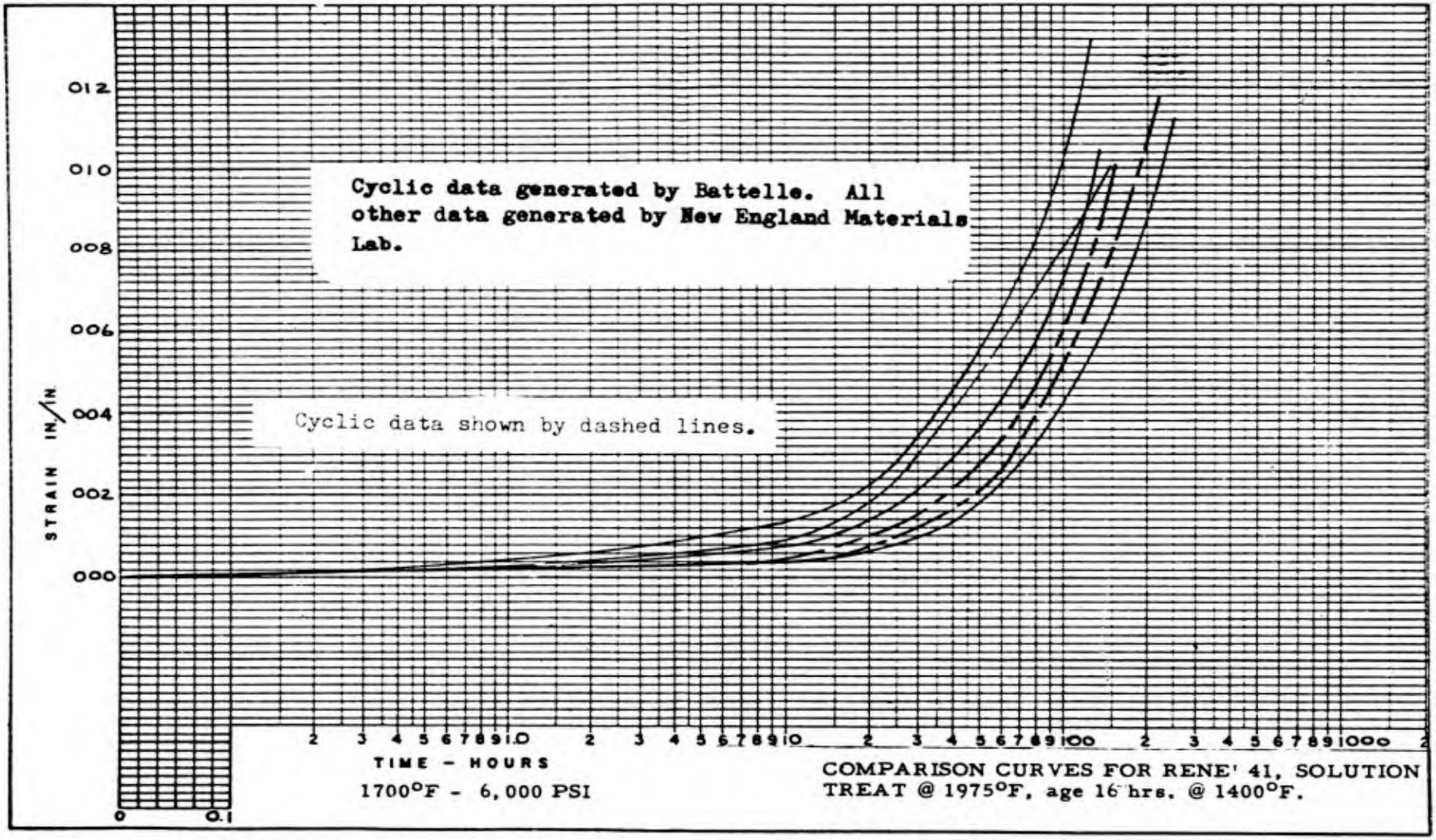

FIGURE 25 - COMPARISON CURVES FOR RENE' 41 1700°F 6,000 psi

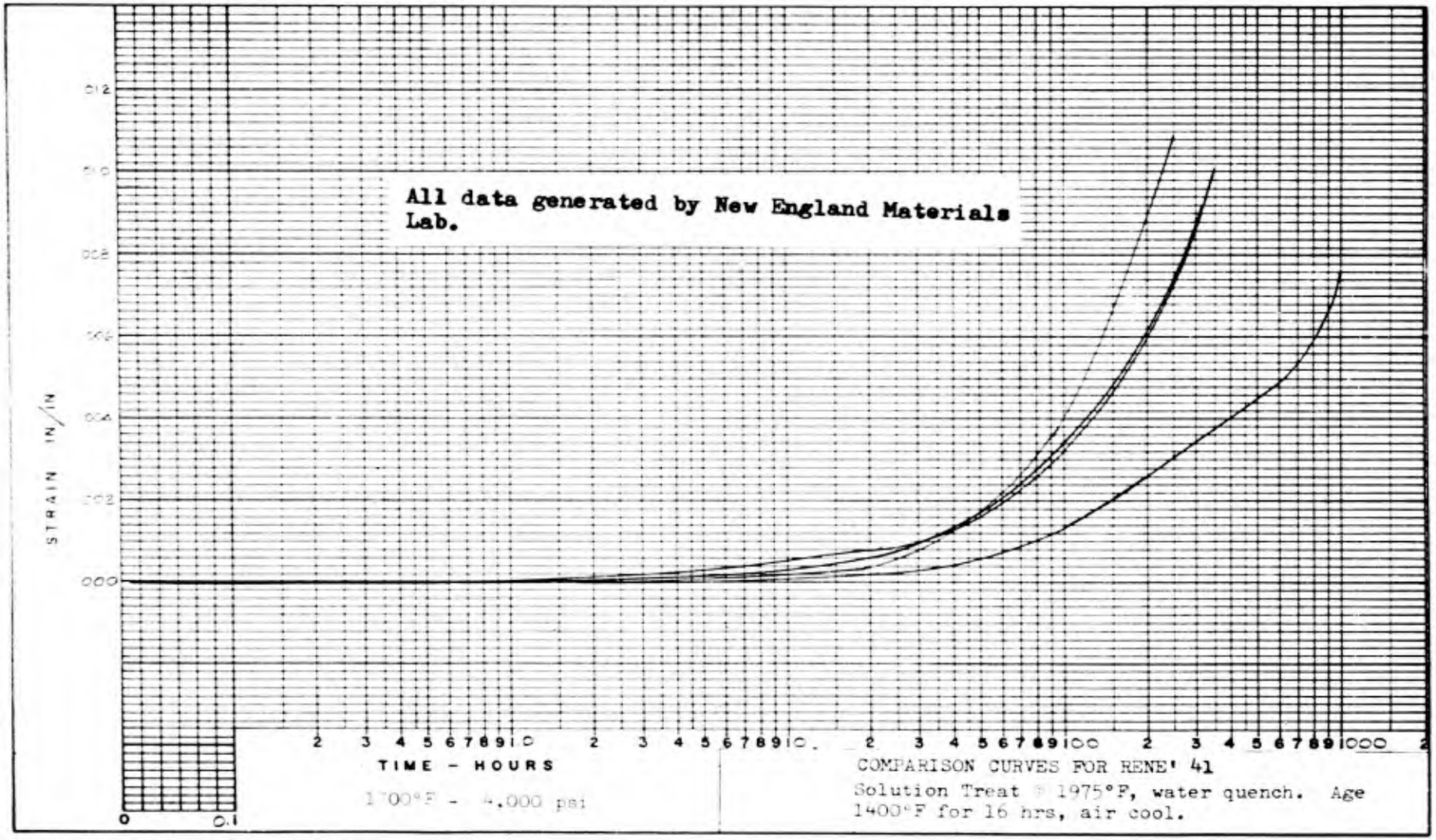

FIGURE 26 - COMPARISON CURVES RENE' 41 1700°F 4000 psi

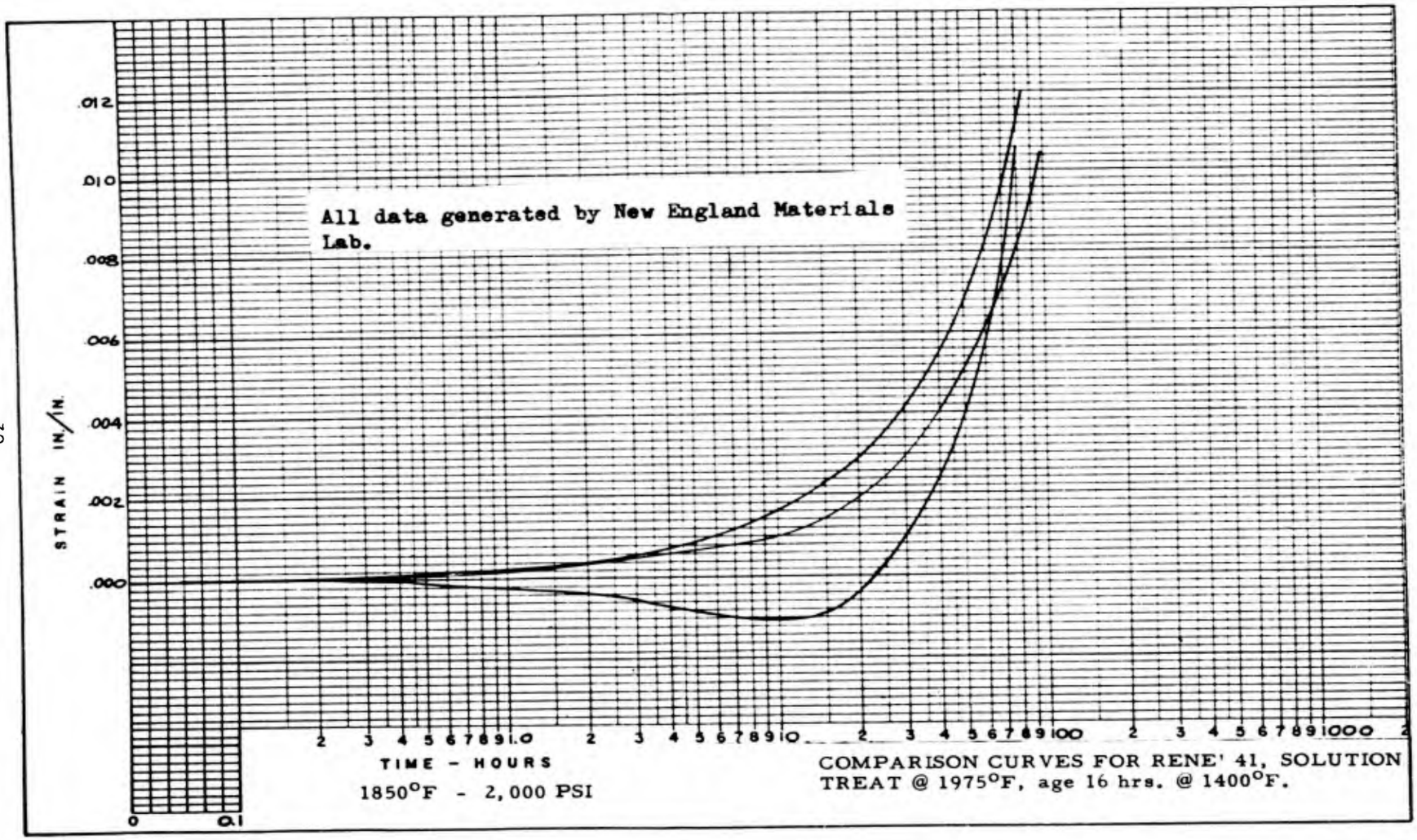

FIGURE 27 - COMPARISON CURVES RENE' 41 1850°F 2000 psi

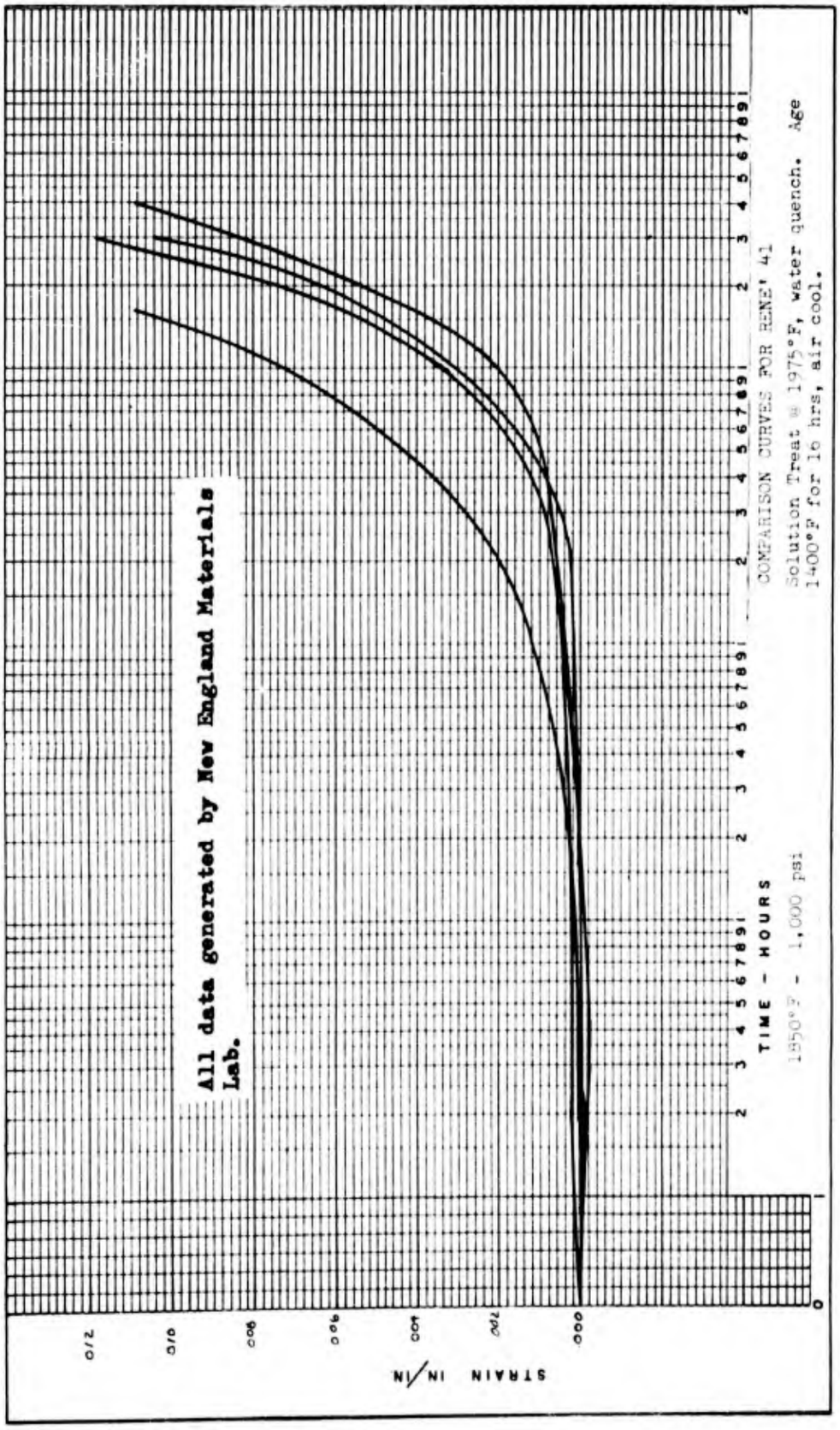

FIGURE 28 - COMPARISON CURVES RENE' 41 1850°F 1000 psi

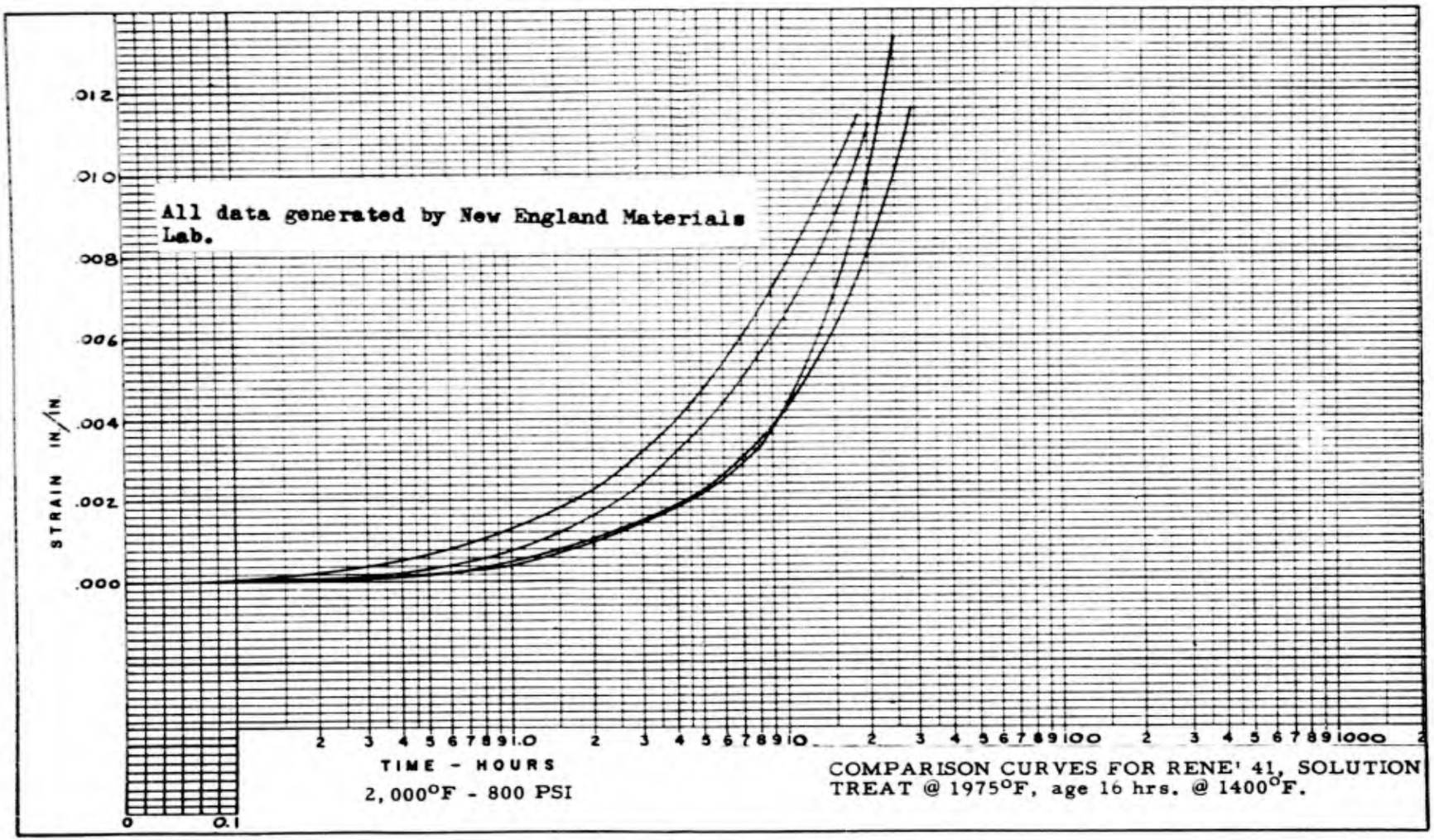

FIGURE 29 - COMPARISON CURVES RENE' 41 2000°F 800 psi

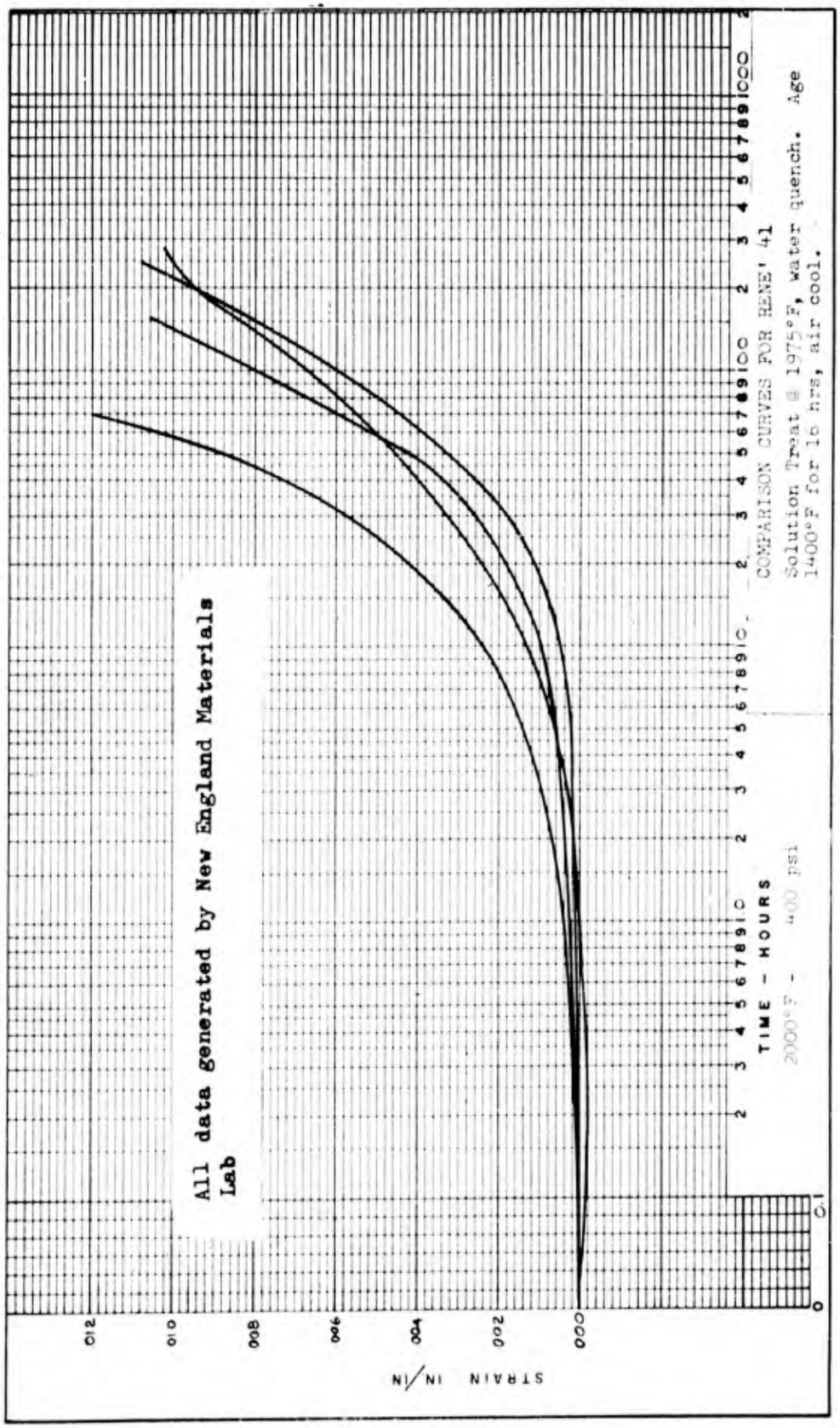

FIGURE 30 - COMPARISON CURVES RENE' 41 2000°F 400 psi

V. DATA ANALYSIS

The activation series equation was used to present the creep data in a comprehensive form.

The constants for the equation were evaluated using the average of the data shown on the comparison curves. Equations formulated for each material are as follows:

Alloy

A-286

$$\epsilon = 7.42 \times 10^{-4} e^{\frac{-8.28 \times 10^3}{T}} \sigma^{2.09 \times 10^2} e^{\frac{-9.25 \times 10^3}{T}} t^{2.7} e^{\frac{-2.49 \times 10^3}{T}}$$

A110AT

$$\epsilon = 346 e^{\frac{-2.241 \times 10^4}{T}} \sigma^{.209} e^{\frac{1.673 \times 10^3}{T}} t^{53} e^{\frac{-6.218 \times 10^3}{T}}$$

Unimach 2

$$\epsilon = 1.97 \times 10^{25} e^{\frac{-7.563 \times 10^4}{T}} \sigma^{6.38 \times 10^{-4}} e^{\frac{8.768 \times 10^3}{T}} t^{39} e^{\frac{-6.633 \times 10^3}{T}}$$

Rene' 41

$$\epsilon = .146 e^{\frac{-1.83 \times 10^4}{T}} \sigma^{.855} e^{\frac{.0279 \times 10^4}{T}} t^{7.89} e^{\frac{-.524 \times 10^4}{T}}$$

$$+ .220 e^{\frac{-1.78 \times 10^4}{T}} \sigma^{.157} e^{\frac{.131 \times 10^4}{T}} t^{27.5} e^{\frac{-.838 \times 10^4}{T}}$$

Derivation of these equations is shown in Appendix IV.

In order to utilize these equations more easily, nomographs were designed. These are presented in Figures 31, 32, 33 and 34. Calculations for the nomographs are shown in Appendix IV.

Use of the nomograph is detailed in Appendix I, pages 83 and 84.

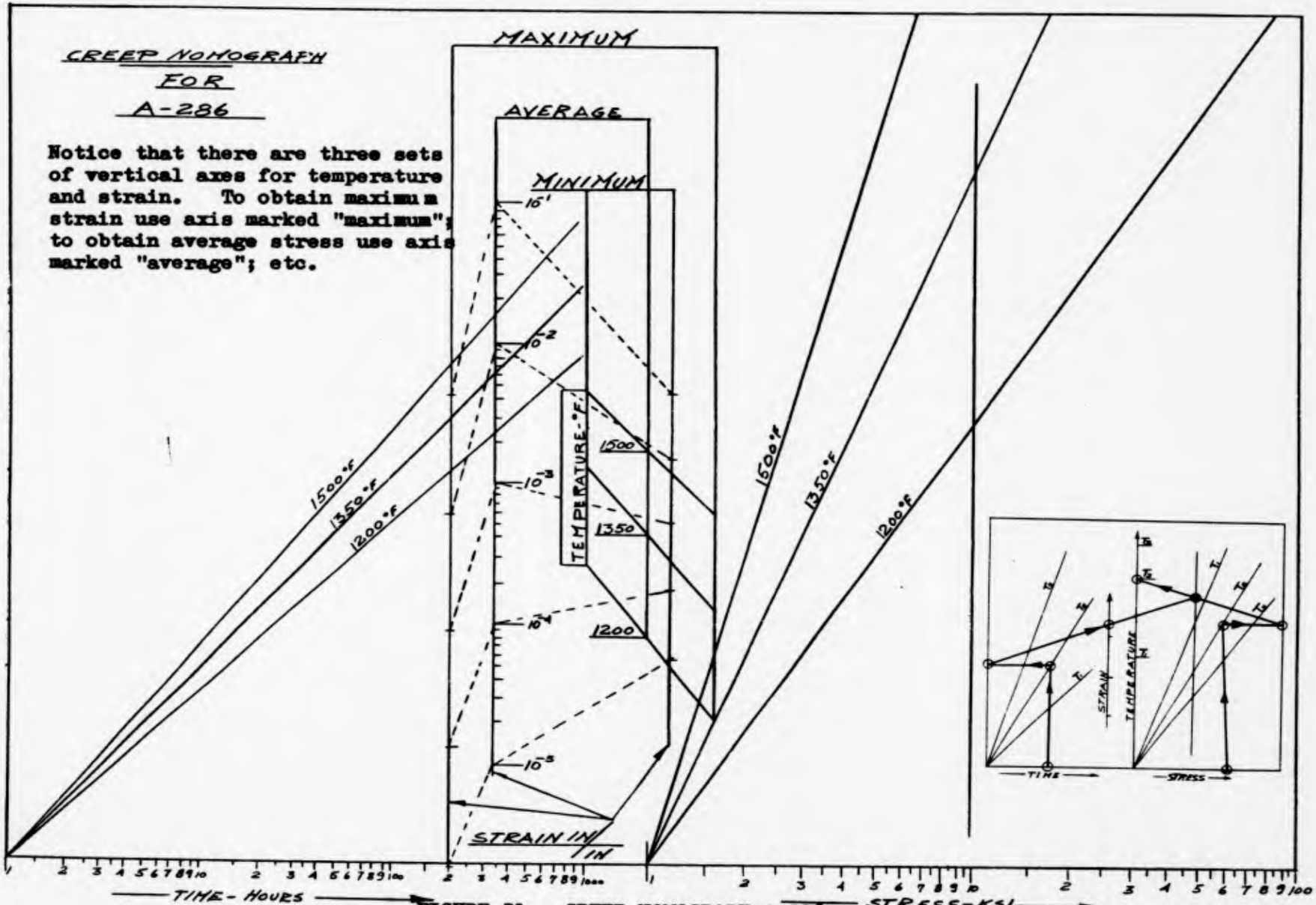

FIGURE 31 - CREEP NOMOGRAPH A-286

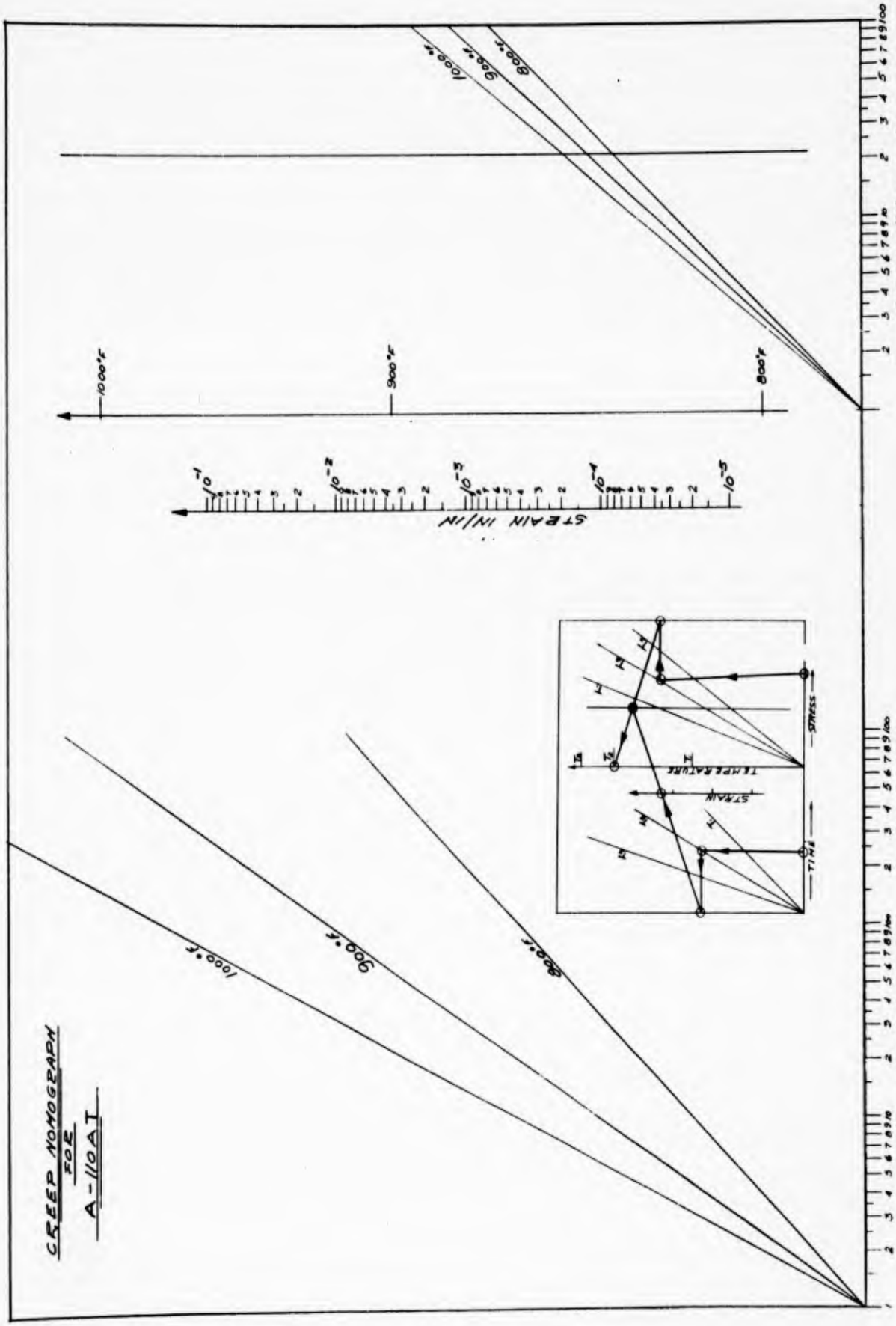

FIGURE 32 - CREEP NOMOGRAPH A110AT

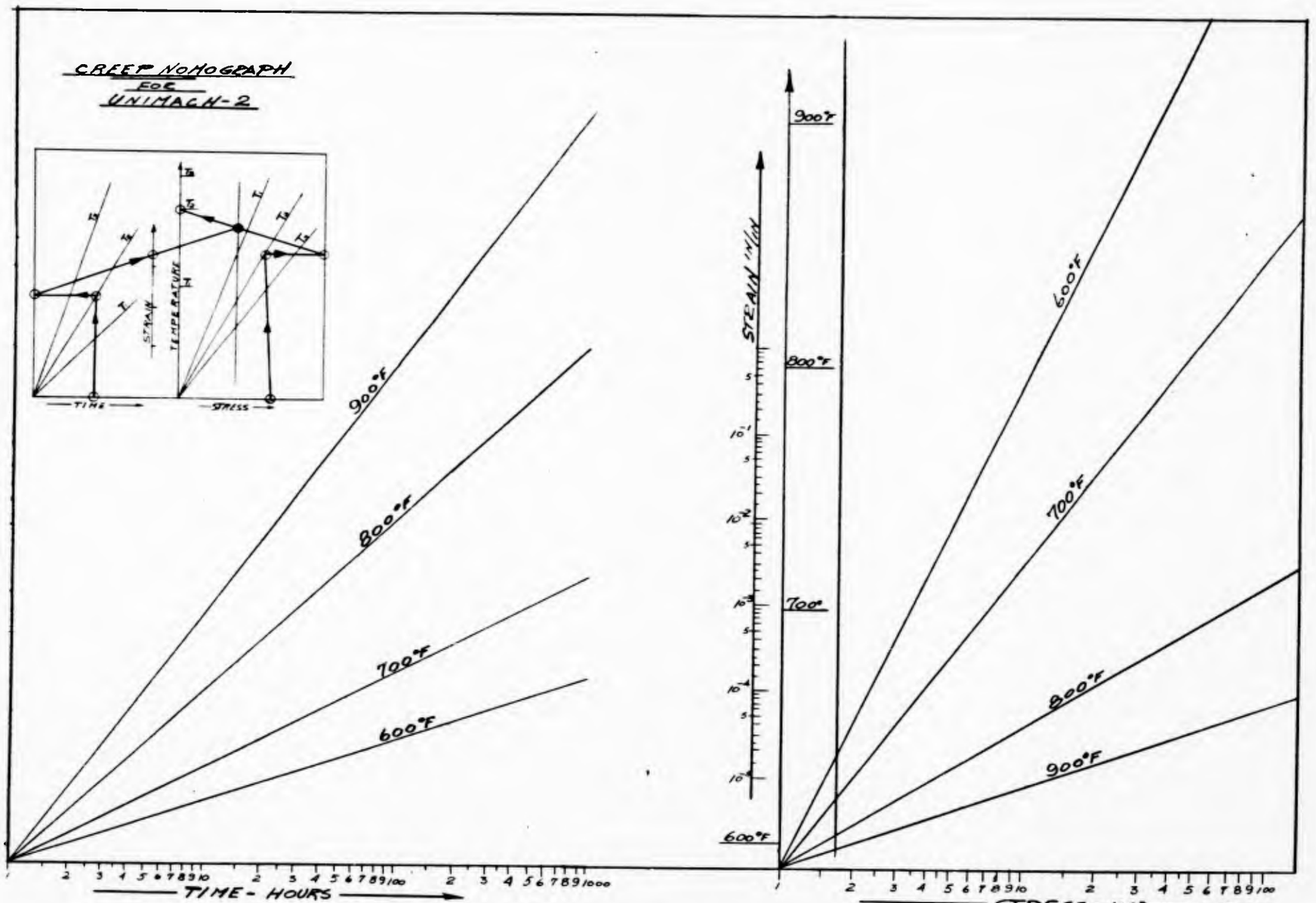

FIGURE 33 - CREEP NOMOGRAPH UNIMACH 2

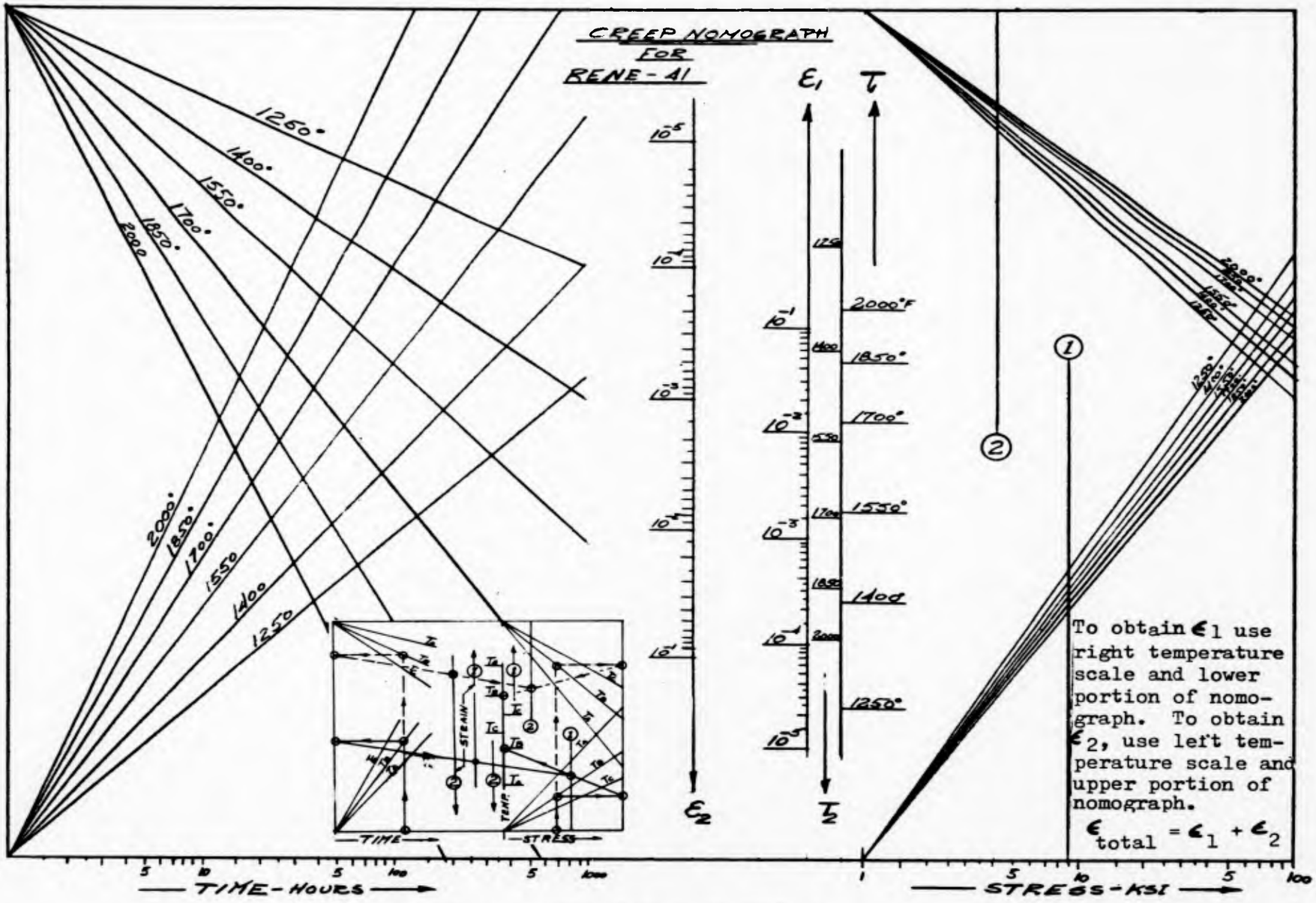

FIGURE 34 CREEP NOMOGRAPH RENE' 41

VI. CONCLUSIONS

Creep data were obtained for A110AT, A-286, and Unimach 2 for comparing with similar data generated on other programs. Scatter in data is greatest for longer times (i.e. 500 to 1000 hours) where the values for strain approach 1%. From the small amount of data available for comparison, it appears that time to reach a given deformation varies by a factor of 4 to 5 in most cases. This appears to be a reasonable correlation.

Creep data were obtained for Rene' 41. Both cyclic stress, cyclic temperature data, and constant stress, constant temperature data were obtained. Results indicate that the creep strain obtained from the specific cycle profile used in this program is cumulative and equal to the creep obtained from the constant stress, constant temperature creep tests.

Test creep curves or tabulated test data are required for transmitting creep data. Basic test data are necessary for formulation of a creep design curve.

It is recommended that, in general, average strain data with respect to time be presented for design purposes. Time and strain are the only creep variables which can be maximized or minimized. For specific applications which may require maximum or minimum creep data, it should be clearly noted which variable is being maximized or minimized.

The nomograph formed from the activation series equation graphically shows general creep behavior over a broad environment. All four creep variables are shown on one graph. The nomographs shown in Figures 32, 33, and 34 were derived from average test data. Figure 31 shows how maximum, average, and minimum data can be presented.

The nomograph provides a means of interpolation. Limits can be imposed and extrapolated areas can be recognized.

VII. RECOMMENDATIONS FOR FURTHER STUDY

The nomographic method of presenting creep data allows interpolation and some degree of extrapolation. Further study is necessary to define the limits of extrapolation. This includes short time testing for long time behavior, and development of an envelope system for program creep study.

The development of a computer program to obtain the equation directly from creep test data would assist in evaluation of creep behavior. A computer program would reduce time and manhours required to obtain the equation from test data.

The few cyclic creep tests completed indicate that further study is necessary to obtain material behavior data under the effect of cyclic conditions. Several effects should be evaluated, e.g. effect of cyclic temperature, effect of cyclic stress, effect of combined cyclic temperature and cyclic stress, and effect of frequency of cycles on creep behavior.

VIII. REFERENCES

1. A. I. Rush and J. W. Freeman, Statistical Evaluation of the Creep Rupture Properties of Four Heat Resistant Alloys in Sheet Form. 1954 ASTM Preprint No. 82.

2. Boeing Airplane Company, Determination of Adaptability of Titanium Alloys. Contract AF 33(600)-33765, AMC TR 58-7-574.

3. Frank J. Gillig and Glen G. Guarnieri, A Study of the Tensile and Creep Rupture Properties of Fifteen Heats of C-110M Titanium Alloy Sheet, WADC TR 55-164.

4. Glen G. Guarnieri, "The Creep-Rupture Properties of Aircraft Sheet Alloys Subjected to Intermittent Load and Temperature". Symposium on Effect of Cyclic Heating and Stressing on Metals at Elevated Temperatures. ASTM Special Publication No. 165.

5. Shepherd, L. A., The Creep Properties of Metals Under Intermittent Stressing and Heating Conditions. WADC TR 53-336.

6. Cornell Aeronautical Laboratory. Intermittent Stressing and Heating of Aircraft Structural Metals. WADC TR 53-24.

7. Larson, F. R. and Miller, J., "A Time-Temperature Relationship for Rupture and Creep Stresses", Trans. ASME 74 (1952) 765-775.

8. Sherby, O. D. and Dorn, J. E., "Creep Correlation in Alpha Solid Solutions of Aluminum", Trans. AIME 194 (1952) 959-964.

9. Hollomon, H. J. and Jaffee, L. D., "Time-Temperature Relation in Tempering Steel", Trans. AIME 162 (1945) 223-249.

10. Manson, S. S. and Haferd, A. M., A Linear Time-Temperature Relation for Extrapolation of Creep and Stress Rupture Data, NACA TN 2890 (1953).

11. Eyring, H., "Viscosity, Plasticity, and Diffusion as Examples of Absolute Reaction Rates", J. Chem. Phy. 4 (1936) 283-293.

12. Kauzmann, W., "Flow Creep of Solid Metals from the Standpoint of the Chemical Rate Theory", Trans. AIME 143 (1941) 57-83.

13. Orr, R. R., Sherby, O. D., and Dorn, J. E., "Correlation of Rupture Data for Metals at Elevated Temperatures", Trans. ASM, Vol. 46 (1954) 113-128.

14. Manson, S. S., "Correlation and Extrapolation of Creep and Stress Rupture Data", MIT Seminar on the Behavior of Metals and Elevated Temperature Design Criteria, 1958.

15. Fountain, R. W. and Korchynsky, M., "The Phenomenon of 'Negative Creep' in Alloys", Trans. ASM 51(1959) 108-119.

16. Metcut Research Associates, Inc., Low Stress Creep Testing of A-286, Report No. 363-1585.

17. Data generated by Joliet Metallurgical Laboratories, Inc., and supplied by WADD.

18. Metcut Research Associates, Inc., Tensile and Creep Properties of A110AT Titanium Alloy.

19. Shimmin, K. D., Applicability of Present Creep Prediction Techniques for Extrapolating Very Long Time Creep Behavior, WADD TR 60-523.

20. Manson, S. S. and Mendelson, A., Optimization of Parametric Constants for Creep-Rupture Data by Means of Least Squares, NASA Memorandum 3-10-59E.

21. Kanter, J. J., "The Problem of Temperature Coefficient of Tensile Creep Rate," Trans. AIME 131 (1938) 385-418.

22. Metcut Research Associates, Inc., Low Stress Creep Testing of Unimach 2 (Thermold J), Report No. 363-1534.

APPENDIX I

CORRELATION OF CREEP DATA BY A POWER FUNCTION ANALOGY

CORRELATION OF CREEP DATA BY A POWER FUNCTION ANALOGY

INTRODUCTION

The practical aim of creep testing is to acquire knowledge containing the time dependence of deformation during continued use of materials at various temperatures and stresses. Through the years many attempts have been made to formulate mathematical expressions for the relations between strain, stress, time, and temperature, both by empirical as well as theoretical treatises. A successful empirical as well as a theoretical treatise of the secondary stage creep alone is not all that is required for intelligent design of creep structures owing to the frequently appreciable magnitude of primary creep.

For creep testing, every measurement has to be carefully taken and the temperatures have to be known with the greatest possible accuracy if the investigator should ever hope to understand the material's behavior. One of the most neglected measurements in creep has been the change in cross-sectional areas. A. V. Gur'er in U.S.S.R. found that for six carbon steels in the elastic range, the material's volume changed due to hardening, but it deformed plastically at constant volume. Stress intensifications can be produced by the formations of localized fissures within the body of the material undergoing test. This is equivalent to a reduction in the stress carrying cross-sectional area of the specimen. It must be pointed out that these internal defects, which are not present in the material initially and would not develop from the application of temperature alone, are developed under the combined effect of time, temperature, and stress and are, therefore, a genuine feature of the creep phenomena. The question, however, still remains: "How are we going to account for this internal defect by external measurements?"

The work done on the second stage creep of metals at elevated temperatures has been concerned with the data correlation in terms of an activation energy defined by the rate theory:

$$\text{RATE} \sim e^{-Q/RT} \tag{31}$$

where Q is the activation energy, R is the gas constant, and T is the absolute temperature. When applied to the process of plastic flow, the rate theory is normally introduced by the assumption that

$$\frac{d\epsilon}{dt} = ke^{-Q/RT} \tag{32}$$

where ϵ is taken as the conventional "engineering" strain and k is an empirical constant. This solution is equivocal since a typical constant load creep curve exhibits regions of different creep behavior. See the figure below.

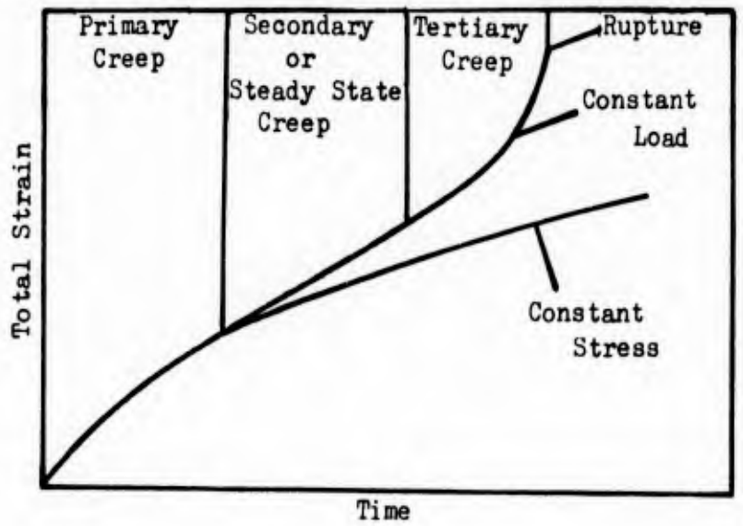

Application of equation 32 invites the use of the secondary creep rate to determine the activation energy. The classical experiment of Andrade, however, demonstrates that a creep curve for constant stress does not exhibit the steady state region of minimum creep rate, but that the rate decreases continuously, and suggests that the distinction between primary and secondary creep is a fictitious one depending upon an arbitrary choice of time scale.

The significance of an activation energy based upon a secondary minimum rate region artificially created by a gradual stress increase is questionable. Application of equation 32 to a constant stress curve, on the other hand, requires either the introduction of another empirical constant or that the activation energy increase markedly with increasing time, an increase that is difficult to explain. The strain-rate approach does not mention the temperature dependence of the activation energy since the quantity

$$\frac{\partial \left[\ln \left(\frac{\partial \epsilon}{\partial t} / k \right) \right]}{\partial \left[\frac{1}{T} \right]} = -Q/R \qquad (33)$$

is roughly constant over the limited temperature range for most creep experiments, and the temperature effects are ordinarily obscured. Several investigators have observed that the slope given by equation 33 is not necessarily constant over an extended temperature range. The thermal dependence of the apparent activation energy observed for self-diffusion in metals is well known and is required in situations involving lattice, grain-boundary, or surface movements of the atoms. Since the creep of a metal under stress also requires atom movements, it would seem that the apparent activation energy for creep should show an analogy of thermal dependence. The empirical approach, however,

does not require specification of a particular mode of atom motion, such as the specialized mode required for movement of dislocations or lattice imperfections which have been envisaged in many fruitful theoretical studies of the problem of plastic deformation. Apparently, creep was first conceived as a self-diffusion process by Kanther who applied it to the steady state concept. Herring has discussed a mechanism of creep by volume diffusion which may become predominant at temperatures nearing the melting point. In this case, strain would be manifested in the migration of grain boundaries and change in grain shape. At lower temperatures atomic motion would be localized at the grain boundaries where movements of relatively rigid grains would produce boundary thickening. Creep at still lower temperatures might require dislocation activity and presumably would involve slip.

It would be fairly obvious from the above discussion that a better knowledge of the phases through which a solid passes before rupture takes place is essential for rational design of structural components for elevated temperature applications.

If the total creep is defined as the time elapsed from application of load until rupture occurs one can in a broad sense speak of it as the sum of the elastic and the plastic creep. However, very little is yet known about the magnitude of these two components, even though the magnitude and the factors affecting the elastic and the plastic components are of greatest importance in any study of the time interval before rupture.

When a load is applied to a specimen, it is believed to pass through the following stages:

1. The elastic portion.

2. The semi-elastic portion, including microcreep.

3. These elastic-viscous portions include micro--as well as macrocreep strain hardening and thermal softening.

4. The plastic portion, mainly macrocreep strain hardening and thermal softening.

It is interesting to note that the volume change of a material decreases as the deformation increases.

It should be understood that creep phenomena are composed of several processes taking place at the same time, but reaching their maximum contributions at different amounts of strain and time. Thermodynamically, this is analagous to reversible and irreversible processes and the deformation process can be defined in terms of change in entropy.

THEORY

For the purpose of derivation of the theory, the deformation of a solid will be divided into two parts--the elastic and the plastic portion. This is done only because it serves to show how the reactions series is obtained. Typical true stress-strain deformation curves are shown below.

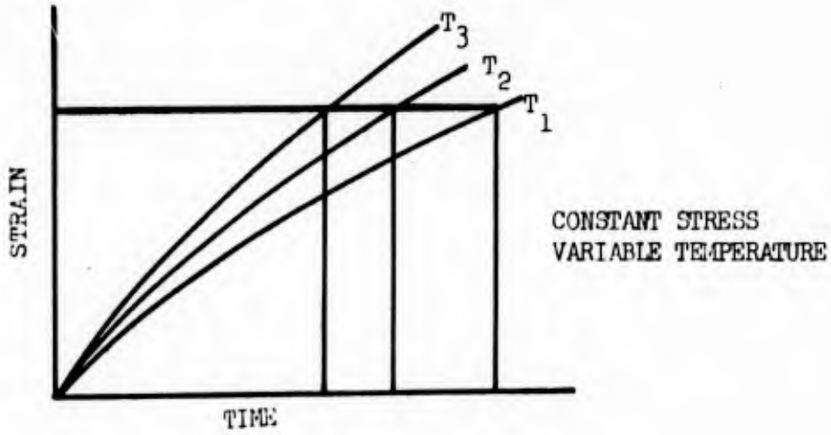

By cross-plotting constant strain data from the above curves, a plot of log time versus the reciprocal of the absolute temperature is obtained and shown below:

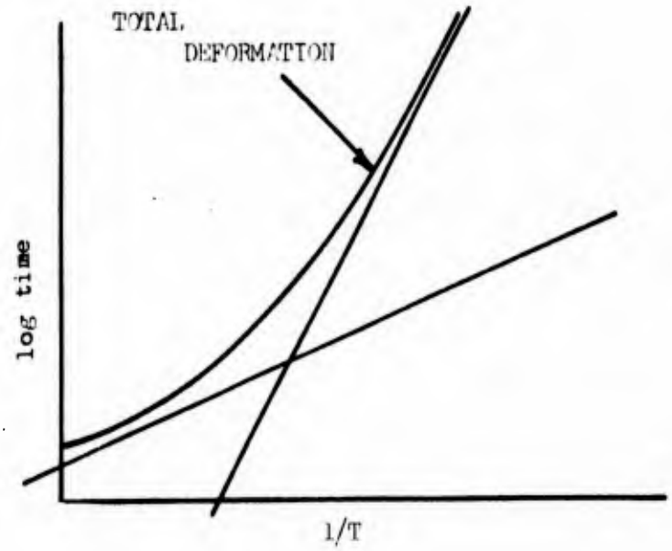

The total deformation curve represents the time interval required in order to reach a given deformation.

By using semilogarithmic paper, it can easily be shown that for most curves with parabolic shape, two straight lines can be drawn with such a position and such a slope that the **sum of their ordinates will at all points be equal to the original parabolic curve.**

The Arrhenius reaction rate theory predicts that for a given reaction, the logarithm of the rate plots as a straight line function of the reciprocal of the absolute temperature. If the parabolic shaped curve is the total deformation, and one of the straight lines represents the elasto-plastic deformation, and the other one the plastic deformation, then the reaction rate representing the plastic deformation is

$$\gamma_p = \frac{dC_p}{dt_p} = -K_p C_p \tag{34}$$

where γ_p is the plastic reaction rate in time units, C_p is concentration of moles per unit volume of material, K_p is reaction velocity constant in concentration units, t_p is units of time.

By re-arranging and integrating the above equation, keeping in mind that the limits of time are from zero to the end of the plastic deformation and the limits of C are from zero to the concentration at rupture, one obtains:

$$\int_0^t t_{dt_p} = -\int_{C_{p_o}}^{C_p} \frac{dC_p}{K_p C_p} \tag{35}$$

Then,

$$t_p = -\frac{1}{K_p} \ln \frac{C_p}{C_{p_o}} \tag{36}$$

Following the same reasoning procedure for the elasto-plastic reaction rate, an expression for the straight line is found:

$$\gamma_E = \frac{dC_E}{dt_E} = -K_E C_E \tag{37}$$

$$\int_0^{t_E} dt_E = \int_{C_{E_o}}^{C_E} -\frac{dC_E}{K_E C_E} \tag{38}$$

$$t_E = -\frac{1}{K_E} \ln \frac{C_E}{C_{E_o}} \tag{39}$$

If these two reactions represent the total reaction, the sum of t_p and t_E must equal the total reaction time. Then, assuming a reaction series,

$$t = t_E + t_p = -\frac{1}{K_E} \ln \frac{C_E}{C_{E_o}} - \frac{1}{K_E} \ln \frac{c_P}{c_{P_o}} \tag{40}$$

$$t = t_E + t_p = \frac{1}{K_E} \ln \frac{C_{E_o}}{C_E} + \frac{1}{K_P} \ln \frac{c_{p_o}}{c_p} \tag{41}$$

Setting $\ln \frac{C_{E_o}}{C_E}$ constant and equal to k_E and $\ln \frac{C_{p_o}}{C_p}$ constant and equal to k_p and

$K = Ae^{-H/RT}$ then $K_E = A_E e^{-H_E/RT}$ and $K_p = A_p e^{-H_p/RT}$

Then:
$$t = \frac{k_E}{A_E e^{-H_E/RT}} + \frac{k_p}{A_p e^{-H_p/RT}} \tag{42}$$

$$t = \frac{k_E}{A_E} e^{H_E/RT} + \frac{k_p}{A_p} e^{H_p/RT} \tag{43}$$

A = proportionality factor characteristic of the system and termed frequency factor.
H = the molal energy of activation.
A_p = the plastic frequency factor.

H_P = The molal energy of activation of the plastic deformation.

H_E = The molal energy of activation of the elasto-plastic deformation.

A_E = **Elasto plastic frequency factor**

R = **The gas constant**

Because of this, the desired equation for the total deformation is established by taking:

$C_1 = k_E/A_E$

$C_2 = H_E/R$

$C_3 = k_P/A_P$

$C_4 = H_P/R$

Then:

$$t = C_1 e^{C_{2/T}} + C_3 e^{C_{4/T}} \qquad (44)$$

C_1 and C_3 are constants containing stress and strain divided by the frequency factor. $C_{2/R}$ and $C_{4/R}$ represent the activation energy of the elasto-plastic and the plastic processes.

It can now be assumed that for a complex material, a reaction series of this nature will represent the total time:

$$t = C_1 e^{C_{2/T}} + C_3 e^{C_{4/T}} + C_5 e^{C_{6/T}} + \ldots (45)$$

Since Equation 45 expresses the total time to reach a given deformation for a given stress, one would like to develop this equation further to express strain as a function of stress, time, and temperature.

$$\epsilon = f(\sigma, t, T)$$

This can be done as follows:

Let

$$C_2, C_4, C_6, \text{etc.} = f(T)$$

$$C_1, C_3, C_5, \text{etc.} = f(\sigma, \epsilon, T)$$

For simplicity, only the first term in the reaction series will be used. Since C_2 is thermal dependent:

$$C_2 = Ke^{-n/T}$$

and

$$C_1 = f(\sigma, \epsilon, T)$$

For constant stress,

$$C_{1(\text{const } \sigma)} = M\epsilon^{-S'e^{-n/T}} \tag{46}$$

and for constant strain,

$$C_{1(\text{const } \epsilon)} = N\sigma^{-\psi e^{E/T}} \tag{47}$$

Therefore,

$$C_1 = \left[C_{1(\text{const } \sigma)}\right]\left[C_{1(\text{const } \epsilon)}\right] = Me^{S'e^{-n/T}} N\sigma^{-\Theta e^{E/T}} \tag{48}$$

However, both M and N are thermal dependent and can therefore be expressed as follows:

$$M\,N = R^{S''e^{-n/T}} \tag{49}$$

Hence:

$$C_1 = R^{S''e^{-n/T}} \epsilon^{S'e^{-n/T}} \sigma^{-\psi e^{E/T}} \tag{50}$$

Substituting the expressions obtained for C_1 and C_2 into equation (45), the following equation results:

$$t = R^{S''e^{-n/T}} \sigma^{-\psi e^{E/T}} \epsilon^{S'e^{-n/T}} e^{\frac{K}{T}e^{-n/T}} \tag{51}$$

Transposing,

$$\epsilon^{S'e^{-n/T}} = R^{-S''e^{-n/T}} e^{-\frac{K}{T}e^{-n/T}} \sigma^{\psi e^{E/T}} t \tag{52}$$

By removing the power on ϵ, the equation takes the form:

$$\epsilon = R^{-(S''/S')} e^{-\frac{K}{T}\frac{1}{S'}} \sigma^{\frac{\psi}{S'}e^{(E+n)/T}} t^{\frac{1}{S'}e^{n/T}} \tag{53}$$

Let:

$$R^{-(S''/S')} = P$$

$$\frac{K}{S'} = \mu$$

$$\frac{\psi}{S'} = D$$

$$E + n = F$$

$$\frac{1}{S'} = S$$

The equation takes the form:

$$\epsilon = Pe^{-\mu/T}\,\sigma^{D e^{F/T}}\,t^{S e^{n/T}} \tag{54}$$

It can be assumed with good reason that equation (54) is the first term in the following power series:

$$\epsilon = P_1 e^{-\mu_1/T}\,\sigma^{D_1 e^{F_1/T}}\,t^{S_1 e^{n_1/T}} + P_2 e^{-\mu_2/T}\,\sigma^{D_2 e^{F_2/T}}\,t^{S_2 e^{n_2/T}} + \ldots\ldots + P_n e^{-\mu_n/T}\,\sigma^{D_n e^{F_n/T}}\,t^{S_n e^{n_n/T}} \tag{55}$$

Rewriting equation (55) for constant temperature, one can obtain Hook's Law as well as the Newtonian Law for viscous behavior:

$$\epsilon = C'_1\,\sigma^{\beta_1}\,t^{\alpha_1} + C'_2\,\sigma^{\beta_2}\,t^{\alpha_2} + \ldots\ldots + C'_n\,\sigma^{\beta_n}\,t^{\alpha_n} \tag{56}$$

Let $\alpha = 0$ and $\beta = 1$, then:

$$\epsilon = C'_1\,\sigma + C'_2\,\sigma + \ldots\ldots + C'_n\,\sigma = \sigma \sum_{o}^{n} C'$$

Setting $\sum_{o}^{n} C' = E$, Hook's Law results:

$$\epsilon = E\,\sigma$$

Differentiating equation (56) with respect to time:

$$\frac{d\epsilon}{dt} = \dot{\epsilon} = C'_1\,\sigma^{\beta_1}\,t_1^{\alpha_1 - 1} + C''_2\,\sigma^{\beta_2}\,t^{\alpha_2 - 1} + \ldots\ldots + C''_n\,\sigma^{\beta_n}\,t^{\alpha_n - 1}$$

By setting $\alpha = \beta = 1$, the equation will express the Newtonian Law of viscous behavior:

$$\dot{\epsilon} = C'_1\,\sigma + C''_2\,\sigma + \ldots\ldots + C''_n\,\sigma = \sigma \sum_{\theta}^{n} C''$$

Setting $\sum_{o}^{n} C'' = \frac{1}{\zeta}$

Since ζ is the coefficient of viscosity or the measure of the metals frictional resistance at the applied stress, then

$$\dot{\epsilon} = \frac{1}{\zeta}\sigma$$

Figures 35 and 36 on the following pages display graphically the equations (45) and (55), as applied to metallic creep.

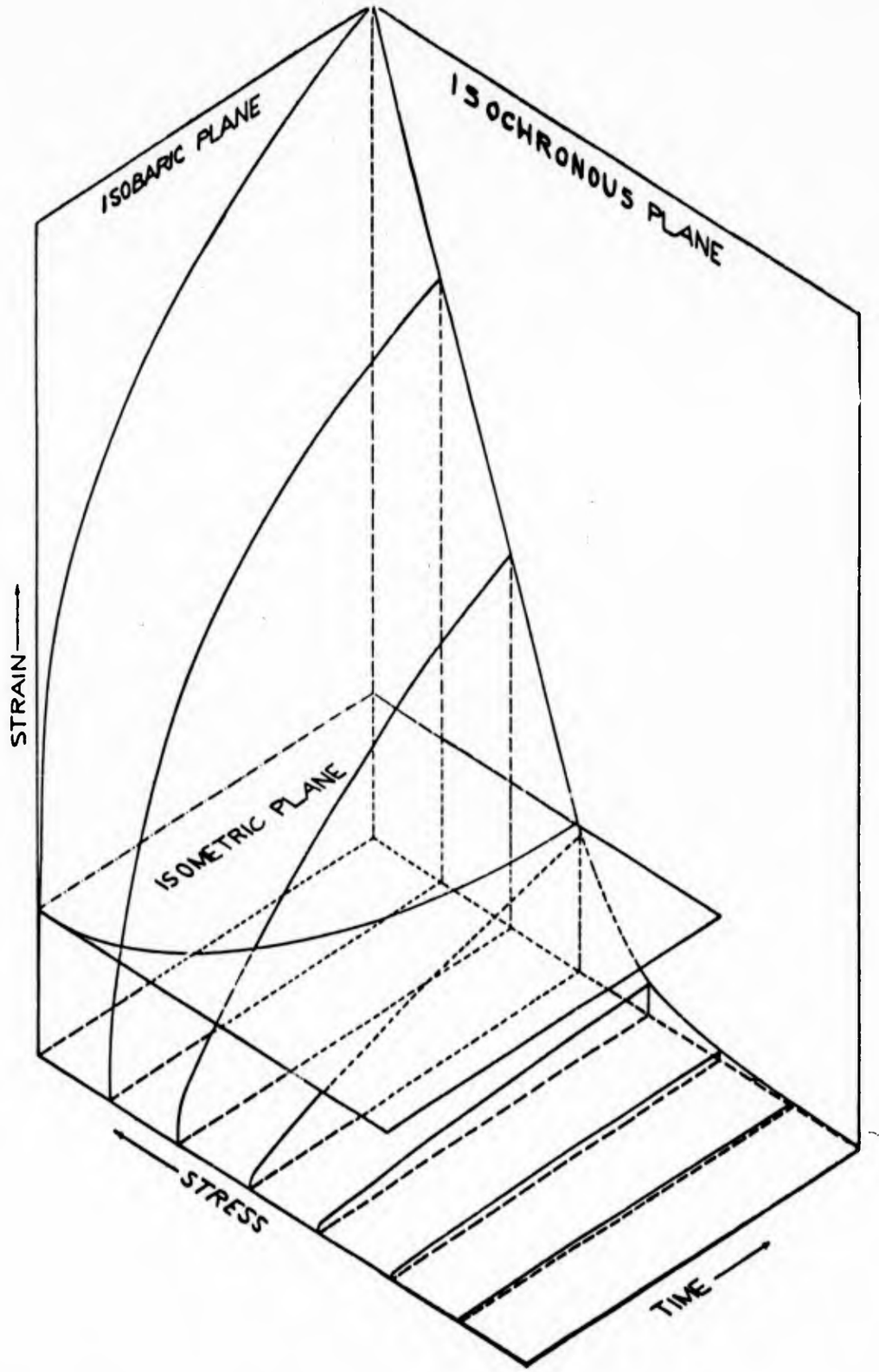

FIGURE 35 - ISOTHERMAL STRESS-STRAIN-TIME SURFACE

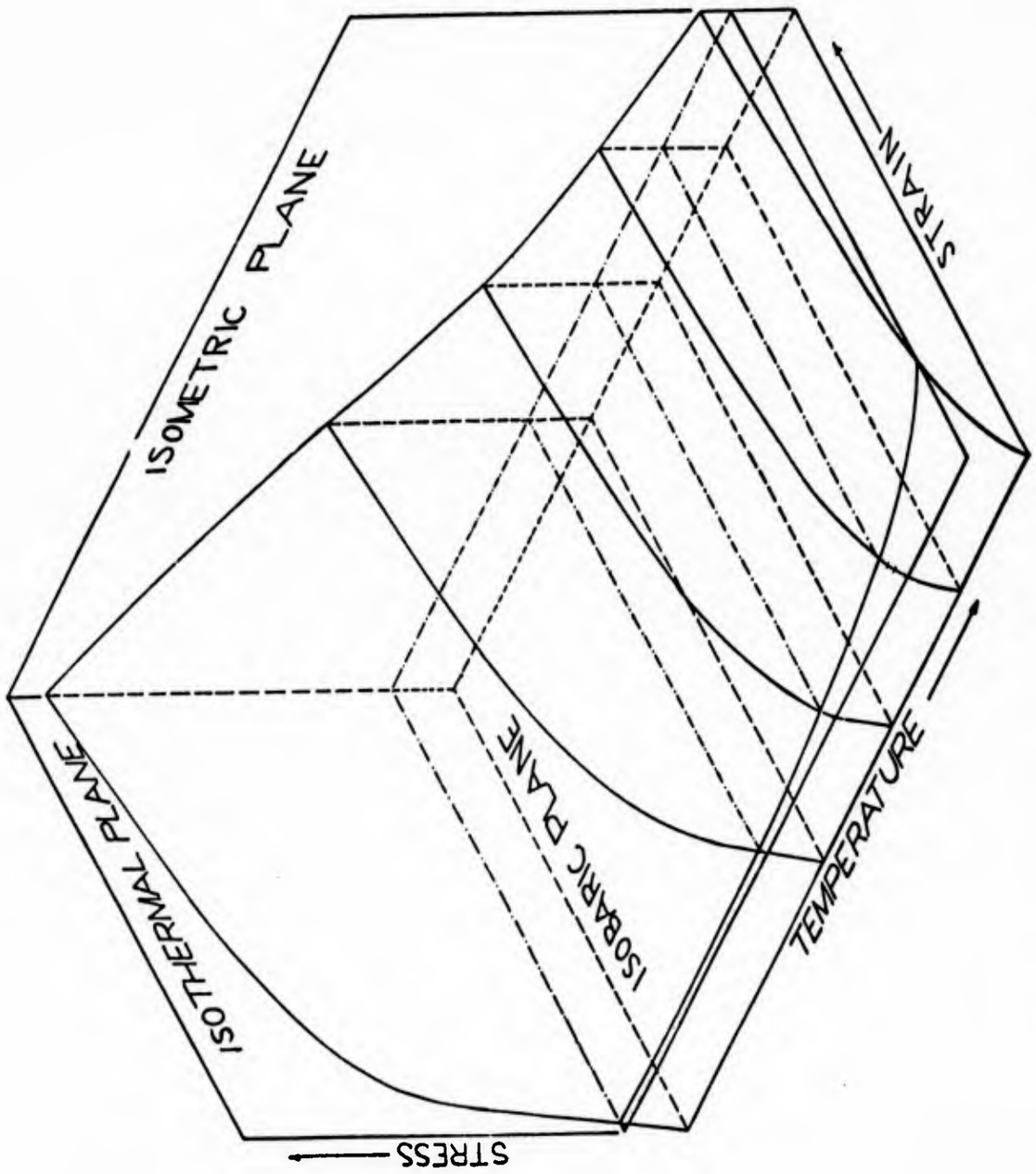

FIGURE 36 - ISOCHRONOUS STRESS-STRAIN-TEMPERATURE SURFACE

APPLICATION OF THE DERIVED EQUATION TO TEST DATA

For simplicity, only the first two items of the derived equation will be used. If higher accuracy is required, more terms can be employed.

By using two terms, we will assume that for a common creep test, only two processes are active, i.e. the elasto-plastic adiabatic semi-reversible process and the plastic irreversible process.

$$\Delta S = \Delta S_{\text{ELASTO-PLASTIC}} + \Delta S_{\text{PLASTIC}} \tag{57}$$

That is to say that the deformation process is represented by the entropy change of the two processes.

The strain equation can be applied to isochronous curves in the form:

$$\epsilon = \epsilon_E + \epsilon_P = C'_1 \sigma^{\beta_1} t^{\alpha_1} + C'_2 \sigma^{\beta_2} t^{\alpha_2} \tag{58}$$

It should be noted that the reversible process does not depend on the path and since our first approach is continuous tension creep, α_1 will be zero, then

$$\epsilon = Pe^{-\mu/T} \sigma^{De^{F/T}} + Le^{-m/T} \sigma^{Ae^{H/T}} t^{Se^{n/T}} \tag{59}$$

However, α_1 will not be zero if creep is cumulated over a period of time. That is to say the elasto-plastic portion will become time dependent.

As pointed out in the previous discussion, if the creep tests were performed at constant stress, true stress-strain curves would be obtained. If the tests were conducted as constant load tests, then the data must be transformed into true stress-strain curves.

For the elasto-plastic portion where the volume is changing, the A. V. Gur'er's method can be used if the hardening coefficient D' is fully defined:

$$\mu_o = 5 - .25 D'/E$$

where μ_o is the transverse coefficient and E is the modulus of elasticity in the longitudinal direction.

However, until further tests have been performed, this equation is only of quantitative value, and any correction of the elasto-plastic portion must be omitted.

Experiments performed in the plastic portion of creep have found that creep proceeds at essentially constant volume, i.e. the volume change is within less than 1%. This will then justify application of P. Ludwik's theory in obtaining true stress strain curves in the plastic range.

If the volumes are assumed constant, the equation of continuity would apply.

$$v_o = v$$

$$a_o \lambda_o = a\lambda$$

For the unstrained state we have

v_o = Volume

ρ_o = Density

a_o = Area

λ_o = Length

and for the material in the strained state we have

v = Instantaneous volume

ρ = Instantaneous density

a = Instantaneous area

λ = Instantaneous length

Now if $v_o = v$ then $\rho_o = \rho$ and $a_o\lambda_o = a\lambda$ or $a_o/a = \lambda/\lambda_o$ and the true reduction in area from tension should be defined as follows:

$$q' = \int_{a_o}^{a} \frac{da}{a} = -\ln {}^{a}/_{a_o} = \ln {}^{a_o}/_{a}$$

Similarly the true change in the length should be defined as:

$$\delta = \int_{\lambda_o}^{\lambda} \frac{d\lambda}{\lambda} = \ln \frac{\lambda}{\lambda_o}$$

now, since $a_o/a = \lambda/\lambda_o$ then:

$$q' = \ln a_o/a = \delta = \ln \lambda/\lambda_o$$

That is to say the true strain equals the reduction in area. However,

$$\delta = \ln \lambda/\lambda_o \quad \text{can be written}$$

$$\delta = \ln \lambda/\lambda_o = \ln \left(\frac{\lambda_o + \Delta\lambda_o}{\lambda_o}\right) = \ln \left(1 + \frac{\Delta\lambda_o}{\lambda_o}\right)$$

Then obviously, $a_o/a = 1 + \epsilon$ or $\frac{a_o}{1+\epsilon} = a$

and it then follows that the true stress in terms of the true strain is

$$\text{TRUE} = p/a_o \quad (1 + \epsilon)$$

In order to show the versitility of the derived equation, the equation will first be applied to a set of isochronous curves, then to a set of basic creep curves.

APPLICATION OF THE DERIVED EQUATION TO ISOCHRONOUS CURVES

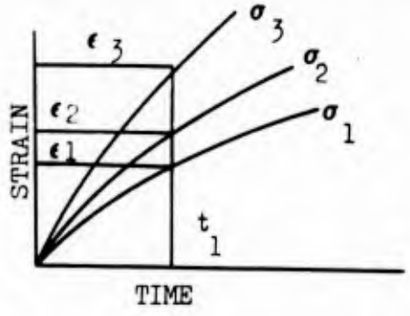

From the basic creep curves, an isochronous curve can be obtained by plotting stress versus strain for a constant time, t_1.

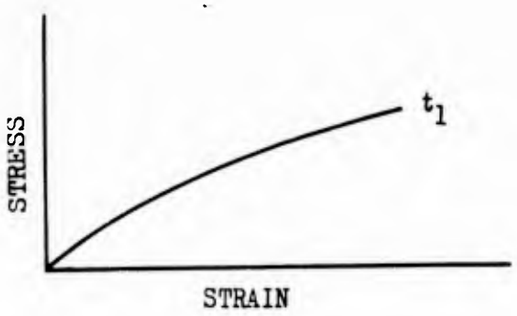

By taking different times, a family of isochronous curves can be constructed. This procedure can be repeated for different temperatures in order to find the temperature effect.

Having plotted the isochronous curves, we are ready to apply the equation

$$\epsilon_{TOTAL} = \epsilon_E + \epsilon_p = C\sigma^{\beta_1} + B\sigma^{\beta_2} \qquad (60)$$

The equation as it is written represents the sum of two lines of log-log paper of slopes β_1 and β_2, respectively.

Since

$$\epsilon_E = C\sigma^{\beta_1} \qquad (61)$$

$$\log \epsilon_E - \log C = \beta \log \sigma$$

and

$$\epsilon_p = B\sigma^{\beta_2} \qquad (62)$$

$$\log \epsilon_p - \log B = \beta_2 \log \sigma$$

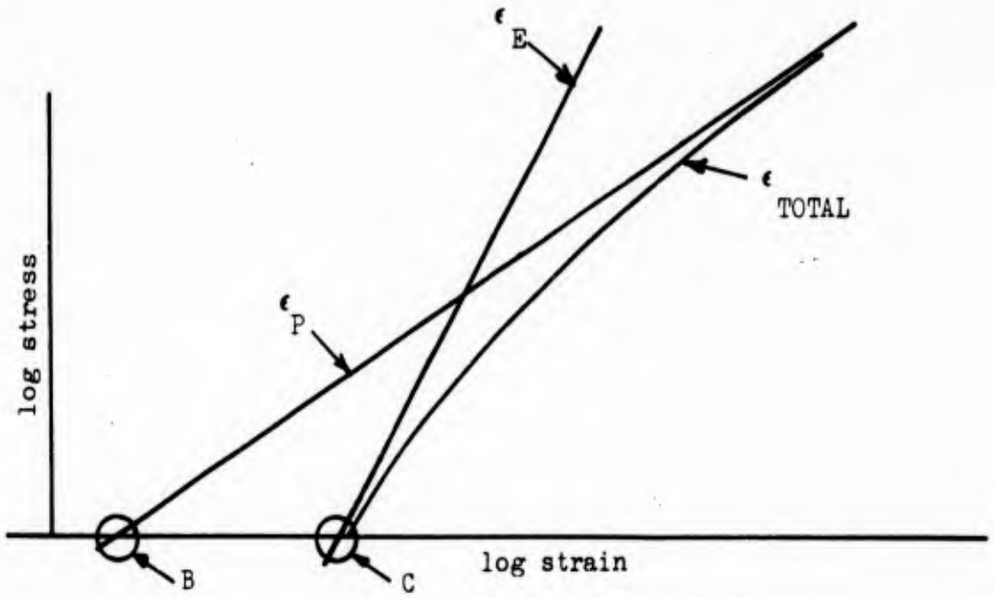

FIGURE 37 - PLOT OF LOG STRESS VS. LOG STRAIN

The lines representing ϵ_E and ϵ_p can be located in such a manner that their sums for any stress will add up to the total strain.

After ϵ_E and ϵ_p have been located, β_1 and β_2 can be calculated as well as the intercepts C and B.

As previously stated, B is time dependent but C is not.

After several values of B have been calculated, the next step is to relate the time effect; this can be done in the following manner:

Since $B = K t^{\alpha}$ (63)

Therefore $\log B - \log K = \alpha \log t$ (64)

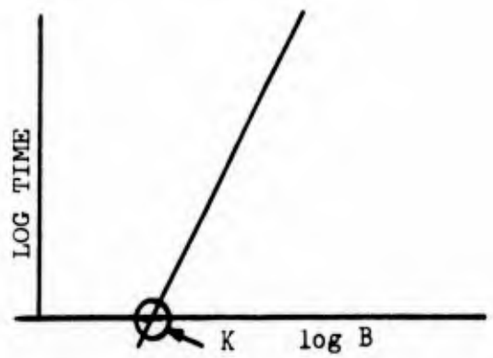

FIGURE 38 - PLOT OF LOG TIME VS. LOG B

Combining Figures 37 and 38:

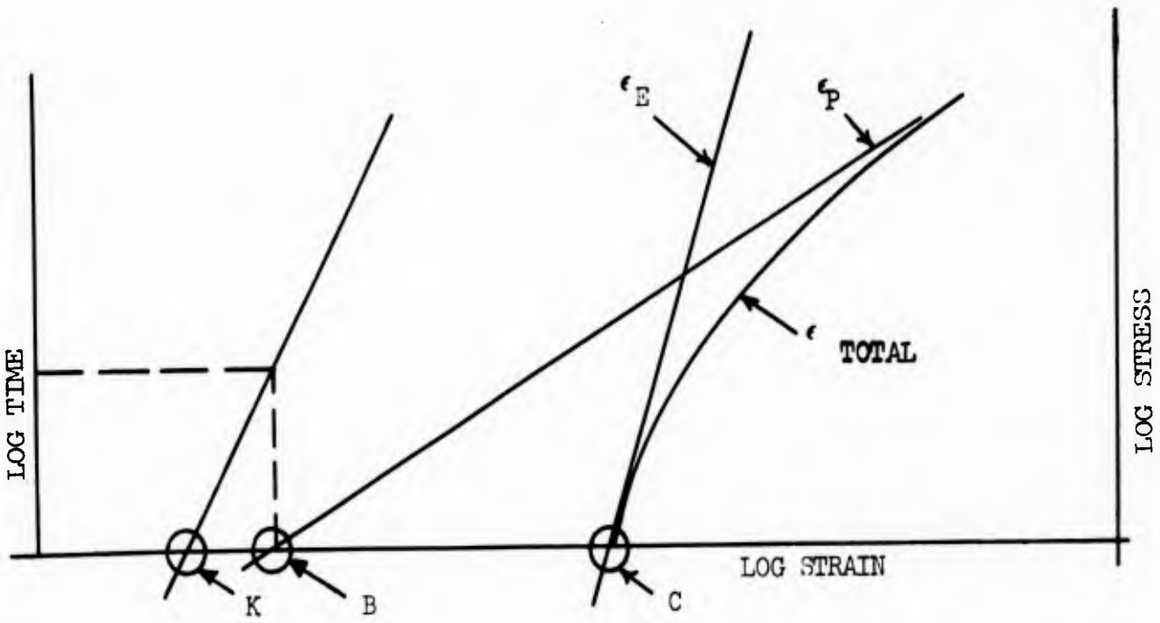

FIGURE 39 PLOT OF LOG TIME, LOG STRAIN AND LOG STRESS

For simplicity let us assume that β_1 and β_2 and α are constant as long as the temperature is constant, then the isochronous family will be represented by a series of parallel plastic lines.

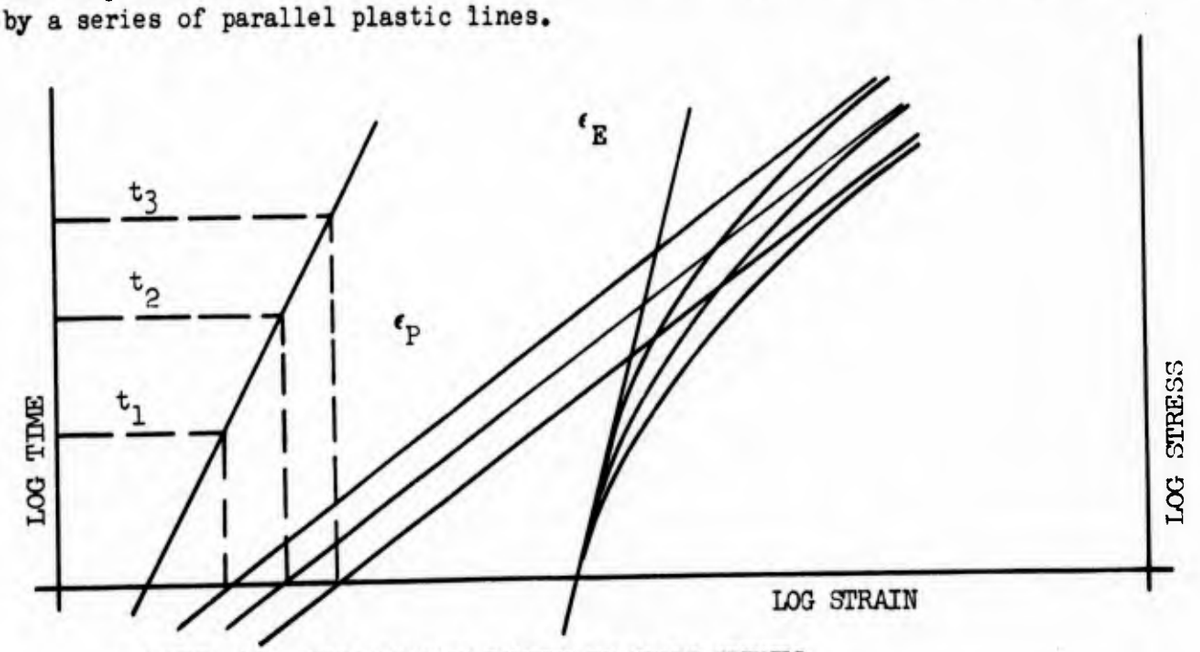

FIGURE 40 ISOCHRONOUS FAMILY OF CREEP CURVES

This procedure is repeated for various temperatures in order that a plot of log C, β_1 , K, α , and β_2 versus the reciprocal of the absolute temperature can be obtained. By so doing the intercepts P, D, L, S, and A will be found, as well as the slope of the lines μ , F, m, n, and H respectively. The slopes of these lines represent the activation energies of the various processes involved.

APPLICATION OF THE DERIVED EQUATION TO BASIC CREEP CURVES

Having obtained the basic creep data, one can plot it as shown below.

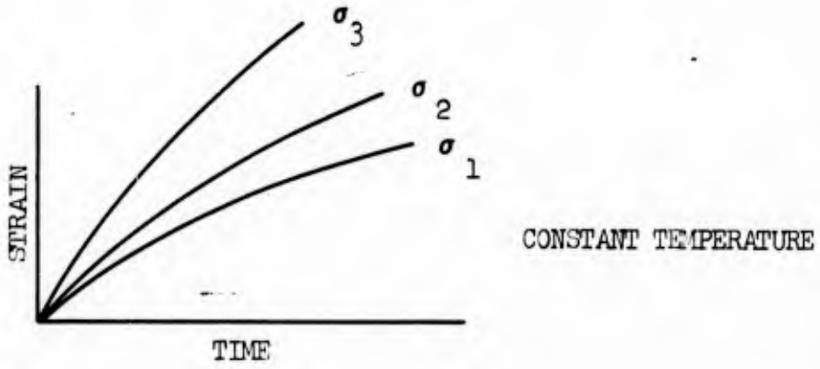

Having plotted the basic creep data in the form shown above, we are ready to apply the equation

$$\epsilon = \epsilon_E + \epsilon_p = C_1' \sigma^{\beta_1} t^{\alpha_1} + C_2' \sigma^{\beta_2} t^{\alpha_2} + \ldots (65)$$

Using only the two first terms of the series and setting $C_1' \sigma^{\beta_1} = K_1$ and $C_2' \sigma^{\beta_2} = K_2$ the following equation results:

$$\epsilon = K_1 t^{\alpha_1} + K_2 t^{\alpha_2} \qquad (66)$$

This equation can be represented by the sum of two lines on log-log paper whose slopes are α_1 , and α_2 , respectively.

Since $$\epsilon_E = K_1 t^{\alpha_1} \qquad (67)$$

$$\log \epsilon_E - \log K_1 = \alpha_1 \log t$$

and

$$\epsilon_p = K_2 t^{\alpha_2} \tag{68}$$

$$\log \epsilon_p - \log K_2 = \alpha_2 \log t$$

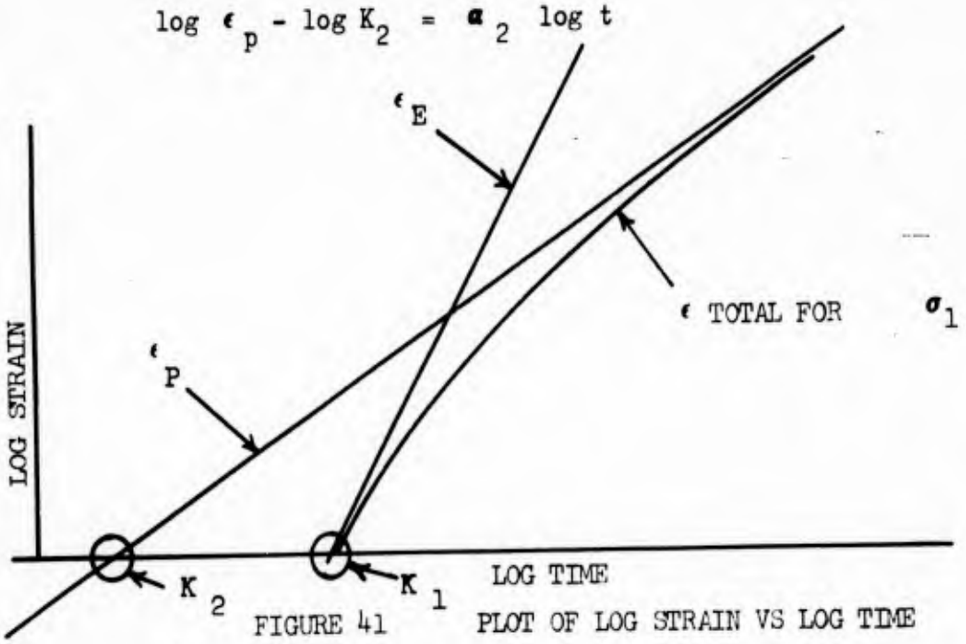

FIGURE 41 PLOT OF LOG STRAIN VS LOG TIME

The lines representing ϵ_E and ϵ_p can be located in such a manner that their sum for any time will equal the total strain.

After ϵ_E and ϵ_p have been located, α_1 and α_2 can be calculated as well as the intercepts K_1 and K_2.

As previously stated, K_2 is time dependent but K_1 is not.

After several values for K_2 have been calculated, the next step is to relate the stresses; this can be done in the following manner:

Since

$$K_2 = C_2' \sigma^{\beta_2} \tag{69}$$

Therefore

$$\log K_2 - \log C_2' = \beta_2 \log \sigma$$

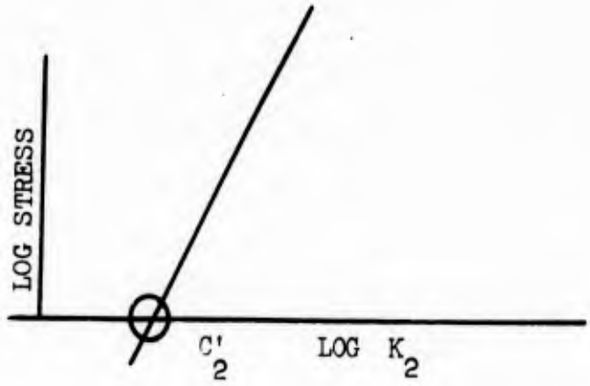

FIGURE 42 PLOT OF LOG STRESS VS LOG K_2

Combining Figures 41 and 42

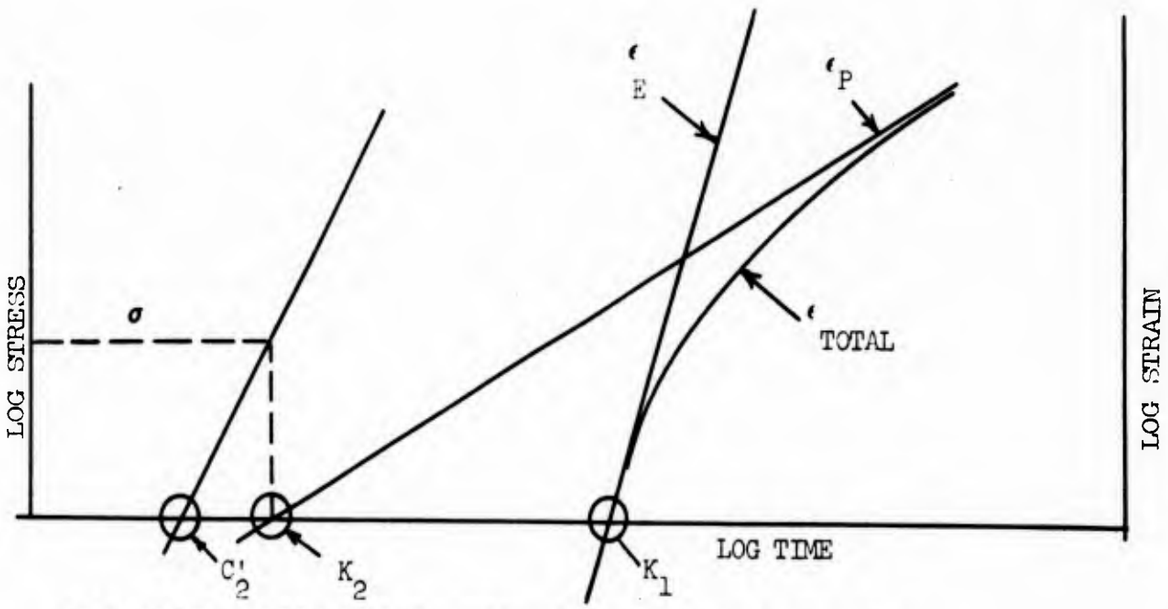

FIGURE 43 PLOT OF LOG STRESS, LOG STRAIN AND LOG TIME

For simplicity assume that β_1, β_2, α_1, and α_2 are constant as long as the temperature is constant. Then the basic creep curve family composed of constant stress curves will be represented by a series of parallel plastic lines.

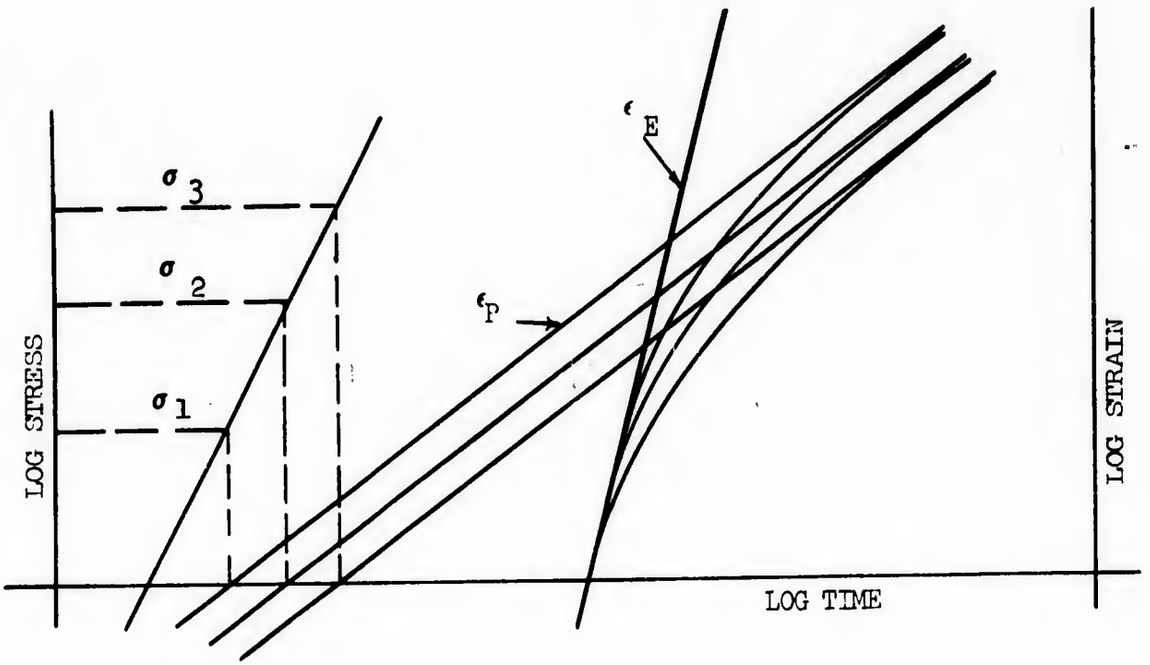

FIGURE 44 FAMILY OF CREEP CURVES

This procedure is repeated for various temperatures in order that a plot of log of K_1, β_1, K_2, β_2, and α_2 versus the reciprocal of the absolute temperature can be obtained. So doing the intercepts P, D, L, S, and A will be found, as well as the slope of the lines μ, F, m, n, and H respectively. The slopes of the lines represent the activation energy for the various processes involved as shown in Figures 45-49. This exercise will produce the numerical constants needed for the application of equation 55 to a metal.

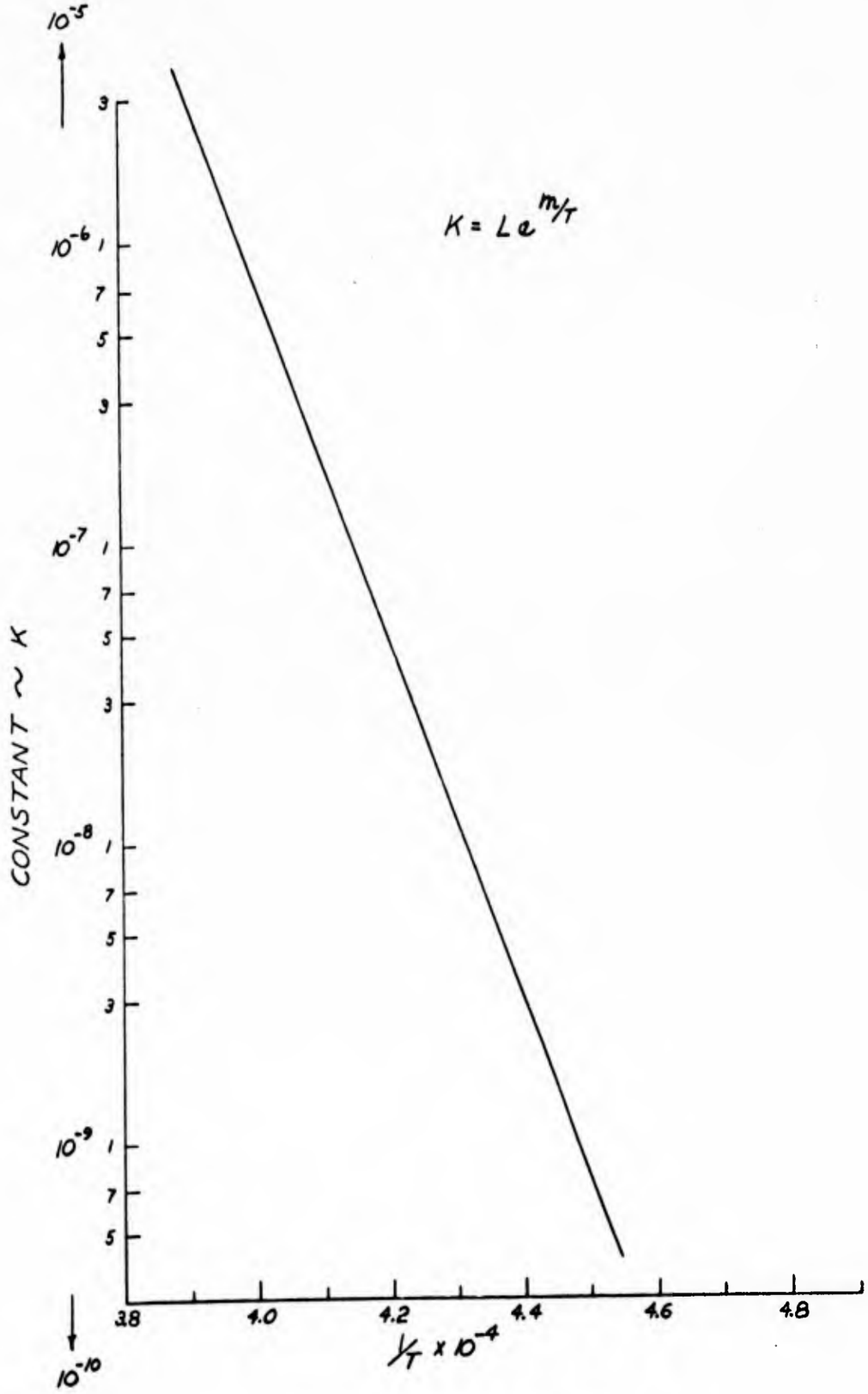

FIGURE 45 - PLOT OF $K = Le^{m/T}$

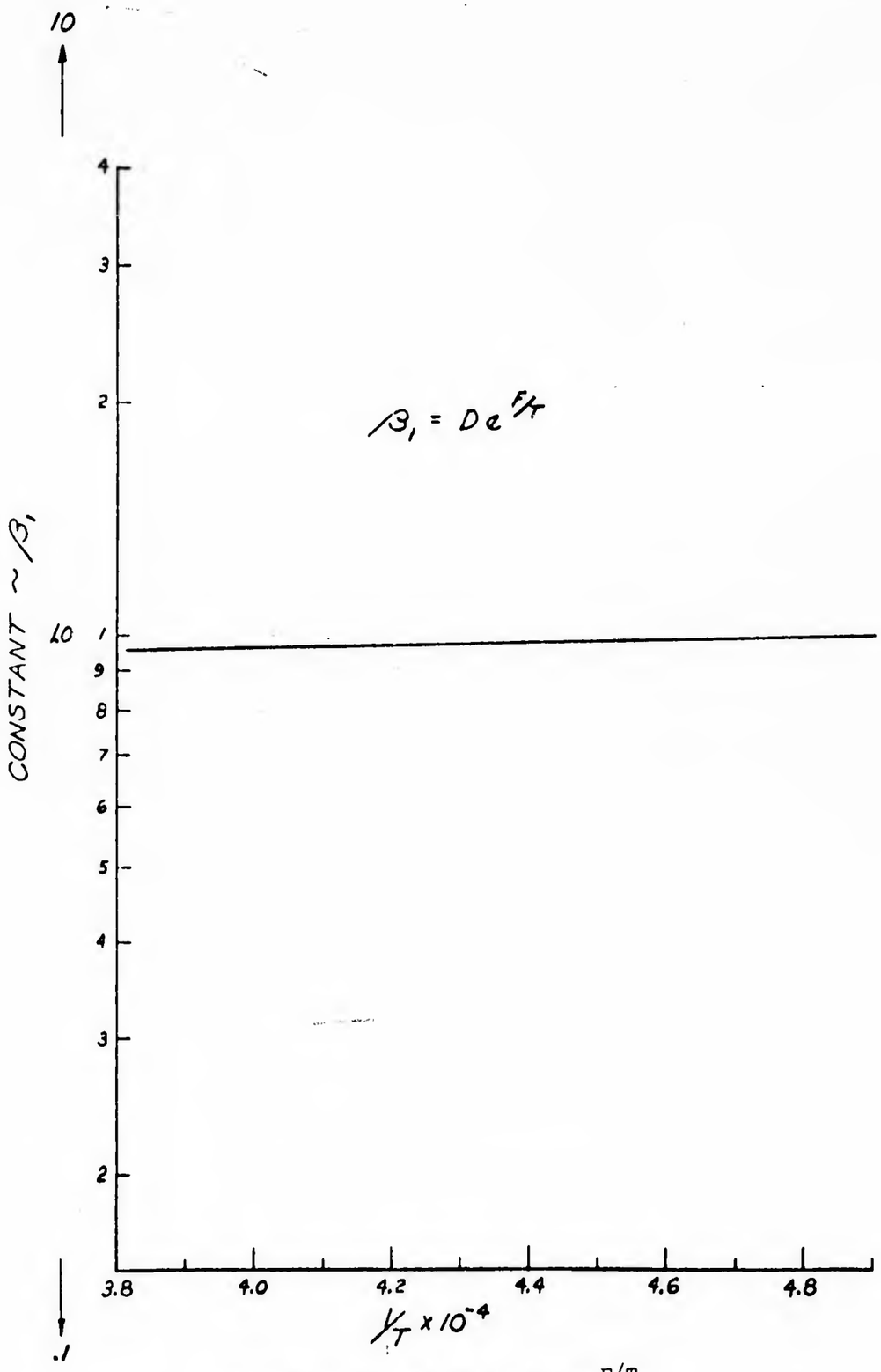

FIGURE 46 - PLOT OF $\beta_1 = De^{F/T}$

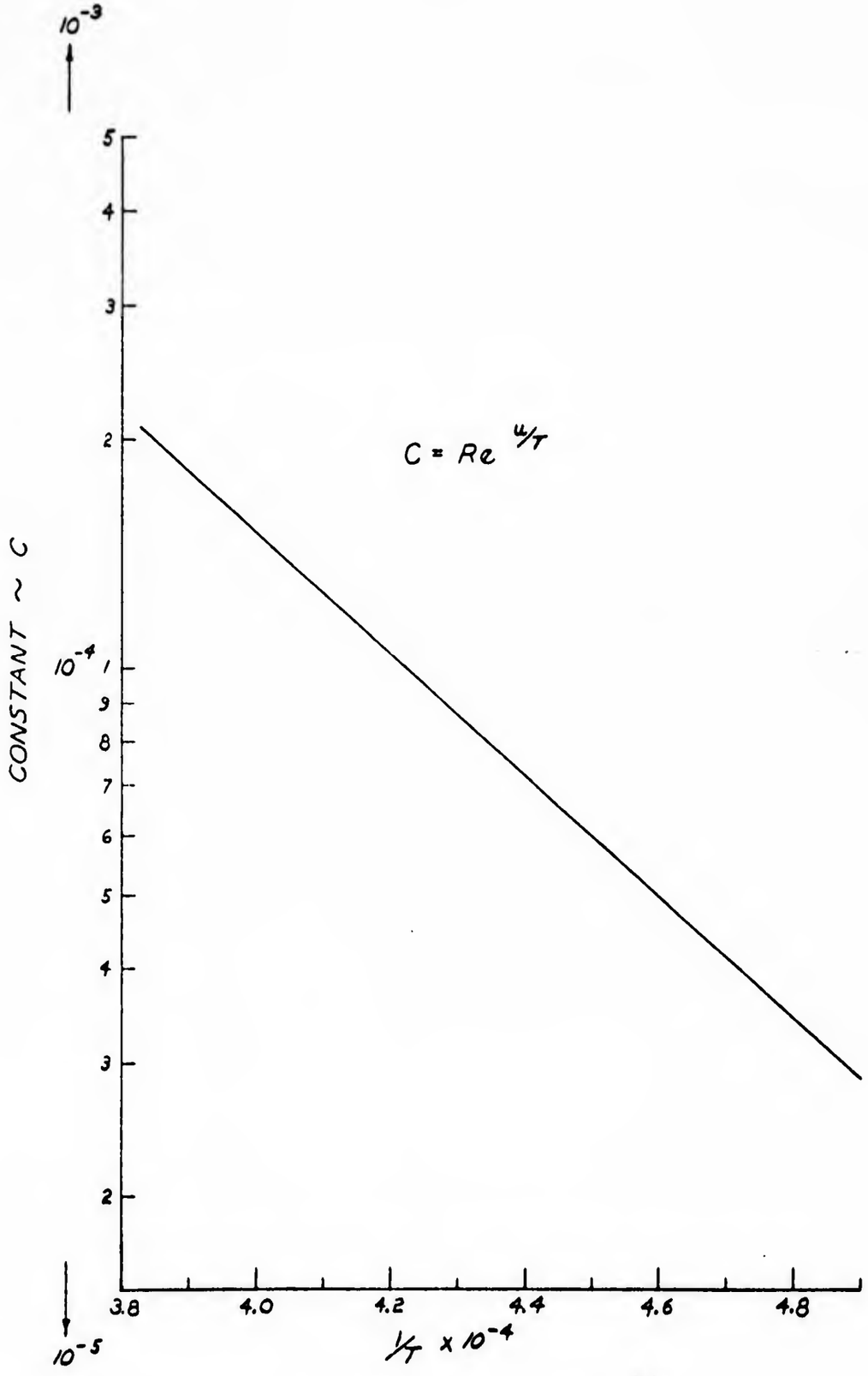

FIGURE 47 - PLOT OF $C = R^{\mu/T}$

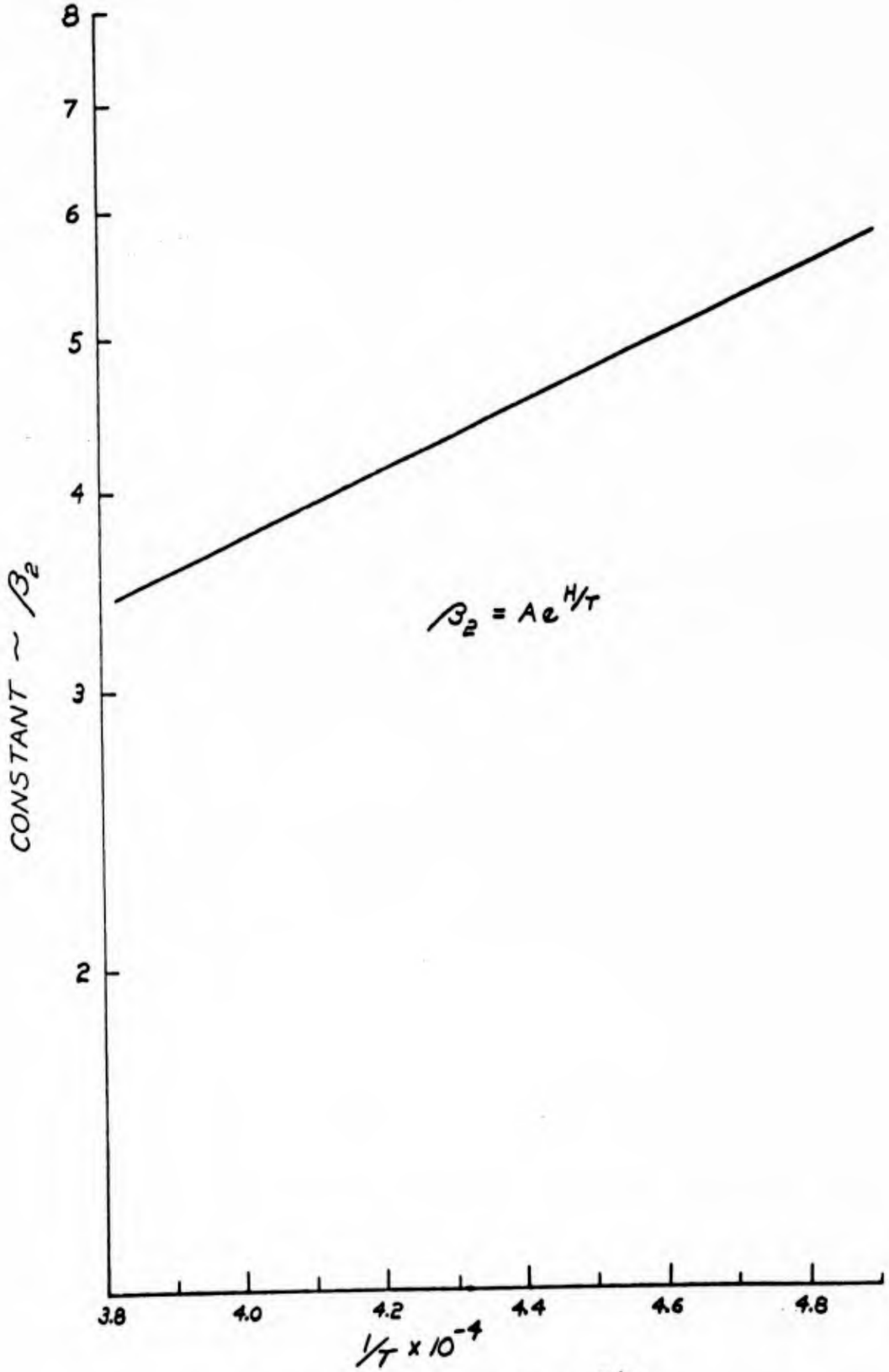

FIGURE 48 - PLOT OF $\beta_2 = Ae^{H/T}$

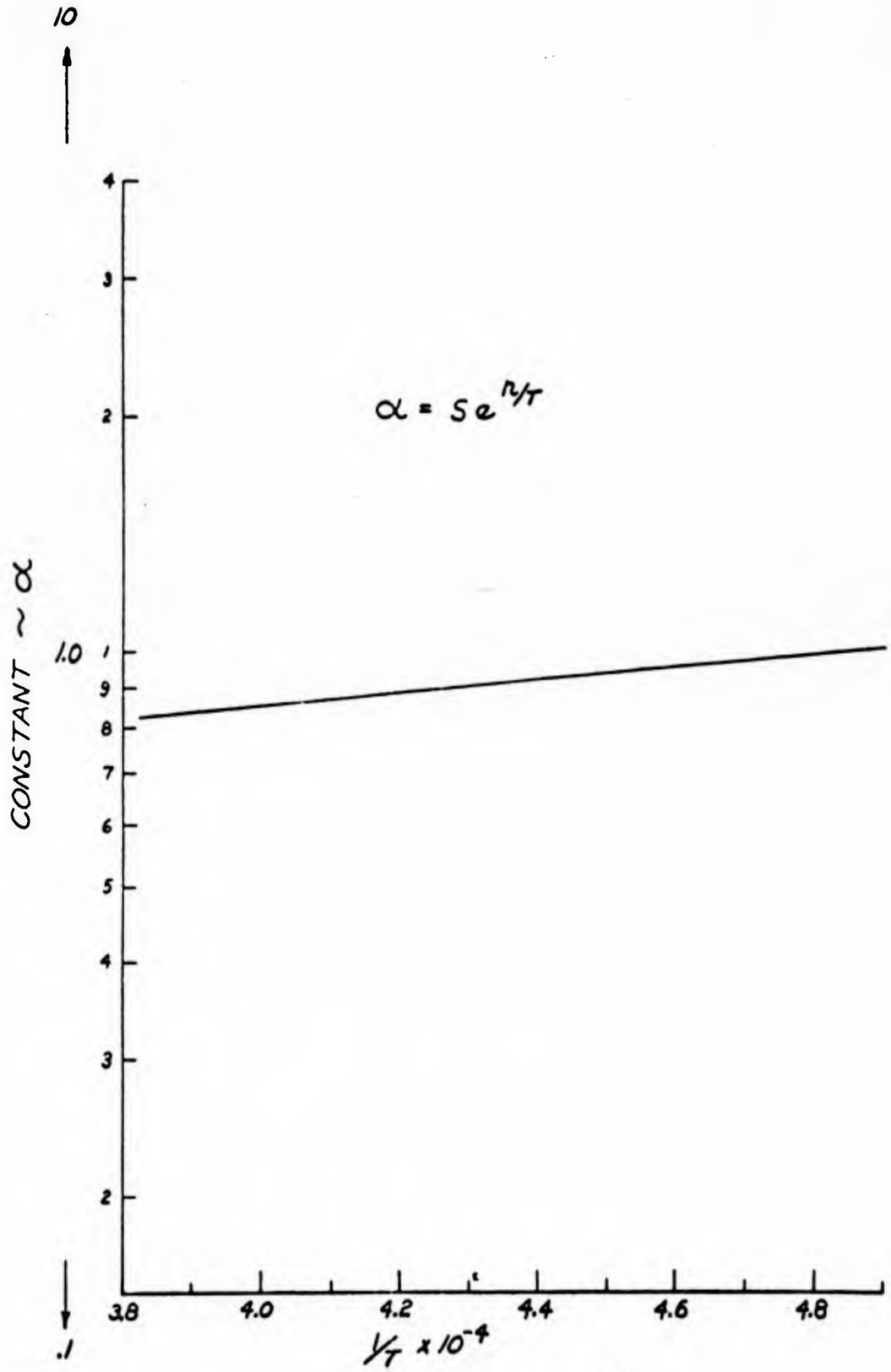

FIGURE 49 - PLOT OF $\alpha = Se^{n/T}$

APPLICATION OF THE DERIVED EQUATION FOR GRAPHICAL PRESENTATION OF CREEP DATA

Having obtained the creep equation for a given metal, it would be convenient to display the creep behavior nomographically.

The basic steps to be taken in order to obtain the nomograph are as follows:

1. Divide the plastic portion of the creep equation into three parts as follows:

$$\epsilon_p = Ae^{-\mu/T} \; \sigma^{De^{F/T}} \; t^{Se^{n/T}} \tag{70}$$

$$\text{Let} \quad X = Ae^{-\mu/T} \quad \text{then} \quad \log X = \frac{\log A}{\mu/T} \tag{71}$$

$$Y = t^{Se^{n/T}} \qquad \log Y = Se^{n/T} \log t \tag{72}$$

$$Z = \sigma^{De^{F/T}} \qquad \log Z = De^{F/T} \log \sigma \tag{73}$$

2. Plot X versus temperature

   Y versus time for different temperatures

   Z versus stress for different temperatures

3. Note the limits of T, σ , and t and let the physical lengths of the x, y, and z axis, to be Lx, Ly, and Lz respectively. Then the scale modulus for each axis can be determined as follows:

$$m_x = \frac{Lx}{X_{MAX} - X_{MIN}}$$

$$m_y = \frac{Ly}{Y_{MAX} - Y_{MIN}}$$

$$m_z = \frac{Lz}{Z_{MAX} - Z_{MIN}}$$

In order to complete the nomograph, an auxiliary axis q must be introduced whose scale modulus is

$$m_q = \frac{(m_y)\ (m_z)}{(m_x + m_z)}$$

and finally, the strain axis ϵ , whose scale modulus is

$$m_\epsilon = \frac{(m_q)\ (m_z)}{(m_q + m_z)}$$

4. The next step is to graphically place the axes with respect to each other, which is done as follows:

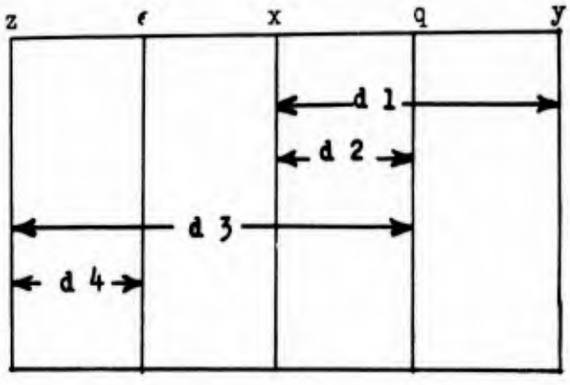

By arbitrarily selecting the (X-Y) distance to equal **d 1** , the (X-q) distance can be calculated as follows:

$$d\ 2 = \left(\frac{m_x}{m_x + m_y}\right) (d\ 1)$$

And by arbitrarily selecting the (q-Z) distance equal to d_3, the distance (Z- ϵ) can be calculated as follows:

$$d_4 = \left(\frac{m_z}{m_z + m_q}\right) d_3$$

Through trial and error, the desired size of the nomograph can be obtained. See Figure 47.

5. Use of the nomograph is illustrated as follows:

Given:	time	=	t_1
	temperature	=	T_2
	stress	=	σ_1
Find:	strain, ϵ		

On Figure 50, locate time (A). Draw a line vertically through t_1 until it intercepts T_2. (B) Draw a horizontal line through this interception point until it crosses the Y axis at (C). Connect T_2 (D) on the X axis with (C) on the Y axis. This line will intercept q at a point (H).

Locate stress (E). Draw a vertical line through this point until it intercepts T_2 (F) . Then draw a horizontal line through (F), until it intercepts Z axis at (G). Connect (G) and (H), and the strain is obtained on the ϵ axis (I).

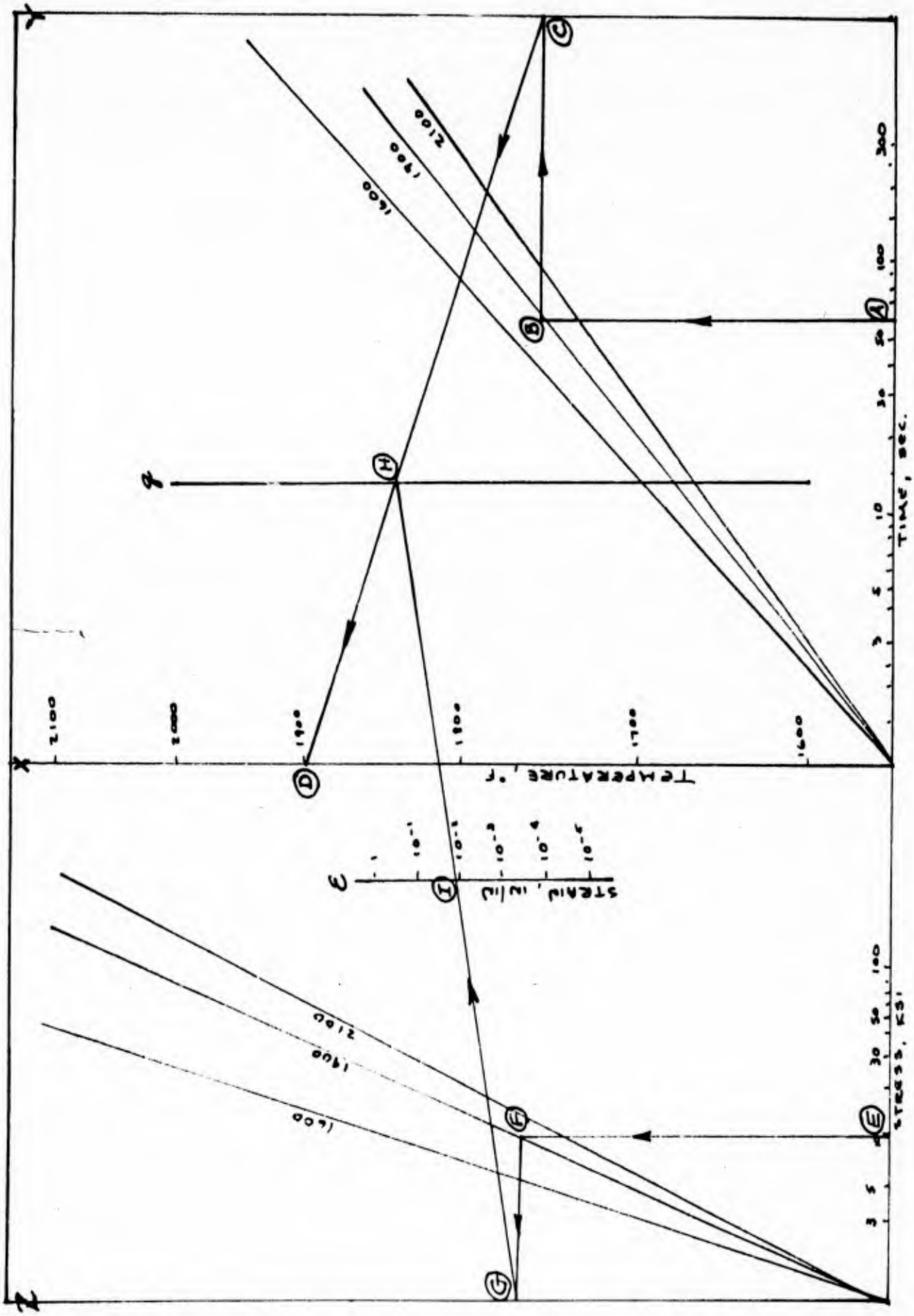

FIGURE 50 - CREEP NOMOGRAPH

APPLICATION OF THE DERIVED EQUATION TO CUMULATIVE CREEP

The temperature is kept constant while the material is deformed first at a constant stress σ_1 from the time t_1 to t_2 then it is deformed at constant stress σ_2 from t_3 to t_4 and finally deformed at a constant stress of σ_n for the time interval t_5 to t_6 as shown below.

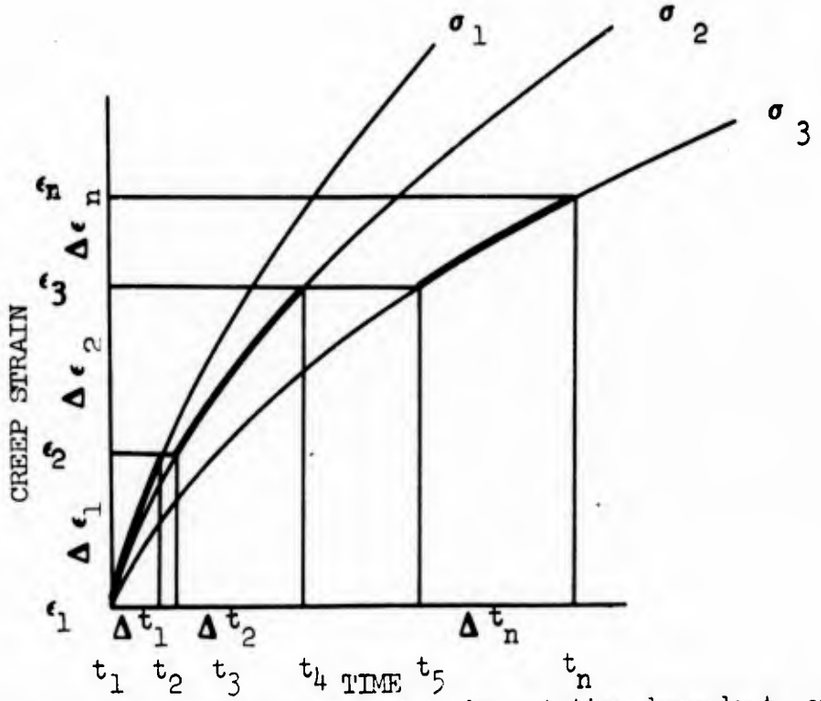

Since the elastic range is assumed to be not time dependent, only the plastic portion must be considered.

The basic creep curves are represented by the equation

$$\epsilon = \epsilon_E + \epsilon_p = C\sigma^{\beta_1} + K t^{\alpha} \sigma^{\beta_2} \tag{74}$$

Therefore

$$\epsilon_p = K t^{\alpha} \sigma^{\beta_2} \tag{75}$$

Setting

$$\Delta \epsilon_1 = \epsilon_2 - \epsilon_1 \quad \text{and} \quad \Delta t_1 = t_2 - t_1$$

$$\Delta \epsilon_2 = \epsilon_3 - \epsilon_1 \quad \text{and} \quad \Delta t_2 = t_4 - t_3$$

$$\Delta \epsilon_n = \epsilon_n - \epsilon_{n-1} \quad \text{and} \quad \Delta t_n = t_n - t_{n-1}$$

Then

$$\epsilon_2 - \epsilon_1 = K \sigma_1^{\beta_2} t_1^{\alpha} \tag{76}$$

$$\epsilon_2 - \epsilon_1 = K \sigma_2^{\beta_2} (t_3 - t_1)^{\alpha} \tag{77}$$

$$\epsilon_3 - \epsilon_2 = K \sigma^{\beta} (t_4 - t_1)^{\alpha} (\epsilon_2 - \epsilon_1) \tag{78}$$

By substitution the equations 76, 77, and 78 will become

$$\Delta \epsilon_1 = K \sigma_1^{\beta_2} \Delta t_1^{\alpha} \tag{79}$$

$$\Delta \epsilon_1 = K \sigma_2^{\beta_2} (t_3 - t_1)^{\alpha} \tag{80}$$

$$\Delta \epsilon_2 = K \sigma_2^{\beta_2} (t_3 - t_1 + \Delta t_2)^{\alpha} - \Delta \epsilon_1 \tag{81}$$

Rearranging equation 80 to obtain

$$t_3 - t_1 = \left(\frac{\Delta \epsilon_1}{K \sigma_2^{\beta_2}} \right)^{\frac{1}{\alpha}}$$

Substituting this result into equation 81 to obtain

$$\Delta \epsilon_2 = K \sigma_2^{\beta} \left[\left(\frac{\Delta \epsilon_1}{A \sigma_2^{\beta_2}} \right)^{\frac{1}{\alpha}} + \Delta t_2 \right]^{\alpha} - \Delta \epsilon_1 \tag{82}$$

Equation 82 can now be written in general terms by setting n equal to the number of cycles.

$$\Delta \epsilon_n = K \sigma_n^{\beta} \left[\sum_{m=1}^{m=n} \left(\frac{\Delta \epsilon_{m-1}}{A \sigma_n^{\beta_2}} \right)^{\frac{1}{\alpha}} + \Delta t_n \right]^{\alpha} - \sum_{m=1}^{m=n} \Delta \epsilon_{m-1} \tag{83}$$

Since the total strain is represented by

$$\epsilon_{Total} = \sum_{m=1}^{m=n} \Delta\epsilon_{m-1} + \Delta\epsilon_{n} \tag{84}$$

the following equation can be obtained by combining equations 83 and 84

$$\epsilon_{Total} = \sum_{m=1}^{m=n} \Delta\epsilon_{m-1} + K\sigma_{n}^{\beta_1} \left[\sum_{m=1}^{m=n} \left(\frac{\Delta\epsilon_{m-1}}{K\sigma_{n}^{\beta_1}} \right)^{\frac{1}{\alpha}} + \Delta t_{n} \right]^{\alpha} \tag{85}$$

or

$$\epsilon_{Total} = K\sigma_{n}^{\beta_1} \left[\sum_{m=1}^{m=n} \left(\frac{\Delta\epsilon_{m-1}}{K\sigma_{n}^{\beta_1}} \right)^{\frac{1}{\alpha}} + \Delta t_{n} \right]^{\alpha} \tag{86}$$

However, since

$$\sum_{m=1}^{m=n} \Delta\epsilon_{m-1} = \sum_{m=1}^{m=n} K \left(\sigma_{m-1}^{\beta_1}\right) \left(\Delta t_{m-1}^{\alpha}\right) \tag{87}$$

the total strain can be expressed

$$\epsilon_{t} = K\sigma_{n}^{\beta_1} \left[\sum_{m=1}^{m=n} \left(\frac{\sigma_{m-1}}{\sigma_{n}} \right)^{\beta_1/\alpha} \left(\Delta t_{m-1}\right) + \cdots\cdots \Delta t_{n} \right]^{\alpha} \tag{88}$$

APPLICATION OF THE DERIVED APPLICATION FOR REVIEWING OTHER CREEP EQUATIONS

Steady state creep and creep rupture characteristics of engineering materials are mostly displayed and correlated by the use of some variation or other of the single activation process:

$$k = Ae^{-Q/RT}$$

See Figure 51. The more commonly known variations of the above equation are the Larson-Miller, the Sherby-Dorn, and the Manson-Haferd methods. These three methods will be discussed separately at first, and then in connection with the derived activation series equation.

The Larson-Miller Method

In 1945 Hollomon and Jaffee derived a graphical relationship between the following tempering parameters: hardness, H; time, t; and temperature, T. This ex post facto type derivation assumes that the tempering is governed by an activation process, hence:

$$h = f_1 (t\, e^{-Q/RT}) \tag{89}$$

It was, however, found that

$$h = f_2 (Q) \tag{90}$$

and that

$$te^{-Q/RT} = t_o = \text{constant} \tag{91}$$

Taking the logarithm of Equation 91 and equating Q from Equations 90 and 91, one obtains:

$$Q = RT \left[\ln (t) - \ln (t_o) \right] = f_2 (h) \tag{92}$$

hence:

$$h = f_3 \left[RT (\ln t/t_o) \right] \tag{93}$$

or

$$\mathbf{h} = f\,(T \ln t/t_o) = f\,\left[T\,(\ln t - \ln t_o)\right] \tag{94}$$

finally letting

$$C_{HJ} = -\ln t_o$$

then

$$\mathbf{h} = f\,\left[T\,(C_{HJ} + \ln t)\right] \tag{95}$$

where the Hollomon-Jaffee tempering parameter is

$$Q/R = \mathbf{HJ} = f\left[T\,(C_{HJ} + \ln t)\right] \tag{96}$$

or, if $K_{HJ} = e^{-C_{HJ}}$ then

$$t = Ae^{Q/RT} = K_{HJ}e^{HJ/T} \tag{97}$$

By 1952 it had been shown by many investigators that creep, diffusion, and tempering appeared to conform to a rate-controlled process; therefore, Larson and Miller proposed that the graphical relationship derived by Hollomon and Jaffee should be directly applicable at a time-temperature relationship for stress rupture and creep.

They assumed, however, that the time to rupture or to reach a given plastic deformation will depend on the summation of the preceding creep rates and that the activation energy will be independent of temperature, but dependent on stress in such a fashion that A will be a fixed value for any material:

$$t = A\,e^{Q/RT} \tag{98}$$

therefore setting $A = e^{-C_{LM}}$

$$Q/R = \mathbf{LM} = f\left[T\,(C_{LM} + \ln t)\right] \tag{99}$$

This relationship is presented graphically in Figure 52.

The Sherby-Dorn Method

In 1952 Sherby and Dorn also proposed a method for correlation of creep and rupture. They found that the total time required to reach stress rupture or a given strain could be expressed by the single term functional relationship:

$$\Theta = t\, e^{-H/RT} \tag{100}$$

Rewriting and setting $\Theta = A$, the equation takes the same form as Equation 91 and Equation 98:

$$t = A\, e^{H/RT} \tag{101}$$

However, Sherby and Dorn assumed that the activation energy, H, is neither stress nor temperature dependent, but made the stipulation that A will be stress dependent. In Figure 52, a sketch is shown of the Sherby-Dorn method.

The Manson-Haferd Method

In 1953 Manson and Haferd studied the Larson-Miller and the Sherby-Dorn parameters and decided that semilog plots of rupture time versus reciprocal of the absolute temperature did not result in true straight lines. They therefore concluded that stress rupture data plotted in this manner could not be represented reliably by either constant stress lines fanning out from a common point or by parallel lines.

Manson and Haferd decided from graphical observations, that at least for some materials and rupture times in excess of 30 hours, the stress rupture data were much better represented by plotting the log of rupture time versus temperature and letting the constant stress lines fan out as straight lines from a common point. The Manson-Haferd method is represented by the following equation:

$$t_r = A' e^{-Q'T} \tag{102}$$

Comparison of the Larson-Miller, the Sherby-Dorn, and the Manson-Haferd and the Activation Series Method

The Larson-Miller, the Sherby-Dorn, and the Manson-Haferd methods have been reviewed. The reason being that these methods have received a wide application for interpretation and extrapolation of steady state creep and

creep rupture. These methods were not intended for use in the Elasto-Plastic Region and will therefore yield great errors as applied to that region. See Figure 53.

It is therefore important that the principals upon which these methods have been based and their limitations are fully understood. For instance, the Larson-Miller method assumes that the frequency factor A is a constant and takes the activation energy to be only stress dependent.

Even though the basic equation for the Manson-Haferd method differs from the Larson-Miller equation, the assumptions for the frequency factor and the activation energy are the same.

The Sherby-Dorn method chooses to make the frequency factor stress dependent (see Figure 54) while the activation energy is assumed constant. See Figure 55.

The activation series makes the frequency factor stress and strain dependent (see Figure 54) while the activation energy is stress and temperature dependent (see Figure 55). It is therefore obvious that the method with the greatest amount of freedom will represent the materials deformation characteristics over the greatest range.

This is brought out in Figure 56 where it is readily seen that the Larson-Miller method favors the primary portion, the Sherby-Dorn method the central portion, and the Manson-Haferd method the final portion of a metal's deformation curve, while the activation series method covers the whole deformation range. The conclusion is, therefore, that the activation series should be used:

$$t = A_1 e^{Q_1/RT} + A_2 e^{Q_2/RT} + \ldots + A_n e^{Q_n/RT} \qquad (103)$$

where

$$A_1 = f(\dot{\epsilon}_1, \sigma_1);\ A_2 = f(\dot{\epsilon}_2, \sigma_2);\ A_n = f(\dot{\epsilon}_n, \sigma_n)$$

$$Q_1 = f(\sigma_1, T_1);\ Q_2 = f(\sigma_2, T_2);\ Q_n = f(\sigma_n, T_n)$$

In Figure 54, the isometric graph shows the relationship between A, $\dot{\epsilon}$, and σ, while Figure 55 is an isometric graph of the Q, σ, and T relationship.

This method will be superior in accuracy and cover the whole deformation range of a metal, i.e. the elastic, the elasto-plastic, the steady state, and the tertiary as well as the rupture region.

$$k = A e^{-Q/RT}$$

Q/R = slope

A = intercept at $1/T = 0$

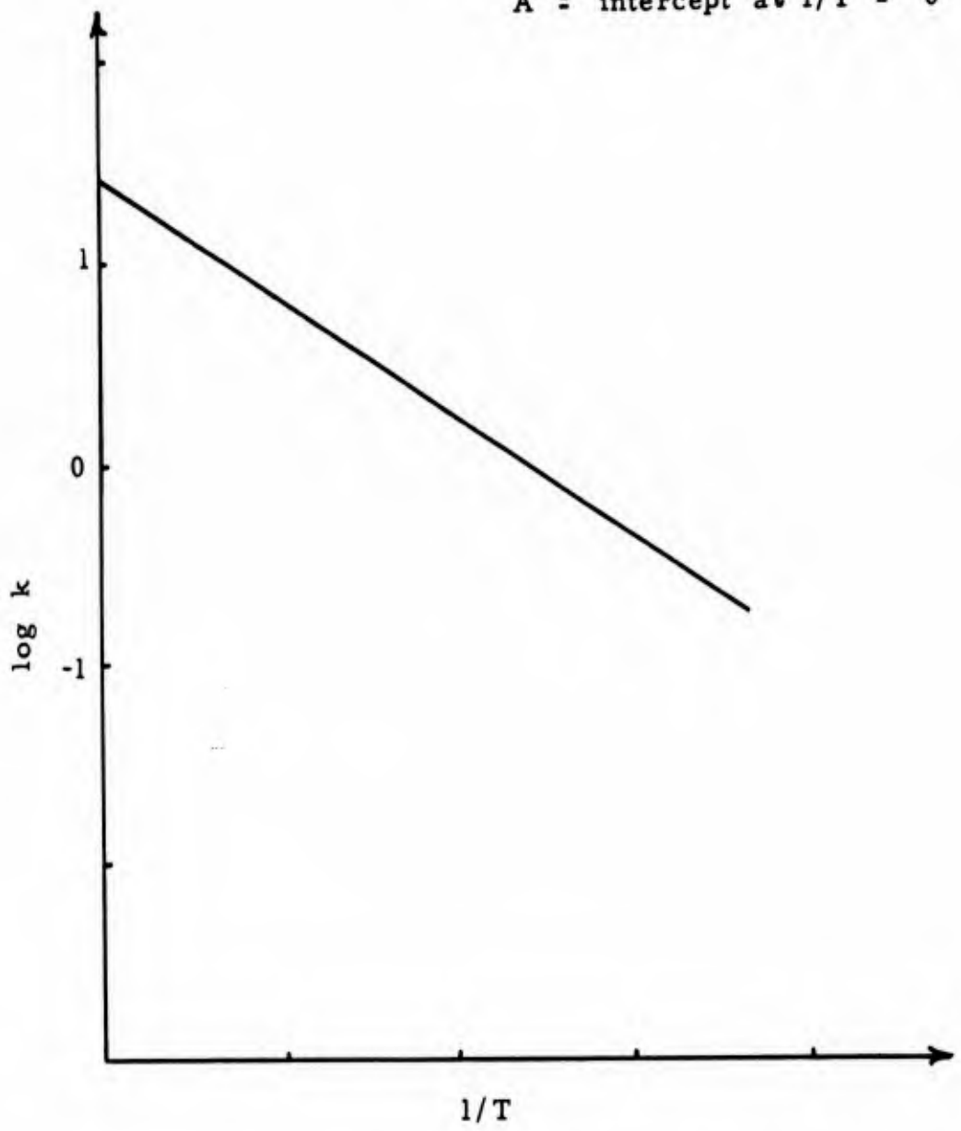

FIGURE 51 - GRAPHICAL REPRESENTATION OF A SINGLE ACTIVATED PROCESS

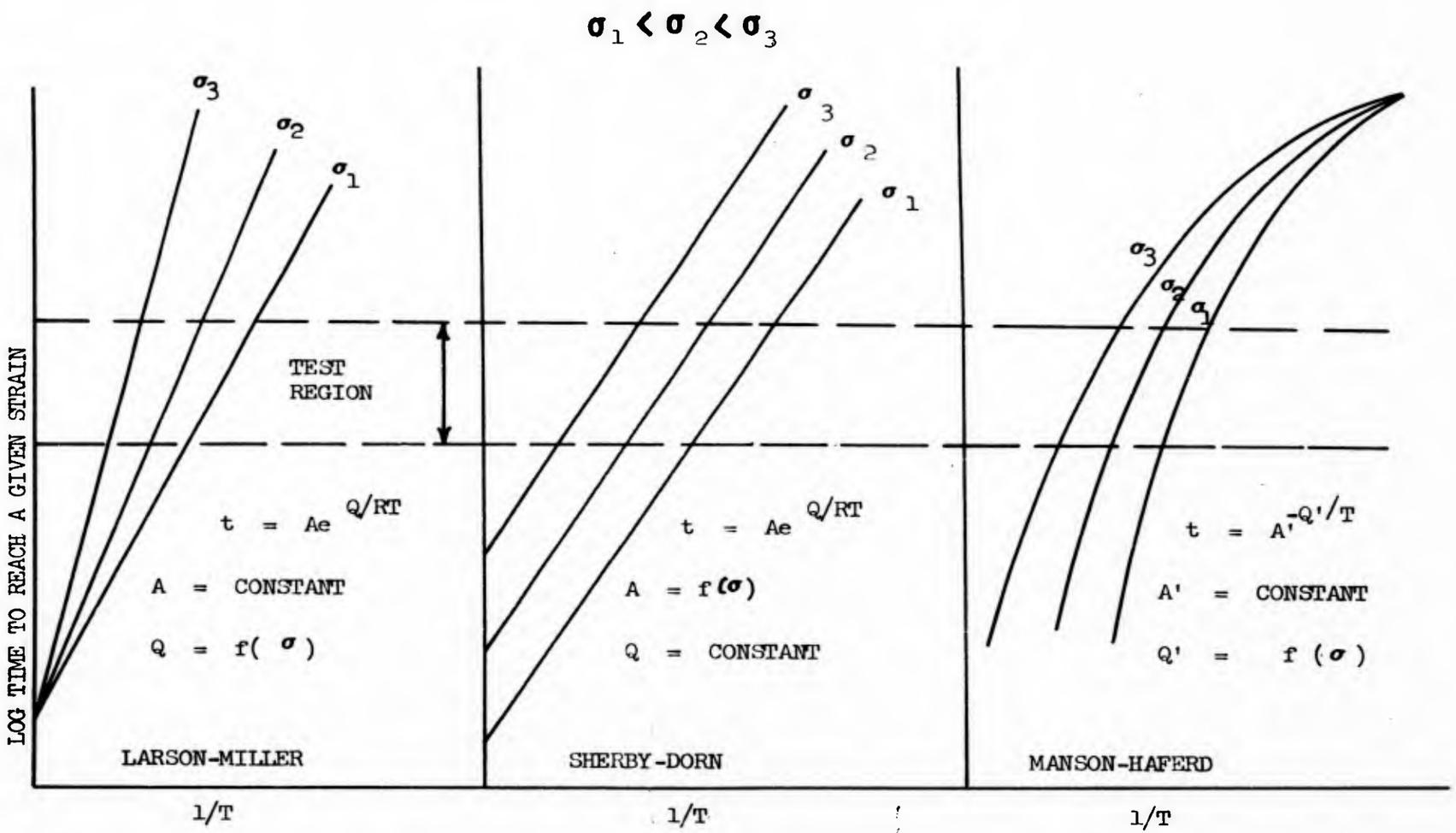

FIGURE 52 - COMPARISON OF CONSTANT STRESS LINES FOR LARSON-MILLER, SHERBY-DORN, AND MANSON-HAFERD METHODS

The error introduced by the use of steady state equations in the elasto-plastic region is shown by the shaded area.

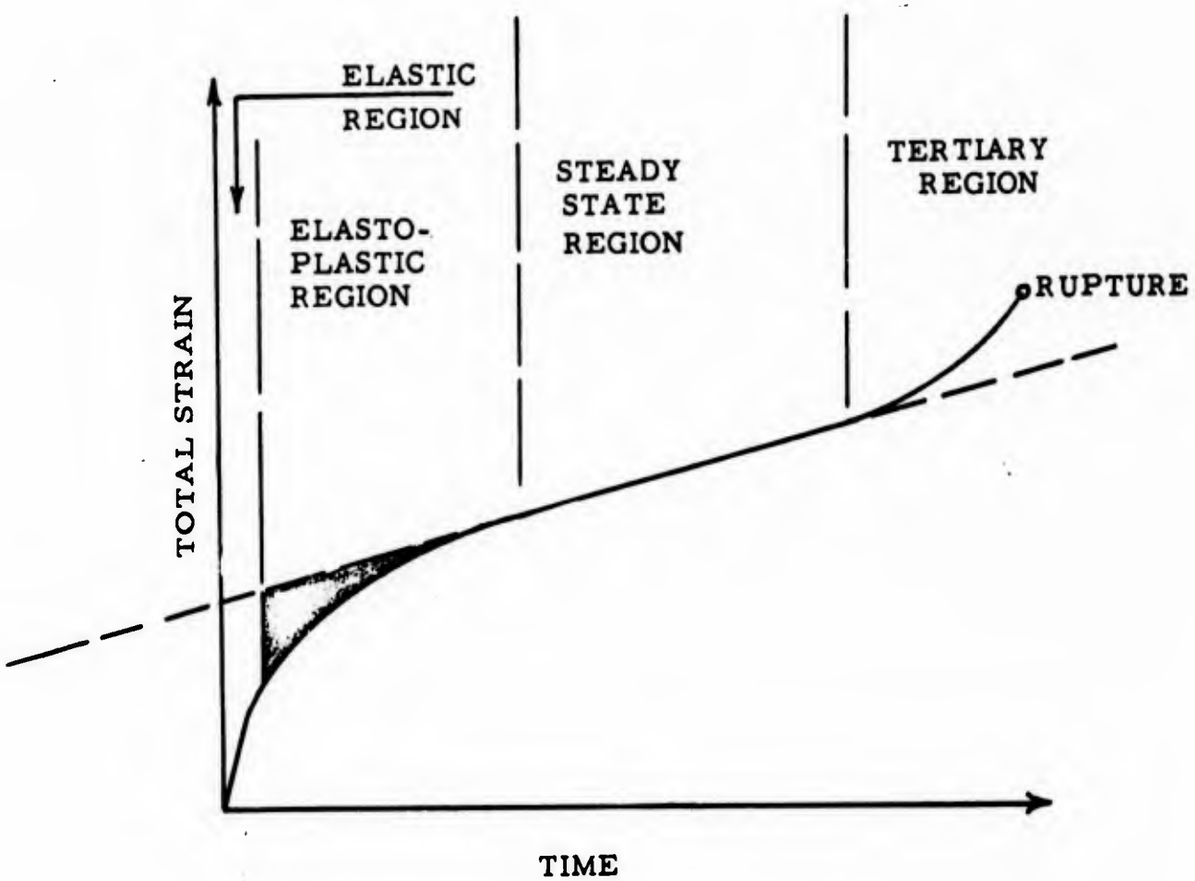

FIGURE 53 - A BASIC ISOBARIC CREEP CURVE

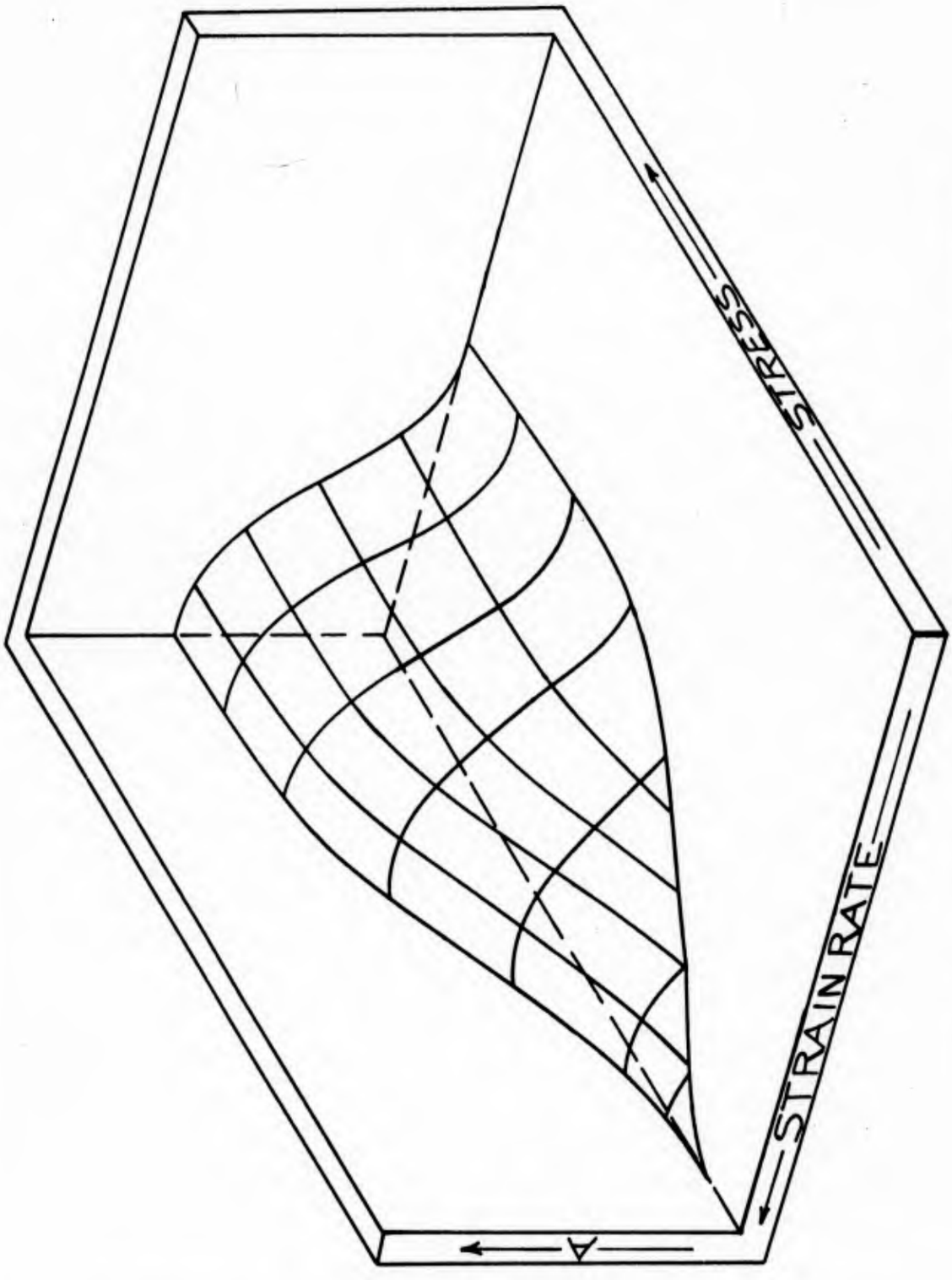

FIGURE 54 - ISOMETRIC STRESS-STRAIN RATE-FREQUENCY FACTOR SURFACE

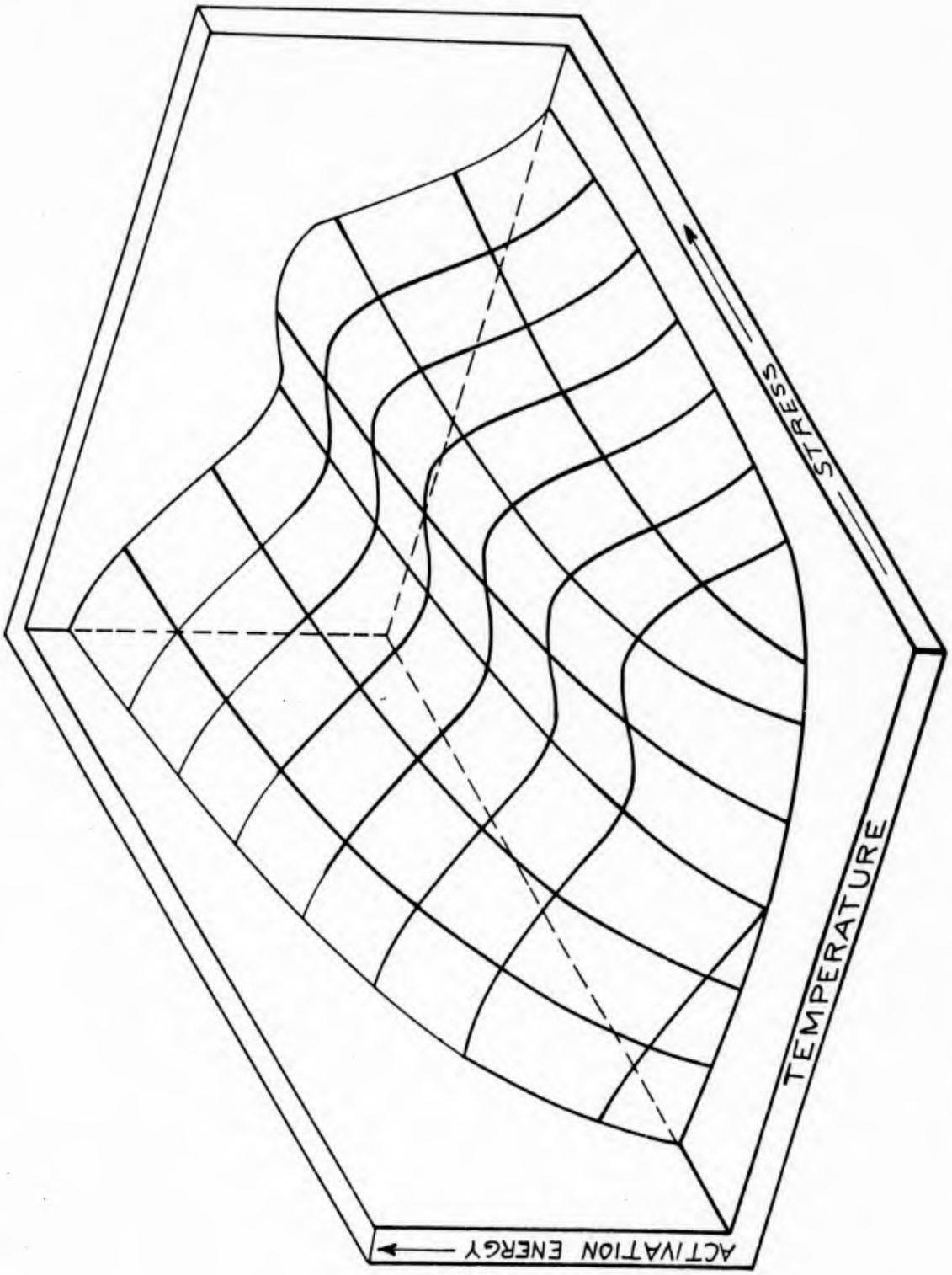

FIGURE 55 - ISOMETRIC STRESS-TEMPERATURE-ACTIVATION ENERGY SURFACE

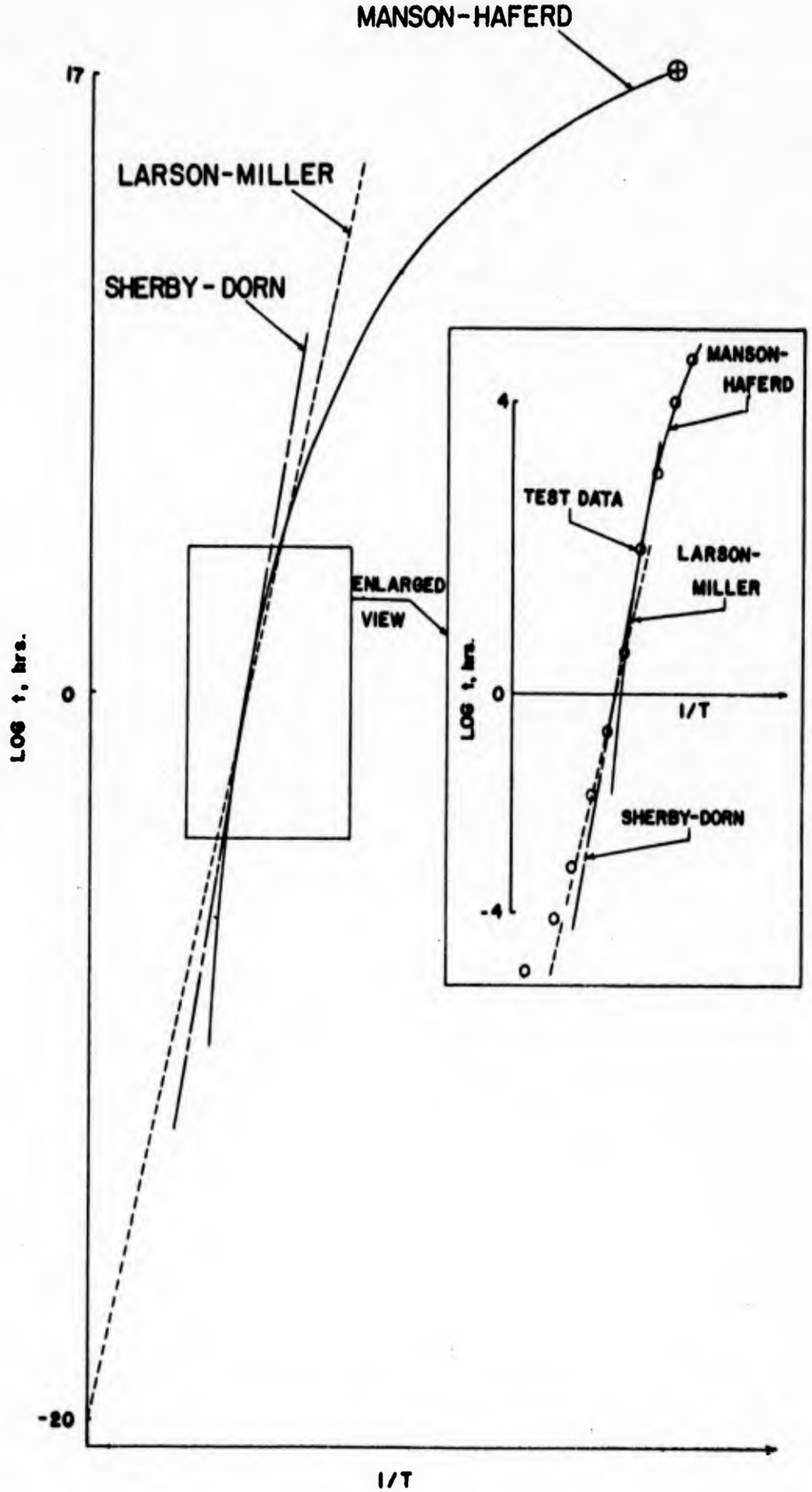

FIGURE 56 - ISOBARIC CREEP DATA REPRESENTED BY MANSON-HAFERD, LARSON-MILLER, AND SHERBY-DORN

APPENDIX II

TEST DATA

TABLE 1 - MATERIAL IDENTIFICATION

CHEMICAL ANALYSIS

MAT'L.	HEAT NUMBER	C	S	Si	Mn	Cr	Ni	Mo	Ti	Al	Fe	B	Co	Zn	N_2	H_2	V	P	OTHER
Rene' 41	R-205	.07	.005	.04	.05	19.04	Bal	9.84	3.17	1.52	.30	.0042	10.85	-	-	-	-	-	-
A110AT	D1-3876673	.042	-	-	.10	-	-	-	Bal.	5.05	.23	-	-	2.60	.022	.0015	-	-	.16
A-286	E 61488	.03	.015	.65	1.48	14.30	26.80	1.10	2.00	.14	Bal.	.003	-	-	-	-	.26	.025	-
Unimach 2	D20223	.49	.008	1.07	.34	4.85	1.50	1.46	-	-	Bal.	-	-	-	-	-	1.05	.024	-

TABLE 2 - TENSILE CONTROL DATA

MATERIAL	TEMP. (°F)	YIELD (PSI)	ULTIMATE (PSI)	
A-286	70	109,600	156,800	
Solution Treated	70	119,500	156,800	
@ 1650°F, Aged	70	117,500	155,300	
16 hrs, @ 1325°F		115,533	156,300	Avg.
	1200	101,500	120,000	
	1200	101,500	119,200	
		101,500	119,600	Avg.
	1500	29,400	36,700	
	1500	37,200	44,300	
	1500	29,100	32,900	
	1500	23,900	26,400	
		29,900	35,075	Avg.
A110AT	75	121,700	126,000	
Mill Annealed	75	121,900	125,700	
	75	126,300	129,400	
		123,300	127,033	Avg.
	800	61,300	76,000	
	800	61,300	75,000	
		61,300	75,500	Avg.
	1000	54,500	70,100	
	1000	53,100	67,300	
		53,800	68,700	
Unimach 2	75	233,000	293,600	
Solution Treated	75	224,700	---	
@ 1800°F	75	220,700	303,000	
Double Aged		226,113	298,300	Avg.
2+2 hrs. @ 800°F				
	600	206,700	275,200	
	600	206,100	275,200	
		206,400	275,200	Avg.
	900	191,100	205,500	
	900	181,900	231,900	
		186,500	218,700	Avg.

TABLE 2 (Concluded)

MATERIAL	TEMP. (°F)	YIELD (PSI)	ULTIMATE (PSI)	
Rene' 41	78	155,400	202,300	
Solution Treated	78	157,200	204,100	
@ 1975°F		156,300	203,200	Avg.
Aged 16 hrs.				
@ 1400°F	1250	125,600	166,500	
	1250	126,100	173,300	
	1250	125,900	160,700	
		125,866	166,833	Avg.
	1400	115,600	136,200	
		114,700	138,600	
		115,300	139,000	
		115,200	137,933	Avg.
	1550	100,400	106,100	
	1550	98,300	102,400	
	1550	97,600	105,200	
		98,766	104,566	Avg.
	1700	53,400	57,600	
	1700	53,800	55,000	
	1700	58,500	60,200	
		55,233	57,600	Avg.
	1850	21,600	24,600	
	1850	20,400	24,400	
	1850	22,000	23,100	
		21,333	24,033	Avg.
	2000	8,150	9,450	
	2000	-----	9,250	
	2000	7,350	9,300	
		7,750	9,333	Avg.

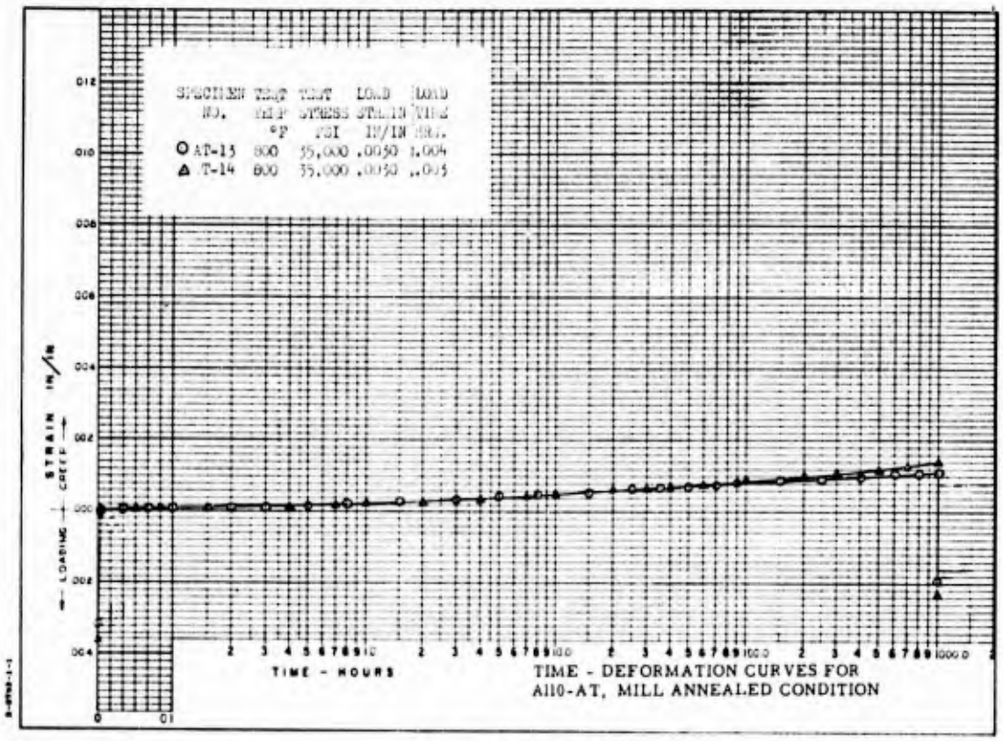

FIGURE 57 - TEST CURVES A110AT 800°F 35,000 psi

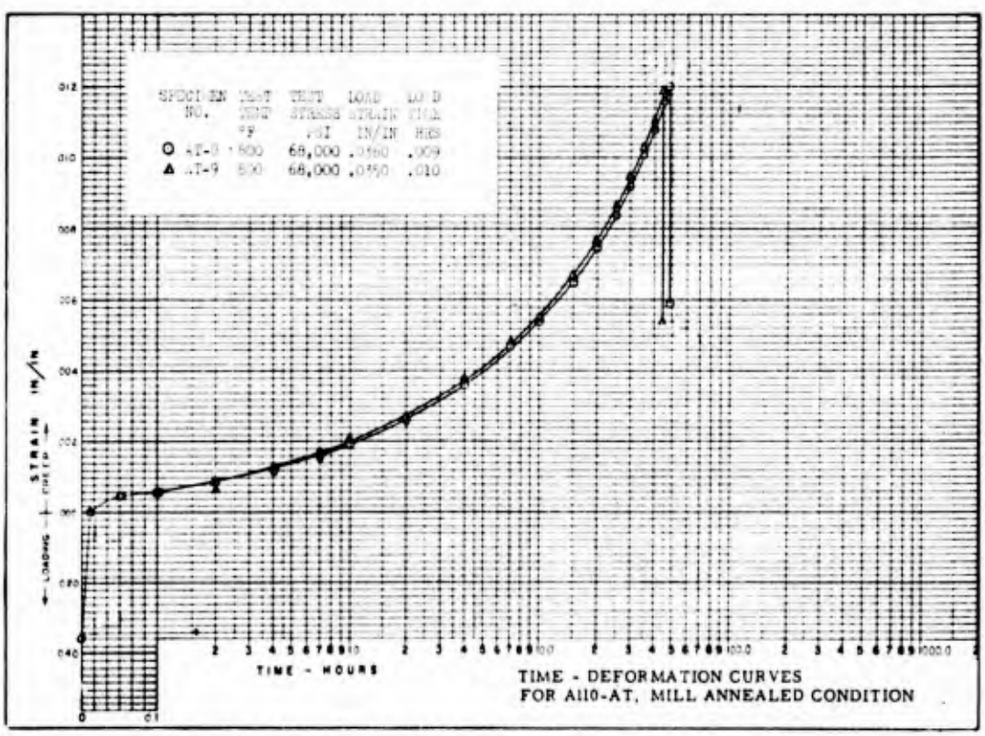

FIGURE 58 - TEST CURVES A110AT 800°F 68,000 psi

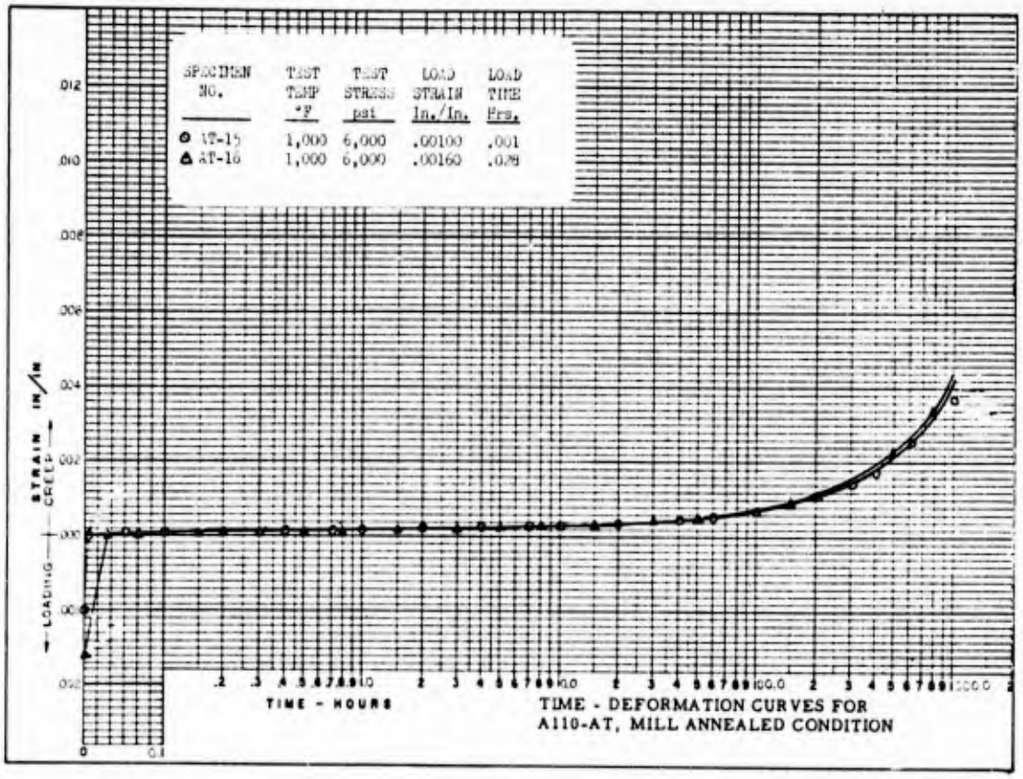

FIGURE 59 - TEST CURVES A110AT 1000°F 6,000 psi

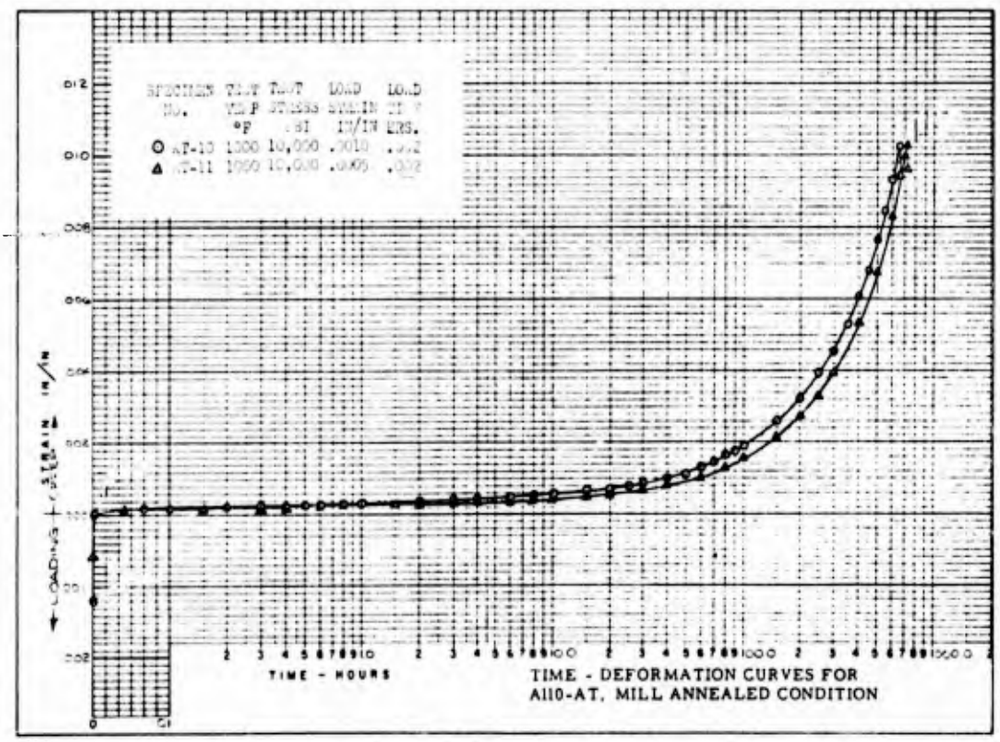

FIGURE 60 - TEST CURVES A110AT 1000°F 10,000 psi

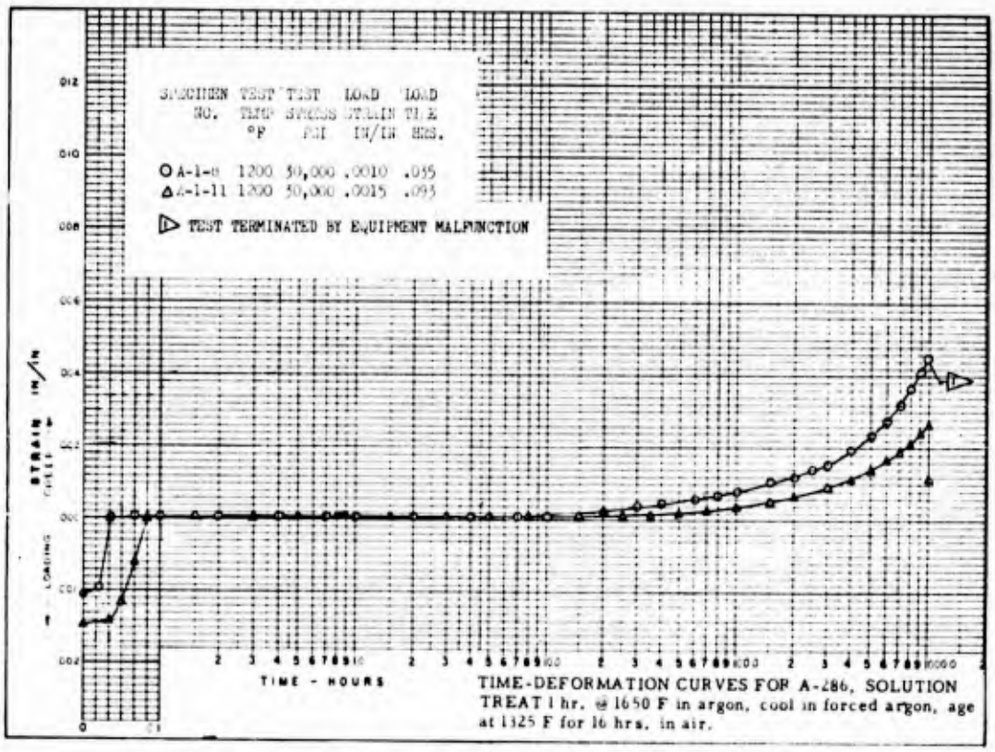

FIGURE 61 - TEST CURVES A-286 1200°F 50,000 psi

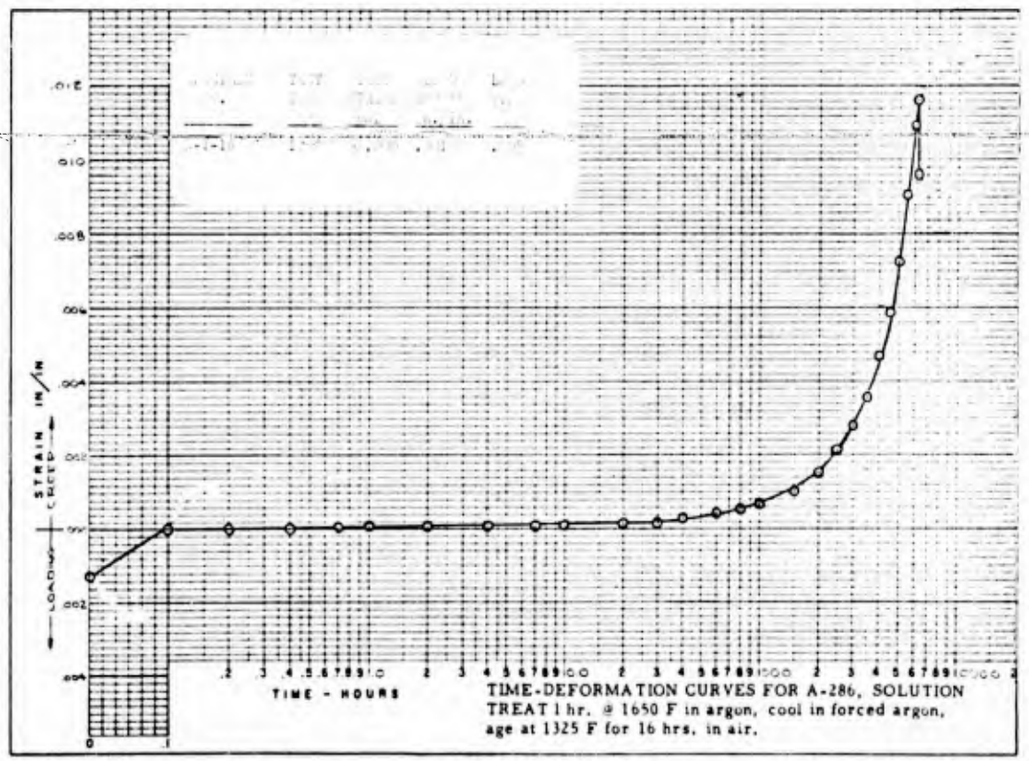

FIGURE 62 - TEST CURVES A-286 1200°F 40,000 psi

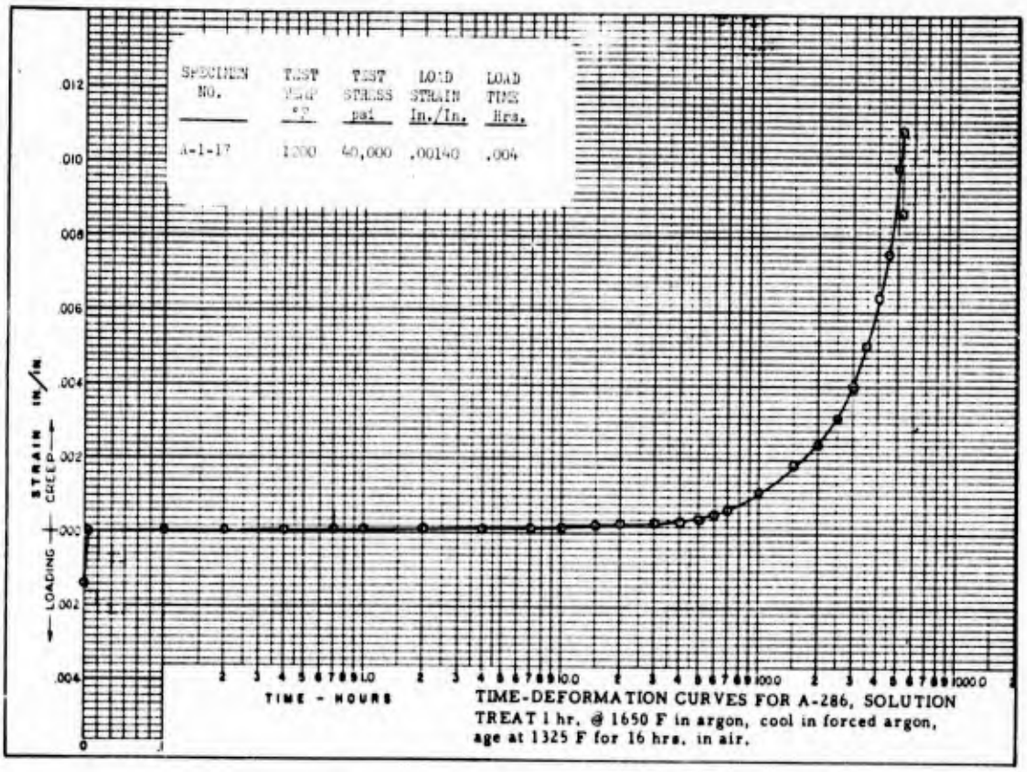

FIGURE 63 - TEST CURVE A-286 1200°F 40,000 psi

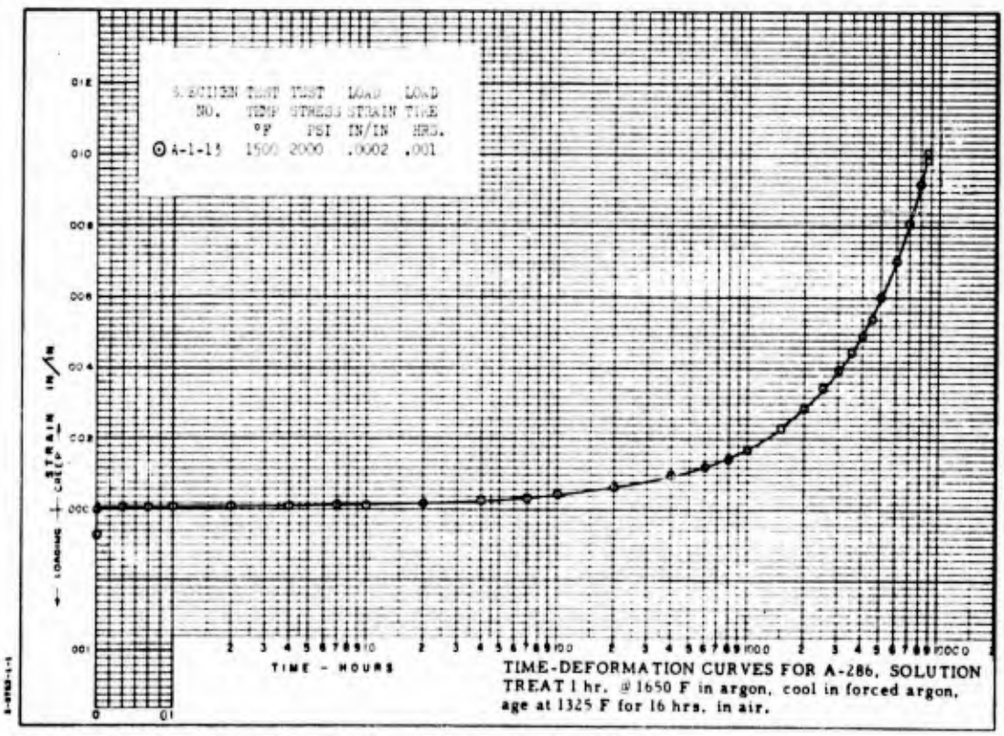

FIGURE 64 - TEST CURVE A-286 1500°F 2000 psi

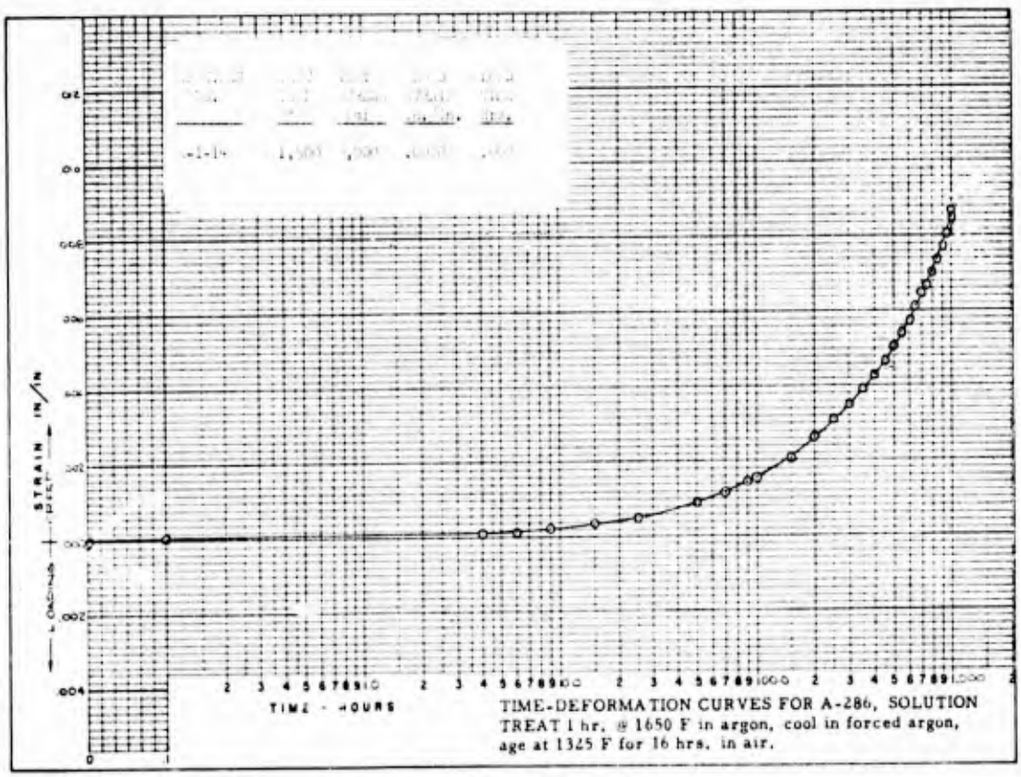

FIGURE 65 - TEST CURVE A-286 1500°F 7000 psi

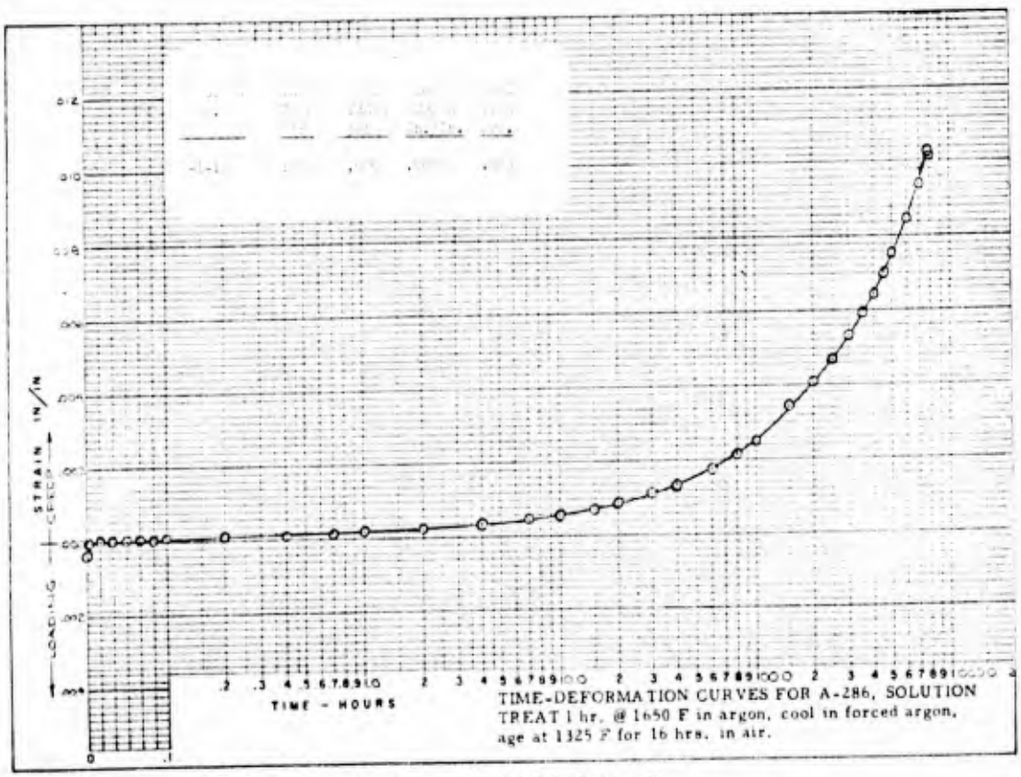

FIGURE 66 - TEST CURVE A-286 1500°F 5000 psi

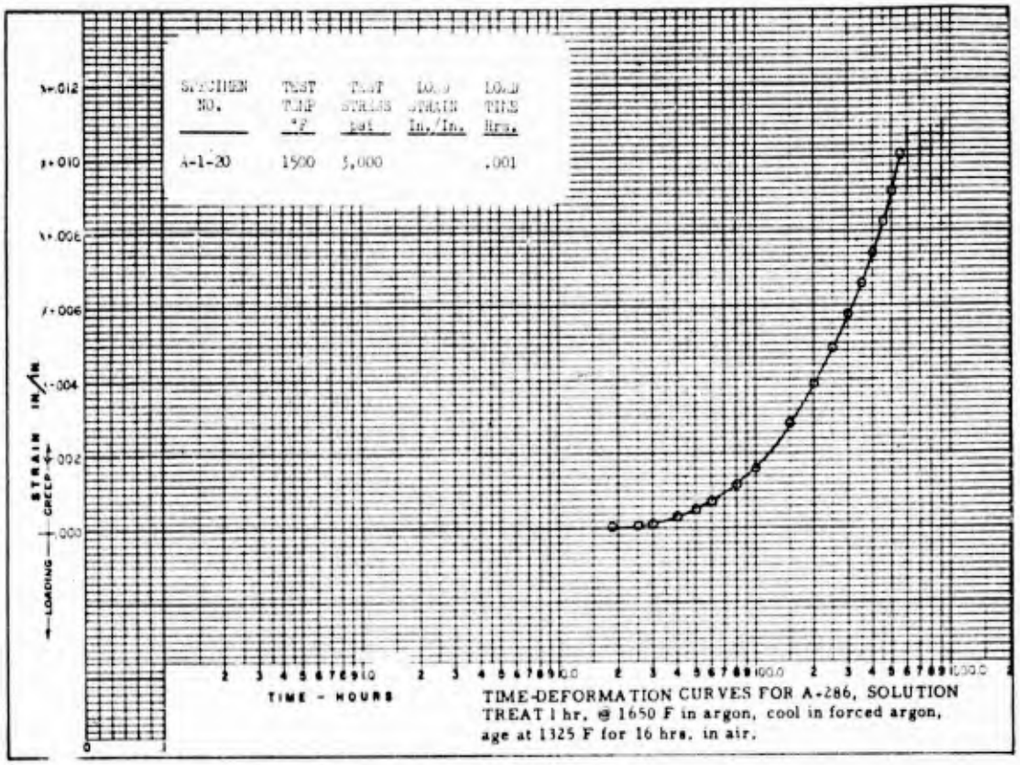

FIGURE 67 - TEST CURVE A-286 1500°F 3000 psi

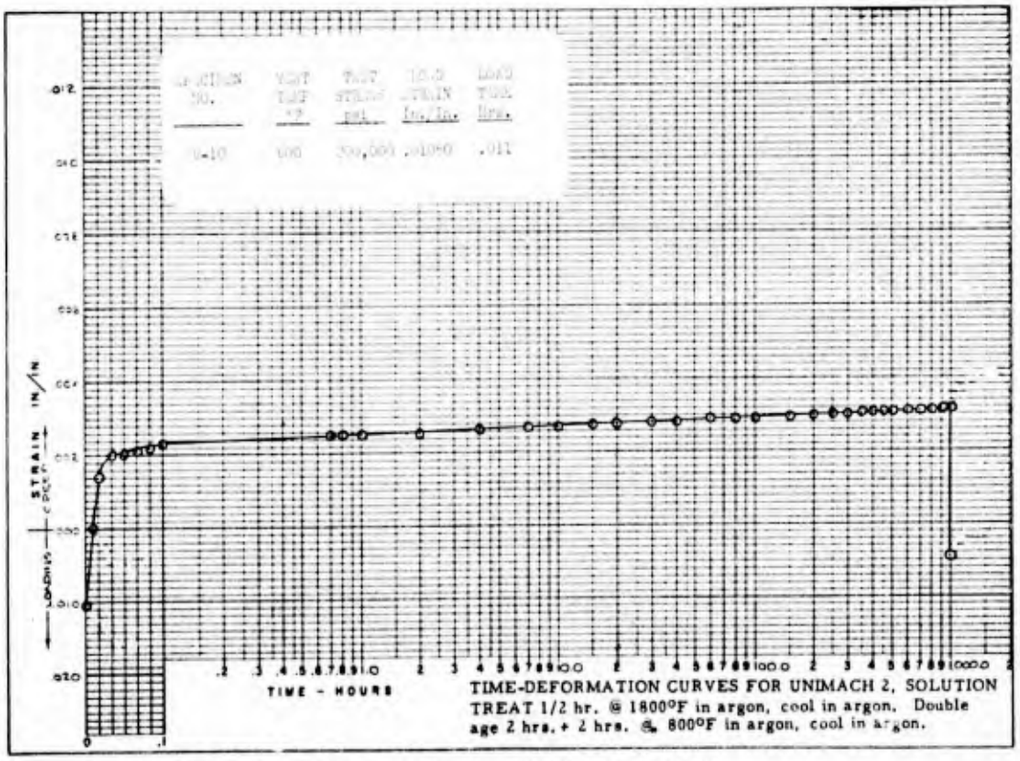

FIGURE 68 - TEST CURVE UNIMACH 2 6000°F 200,000 psi

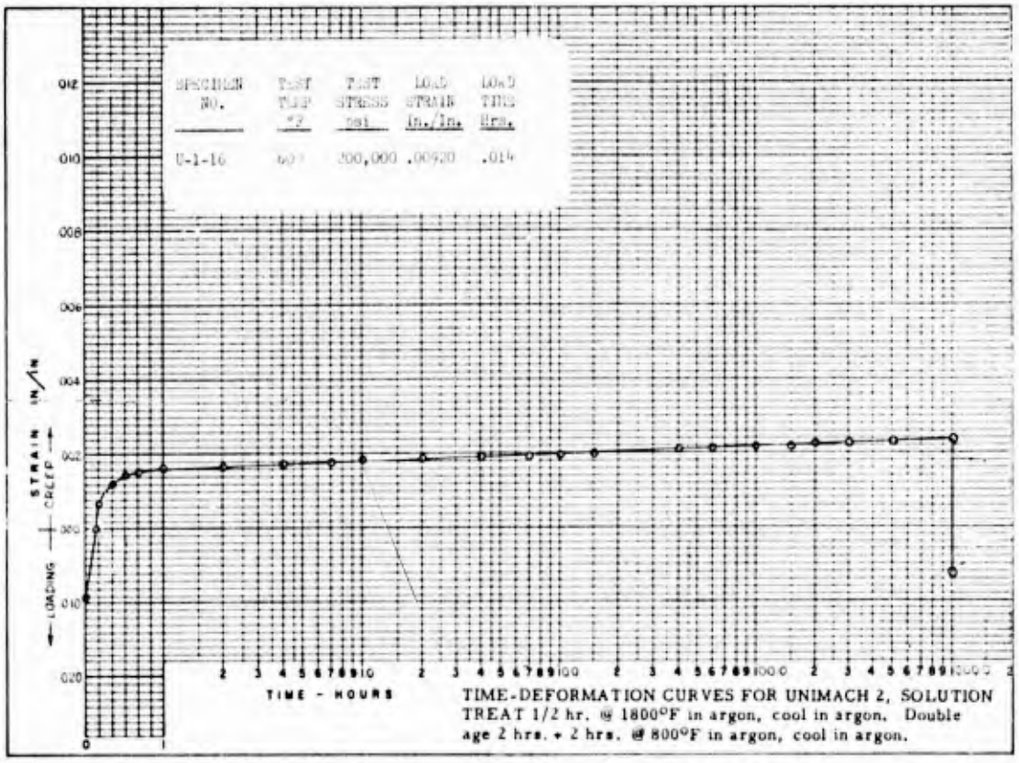

FIGURE 69 - TEST CURVE UNIMACH 2 600°F 200,000 psi

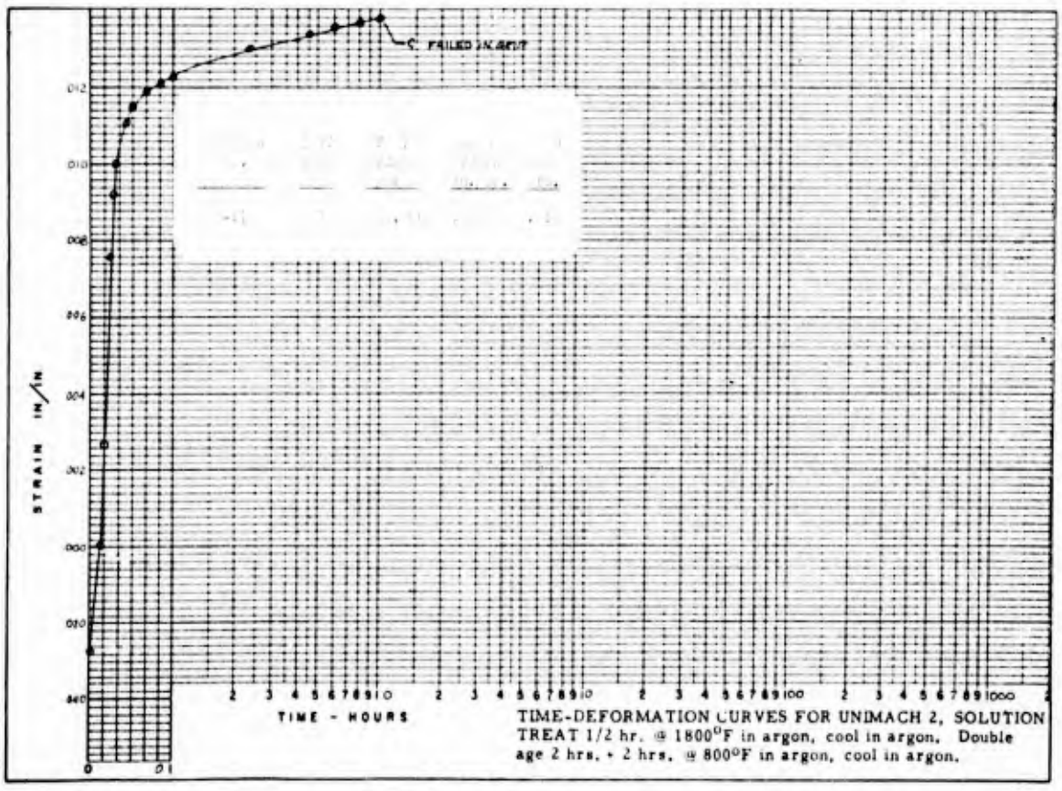

FIGURE 70 - TEST CURVE UNIMACH 2 600°F 250,000 psi

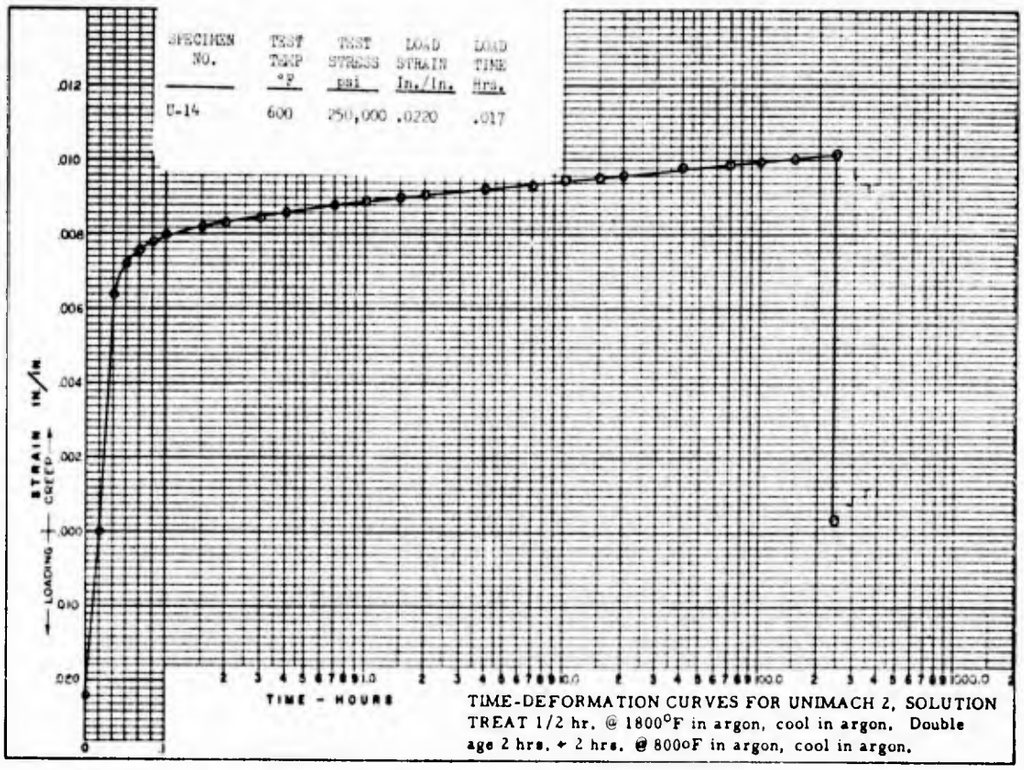

FIGURE 71 - TEST CURVE UNIMACH 2 600°F 250,000 psi

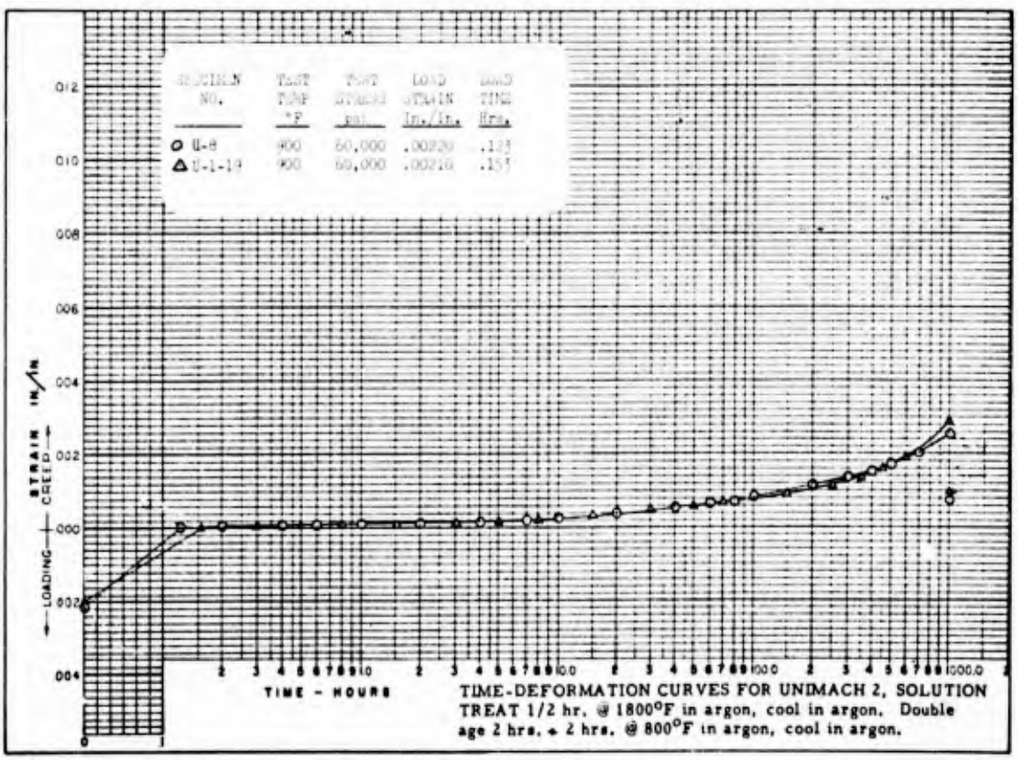

FIGURE 72 - TEST CURVES UNIMACH 2 900°F 60,000 psi

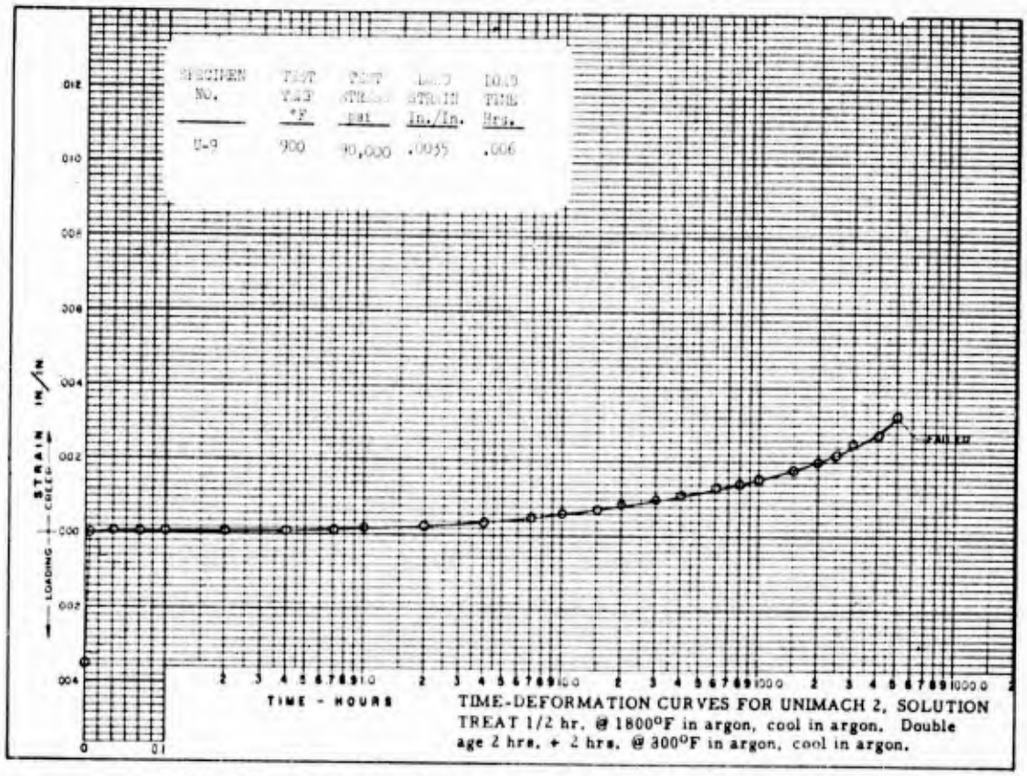

FIGURE 73 - TEST CURVE UNIMACH 2 900°F 90,000 psi

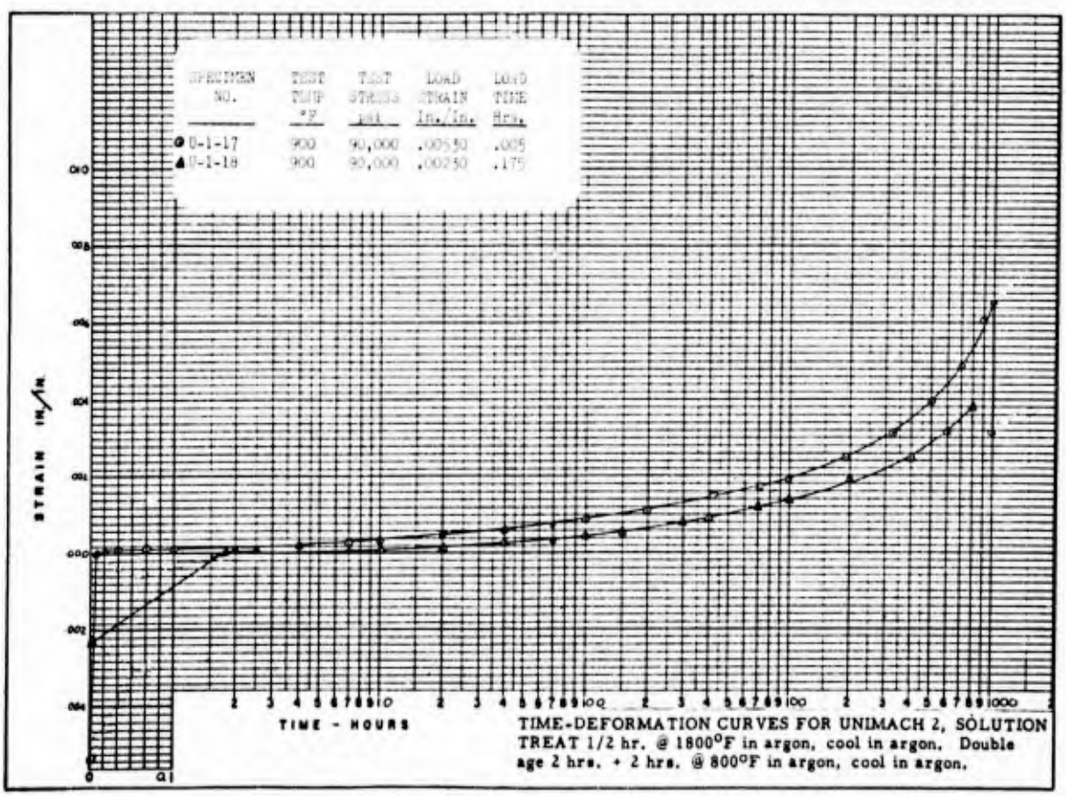

FIGURE 74 - TEST CURVES UNIMACH 2 900°F 90,000 psi

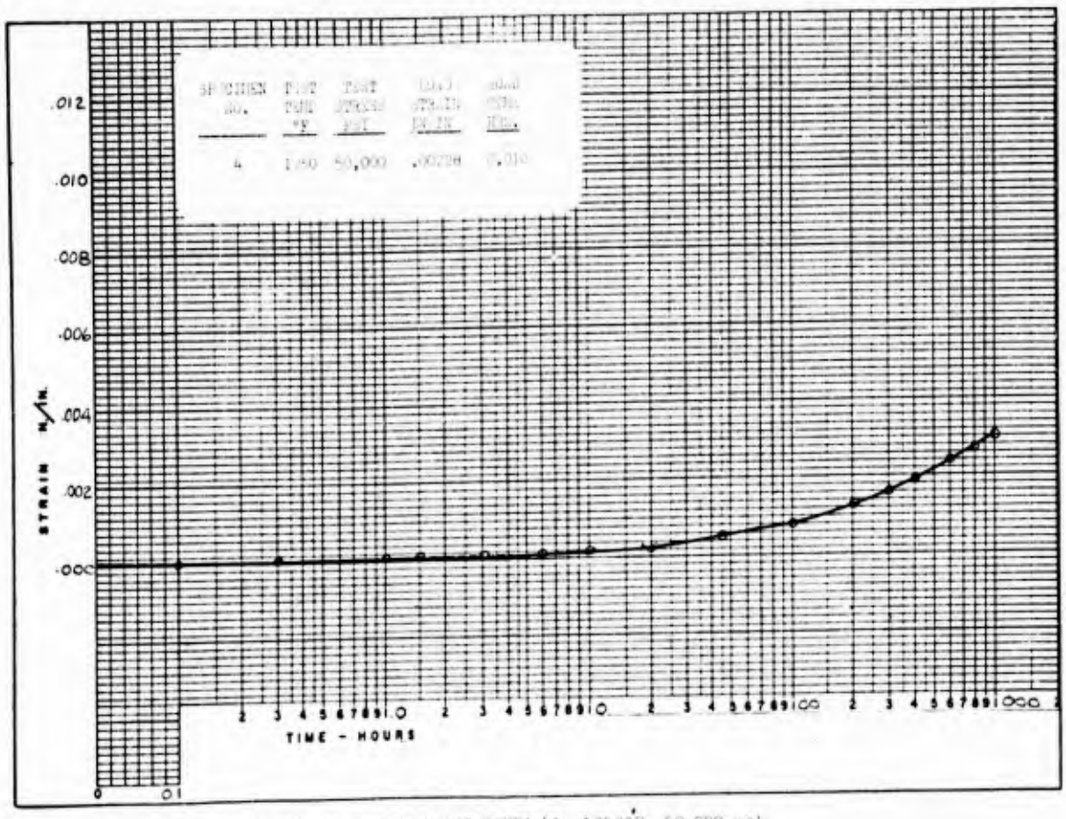

FIGURE 75 - TEST CURVE RENE' 41 1250°F 50,000 psi

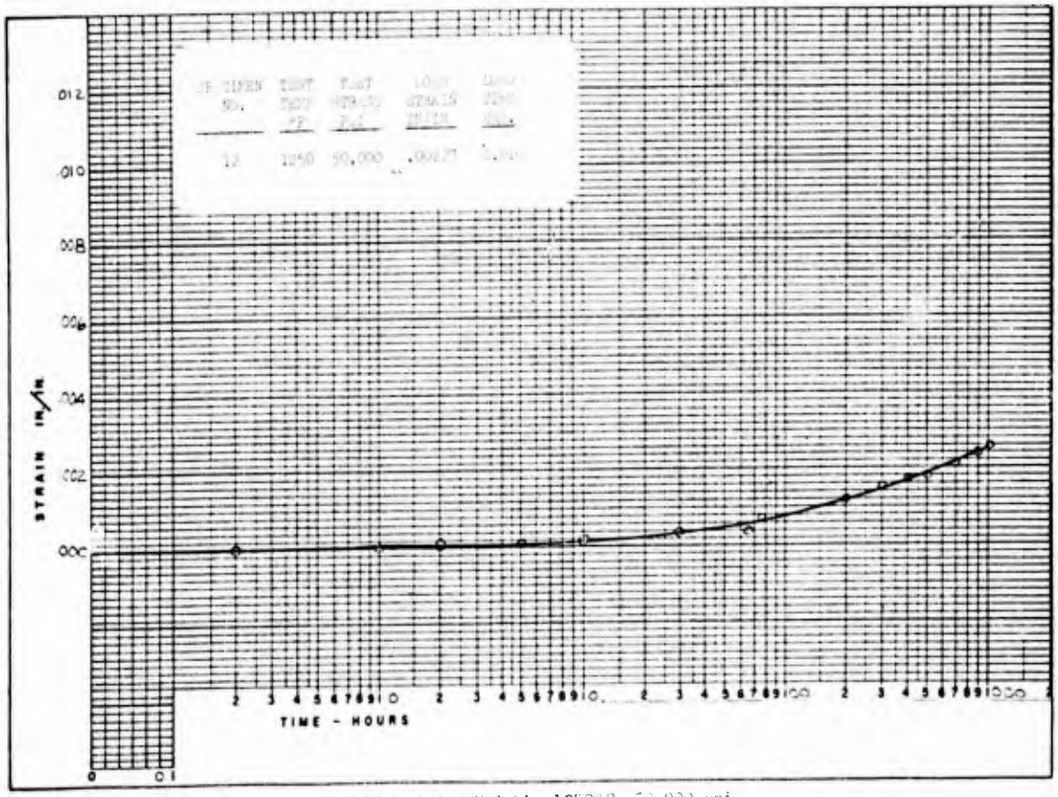

FIGURE 76 - TEST CURVE RENE' 41 1250°F 50,000 psi

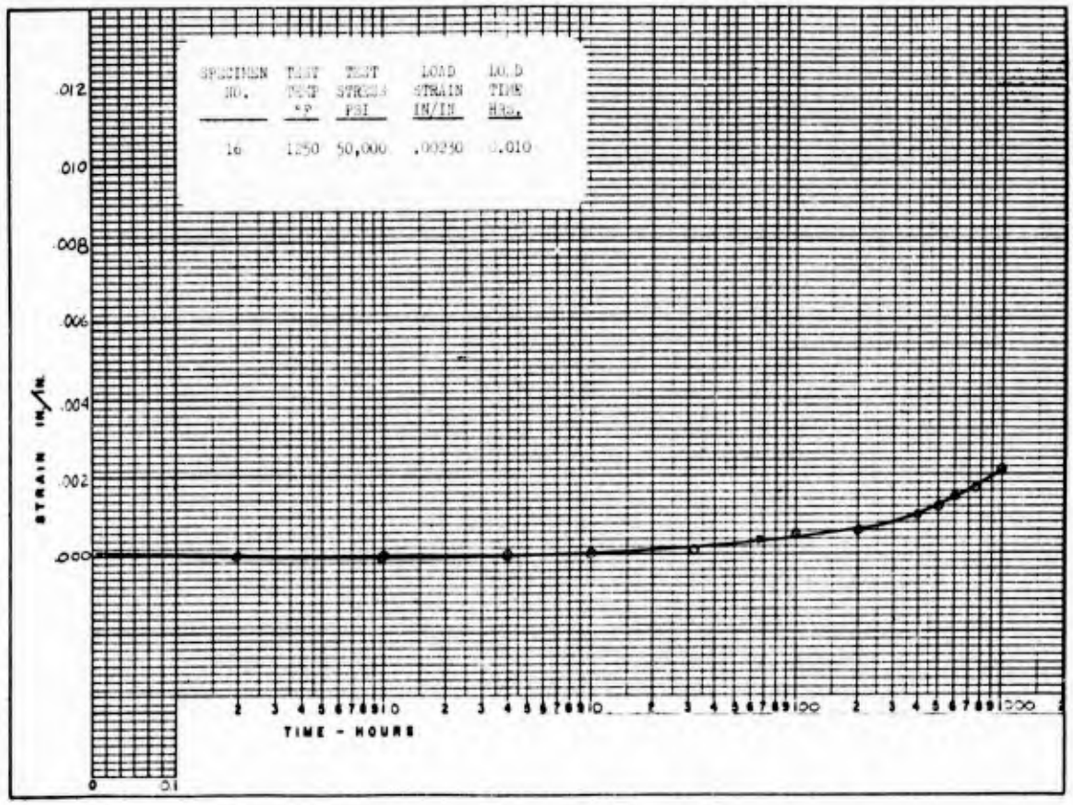

FIGURE 77 - TEST CURVE RENE' 41 1250°F 50,000 psi

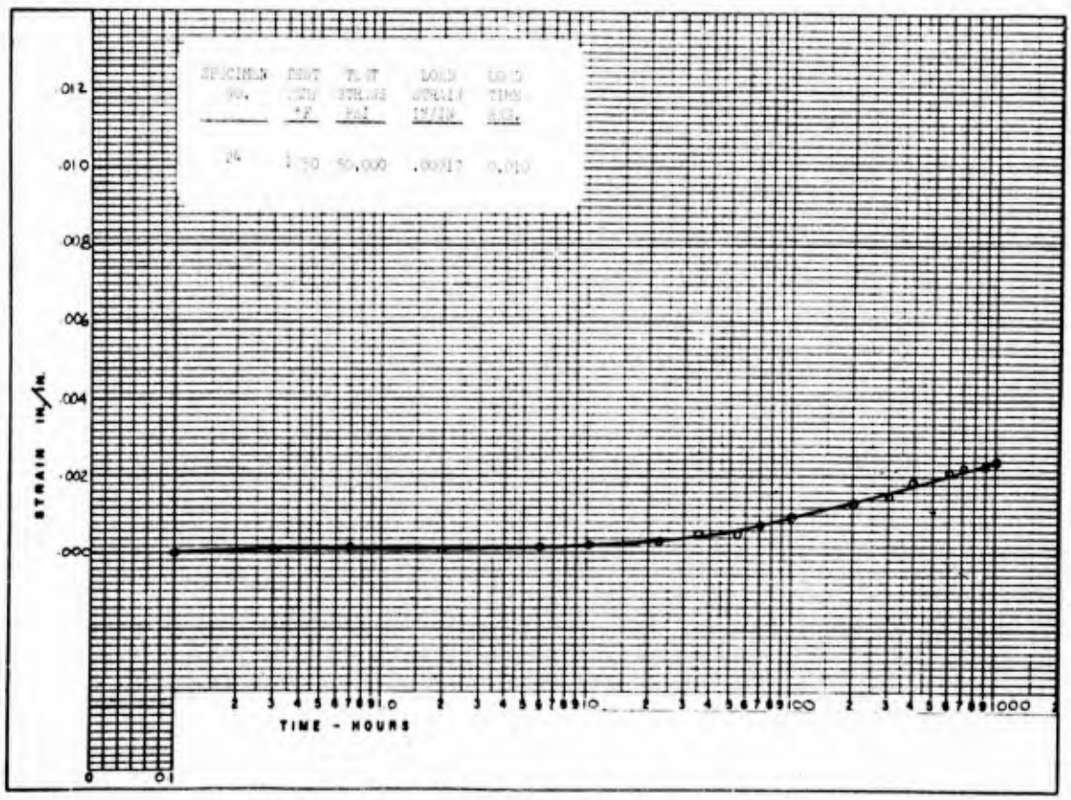

FIGURE 78 - TEST CURVE RENE' 41 1250°F 50,000 psi

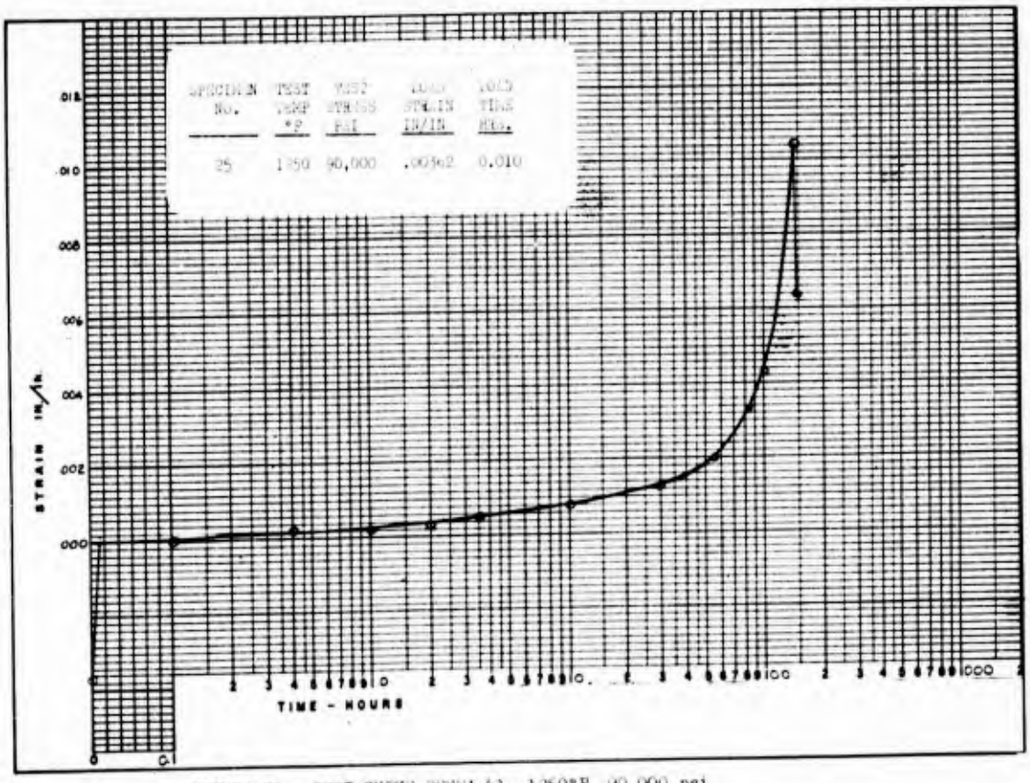

FIGURE 79 - TEST CURVE RENE' 41 1250°F 90,000 psi

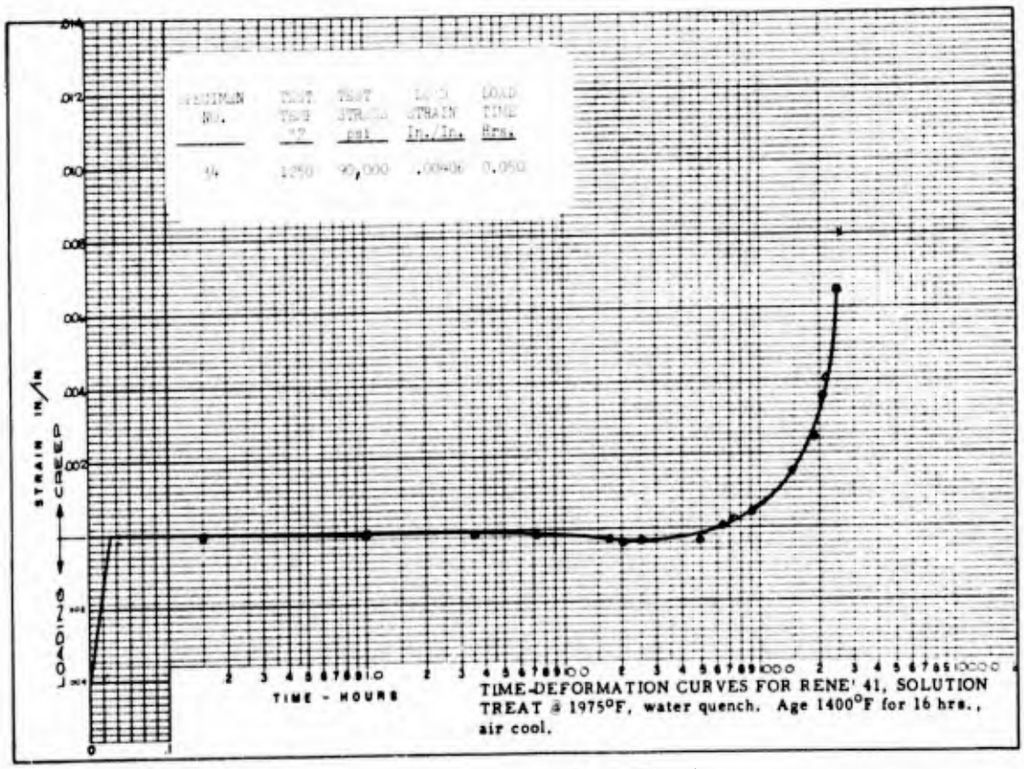

FIGURE 80 - TEST CURVE RENE' 41 1250°F 90,000 psi

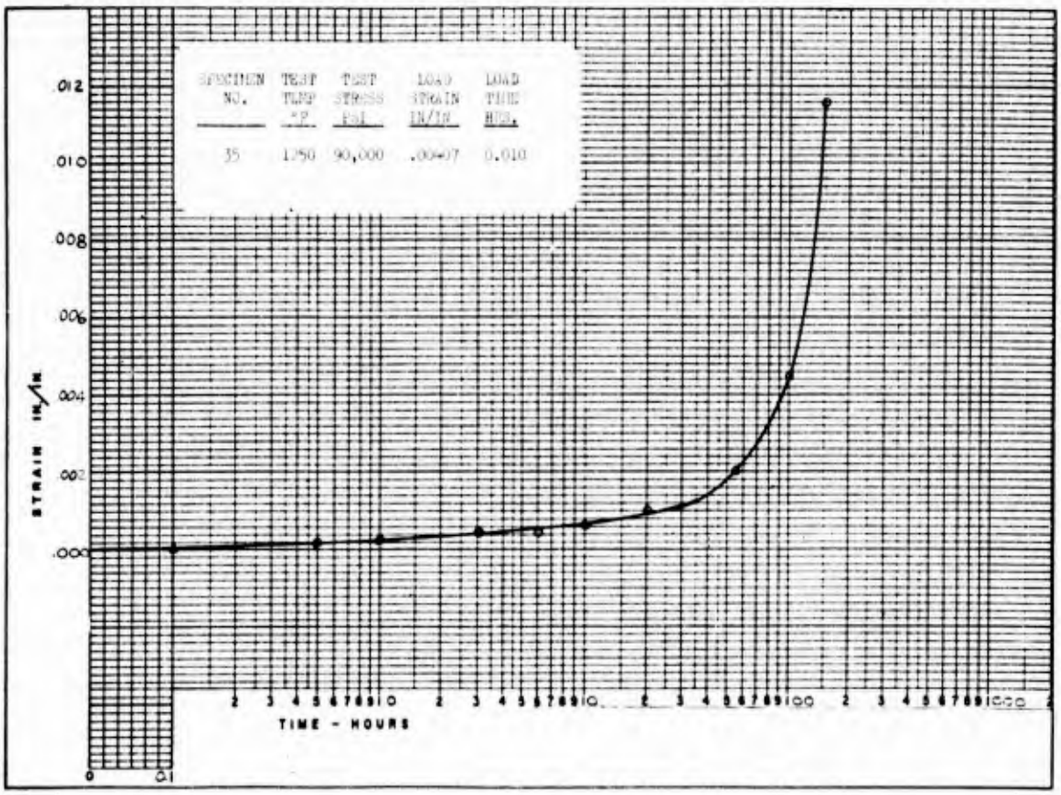

FIGURE 81 - TEST CURVE RENE' 41 1250°F 90,000 psi

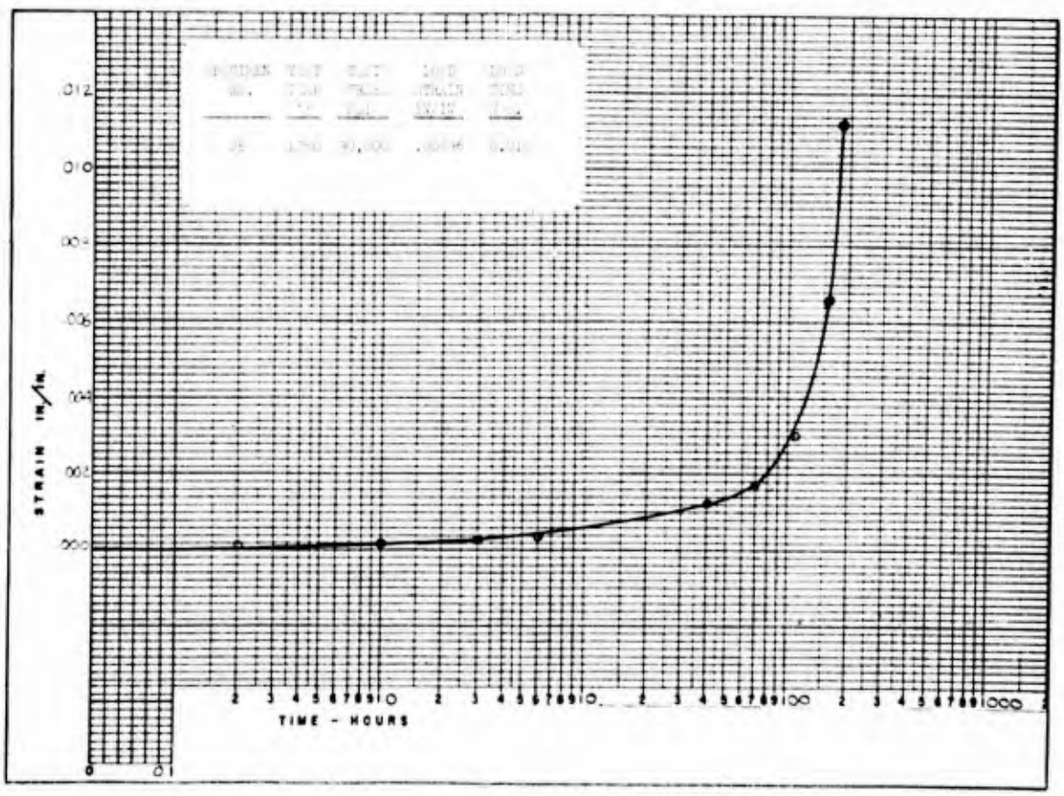

FIGURE 82 - TEST CURVE RENE' 41 1250°F 90,000 psi

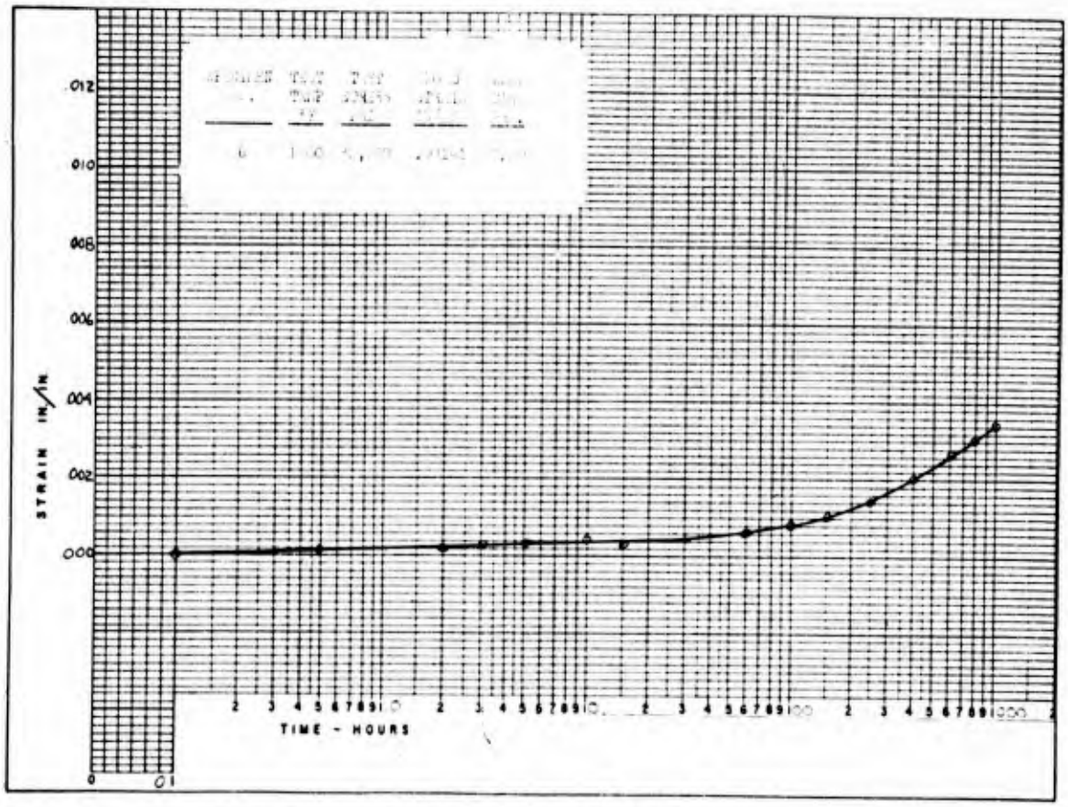

FIGURE 83 - TEST CURVE RENE' 41 1400°F 30,000 psi

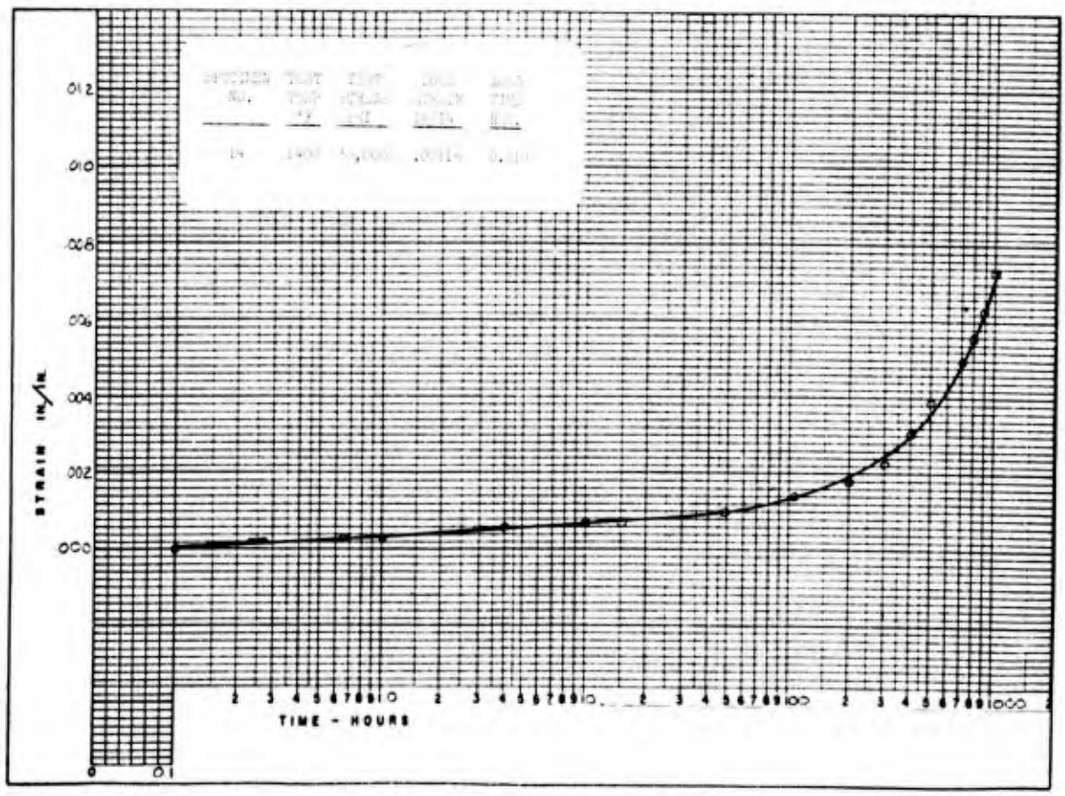

FIGURE 84 - TEST CURVE RENE' 41 1400°F 30,000 psi

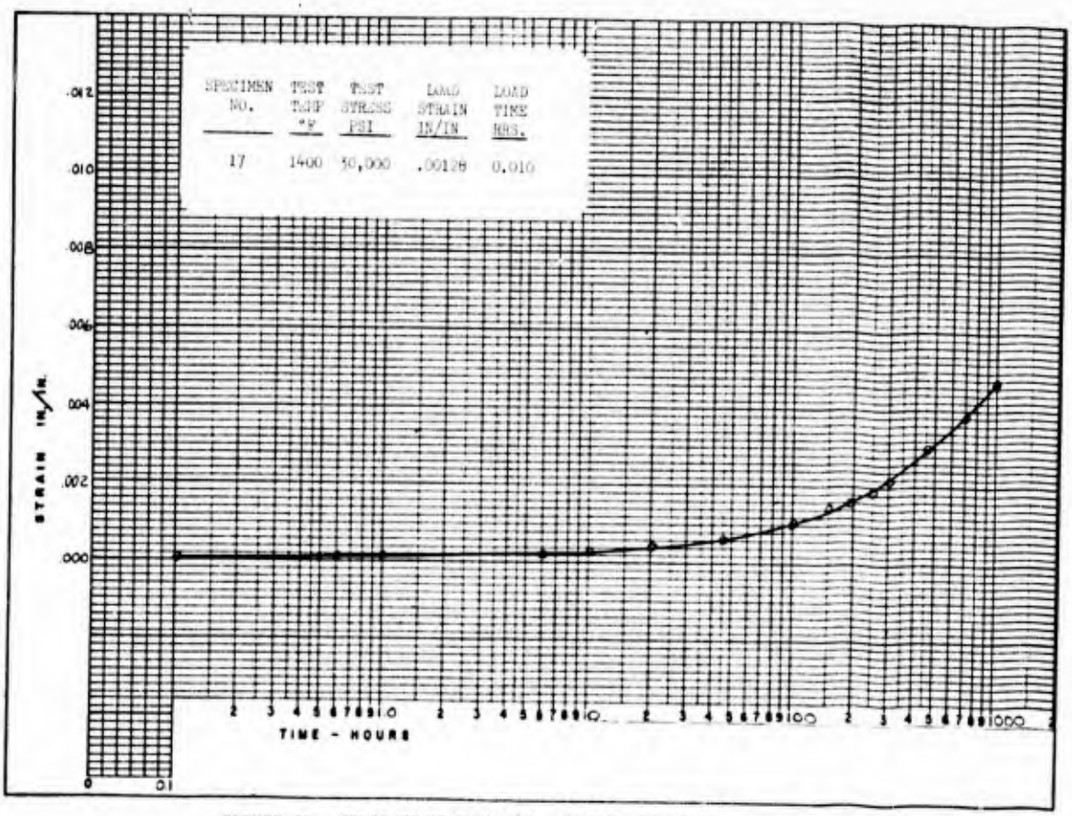

FIGURE 85 - TEST CURVE RENE' 41 1400°F 50,000 psi

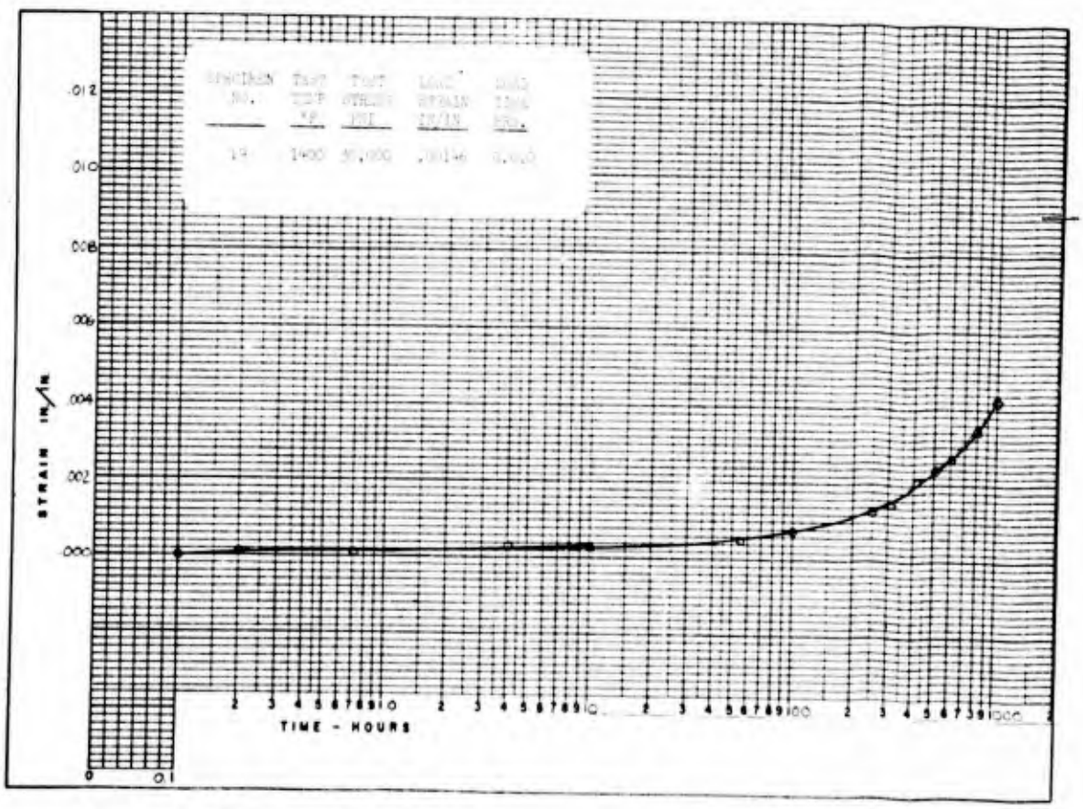

FIGURE 86 - TEST CURVE RENE' 41 1400°F 50,000 psi

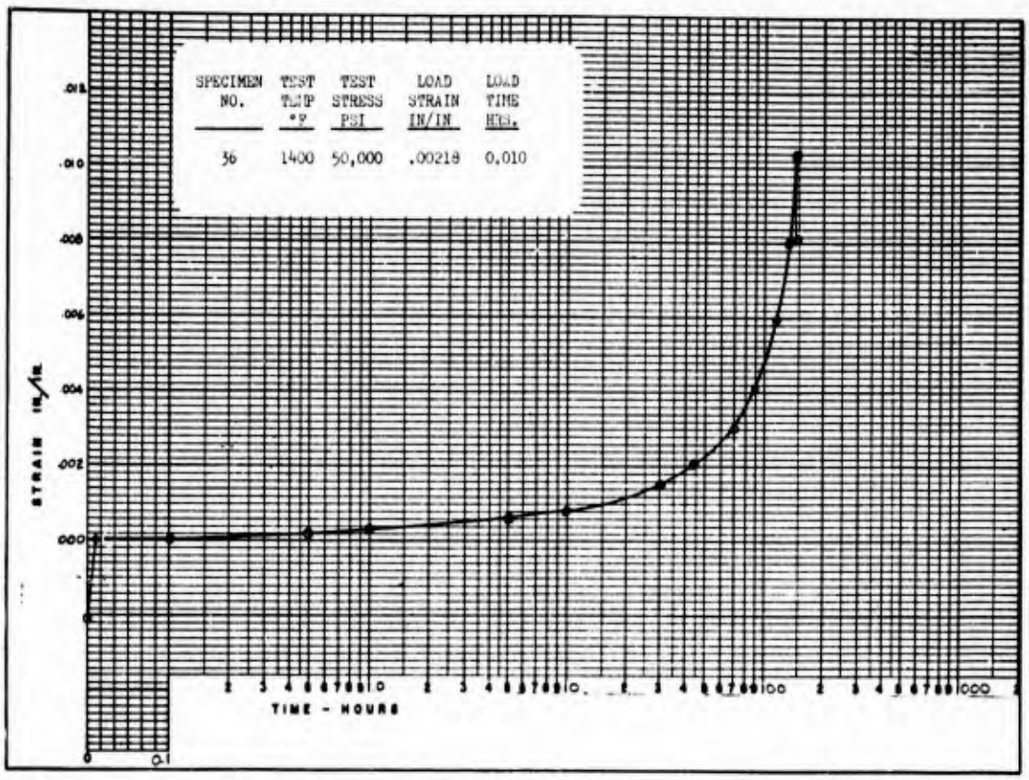

FIGURE 87 - TEST CURVE RENE' 41 1400°F 50,000 psi

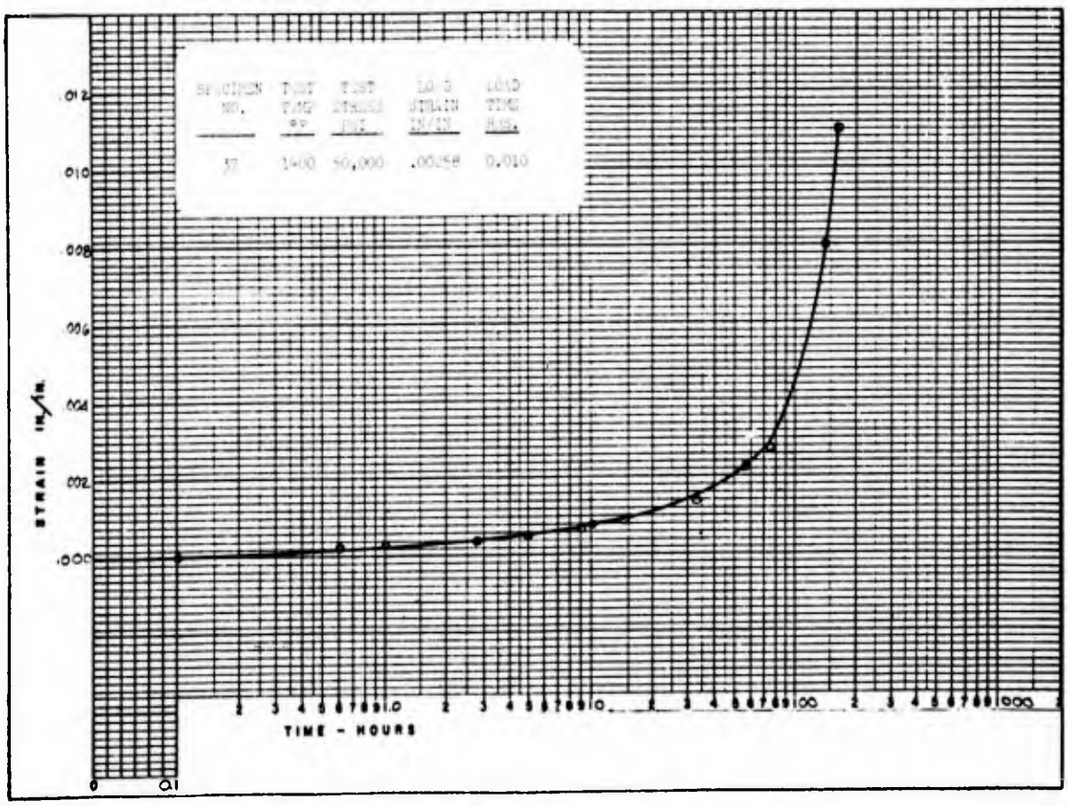

FIGURE 88 - TEST CURVE RENE' 41 1400°F 50,000 psi

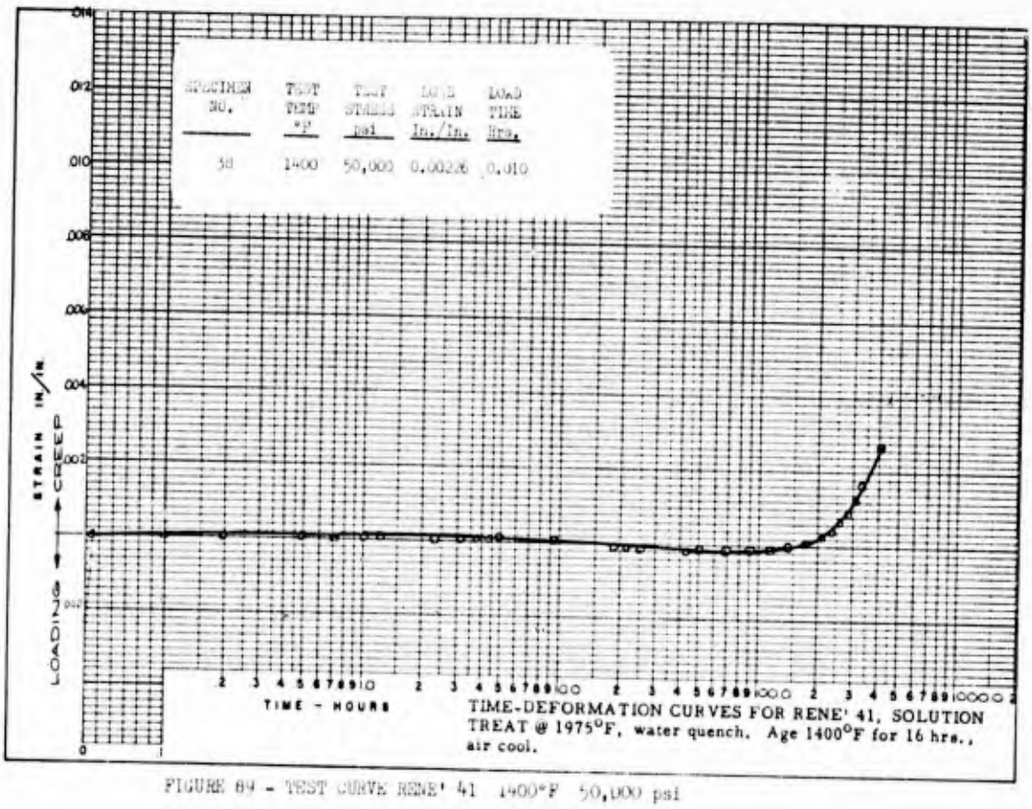

FIGURE 89 - TEST CURVE RENE' 41 1400°F 50,000 psi

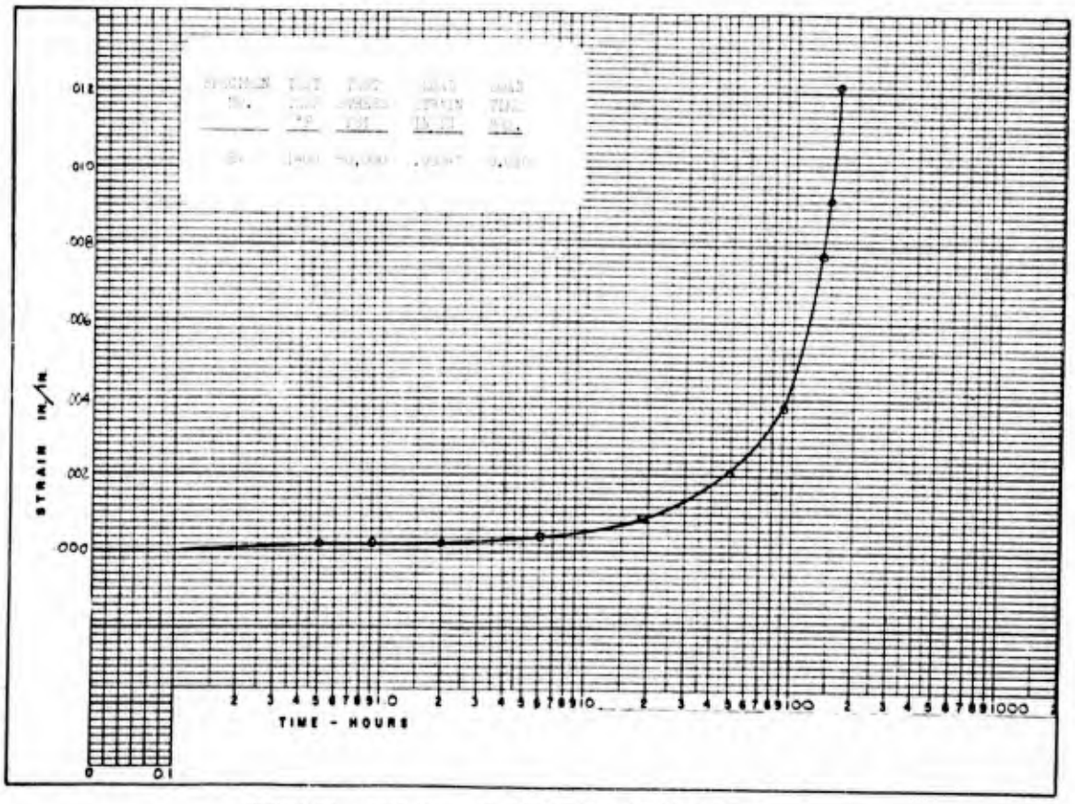

FIGURE 90 - TEST CURVE RENE' 41 1400°F 50,000 psi

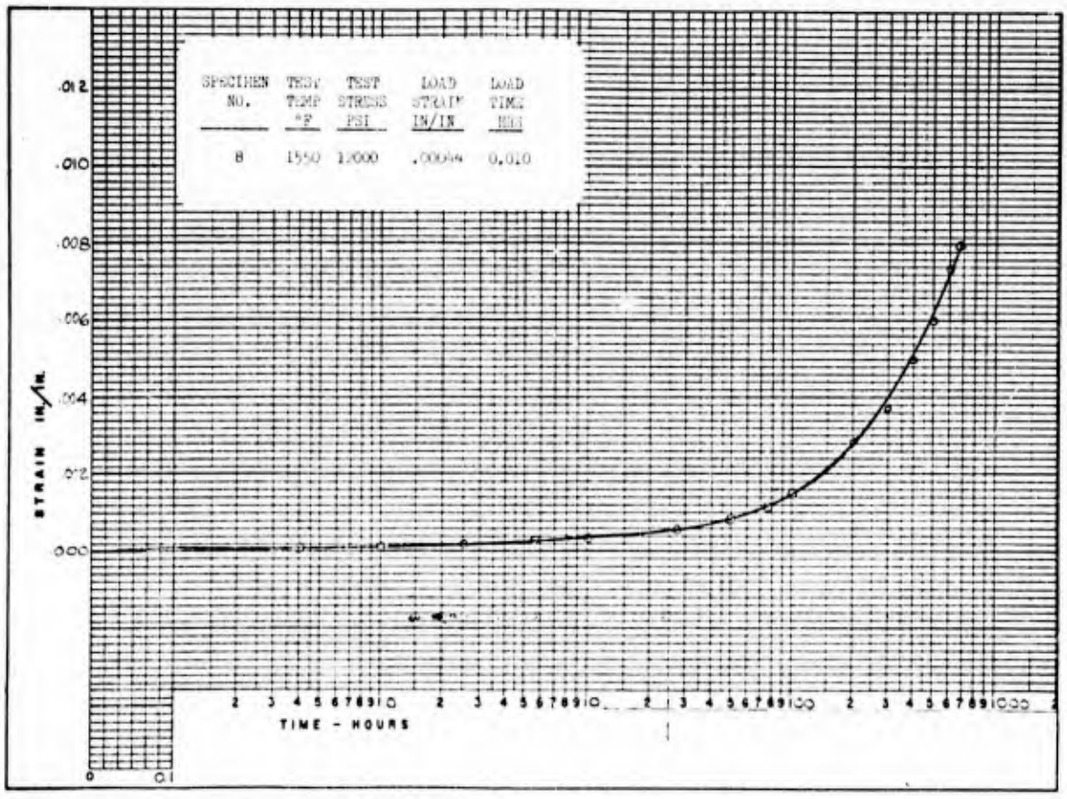

FIGURE 91 - TEST CURVE RENE' 41 1550°F 12,000 psi

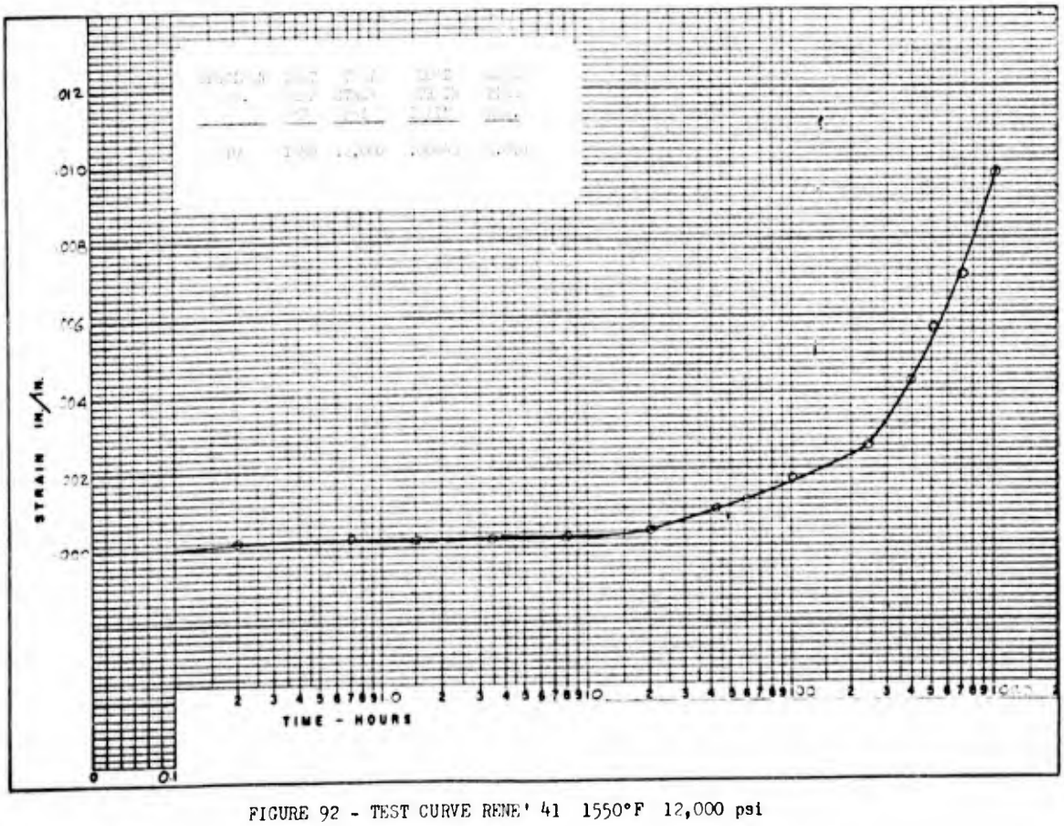

FIGURE 92 - TEST CURVE RENE' 41 1550°F 12,000 psi

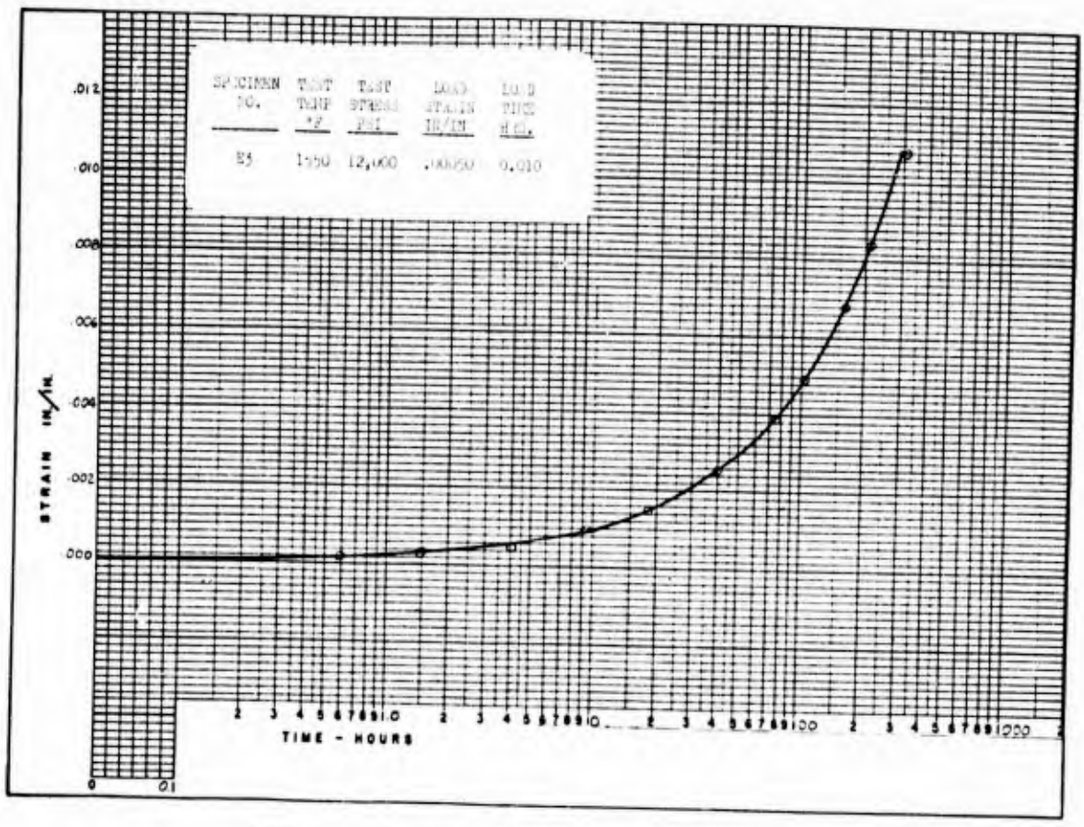

FIGURE 93 - TEST CURVE RENE' 41 1550°F 12,000 psi

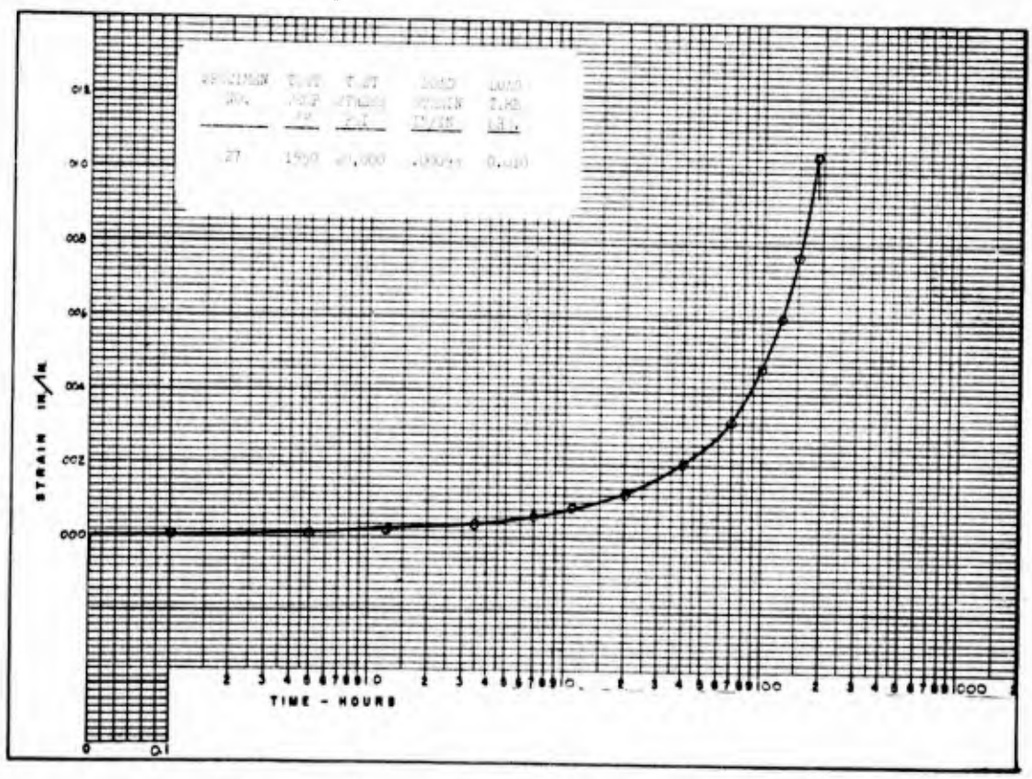

FIGURE 94 - TEST CURVE RENE' 41 1550°F 20,000 psi

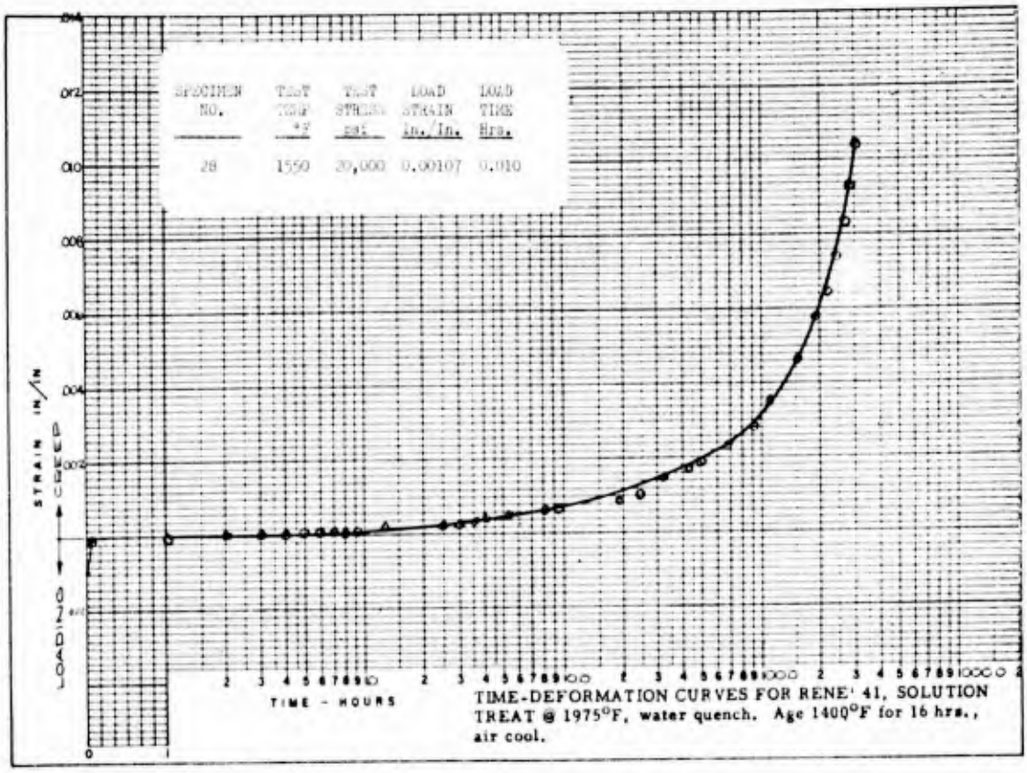

FIGURE 95 - TEST CURVE RENE' 41 1550°F 20,000 psi

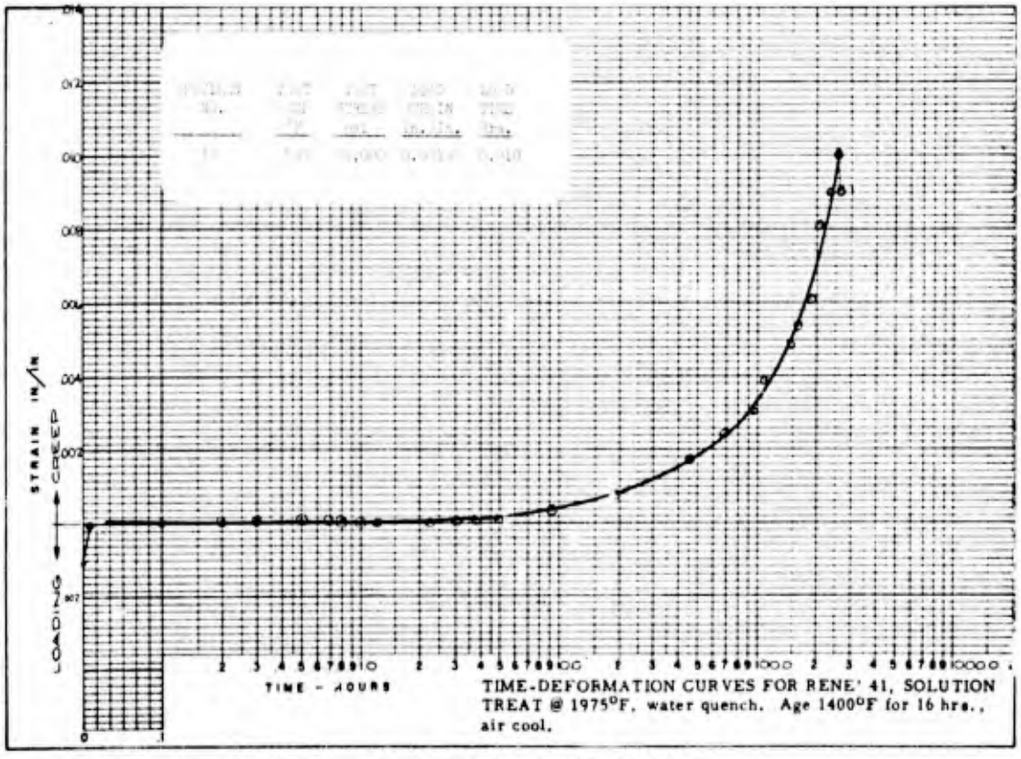

FIGURE 96 - TEST CURVE RENE' 41 1550°F 20,000 psi

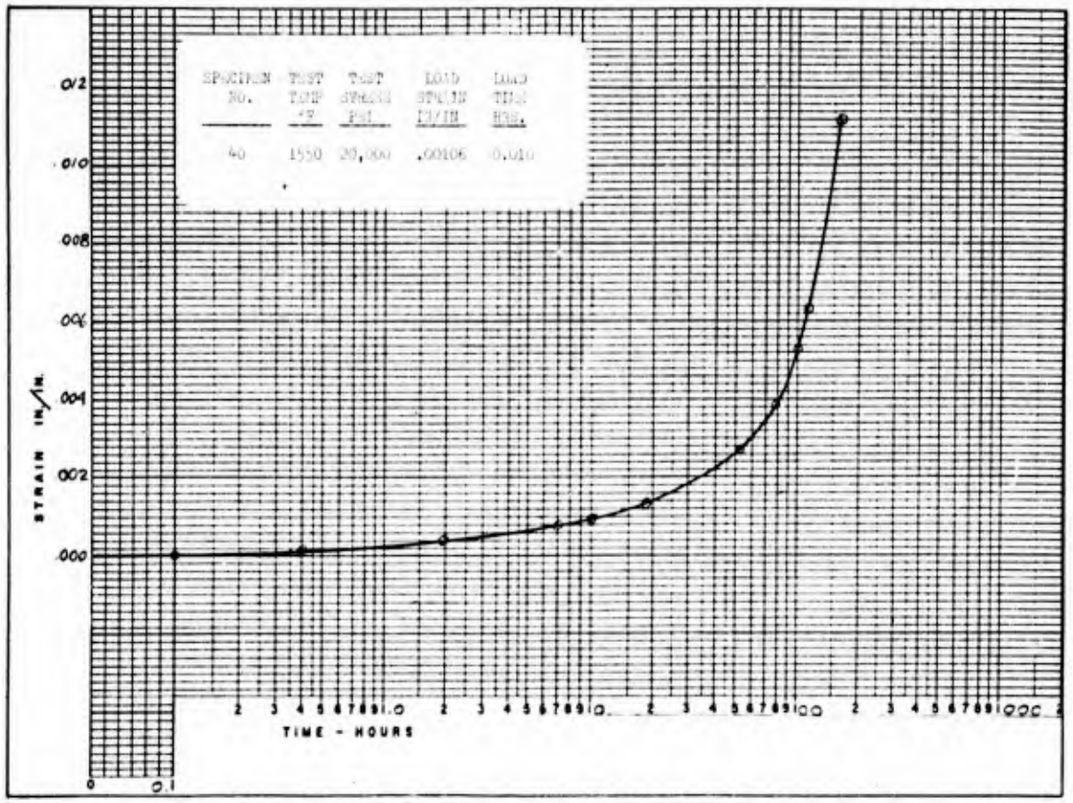

FIGURE 97 - TEST CURVE RENE' 41 1550°F 20,000 psi

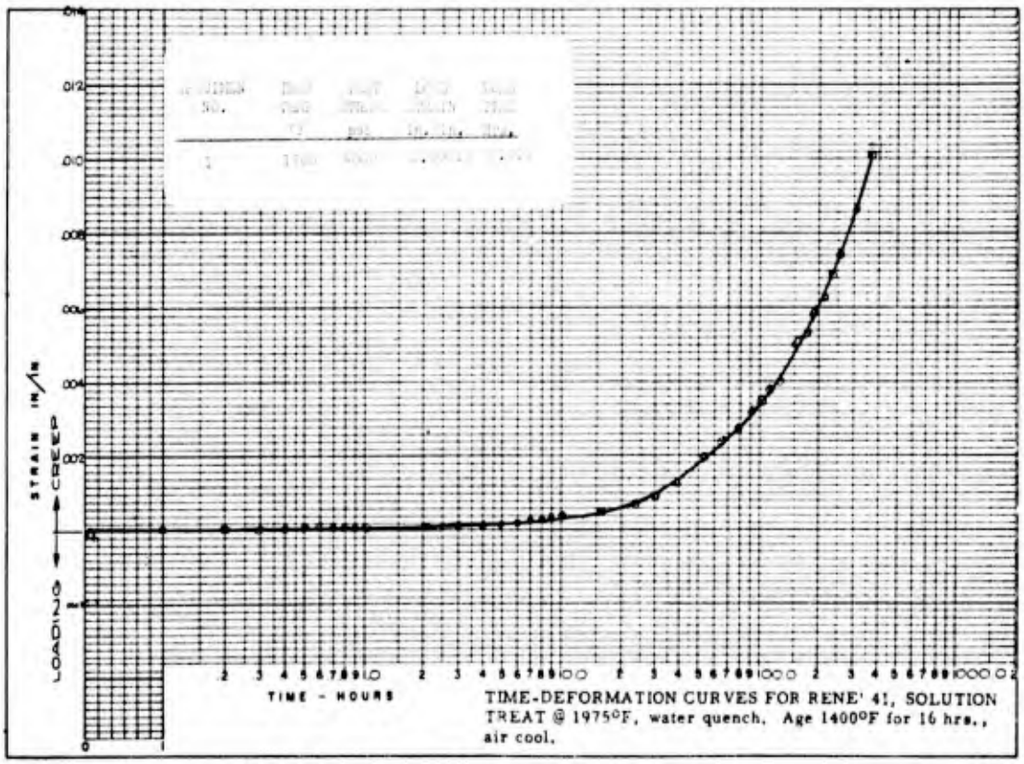

FIGURE 98 - TEST CURVE RENE' 41 1700°F 4,000 psi

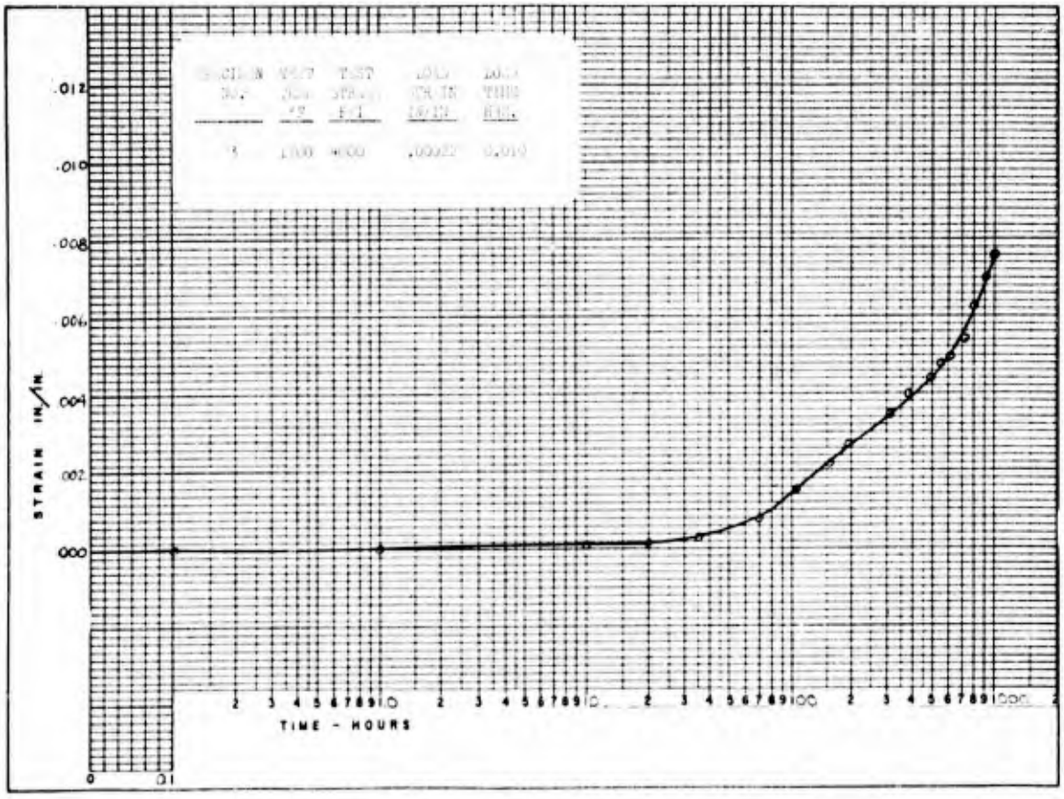

FIGURE 99 - TEST CURVE RENE' 41 1700°F 4,000 psi

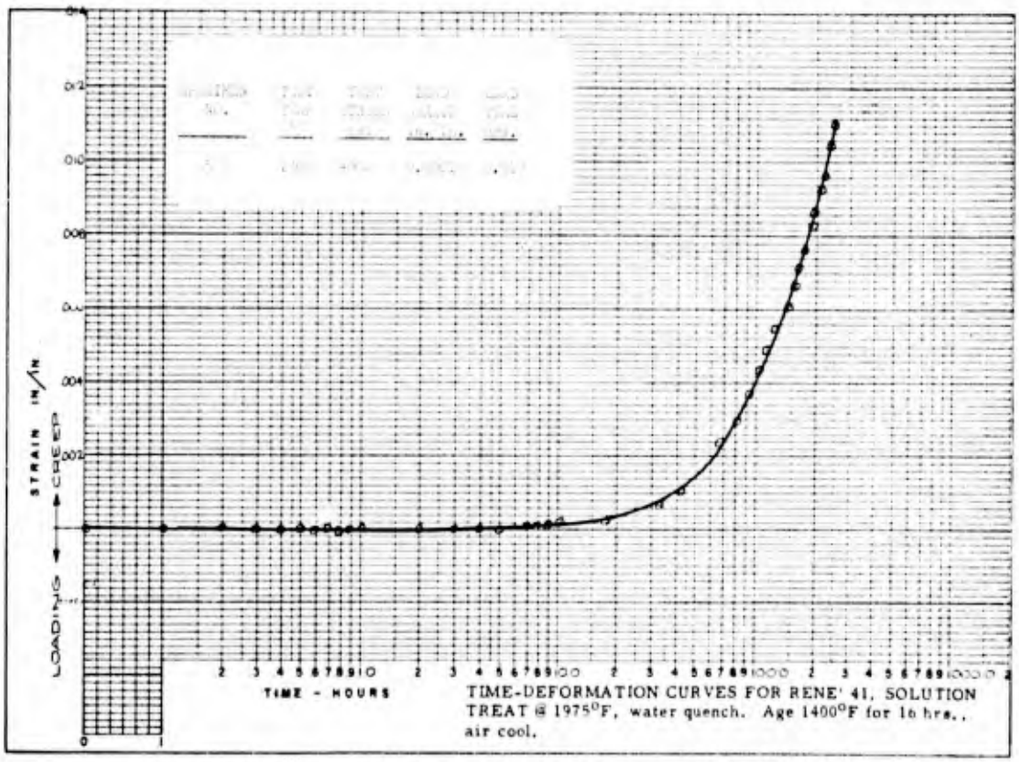

FIGURE 100 - TEST CURVE RENE' 41 1700°F 4,000 psi

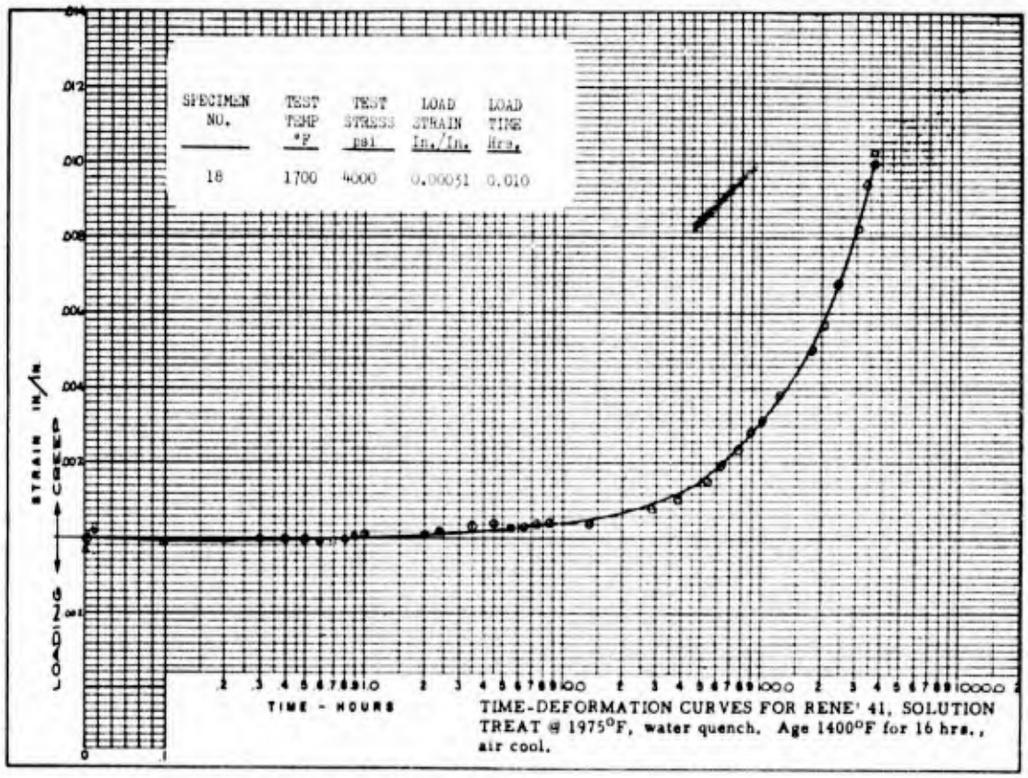

FIGURE 101 - TEST CURVE RENE' 41 1700°F 4,000 psi

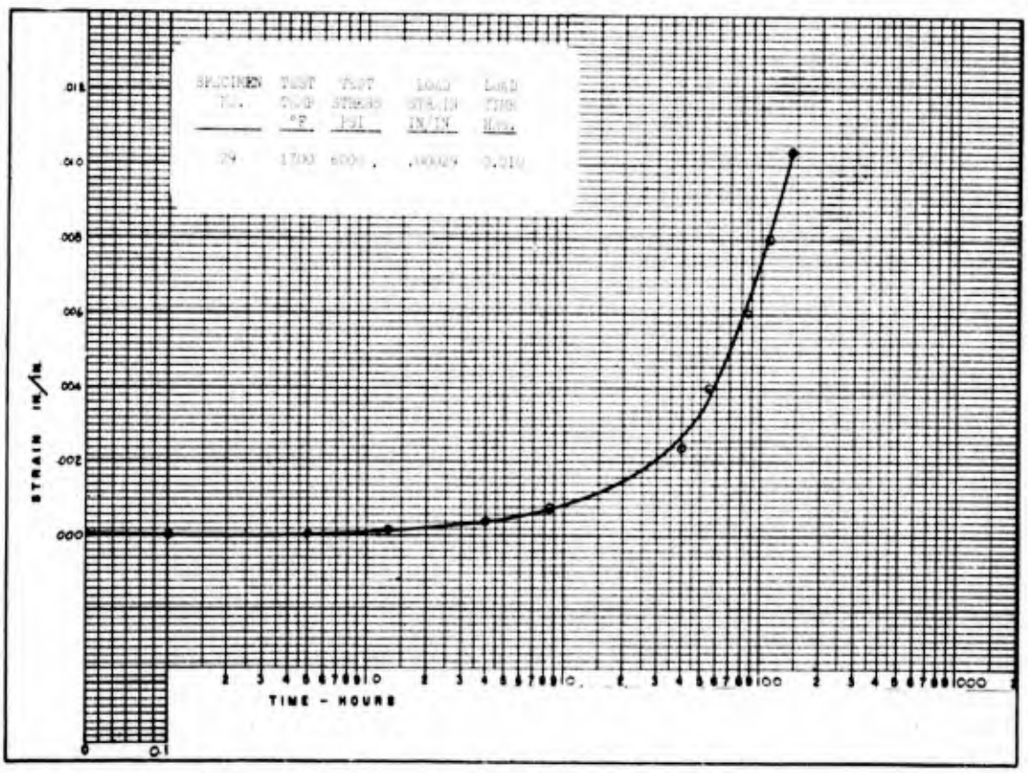

FIGURE 102 - TEST CURVE RENE' 41 1700°F 6,000 psi

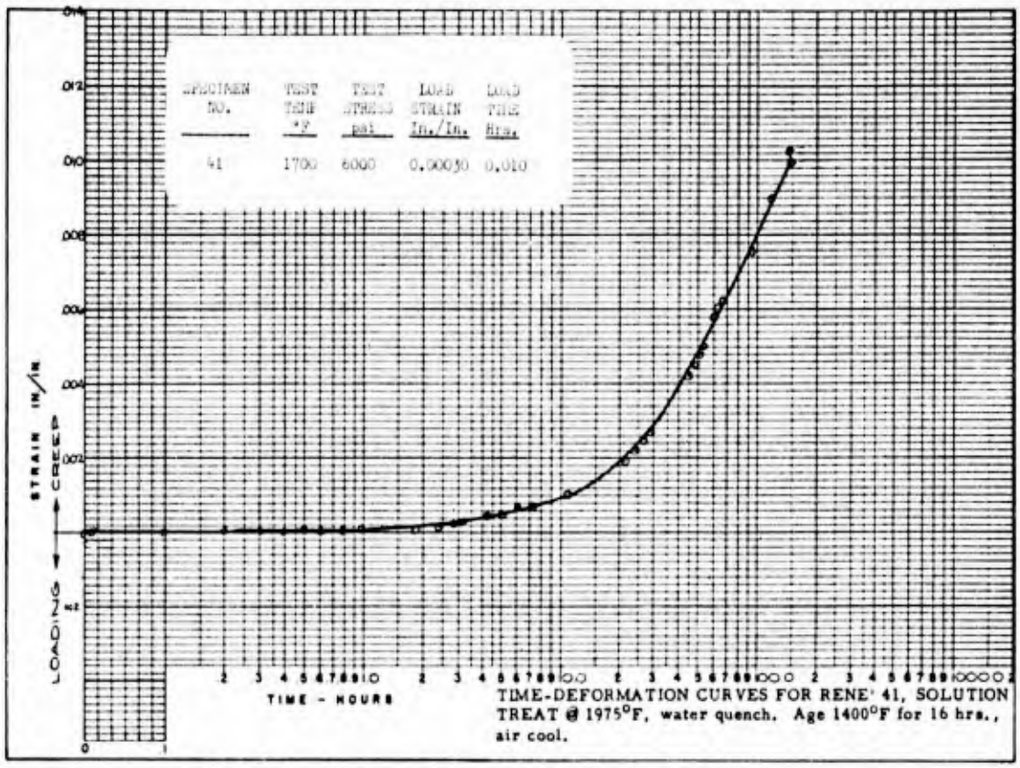

FIGURE 103 - TEST CURVE RENE' 41 1700°F 6,000 psi

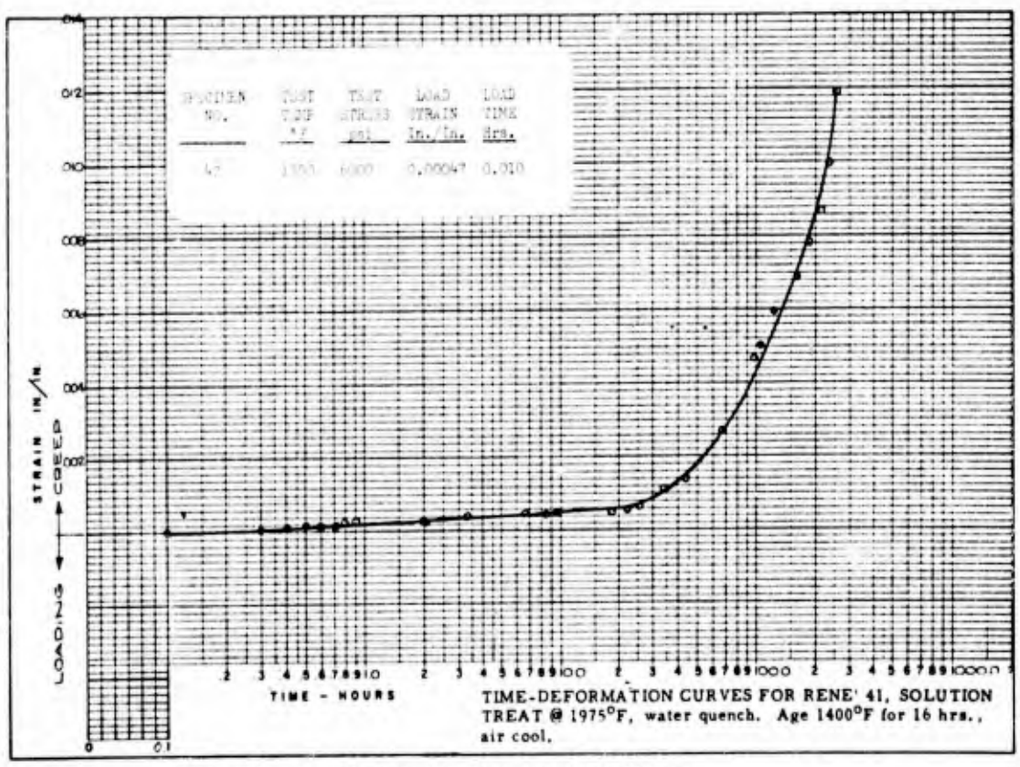

FIGURE 104 - TEST CURVE RENE' 41 1700°F 6,000 psi

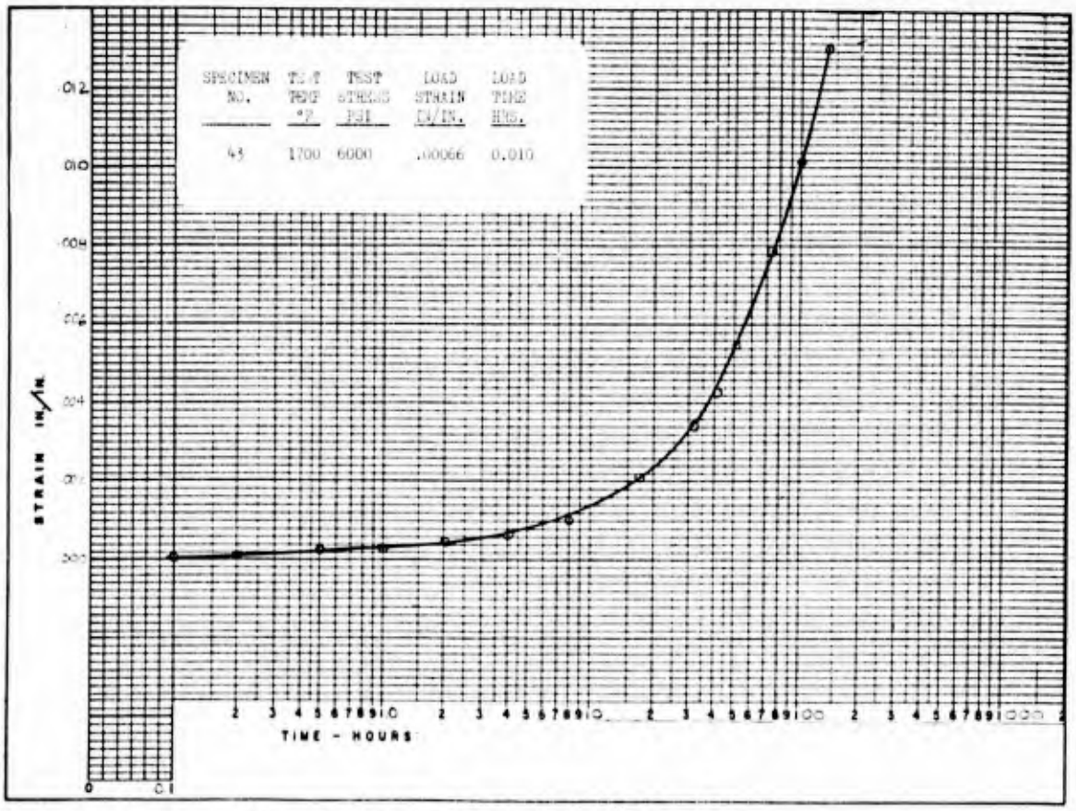

FIGURE 105 - TEST CURVE RENE' 41 1700°F 6,000 psi

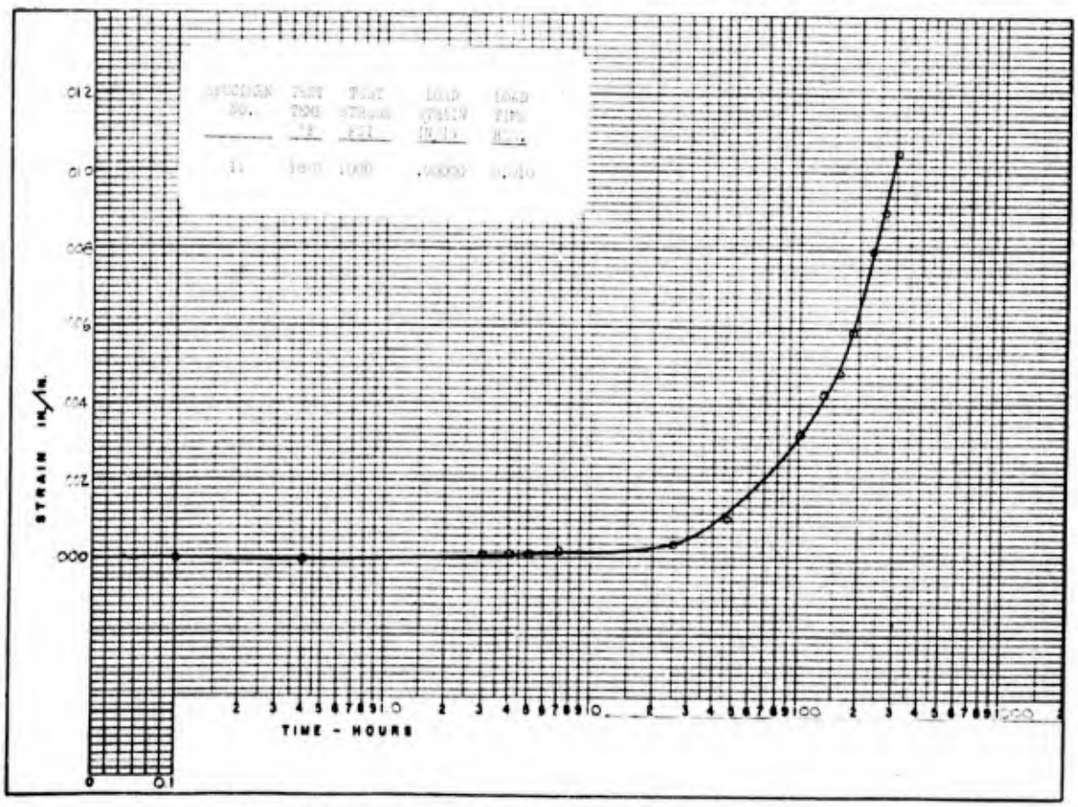

FIGURE 106 - TEST CURVE RENE' 41 1850°F 1000 psi

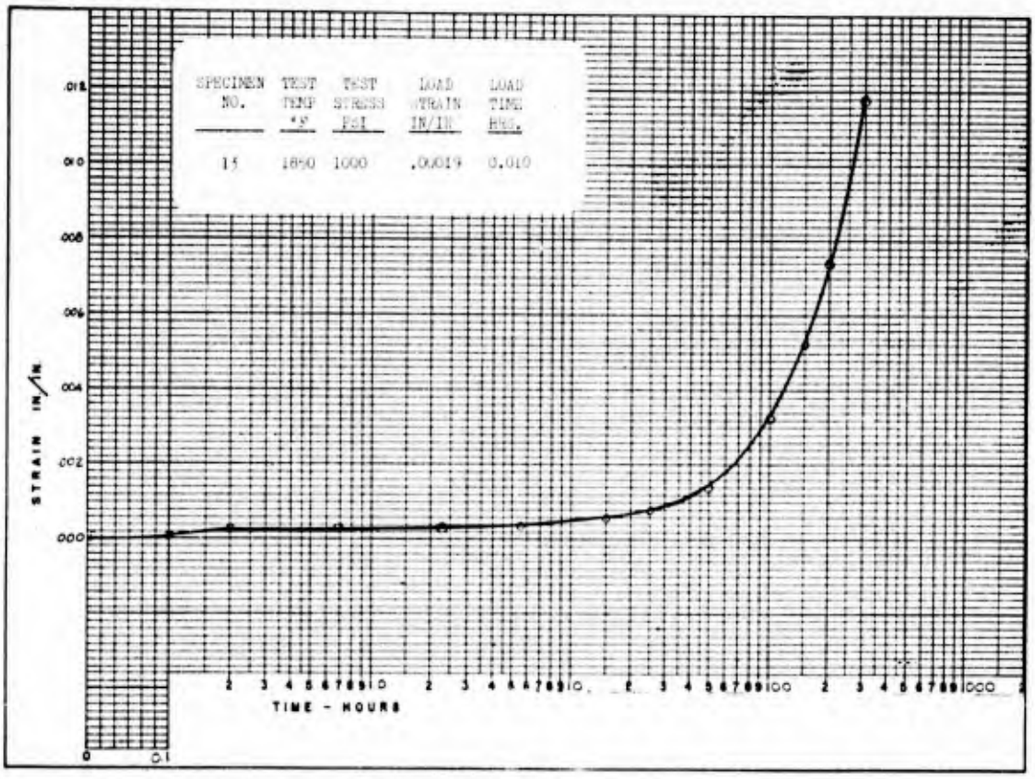

FIGURE 107 - TEST CURVE RENE' 41 1850°F 1000 psi

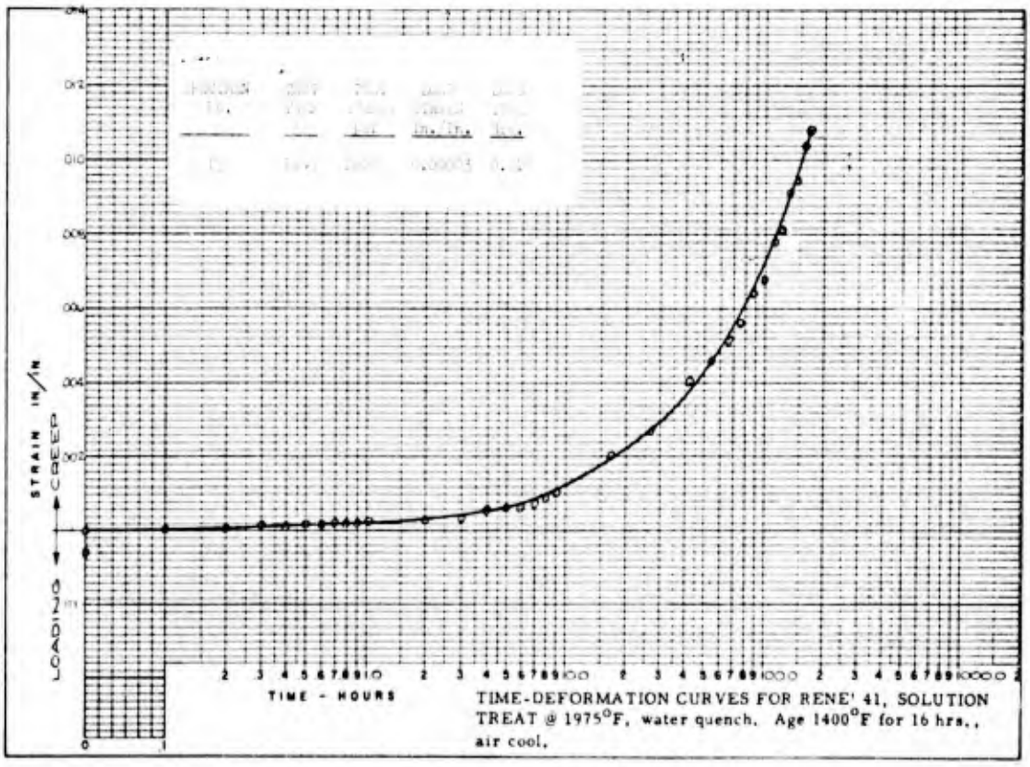

FIGURE 108 - TEST CURVE RENE' 41 1850°F 1000 psi

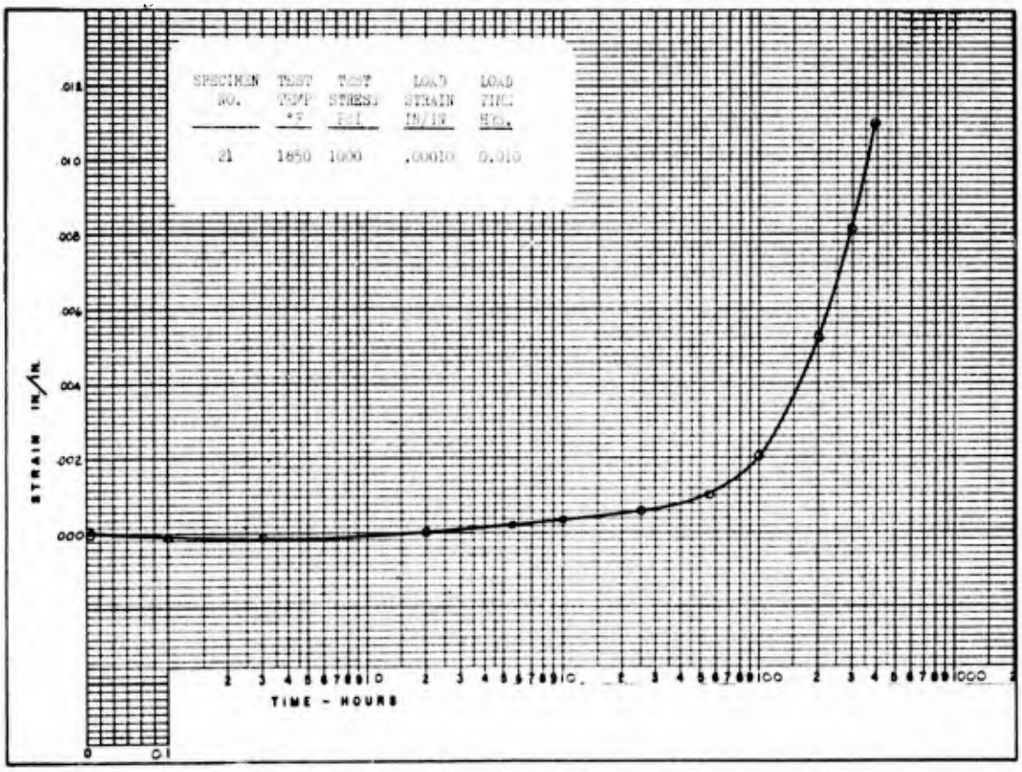

FIGURE 109 - TEST CURVE RENE' 41 1850°F 1000 psi

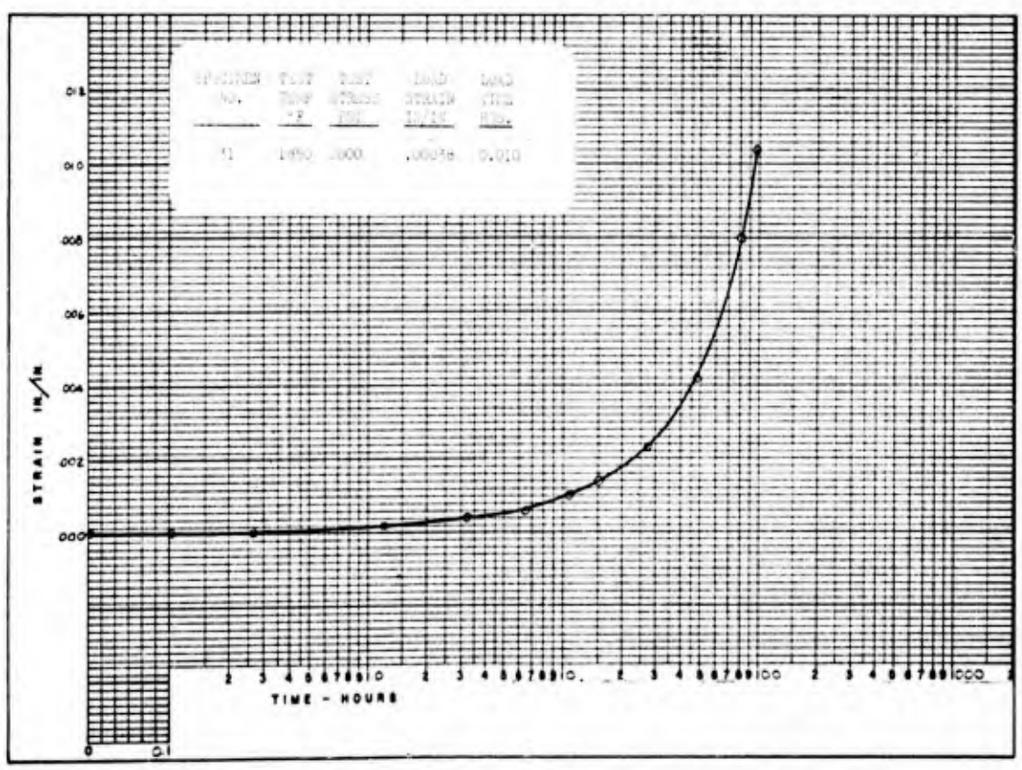

FIGURE 110 - TEST CURVE RENE' 41 1850°F 2,000 psi

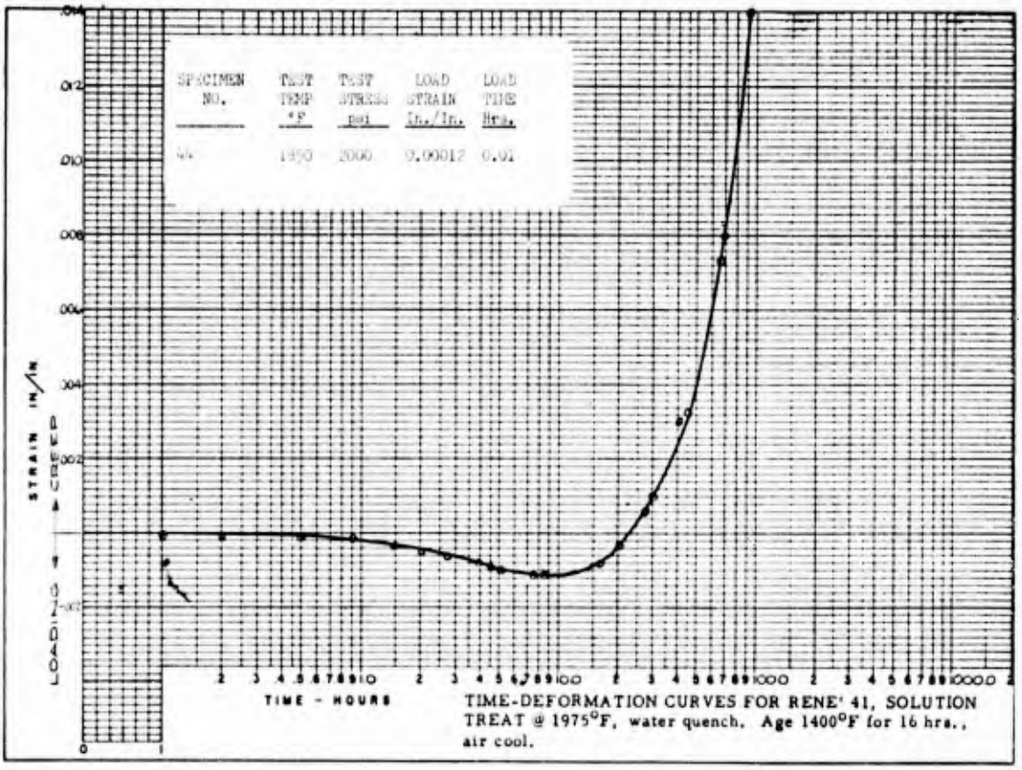

FIGURE 111 - TEST CURVE RENE' 41 1850°F 2,000 psi

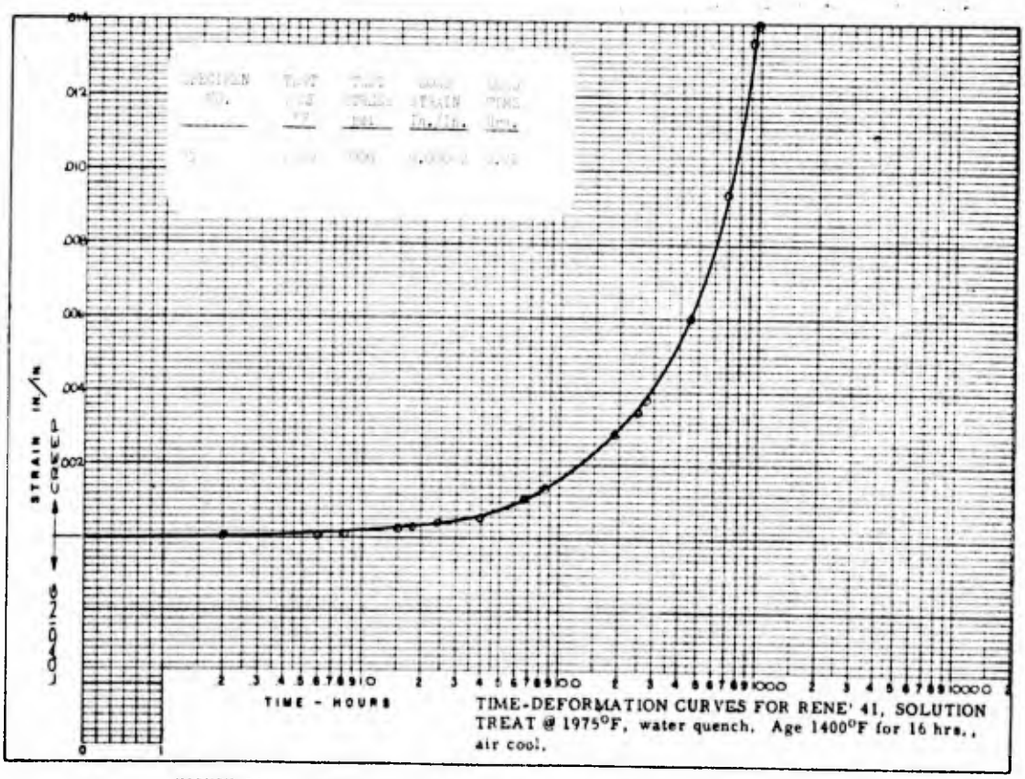

FIGURE 112 - TEST CURVE RENE' 41 1850°F 2000 psi

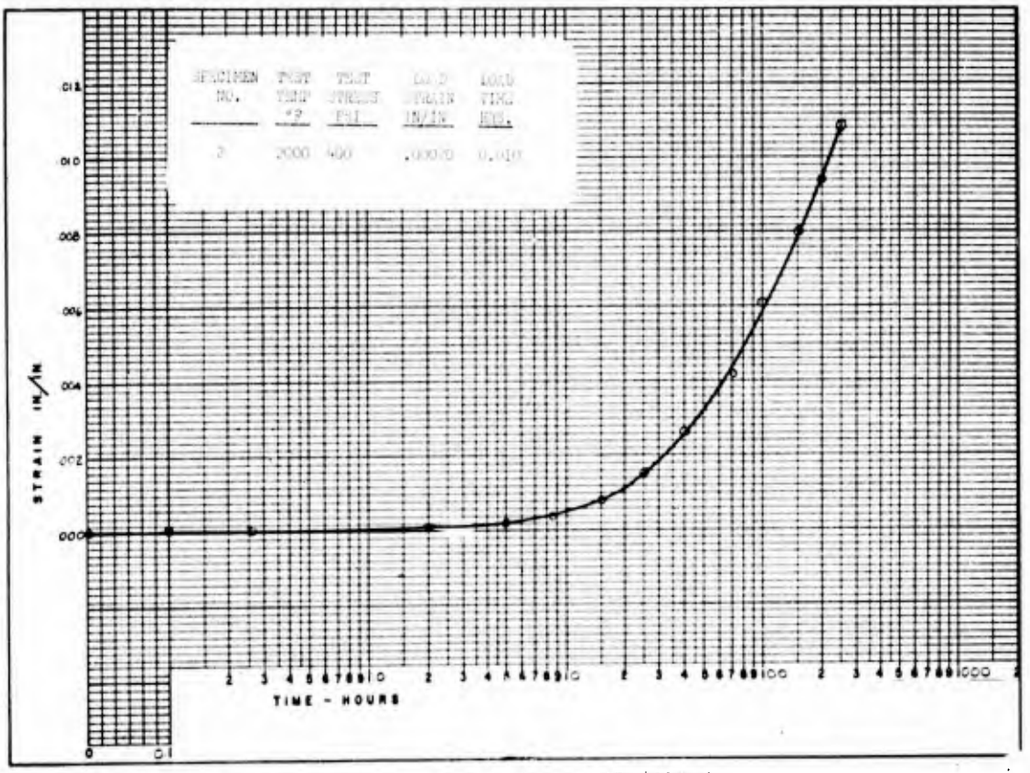

FIGURE 113 - TEST CURVE RENE' 41 2000°F 400 psi

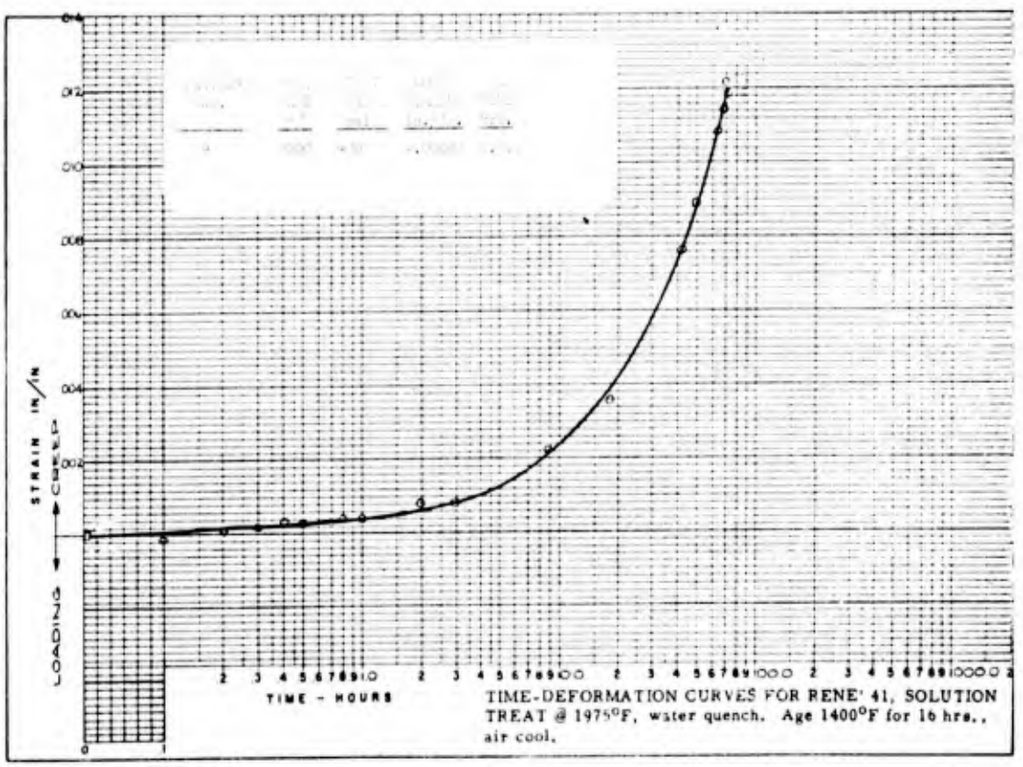

FIGURE 114 - TEST CURVE RENE' 41 2000°F 400 psi

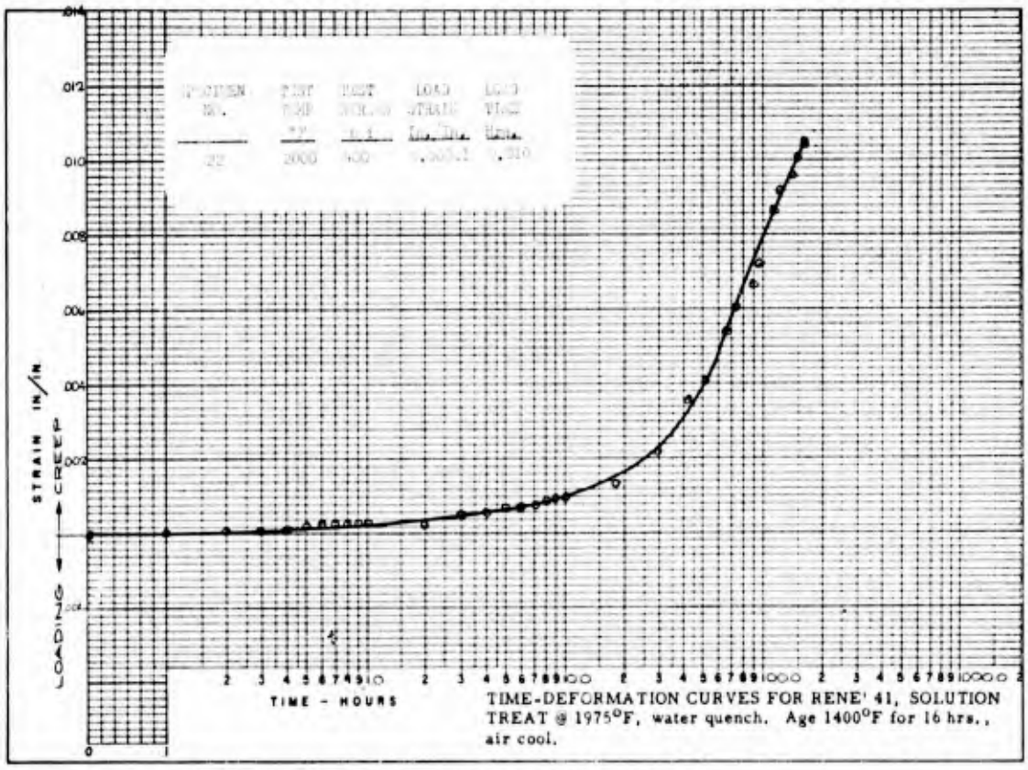

TIME-DEFORMATION CURVES FOR RENE' 41, SOLUTION TREAT @ 1975°F, water quench. Age 1400°F for 16 hrs., air cool.

FIGURE 115 - TEST CURVE RENE' 41 2000°F 400 psi

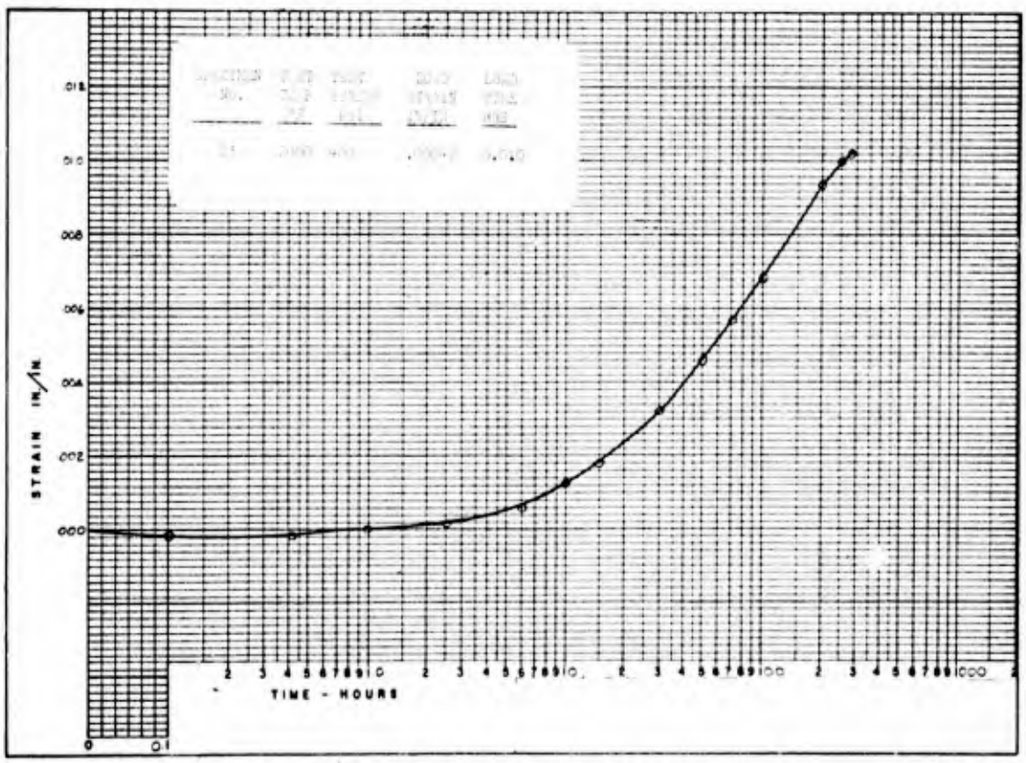

FIGURE 116 - TEST CURVE RENE' 41 2000°F 400 psi

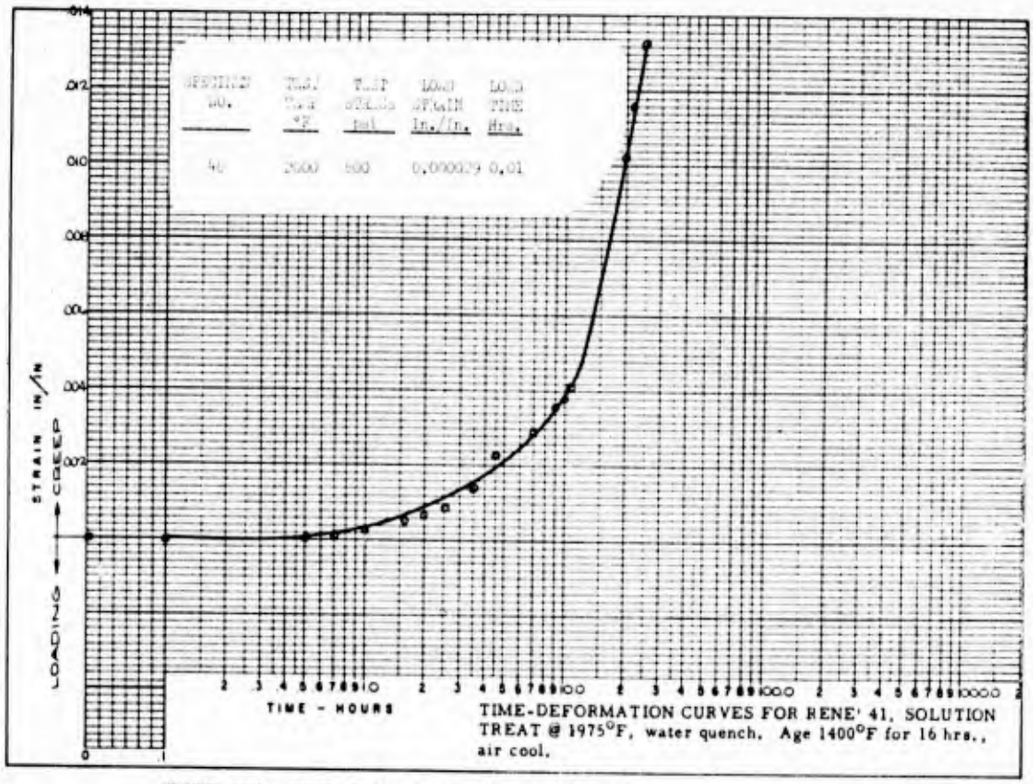

FIGURE 117 - TEST CURVE RENE' 41 2000°F 800 psi

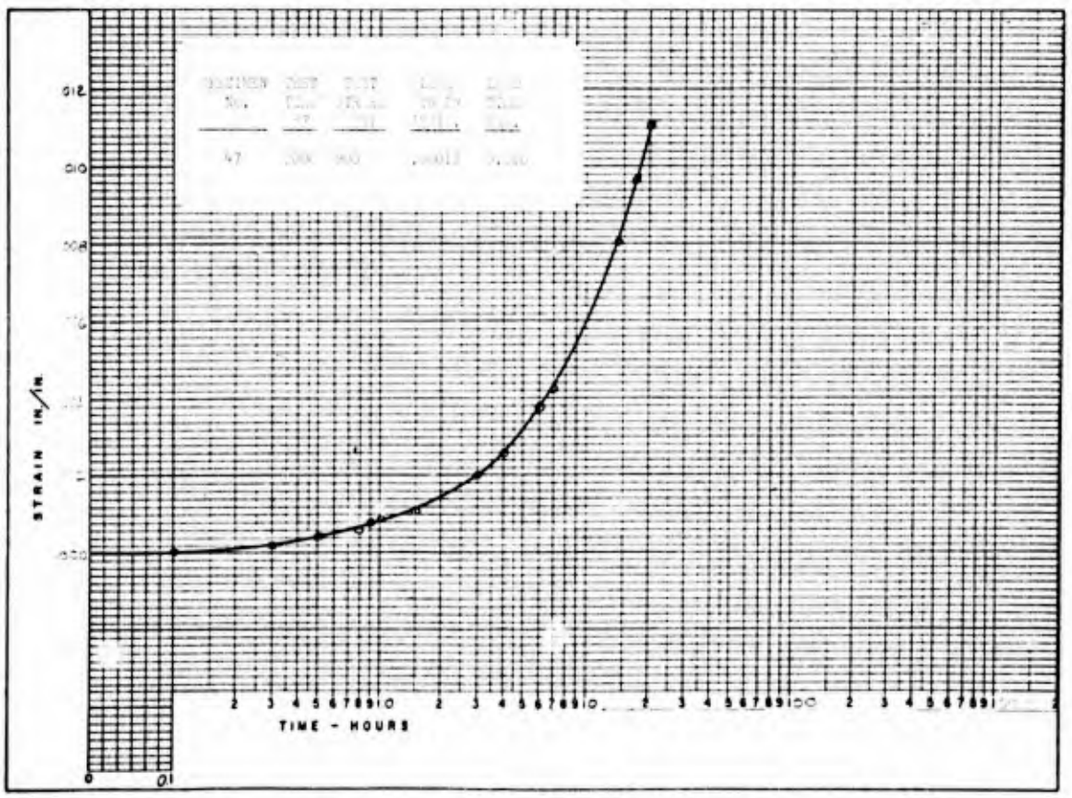

FIGURE 118 - TEST CURVE RENE' 41 2000°F 800 psi

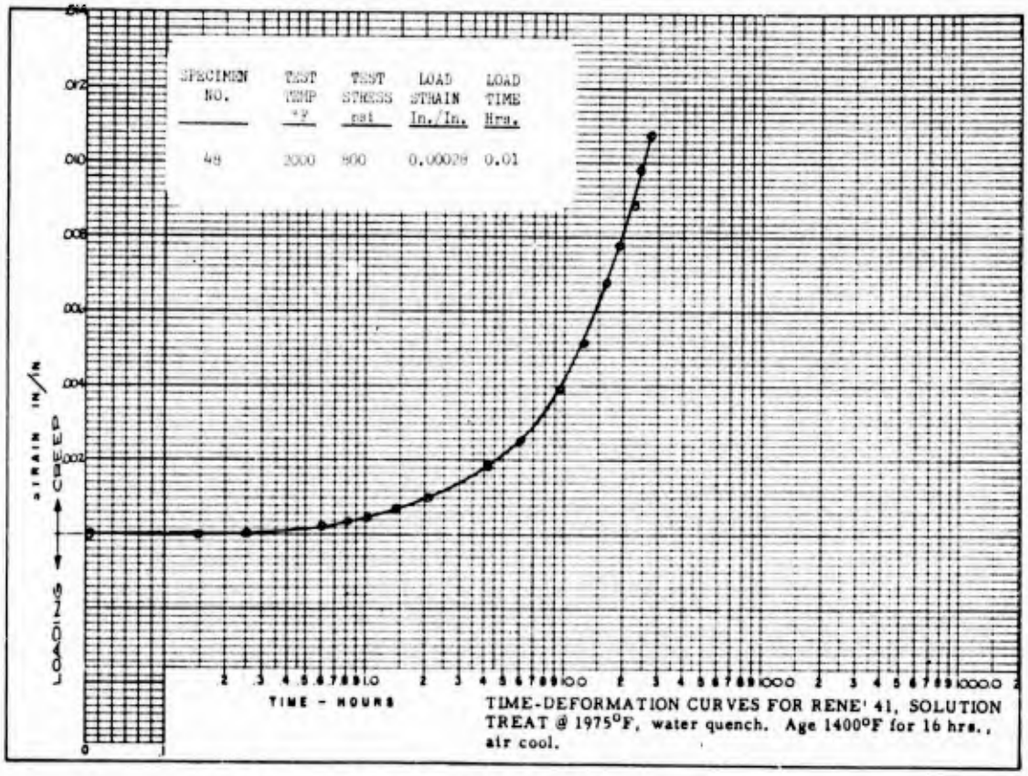

FIGURE 119 - TEST CURVE RENE' 41 2000°F 800 psi

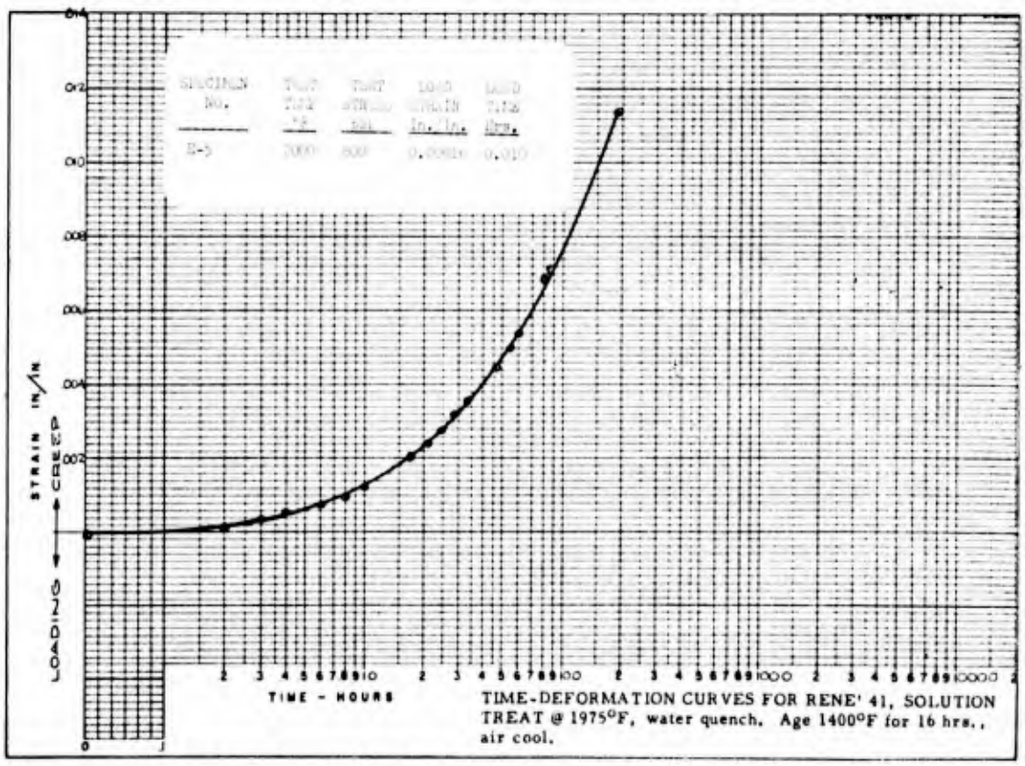

FIGURE 120 - TEST CURVE RENE' 41 2000°F 800 psi

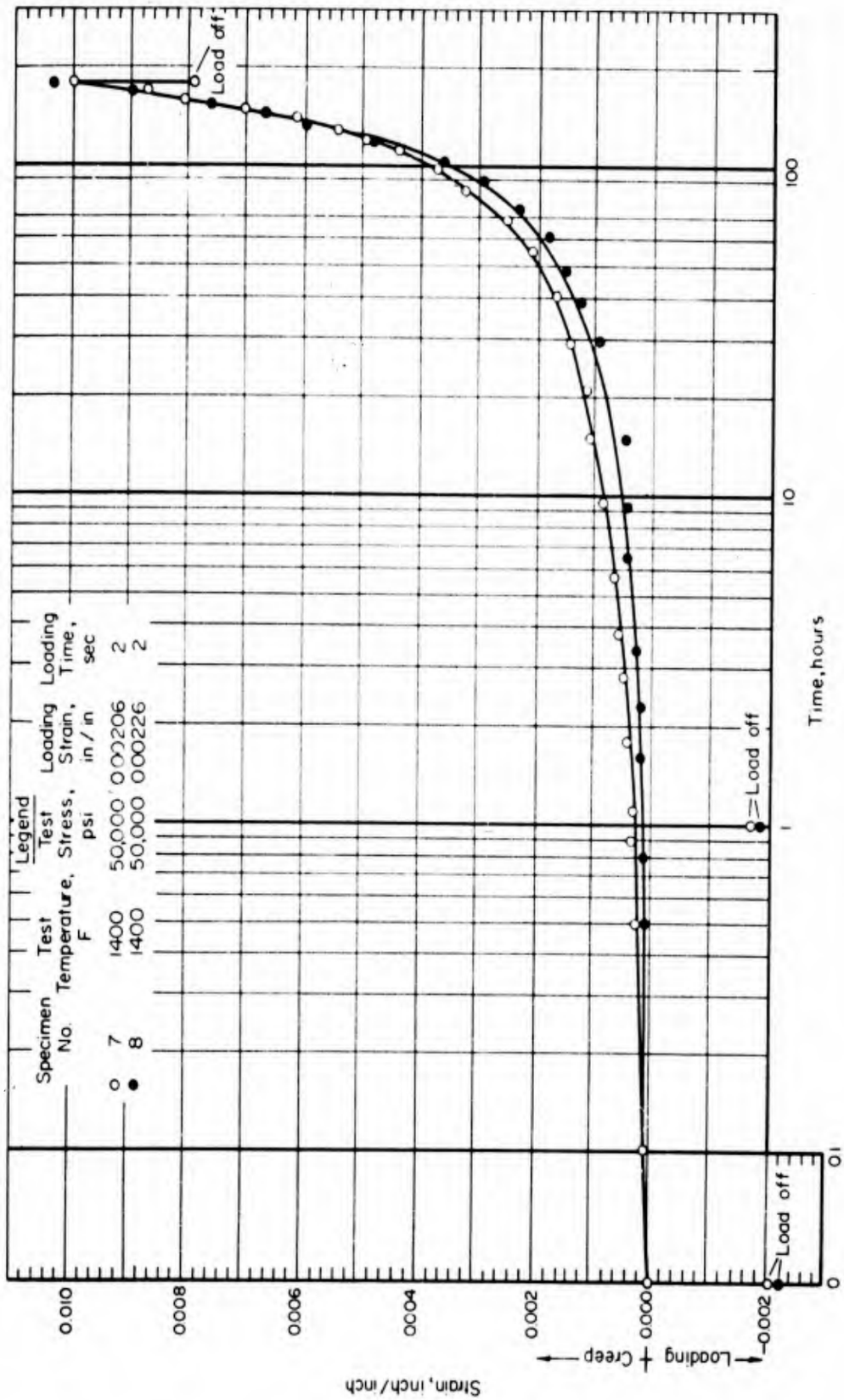

TIME DEFORMATION CURVES FOR RENE' 41 AT 1400 F -- CYCLED

FIGURE 121 - TEST CURVE RENE' 41 1400°F 50,000 psi CYCLED

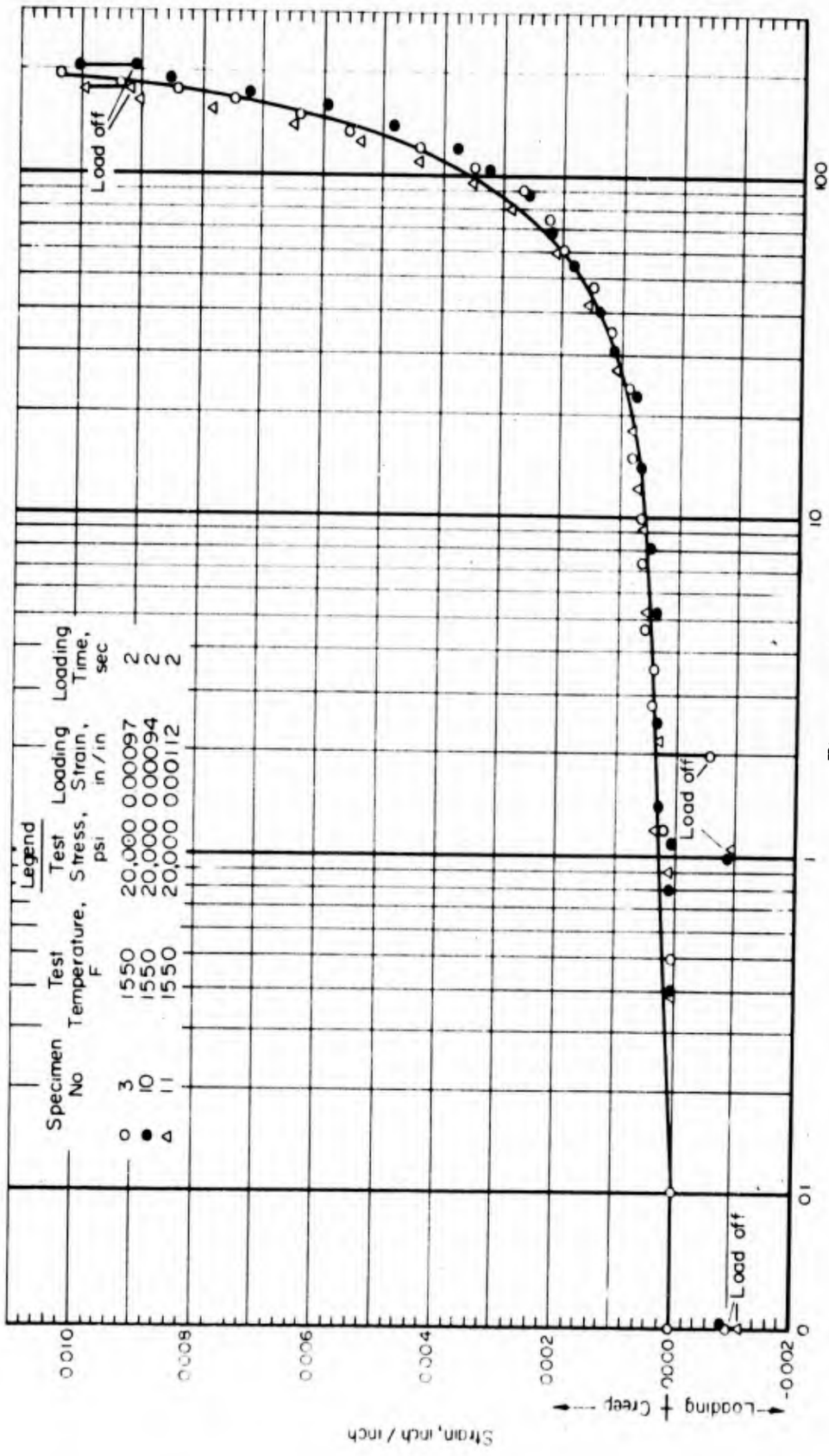

TIME - DEFORMATION CURVES FOR RENE' 41 AT 1550 F--CYCLED

FIGURE 122 - TEST CURVE RENE' 41 1550°F, 20,000 PSI CYCLED

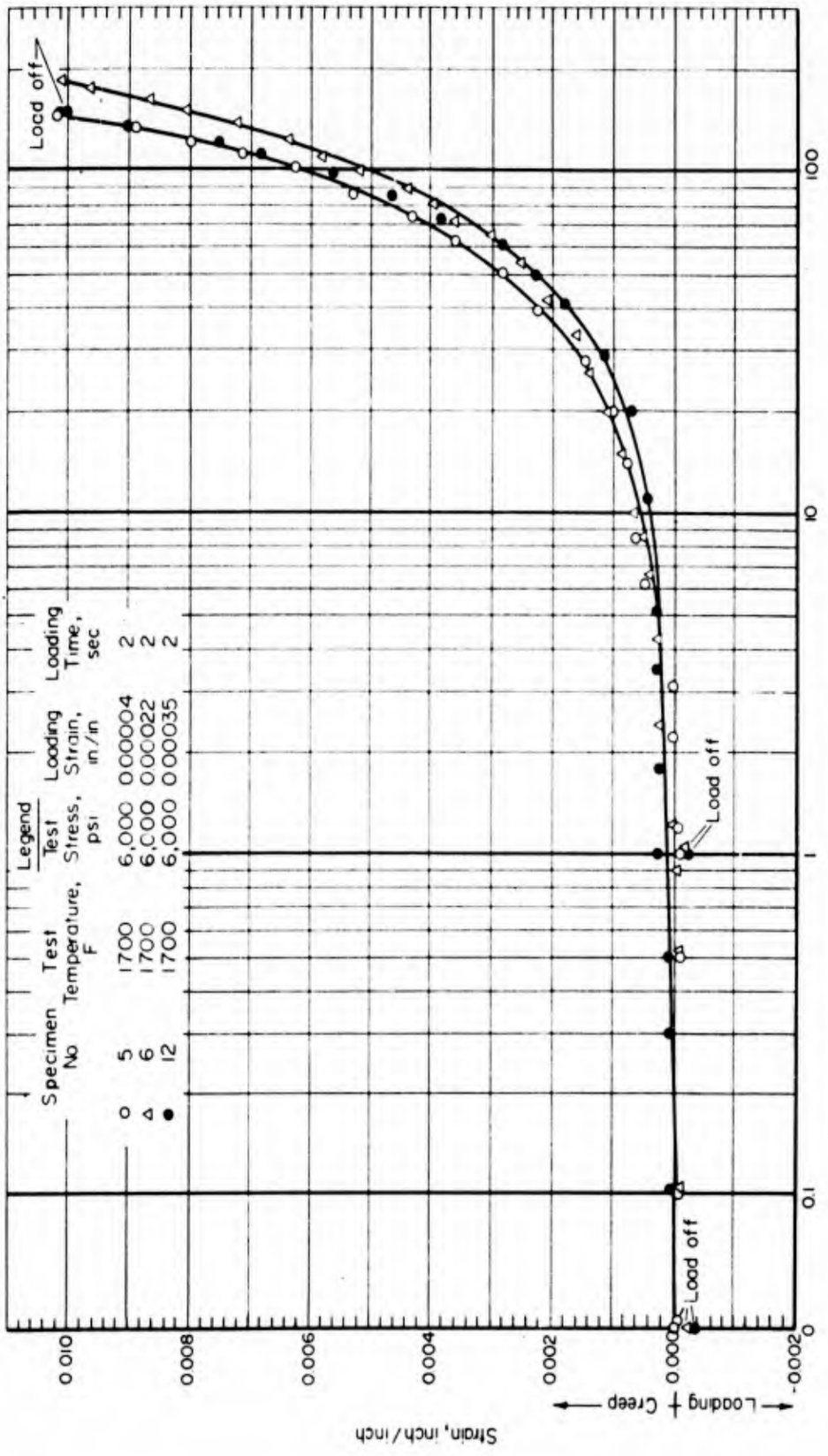

TIME-DEFORMATION CURVES FOR RENE' 41 AT 1700 F -- CYCLED

FIGURE 123 - TEST CURVE RENE' 41 1700°F 6,000 psi CYCLED

APPENDIX III

TEST PROCEDURES AND EQUIPMENT

BOEING TEST PROCEDURE FOR A-286, A110AT, AND UNIMACH 2

TEST EQUIPMENT

Tests were conducted in a temperature controlled laboratory (72°F ± 1°F) in machines mounted on a concrete floor isolated from external shock and vibration.

The tests were conducted in BAC 10,000 pound and Riehle MCR-20, 20,000 pound shock mounted, constant load, dead-weight, lever arm type test machines with automatic beam leveling. Pin grips terminating in self-aligning universal joints were used to insure axial loading of the specimen.

Strain-time curves were autographically recorded using a Riehle model DHK-20B extensometer in conjunction with Riehle model CDR-1 strip chart recorder.

Riehle averaging extensometers calibrated with individual strain-time strip chart recorders giving ASTM extensometer class B-1 accuracy of ± 0.0001 inches or better were used for strain measurement. The extensometers were calibrated before each test using a Riehle extensometer comparator which in itself is accurate to within ± 0.000002 inches.

Load-time curves were autographically recorded using a strain gage load cell, with the test specimen, in conjunction with a Leeds and Northrup Speedomax Model S adjustable zero adjustable range strip chart recorder.

Temperature was measured with chromel-alumel thermocouples attached at the center and ends of the 2.0 inch gage section. A Leeds and Northrup Model "G" Speedomax in conjunction with a Leeds and Northrup two action D.A.T. control was used as a temperature indicated recorder controller. Temperature checks were accomplished with a Leeds and Northrup Model 8662 portable potentiometer. A standard Marshall creep furnace equipped with external shunts was used as the test chamber. The test specimen is shown in Figure 124.

TEST PROCEDURE

In order to be sure that heat treatment produced the desired material strength, seven specimens of each material were tensile tested to failure at temperatures identical to those used in the creep tests.

A mechanical dynamometer was placed in the creep machine and dead weights were added to the beam until the predetermined test load was registered. The dynamometer was then removed and the specimen with extensometer and thermocouples attached was inserted to tandem with a load cell into the setup as shown in Figures 126 through 129.

The specimens were heated to test temperature at 20°F ± 5°F per minute. Care was taken not to over heat the specimen. A temperature gradient of less than 2.5°F and 5.0°F in the BAC and Riehle machines respectively over the two inch gage length was obtained by varying the external shunting of the furnace. The stabilized temperature gradient was accomplished and the test specimen

loaded with 2.8 hours $\pm$ 0.5 hours after the test temperature was first reached. The indicated test temperature was maintained to within 1.0°F and 2.5°F in the BAC and Riehle machines respectively throughout the test. The load was applied with a fixed head-travel rate of 0.32 and 0.01 inches per minute in the BAC and Riehle machines respectively.

The thermocouple survey at 1500°F for 1000 hours indicated that there was no thermocouple deterioration problem.

The gage width and thickness dimensions were measured with a micrometer caliper to the nearest 0.0002 inch.

NEW ENGLAND MATERIALS LABORATORY TEST PROCEDURE FOR RENE' 41

TEST EQUIPMENT

The conventional creep tests were performed by New England Materials Laboratory, Medford, Massachusetts.

The creep tests were performed on test frames consisting principally of a single vertical section of 8 inch steel channel which provides support for the loading beam and test furnace. Two small support legs project to the rear of the vertical member to give the frame lateral stability. Hardened steel fulcrum blanks are mounted at the top of the frame and a 1 inch thick steel base plate bolted to the concrete floor provides an anchor for the specimen loading system.

Loading of the test specimens was accomplished by means of a simple uniform cross section steel beam, with hardened steel knife edges at three points of contact; the fulcrum, the specimen loading shackle, and the weight pan pivot accuracy of the loading system is within .1% of calibrated load.

The test furnaces used are resistance heated tube furnaces with sight ports front and rear to permit optical creep measurement. Each furnace is provided with 10 shunt braces spaced evenly along the heating element to allow the necessary adjustment of temperature along the specimen and adapter assembly.

Three thermocouples were attached to each test specimen, one at the center of the gage section and one at each end. The center thermocouple was the control couple and provided the temperature record. The other two couples were checked periodically with a potentiometer. Temperature was controlled by Honeywell "Electronik" potentiometric indicating controllers with a response sensitivity of $\pm 1°F$. Temperature was recorded on a Western 24 point recorder of comparable sensitivity.

Creep was measured optically with a filar eyepiece micrometer microscope (110X). The creep gage consisted of a length of 20 mil platinum wire attached at one end of the specimen gage and a length of small diameter platinum tube attached at the opposite end. The platinum wire was notched at intervals of approximately 0.010 inch and extended into the tube. As the specimen elongated, the wire was withdrawn from the tube and the deformation was determined by measuring the change in the distance from a reference notch on the wire to the tip of the platinum tube. Two gages were mounted on each specimen (on opposite sides). Readings taken from opposite sides of the specimen were averaged. The measuring microscope reads directly in increments of 0.0005 mm (0.0000197 inch).

Clamps were used to mount the platinum creep gages. The clamps consisted of rectangular pieces of chromium alloy with a saw cut slot which fit over the specimen gage. The clamping action was provided by the difference in expansion coefficients of the chromium and the Rene' 41.

The test specimen is shown in Figure 125.

TEST PROCEDURE

Specimens were placed in the test furnaces and brought to temperature as quickly as possible. Specimens were held at test temperature for approximately two hours before the load was applied. A hydraulic jack was used to apply the load.

Microscope readings were taken immediately before and after application of load and then periodically at intervals determined by the estimated duration of the test. Readings were taken immediately before and after removal of the load.

BATTELLE TEST PROCEDURE FOR RENE' 41 CYCLIC TESTING

THERMAL CYCLE

The basic thermal cycle consisted of the following steps which were performed in sequence:

1. Heat rapidly to maximum test temperature.
2. Apply maximum stress.
3. Maintain maximum temperature and stress for 1 hour.
4. Unload.
5. Cool rapidly to below 300°F.

The maximum temperatures used in this program were 1400, 1550 and 1700°F. The maximum stresses corresponding to these temperatures were 50,000, 20,000 and 6,000 psi, respectively. The minimum temperature was specified as any temperature below 300°F and generally ranged between 200 and 300°F during these tests. The minimum stress for all specimens was approximately 225 psi, which resulted from the weight of the lower specimen grip and retaining nut.

The average time required for performing each of the steps in the basic cycle was as follows:

Specimens	Maximum Temp. °F	Heating Time, Sec.	Loading Time, Sec.	Unloading Time, Sec.	Cooling Time, Sec.
7, 8	1400	30	2	2	30
3, 10, 11	1550	34	2	2	36
5, 6, 12	1700	38	2	2	41

Originally, all tests were to be continued until 1000 hours had been accumulated at maximum temperature and stress, until 1 percent creep had been accumulated, or until rupture, whichever occurred first. However, 1 percent creep was reached at times on the order of 150 to 200 hours and most of the tests were discontinued after 1 percent creep had been accumulated.

TEST EQUIPMENT AND PROCEDURE

All cyclic creep tests were made in standard Battelle-type creep testing frames shown in Figure 130. These machines were previously calibrated and found to be well within the permissible variations specified in ASTM Standard E139-58T for accuracy and axiality of loading. A close-up view of one test unit with the furnace in the raised position is shown in Figure 131.

Specimens were heated to temperature by a combination of radiant heating from a Chromel-wound creep test furnace and by auxiliary self-resistance heating supplied by a 1-kva transformer. A short stainless steel lead was welded to the top shoulder of each specimen to enable the auxiliary power lead to be connected to the specimen while the furnace was in the raised position.

The auxiliary heating was applied to the specimen for 28 seconds at the beginning of each cycle and was then applied intermittently, as required, until the furnace was reheated sufficiently to maintain specimen temperature within the desired limits. The period of intermittent heating was approximately 2 minutes per cycle.

Cooling was accomplished be means of a fan, which was turned on automatically when the furnace was lifted to the raised position at the end of each cycle.

Loading and unloading of the specimen was accomplished by lowering or raising the lever arm on the top of the creep machine by means of a hand wheel and threaded jack.

Temperature was indicated by means of calibrated 22-gage Chromel-Alumel thermocouples wired to the center and near each end of the gage section, as shown in Figure 131, and was measured by means of a semi-precision potentiometer. The temperature indicated by the center and top thermocouples was recorded continuously during the first five cycles of each test, and that of the bottom thermocouple was checked frequently during this period. For the remainder of the test, the center thermocouple was monitored continuously during reheating to temperature and for a few minutes of each cycle; the top thermocouple was recorded at regular 3-minute intervals; and the bottom thermocouple was used for controlling furnace temperature. The temperature indicated by each thermocouple was measured and recorded four times daily.

During rapid heating and intermittent application of the auxiliary power, an effort was made to keep the temperature indicated by the center thermocouple at the desired test temperature. The temperature indicated by the top and the bottom thermocouples lagged behind that of the center thermocouple during rapid heating and for the first few minutes of each cycle. This variation in temperature was caused by the cooling effect of the extensometer clamps on either end of the gage length. The variation between the indicated temperature for each of the thermocouples and the desired test temperature was within the range +6, -20°F during the first 10 minutes at maximum temperature and +3°F for the duration of the cycle.

In the case of Specimens 1 and 2, overheating of the center of the specimen occurred during rapid reheating to temperature during the early part of the test. This happened because initially an end thermocouple was being monitored during reheating, the center thermocouple being used for recording. In subsequent tests, the thermocouples were used as described above.

Strain was indicated by means of platinum strip extensometers which were clamped to the ends of the 2-inch gage section. Because the specimens were not straight, extensometers were mounted on opposite sides of the specimen, as shown in Figure 131, in order to minimize the effect of straightening the

specimens during loading. Strain was measured optically by means of a calibrated 20-power filar micrometer microscope on which the smallest division is 0.00005 inch. The readings from the two extensometers were then averaged before recording.

All the specimens, particularly Specimens 7 to 12, were bowed when received. Consequently, the extensometer strip mounted on the convex side of the arc indicated a very low, or even negative, value of strain when the applied load straightened the specimen, and the extensometer on the concave side indicated too high a value. Although the two values were averaged, the error incurred in the observed loading and unloading strain values is apparent. This error would not be expected in the creep readings, since these were taken only when the specimen was loaded and reasonably straight.

During the first cycle only, strain was measured at maximum temperature, both before and after loading and after unloading in order to determine the initial loading and unloading strains. During subsequent cycles, strain was measured only when the specimen was at maximum temperature and stress. Sufficient readings were made to define the creep-time curve adequately, with no fewer than one reading being made during each three cycles of test.

The atmosphere was air for all tests.

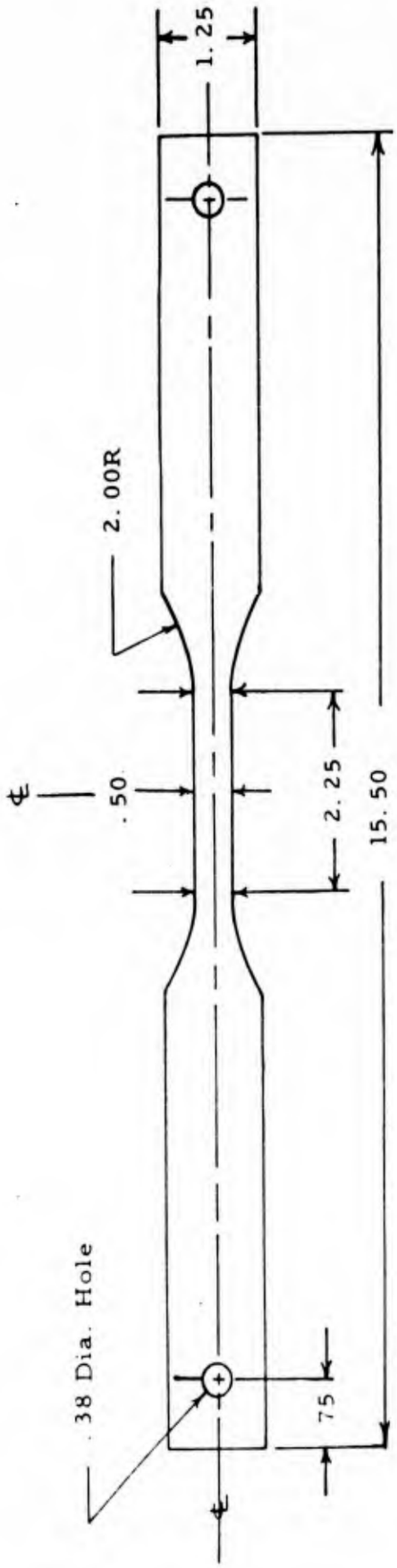

Tensile and Creep Specimen

Room and Elevated Temperature Testing

FIGURE 124 - TEST SPECIMEN

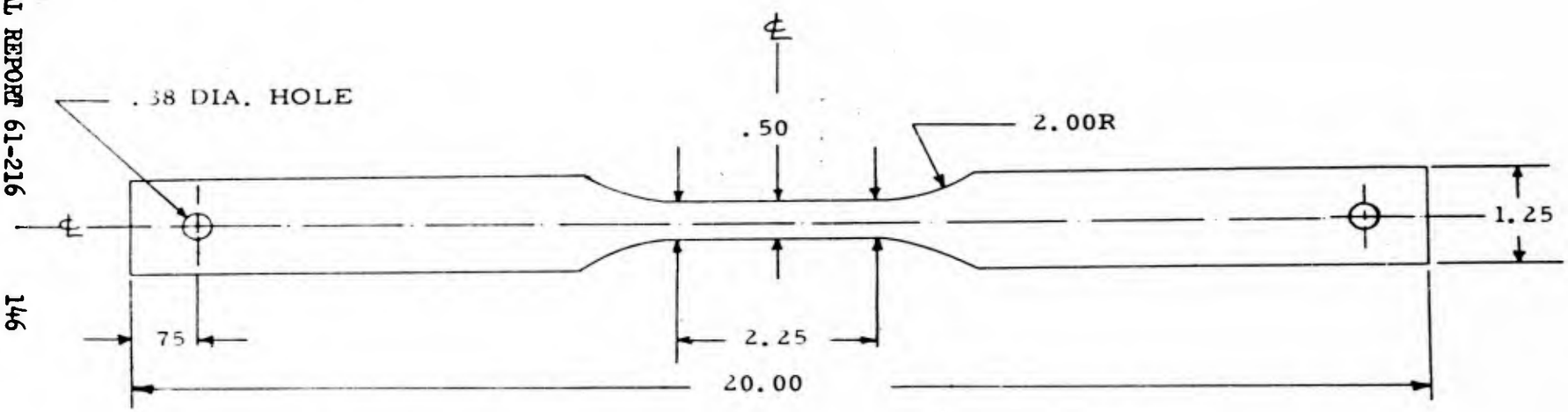

Creep Specimen

For Rene' 41 Only

FIGURE 125 - TEST SPECIMEN - RENE' 41

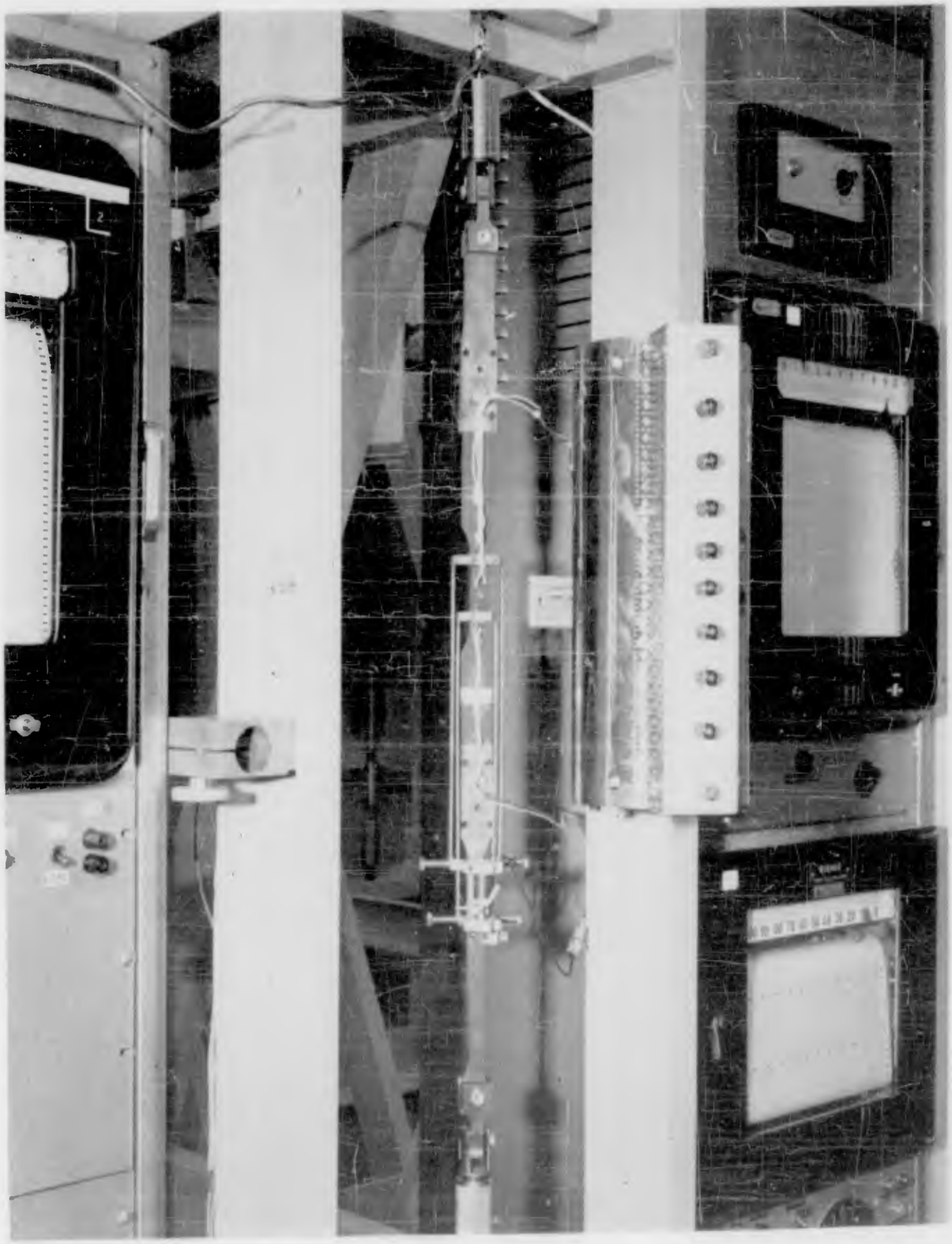

FIGURE 126 - SPECIMEN INSTALLATION BAC CREEP TESTS
DEAD LOAD LEVER ARM CREEP MACHINE

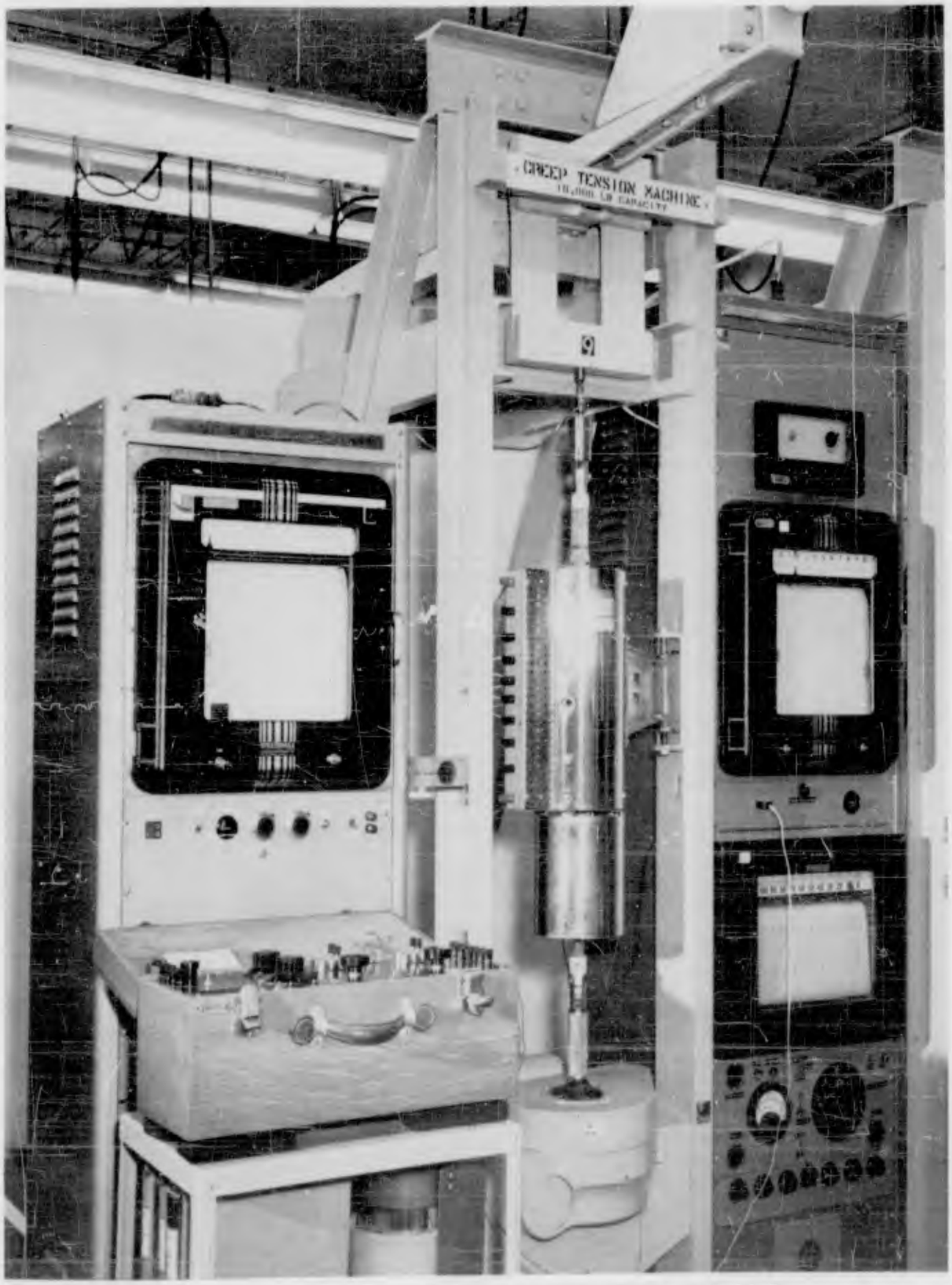

FIGURE 127 - TEST SETUP BAC CREEP TESTS DEAD LOAD
LEVER ARM CREEP MACHINE

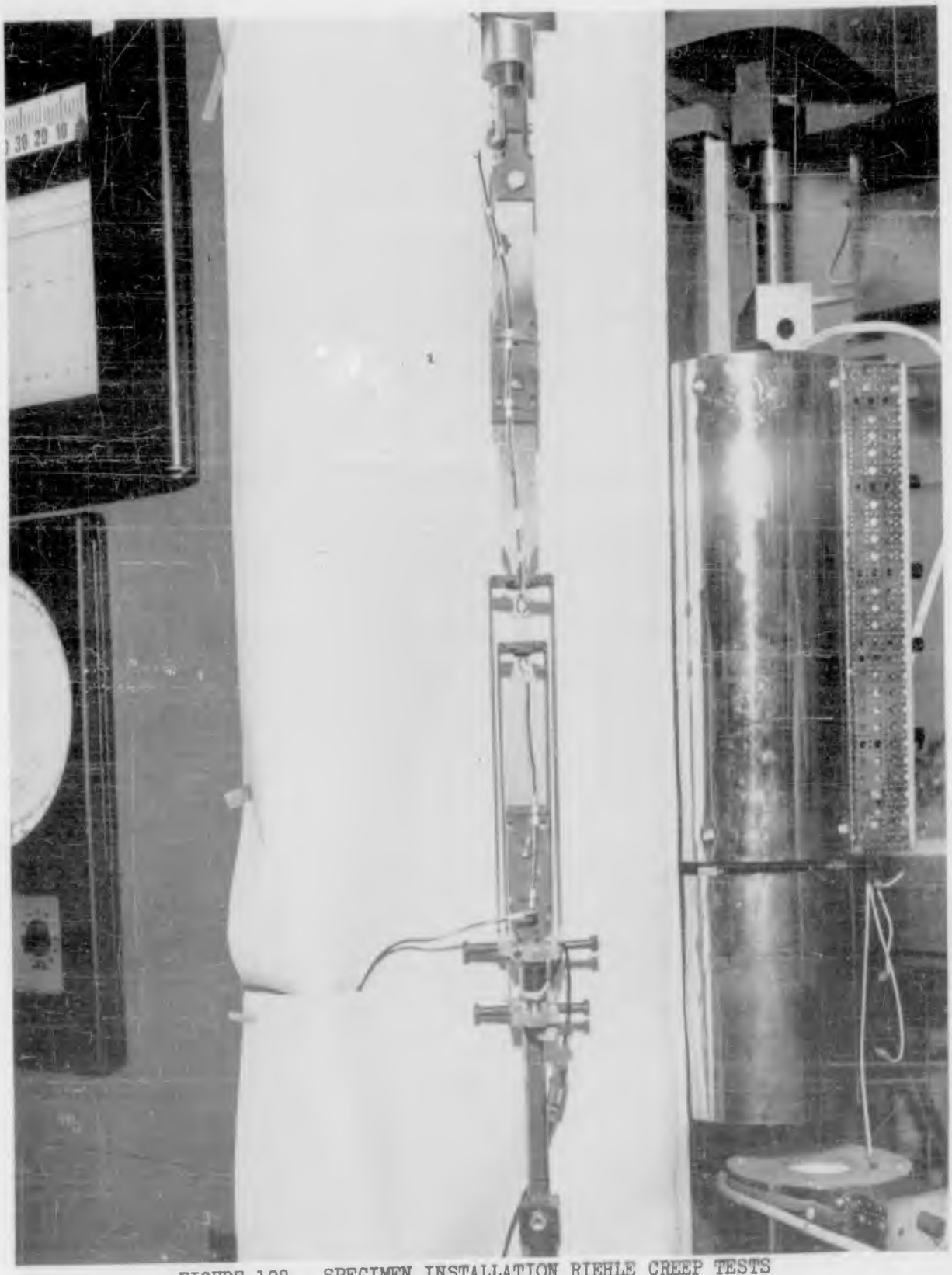

FIGURE 128 - SPECIMEN INSTALLATION RIEHLE CREEP TESTS
DEAD LOAD LEVER ARM CREEP MACHINE

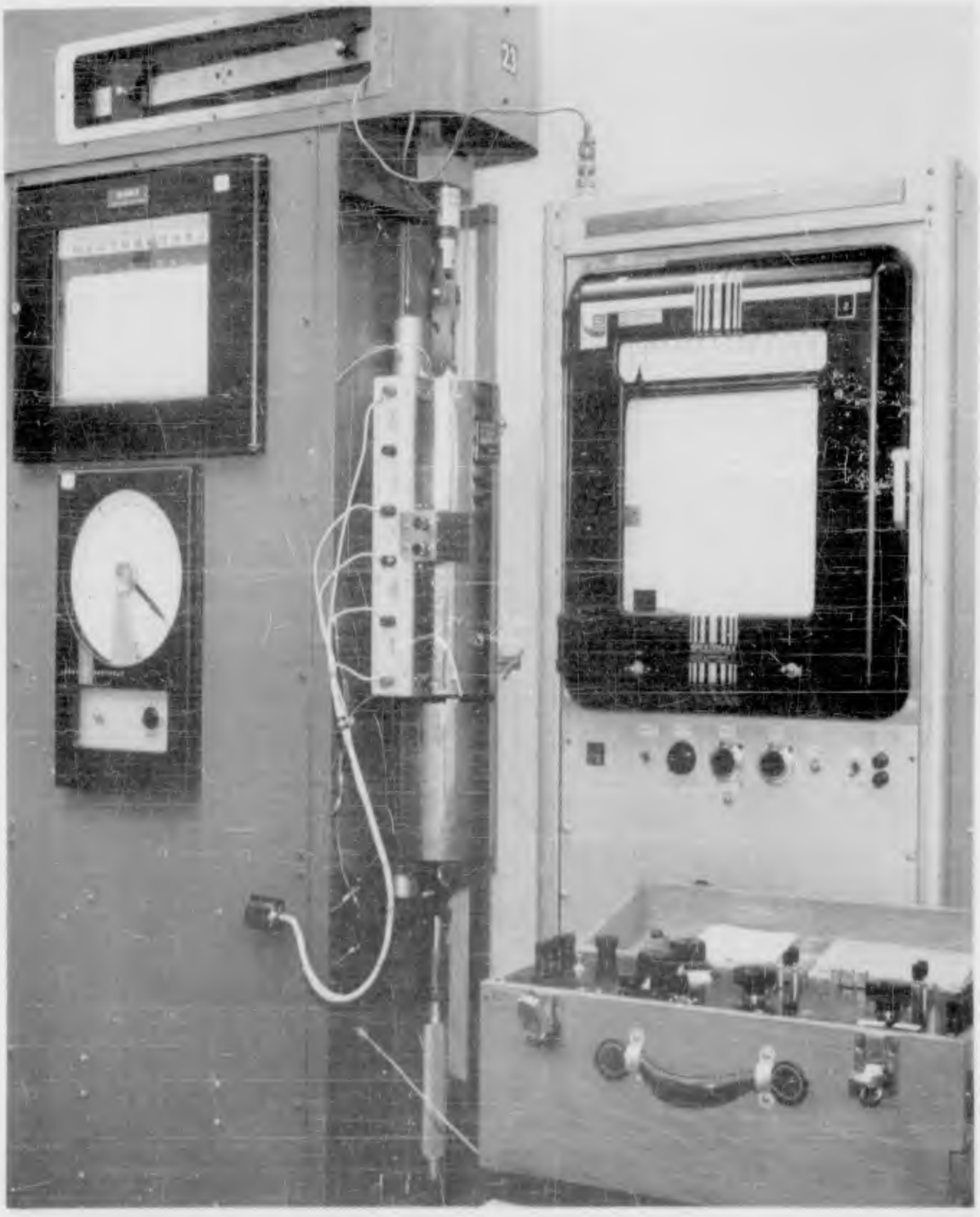

FIGURE 129 - TEST SETUP RIEHLE CREEP TESTS DEAD LOAD
LEVER ARM MACHINE

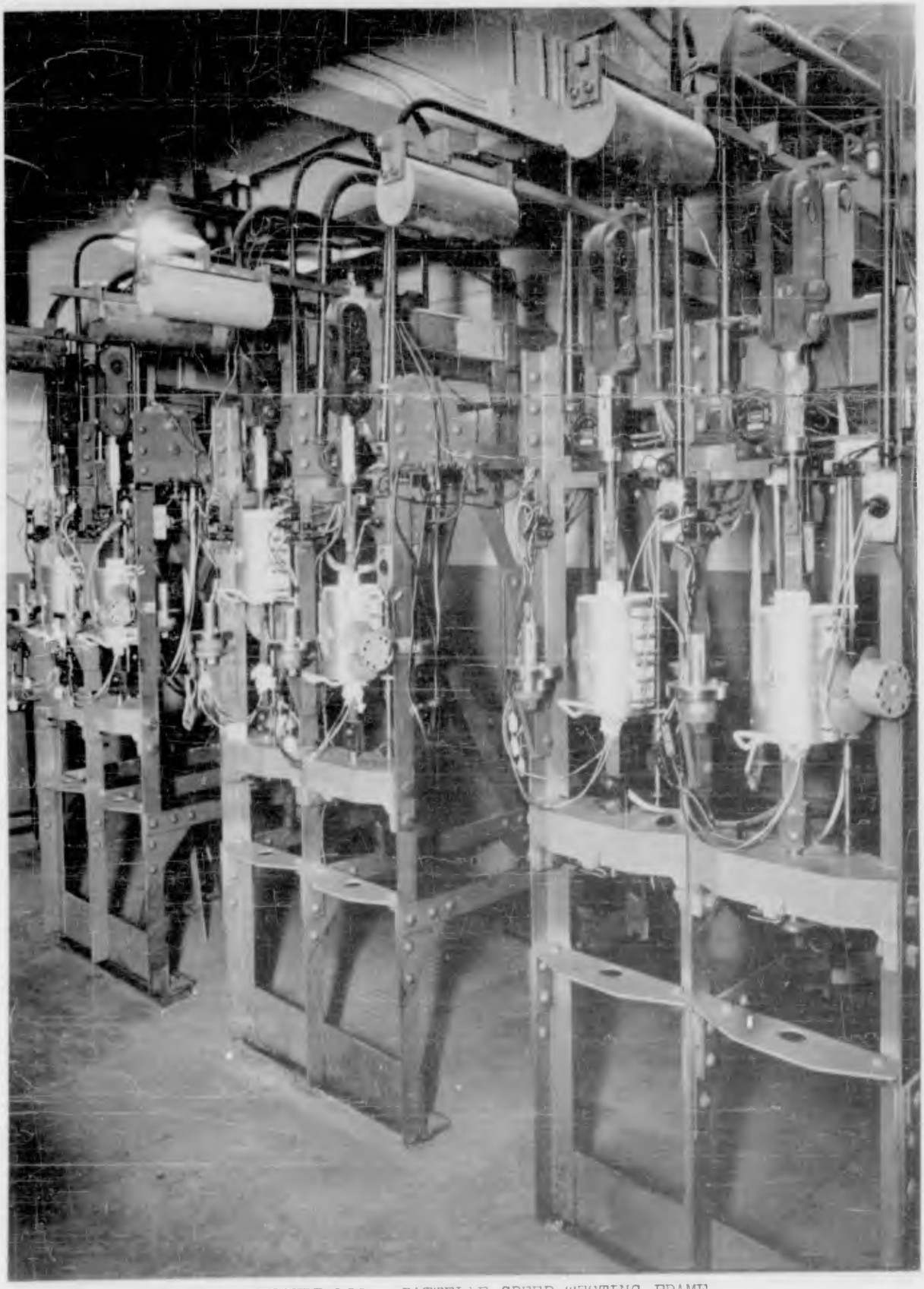

FIGURE 130 - BATTELLE CREEP TESTING FRAME

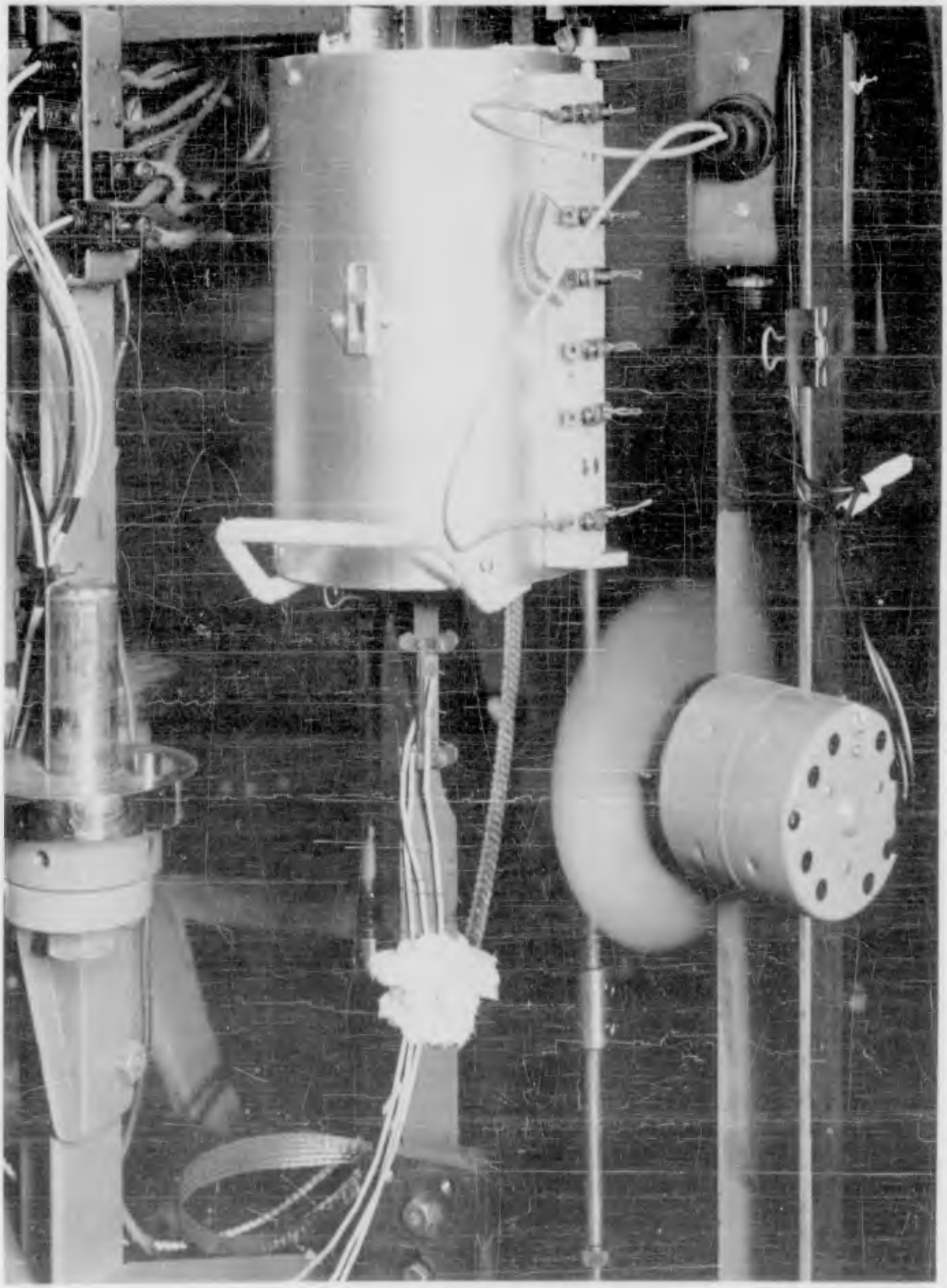

FIGURE 131 - BATTELLE CREEP TEST SETUP

APPENDIX IV

CALCULATIONS

CALCULATIONS

The following calculations illustrate the application of the equation derived in Appendix I to test data. Calculations are shown for A286 from test data included in Appendix II.

In addition, calculations are detailed for the nomograph shown in Figure 31.

CALCULATION OF CREEP EQUATION FOR A286 DATA

Given: Strain-Time curves for A286 at 1200°

Problem: Determine numerical values for the constants K, β , α , for A286 by least squares method.

Equations Used:

$$\epsilon = K \sigma^{\beta} t^{\alpha} \tag{104}$$

$$\beta = \frac{\overline{(\log \sigma^2)} - (\overline{\log \sigma})^2}{(\log \epsilon \log \sigma) - (\log \epsilon)(\log \sigma)} \tag{105}$$

$$\log B = \log \bar{\epsilon} - \beta \log \bar{\sigma} \tag{106}$$

$$\alpha = \frac{\overline{\log B \log t} - (\overline{\log B})(\overline{\log t})}{(\log t)^2 - (\overline{\log t})^2} \tag{107}$$

$$K = \overline{\log \epsilon} - \alpha \overline{\log t} \tag{108}$$

Plot the A286 strain-time data at 1200° as in Figure 132.

Solution: Using Equation 105 above, compute the slope of the regression line through the data points for 500 hours in the following manner:

1.	$\epsilon \times 10^{-4}$	$\sigma \times 10$	$\log \epsilon$	$\log \sigma$	$(\log \sigma)^2$	$\log \epsilon \log \sigma$
	73	4	1.863	.602	.362	1.122
	13.8	3	1.140	.477	.228	.544
	24.0	3	1.380	.477	.228	.658
	33.5	3	1.525	.477	.228	.727
	60.0	3	1.778	.477	.228	.848
	22.0	2.5	1.342	.398	.158	.535
	7.0	1.5	0.845	.176	.031	.149
TOTAL	233.3	20.0	9.873	3.0840	1.463	4.583
AVG.	33.3	2.9	1.410	.441	.209	.654

2. $$\beta = \frac{\overline{(\log \sigma)^2} - (\overline{\log \sigma})^2}{\log \epsilon \log \sigma - (\log \epsilon)(\log \sigma)} \quad \frac{.209 - (.441)^2}{.654 - (1.410)(.441)} = \frac{.209 - .194}{.654 - .621}$$

$$\beta = \frac{.015}{.032} = .469$$

3. This procedure is repeated for each time increment used; in this case 200, 100, 50, and 10 hours with the resulting values for β

β_{500} hours = .469

β_{200} hours = .485

β_{100} hours = .602

β_{50} hours = 1.230

β_{10} hours = 1.07

$\beta_{Avg.}$ = .771

4. Taking the arithmetic average of the β's draw parallel lines through the centroid of the data points for each time. See Figure 132.

5. Compute the constant, B, for each of these lines in the following manner:

$$\log B = \log \bar{\epsilon} - \beta \log \bar{\sigma}$$

Using 500 hours for example:

$$\log B_{500 \text{ hours}} = \log 3.33 \times 10^{-3} - (.771)(\log 29)$$

$$= (7.51851-10) - (.771)(1.46240)$$

$$= (7.51851-10) - 1.12751$$

$$= 6.39100-10$$

$$B_{500 \text{ hours}} = 2.46 \times 10^{-4}$$

6. Repeating this for each time,

B_{500} hours = 2.46×10^{-4}

B_{200} hours = 1.55×10^{-4}

B_{100} hours = 8.60×10^{-5}

B_{50} hours = 5.50×10^{-5}

B_{10} hours = 2.25×10^{-5}

Note that the intercepts of the constant time lines with the stress level equal to one (1) are the same as the computed values of B.

7. Plot log time versus B. See Figure 133.

8. Compute by least squares, the regression line and its slope, α , for these points:

	t	B x 10^{-5}	log t	log B	$(\log t)^2$	log t log B
	10	2.25	1.00000	.35218	1.0000	.35218
	50	5.5	1.69897	.74036	2.88650	1.25785
	100	8.6	2.00000	.93450	4.00000	1.86900
	200	15.5	2.30103	1.19033	5.29470	2.73899
	500	24.6	2.69897	1.38021	7.28440	3.72515
TOTAL	860	56.45	9.69895	4.59760	20.46550	9.94315
AVG.	172	11.3	1.93979	.91952	4.09310	1.98863

9. $$\alpha = \frac{\overline{\log B \log t} - (\overline{\log B})(\overline{\log t})}{\overline{\log t^2} - (\overline{\log t})^2}$$

$$\alpha = \frac{1.98863 - (.91952)(1.9397)}{4.09310 - (1.93979)^2} = \frac{1.98863 - 1.78367}{4.09310 - 3.76278}$$

$$\alpha = \frac{.20495}{.33032} = .62045$$

10. Using equation 108:

$$K = \overline{\log B} - \alpha \overline{\log t}$$

$$K = 5.91952 - (.62045)(1.93979)$$

$$= 4.7159 \times 10^{-5}$$

Note that this value is the same as the intercept of the regression line through the points and time equal to one (1) hours.

11. Substituting into equation 104 above, the following equation for A286 at 1200°F was obtained:

$$\epsilon = 4.72 \times 10^{-5} \quad \sigma^{.771}_{t}{}^{.620}$$

12. This same procedure was followed for A286 at 1300° and 1500° with the resulting equations:

$$\epsilon = 1.73 \times 10^{-5} \quad \sigma^{1.83}_{t}{}^{.773} \qquad \text{for } 1500°F$$

$$\epsilon = 6.09 \times 10^{-6} \quad \sigma^{1.199}_{t}{}^{.660} \qquad \text{for } 1300°F$$

13. To obtain the general form of the equation, the equations for constant temperature were combined. Plot:

$$\log K \text{ vs } \frac{1}{T},$$

$$\log \beta_2 \text{ vs } \frac{1}{T},$$

and

$$\log \alpha \text{ vs } \frac{1}{T}$$

when T is absolute temperature in °R.

14. Let $K = Le^{m/T}$

$\beta_2 = Ae^{H/T}$

$\alpha = Se^{n/T}$

The slopes of the regression lines are m, H, and n respectively. The values for L, A, and S were computed mathematically using method shown in Step 10.

15. The following values were obtained:

$$K = 7.42 \times 10^{-4} e^{-8.28 \times 10^3/T}$$

$$\beta_2 = 2.09 \times 10^2 e^{-9.35 \frac{x}{T} 10^3/T}$$

$$\alpha = 2.7 e^{-2.47 \times 10^3/T}$$

The general equation then becomes:

$$\epsilon = 7.42 \times 10^{-4} e^{8.28 \times 10^3/T} \quad 2.09 \times 10^2 e^{-9.35 \times 10^3/T}_t \, 2.7e^{-2.47 \times 10^3/T} \tag{59}$$

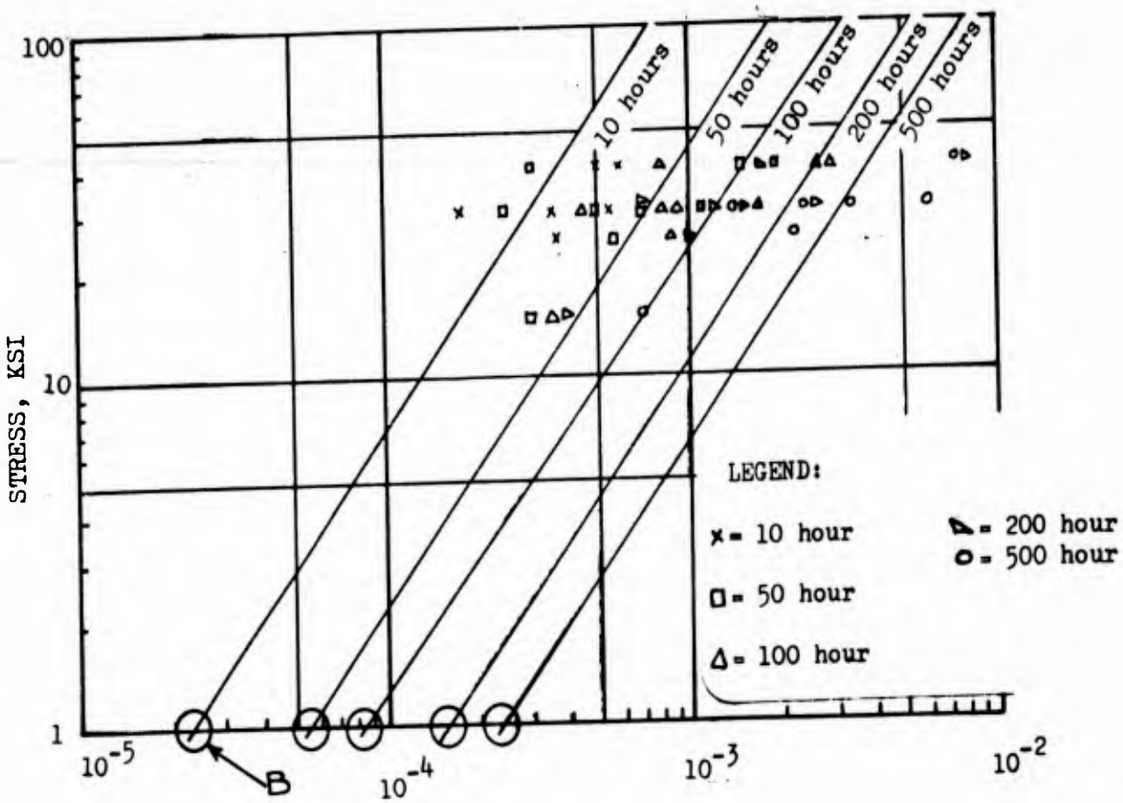

FIGURE 132 - PLOT OF STRESS VS. STRAIN

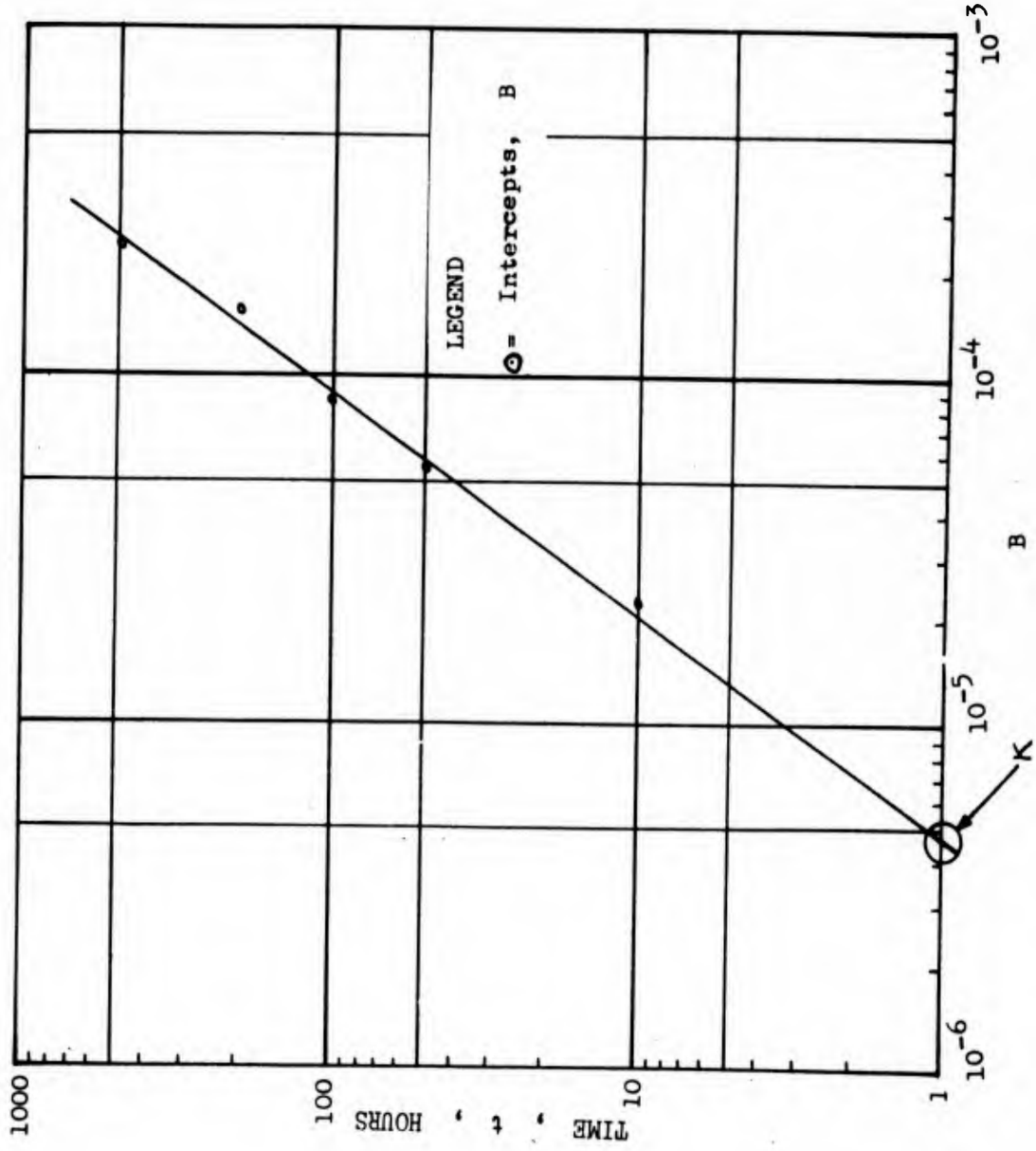

FIGURE 133 - PLOT OF K VS. TIME

CALCULATION OF NOMOGRAPH FOR A286

Consider the equation

$$\epsilon = 7.42 \times 10^{-4} e^{\frac{-8.28 \times 10^3}{T}} \sigma^{2.09 \times 10^2} e^{\frac{-9.25 \times 10^3}{T}} t^{2.7} e^{\frac{-2.49 \times 10^3}{T}} \quad (109)$$

By letting $$x = 7.42 \times 10^{-4} e^{\frac{-8.28 \times 10^3}{T}} \quad (110)$$

$$y = \sigma^{2.09 \times 10^2} e^{\frac{-9.25 \times 10^3}{T}} \quad (111)$$

$$z = t^{2.7} e^{\frac{-2.49 \times 10^3}{T}} \quad (112)$$

Equation 109 takes the form:

$$\epsilon = x \quad y \quad z \quad (113)$$

or

$$\log \epsilon = \log x + \log y + \log z \quad (114)$$

Equation 114 can be expressed by a simple alignment chart.

Equations 110 and 111 and 112 can be plotted and the x, y, and z axes aligned to form a nomograph.

1. Plot equation 110; x vs. T:

T	$\frac{8.28 \times 10^3}{T}$	$e^{\frac{-8.28 \times 10^3}{T}}$	x
1200°F = 1660°R	4.99	.00672	4.99×10^{-6}
1350°F = 1810°R	4.57	.01037	7.69×10^{-6}
1500°F = 1960°R	4.32	.01471	1.091×10^{-5}

Let the x scale = 15", and the limits of x be 2×10^{-6} and 6.7×10^{-5}.

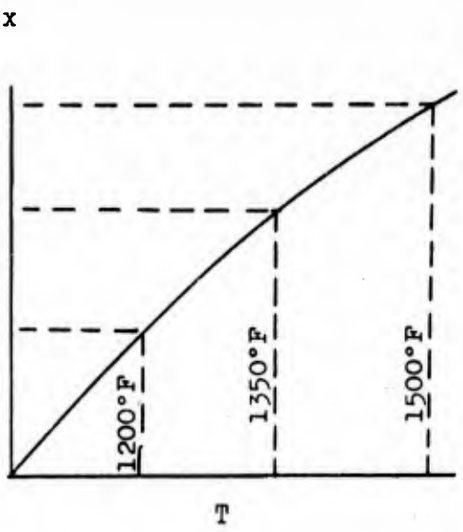

Mark off, on the x line, values corresponding to the temperatures.

2. Plot equation 111; y vs. σ for T_1, T_2, T_3:

T	$\frac{-9.25\times10^3}{T}$	e $^{\frac{-9.25\times10^3}{T}}$	$2.09 \times 10^2 e^{\frac{-9.25\times10^3}{T}}$	σ	y
1200°F = 1660°R	-5.57	.00382	.798	30 KSI	15.09
				40	19.02
1350°F = 1810°R	-5.11	.00604	1.26	7	11.61
				10	18.20
1500°F = 1960°R	-4.72	.00893	1.87	2	3.66
				3	7.80

Let the y scale = 15" and the limits of y be 1 and 33.5

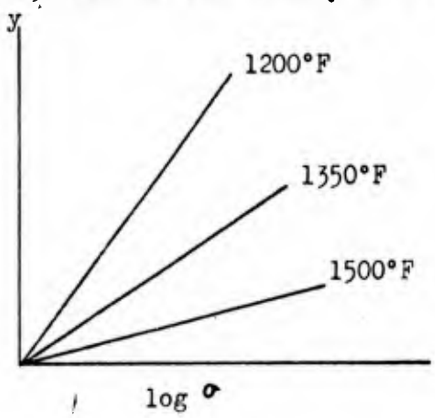

To obtain other temperature lines,

Plot $\frac{1}{T}$ vs. the exponent of σ in equation 111.

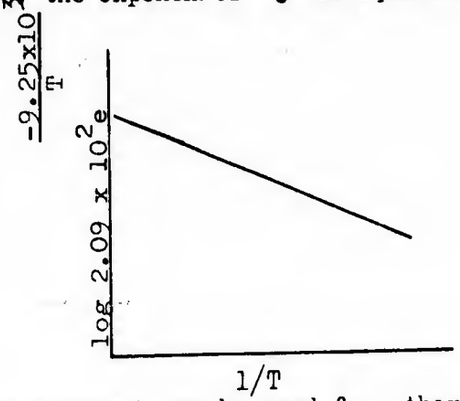

Values of the exponent can be read for other temperatures. Pick a value for σ (e.g. 10 KSI) and determine y from $y = \sigma^{\exp}$ for each temperature. These values can then be plotted on the y vs. σ plot.

3. Plot equation 112; z vs. t for T_1, T_2, T_3:

T	$\frac{-2.49 \times 10^3}{T}$	$e^{\frac{-2.49 \times 10^3}{T}}$	$2.7e^{\frac{-2.49 \times 10^3}{T}}$	t	z
1200°F = 1660°R	-1.5	.223	.602	10 hr	4.00
				100 hr	16.00
				500 hr	42.15
1350°F = 1810°R	-1.38	.252	.680	10	4.79
				100	22.9
1500°F = 1960°R	-1.27	.281	.759	10	5.74
				100	33

Let the z scale = 15" and the limit of z be 1 and 1000.

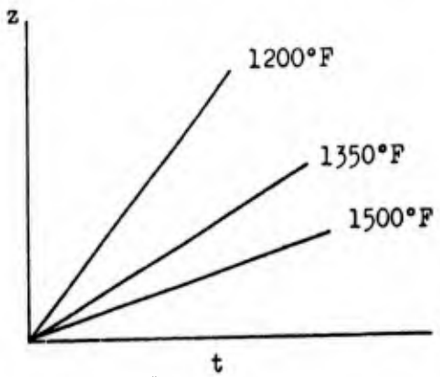

To obtain other temperature lines, plot $\frac{1}{T}$ vs. the exponent of t in equation 112.

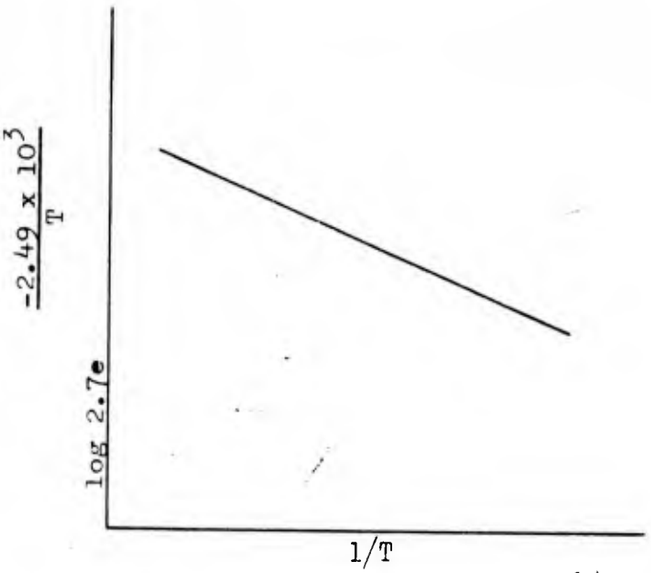

Values of the exponent can be read for other temperatures. Pick a value for t (e.g. 100 hrs), and determine z from $z = t^{\text{exp.}}$ for each temperature. These values can then be plotted on the z vs. t plot.

4. Assemble the plots of x, y, and z as follows:

Using standard nomographic procedures determine scale modulus for each vertical axis:

Line	Limits	Length	Scale Modulus
x	2×10^{-6} to 6.7×10^{5}	15"	$m_1 = 9.83$
y	1 to 33.5	15"	$m_2 = 9.83$
q			$m_3 = 4.92$
z	1 to 1000	15"	$m_4 = 5$
ϵ			$m_5 = 2.48$

$$m_1 = \frac{15}{\log 6.7 \times 10^{-5} - \log 2 \times 10^{-6}} = \frac{15}{1.5251} = 9.83$$

$$m_2 = \frac{15}{\log 33.5 - \log 1} = \frac{15}{1.525} = 9.83$$

$$m_3 = \frac{m_1 m_2}{m_1 + m_2} = \frac{(9.83)(9.83)}{19.66} = 4.915$$

$$m_4 = \frac{15}{\log 1000 - \log 1} = \frac{15}{3} = 5$$

$$m_5 = \frac{(m_4)(m_3)}{m_4 + m_3} = \frac{(4.92)(5)}{9.92} = 2.48$$

Let the distance between x and y = 10".

Then the distance between x and the auxilliary line q is:

$$\left(\frac{m_1}{m_1 + m_2}\right) \quad 10 = \left(\frac{9.83}{19.66}\right) \quad 10 = 5"$$

Let the distance between q and z = 15".

Then the distance from z to ϵ is:

$$\left(\frac{m_4}{m_3 + m_4}\right) \quad 15 = \left(\frac{5}{9.92}\right) \quad 15 = 7.56"$$

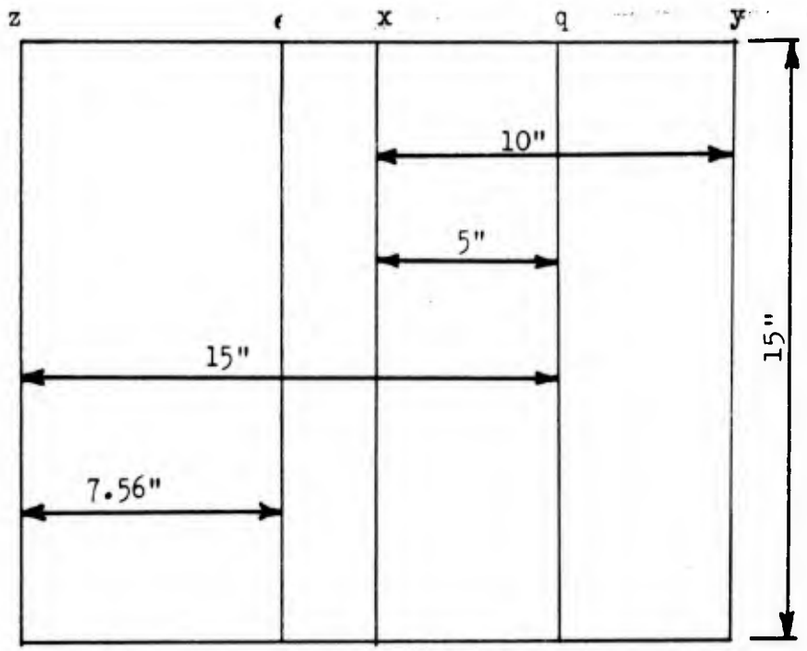

5. For simplicity in usage, mark only the scales which are used: i.e. temperature, time, stress, strain.

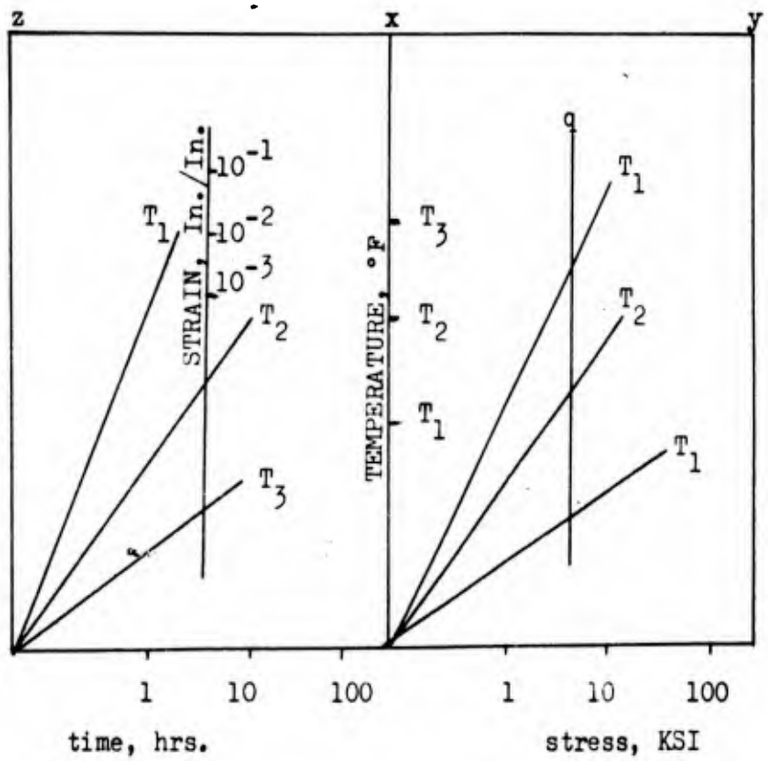

BOEING AIRPLANE COMPANY, Seattle, Wash.
PRESENTATION OF CREEP DATA FOR DESIGN PURPOSES, by M. N. Aarnes and M. M. Tuttle, 169 p. incl. figs., tables and refs. (Project 7381; Task 73812)
(ASD TR 61-216) (Contract AF 33(616)-7201)
Unclassified Report

This program was conducted to obtain additional and comparative creep data, to compare creep data from several sources, and to recommend what values to present and in what form to present creep data for design purposes.

Conventional long time creep tests were performed on A-286 at 1200°F and 1500°F; Allo AT at 800°F and 1000°F; and Unimach 2 at 600°F and 900°F for purposes of comparing with existing similar data. Conventional creep

(over)

tests were performed on Rene' 41 at 1250, 1400, 1550, 1700, 1850, and 2000°F.

Data were analyzed and are presented in the form of activation series equations. Nomographs were derived for each material.

Cyclic creep tests were performed on Rene' 41 in which both stress and temperature were cycled. Cyclic data were found to be comparable to the constant stress constant temperature data.

UNCLASSIFIED

BOEING AIRPLANE COMPANY, Seattle, Wash.
PRESENTATION OF CREEP DATA FOR DESIGN PURPOSES, by M. N. Aarnes and M. M. Tuttle, 169 p. incl. figs., tables and refs. (Project 7381; Task 73812)
(ASD TR 61-216) (Contract AF 33(616)-7201)
Unclassified Report

This program was conducted to obtain additional and comparative creep data, to compare creep data from several sources, and to recommend what values to present and in what form to present creep data for design purposes.

Conventional long time creep tests were performed on A-286 at 1200°F and 1500°F; Allo AT at 800°F and 1000°F; and Unimach 2 at 600°F and 900°F for purposes of comparing with existing similar data. Conventional creep

(over)

tests were performed on Rene' 41 at 1250, 1400, 1550, 1700, 1850, and 2000°F.

Data were analyzed and are presented in the form of activation series equations. Nomographs were derived for each material.

Cyclic creep tests were performed on Rene' 41 in which both stress and temperature were cycled. Cyclic data were found to be comparable to the constant stress constant temperature data.

UNCLASSIFIED
UNCLASSIFIED
UNCLASSIFIED
UNCLASSIFIED
UNCLASSIFIED
UNCLASSIFIED
UNCLASSIFIED

BOEING AIRPLANE COMPANY, Seattle, Wash.
PRESENTATION OF CREEP DATA FOR DESIGN PURPOSES, by M. N. Aarnes and M. M. Tuttle, 169 p. incl. figs., tables and refs. (Project 7381; Task 73812)
(ASD TR 61-216) (Contract AF 33(616)-7201)
Unclassified Report

This program was conducted to obtain additional and comparative creep data, to compare creep data from several sources, and to recommend what values to present and in what form to present creep data for design purposes.

Conventional long time creep tests were performed on A-286 at 1200°F and 1500°F; A110AT at 800°F and 1000°F; and Unimach 2 at 600°F and 900°F for purposes of comparing with existing similar data. Conventional creep

(over)

tests were performed on Rene' 41 at 1250, 1400, 1550, 1700, 1850, and 2000°F.

Data were analyzed and are presented in the form of activation series equations. Nomographs were derived for each material.

Cyclic creep tests were performed on Rene' 41 in which both stress and temperature were cycled. Cyclic data were found to be comparable to the constant stress constant temperature data.

UNCLASSIFIED

UNCLASSIFIED

UNCLASSIFIED

UNCLASSIFIED

BOEING AIRPLANE COMPANY, Seattle, Wash.
PRESENTATION OF CREEP DATA FOR DESIGN PURPOSES, by M. N. Aarnes and M. M. Tuttle, 169 p. incl. figs., tables and refs. (Project 7381; Task 73812)
(ASD TR 61-216) (Contract AF 33(616)-7201)
Unclassified Report

This program was conducted to obtain additional and comparative creep data, to compare creep data from several sources, and to recommend what values to present and in what form to present creep data for design purposes.

Conventional long time creep tests were performed on A-286 at 1200°F and 1500°F; A110AT at 800°F and 1000°F; and Unimach 2 at 600°F and 900°F for purposes of comparing with existing similar data. Conventional creep

(over)

tests were performed on Rene' 41 at 1250, 1400, 1550, 1700, 1850, and 2000°F.

Data were analyzed and are presented in the form of activation series equations. Nomographs were derived for each material.

Cyclic creep tests were performed on Rene' 41 in which both stress and temperature were cycled. Cyclic data were found to be comparable to the constant stress constant temperature data.

UNCLASSIFIED

UNCLASSIFIED

UNCLASSIFIED

UNCLASSIFIED

BOEING AIRPLANE COMPANY, Seattle, Wash.
PRESENTATION OF CREEP DATA FOR DESIGN PURPOSES, by M. N. Aarnes and M. M. Tuttle, 169 p. incl. figs., tables and refs. (Project 7381; Task 73812)
(ASD TR 61-216) (Contract AF 33(616)-7201)
Unclassified Report

This program was conducted to obtain additional and comparative creep data, to compare creep data from several sources, and to recommend what values to present and in what form to present creep data for design purposes.

Conventional long time creep tests were performed on A-286 at 1200°F and 1500°F; A110AT at 800°F and 1000°F; and Unimach 2 at 600°F and 900°F for purposes of comparing with existing similar data. Conventional creep

(over)

UNCLASSIFIED

BOEING AIRPLANE COMPANY, Seattle, Wash.
PRESENTATION OF CREEP DATA FOR DESIGN PURPOSES, by M. N. Aarnes and M. M. Tuttle, 169 p. incl. figs., tables and refs. (Project 7381; Task 73812)
(ASD TR 61-216) (Contract AF 33(616)-7201)
Unclassified Report

This program was conducted to obtain additional and comparative creep data, to compare creep data from several sources, and to recommend what values to present and in what form to present creep data for design purposes.

Conventional long time creep tests were performed on A-286 at 1200°F and 1500°F; A110AT at 800°F and 1000°F; and Unimach 2 at 600°F and 900°F for purposes of comparing with existing similar data. Conventional creep

(over)

UNCLASSIFIED

tests were performed on Rene' 41 at 1250, 1400, 1550, 1700, 1850, and 2000°F.

Data were analyzed and are presented in the form of activation series equations. Nomographs were derived for each material.

Cyclic creep tests were performed on Rene' 41 in which both stress and temperature were cycled. Cyclic data were found to be comparable to the constant stress constant temperature data.

UNCLASSIFIED

tests were performed on Rene' 41 at 1250, 1400, 1550, 1700, 1850, and 2000°F.

Data were analyzed and are presented in the form of activation series equations. Nomographs were derived for each material.

Cyclic creep tests were performed on Rene' 41 in which both stress and temperature were cycled. Cyclic data were found to be comparable to the constant stress constant temperature data.

UNCLASSIFIED

UNCLASSIFIED

UNCLASSIFIED

UNCLASSIFIED

BOEING AIRPLANE COMPANY, Seattle, Wash.
PRESENTATION OF CREEP DATA FOR DESIGN PURPOSES, by M. N. Aarnes and M. M. Tuttle, 169 p. incl. figs., tables and refs. (Project 7381; Task 73812)
(ASD TR 61-216) (Contract AF 33(616)-7201)
Unclassified Report

This program was conducted to obtain additional and comparative creep data, to compare creep data from several sources, and to recommend what values to present and in what form to present creep data for design purposes.

Conventional long time creep tests were performed on A-286 at 1200°F and 1500°F; A110AT at 800°F and 1000°F; and Unimach 2 at 600°F and 900°F for purposes of comparing with existing similar data. Conventional creep

(over)

tests were performed on Rene' 41 at 1250, 1400, 1550, 1700, 1850, and 2000°F.

Data were analyzed and are presented in the form of activation series equations. Nomographs were derived for each material.

Cyclic creep tests were performed on Rene' 41 in which both stress and temperature were cycled. Cyclic data were found to be comparable to the constant stress constant temperature data.

UNCLASSIFIED

BOEING AIRPLANE COMPANY, Seattle, Wash.
PRESENTATION OF CREEP DATA FOR DESIGN PURPOSES, by M. N. Aarnes and M. M. Tuttle, 169 p. incl. figs., tables and refs. (Project 7381; Task 73812)
(ASD TR 61-216) (Contract AF 33(616)-7201)
Unclassified Report

This program was conducted to obtain additional and comparative creep data, to compare creep data from several sources, and to recommend what values to present and in what form to present creep data for design purposes.

Conventional long time creep tests were performed on A-286 at 1200°F and 1500°F; A110AT at 800°F and 1000°F; and Unimach 2 at 600°F and 900°F for purposes of comparing with existing similar data. Conventional creep

(over)

tests were performed on Rene' 41 at 1250, 1400, 1550, 1700, 1850, and 2000°F.

Data were analyzed and are presented in the form of activation series equations. Nomographs were derived for each material.

Cyclic creep tests were performed on Rene' 41 in which both stress and temperature were cycled. Cyclic data were found to be comparable to the constant stress constant temperature data.

UNCLASSIFIED

UNCLASSIFIED